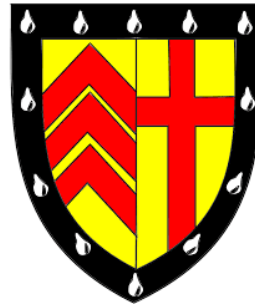


Maxime Pierre Fabrice Couturier

**Substrate elucidation and mutasynthesis:
Characterisation of the biosynthetic pathway of a
tripyrrolic secondary metabolite, prodigiosin**



This dissertation is submitted for the degree of Doctor of Philosophy

University of Cambridge

Clare College

September 2019

Declaration

I hereby declare that:

This thesis is the result of my own work and includes nothing which is the outcome of work done in collaboration except as declared in the Preface and specified in the text.

This thesis is not substantially the same as any that I have submitted, or, is being concurrently submitted for a degree or diploma or qualification at the University of Cambridge or any other University. I further state that no substantial part of my thesis has already been submitted, or, is being concurrently submitted for any such degree, diploma or other qualification at the University of Cambridge or any other University or similar institution.

This dissertation does not exceed 60,000 words, including abstract, tables, and footnotes, but excluding table of contents, diagrams, figure captions, list of abbreviations, bibliography, appendices and acknowledgements.

Maxime Couturier

Cambridge, September 2019

Abstract

Substrate elucidation and mutasynthesis: Characterisation of the biosynthetic pathway of a tripyrrolic secondary metabolite, prodigiosin

Maxime Pierre Fabrice COUTURIER

A wide variety of biological activity can be found in the realm of secondary metabolites. The tripyrrole prodigiosin illustrates this perfectly with activities ranging from antimicrobial to immunosuppressive and anticancer. Microorganisms producing the red pigment prodigiosin were first isolated more than 150 years ago. Yet, its structure was only elucidated in the 1960s and the biosynthetic pathway remained mainly unknown until the 2000s. This secondary metabolite results from a bifurcated pathway where monopyrrole 2-methyl-3-pentyl-1*H*-pyrrole (MAP) and bipyrrrole 4-methoxy-1*H*,1'*H*-2,2'-bipyrrrole (MBC) are produced independently before condensation. As MBC is an intermediate in the synthesis of other natural products, the enzymes involved in its formation have been well characterised. In contrast, the three enzymes – PigD, PigE and PigB – involved in the formation of MAP are specific to the biosynthesis of prodigiosin and less is known about them. This thesis focuses on the latter two enzymes.

PigE was first described as a transaminase catalysing the transformation of 3-acetyloctanal into 3-acetyloctylamine (which cyclises to form dihydroMAP) and this activity has been confirmed by feeding intermediates to various gene-knockout strains. However, *in vitro* studies have demonstrated that 3-acetyloctanal could not be the product of PigD. In addition, bioinformatics analysis of its amino acid sequence showed that PigE has two domains: a transaminase C-terminal moiety and an unspecified N-terminal one, which we propose is a thioester reductase that converts a 3-acetyloctanoyl thioester to 3-acetyloctanal. Attempted chemical complementation of a *pigD*-knockout strain of *Serratia* using synthetic thioester, carboxylic acid and aldehyde substrates showed that both the thioester and the aldehyde can be used for pigment production, indicating that a thioester reductase is involved in prodigiosin biosynthetic pathway. Furthermore, the PigE protein was expressed in a heterogeneous host, purified and submitted to a number of activity and kinetic assays, which demonstrated that it can reduce a 3-acetyloctanoyl thioester substrate.

The oxidation of dihydroMAP to MAP had previously been shown to be catalysed by an FAD-dependent oxidase PigB. The kinetics of HapB, a homologue of PigB had been studied by a previous group member. To take this project further we studied the substrate flexibility of the

Preface

enzyme and used it to form new analogues of prodigiosin by mutasynthesis. Ten analogues of dihydroMAP with modifications either in the C2 or C3 positions were synthesised. Both extensions and truncations in the length of the chain at the C3 position could be accepted, whereas alkyl chains longer than 3 carbons on the C2 position could not be accommodated. Similar results were found *in vivo* when the analogues were fed to a *pigD*-knockout strain of *Serratia*, showing that PigB and the condensing enzyme PigC shared similar flexibility. Eight analogues of prodigiosin were hence obtained and their antimicrobial activities against Gram-positive and Gram-negative bacteria were assessed.

Acknowledgement

I would like to take this opportunity to express my gratitude to my supervisor Dr. Finian J. Leeper. Not only did he guide me through these four years, but he also always encouraged me to give my best in everything. I would also like to thank him for the time he spent proof-reading this work and the other reports I submitted over the years. I would also like to thank Prof. George P.C. Salmond for welcoming me in his lab in the Biochemistry Department and useful input all along this project.

I am also extremely grateful to the Frances and Augustus Newman foundation and the BBSRC DTP for funding this PhD. Nothing would have been possible without them.

A big thanks to the members of both labs for their support and friendship. In particular, I would like to thank Dr Rita Monson, who taught me microbiology and molecular biology with a rare patience and Dr Annabel Murphy for her all her helpful inputs and advice. A great thank you as well to Dr Emma Radoux and Flaviu Bulat who welcomed me in the Leeper lab and took the time to make sure I was starting off on the right foot, and to Danny Parle, Matt Corney and Alex Chan for bearing me in the last year.

I also would like to thank my academic mentor, Dr Anthony Coyne who was always there when I needed support or advice.

A great thank you also to the technical teams both in the Chemistry and Biochemistry departments: research would not be possible without you!

I feel extremely fortunate to have spent the past few years as part of the University of Cambridge and Clare College. This place gathers brilliant minds from all imaginable backgrounds – who would have thought you could do a PhD in music – to form one of the most stimulating environments I have ever encountered.

I would also like to take this opportunity to thank Prof. Sam Zard who taught me chemistry in the Ecole Polytechnique and without whom I probably would not be here today.

A warm thank you to my family for their constant support. To my parents for always finding ways to motivate me and to put things in perspective. To my brothers, whose role in this project I am still trying to determine, but it was certainly crucial. Finally, a *grand merci* to Vinny, well, for everything...

Pour la patrie,

Les sciences

Et la gloire

Table of contents

Declaration.....	i
Abstract.....	ii
Acknowledgement.....	v
Table of contents.....	vi
List of abbreviations.....	xi
Chapter 1. Prodigiosin: structure, synthesis and biosynthesis.....	1
1. Structure of prodiginines.....	1
2. Discovery and elucidation of the structure of prodigiosin.....	3
3. Elucidation of prodigiosin biosynthetic pathway.....	5
3.1. Biosynthesis of MBC ^{24,31}	7
3.2. Biosynthesis of MAP 9.....	9
3.3. Biosynthesis of 2-undecylpyrrole B.....	11
3.4. Condensation: PigC.....	12
3.5. Formation of cyclized prodiginines.....	13
4. Related compounds.....	13
4.1. Marineosin.....	13
4.2. Roseophilin.....	14
4.3. Tambjamines.....	15
5. Biological properties of prodiginines.....	16
5.1. Antimalarial.....	16
5.2. Antifungal.....	17
5.3. Anti-bacterial.....	17
5.4. Immunosuppressive.....	18
5.5. Antitumour.....	19
6. The role of thioester in biosynthesis.....	23

Preface

7. Aims of the project	25
Chapter 2. Mutasythesis of new prodiginines by exploiting the substrate flexibility of dihydropyrrole oxidase PigB	26
1. Objectives	26
2. Elucidation of the structure of PigB's substrate.....	28
3. Synthesis of novel analogues of H ₂ MAP	30
3.1. Modifications in the C2 and the C3 position.....	30
3.2. Preliminary study of modifications of the substituent on the C4 position.....	32
3.3. Toward a general methodology	33
4. <i>In vitro</i> characterisation of PigB homologue, HapB	35
4.1. Comparison between HapB and PigB.....	35
4.2. Substrate flexibility of HapB	38
5. Mutasythesis	39
5.1. Qualitative results of complementation assay	39
5.2. Quantitative results	40
6. Enantioselectivity of PigB	43
7. Conclusion and future work	49
Chapter 3. Antimicrobial activity of prodigiosin analogues	50
1. Construction of a prodigiosin producing strain suitable for antibiotic assays.....	50
2. Antibiotic assay	52
2.1. Preliminary studies.....	52
2.2. Disc diffusion assay	53
2.3. Half maximal growth inhibition (GI ₅₀) experiments	57
3. Preliminary anti-cancer activity assay.....	58
4. Investigation of hyper-producing strain for yield improvement	59
5. Other potential applications of prodigiosin analogues	61
6. Conclusion and future work	62
Chapter 4. Characterisation of PigE.....	63

Preface

1. Overview and aims of the project.....	63
1.1. Overview of potential characteristics of PigE.....	63
1.2. PigE: a potential bifunctional thioester reductase - aminotransferase	64
2. Bioinformatic analysis of PigE	66
2.1. NCBI Basic Local Alignment Search Tool (BLAST) ¹⁷⁶	66
2.2. PHYRE ¹⁴⁷	67
2.3. Comparison with TamH.....	69
3. Synthesis of PigE potential substrate(s).....	70
3.1. Method A: from ethyl acetoacetate to 3-acetyloctanal	70
3.2. Method B: From 2-octanone to 3-acetyloctanoic acid.....	72
4. Complementation experiments.....	74
4.1. Qualitative assay	74
4.2. Conditions for quantitative complementation assay with PigE substrate	75
4.3. Complementation assays with thioester 68	77
4.4. Investigation in the role of PigE in the thioester reduction	81
5. <i>In vitro</i> characterisation of pigE	86
5.1. Construction of BL21 pPigE and expression of the protein	86
5.2. Protein expression and purification.....	87
5.3. Protein characterisation	90
5.4. Cell extracts assays	93
5.5. LC-MS	100
6. Conclusions and perspective	103
Chapter 5. Toward an <i>in vivo</i> characterisation of PigD.....	104
1. Overview and aim of the project	104
2. Bioinformatics analyses	105
3. The PigD product is not secreted	106
4. Synthesis of the unlabelled potential substrate	107
4.1. Knoevenagel condensation	107

Preface

4.2. Wittig reaction.....	108
4.3. Formation of the aldehyde 17.....	109
5. Deuterium labelling.....	109
Chapter 6. Conclusions and future work.....	112
Chapter 7 Materials and methods.....	114
1. Biological chemistry.....	114
1.1. General considerations.....	114
1.2. Media and buffers.....	114
1.3. PCR.....	117
1.4. Cloning.....	118
1.5. Conjugation.....	119
1.6. Transduction.....	119
1.7. Protein expression and purification.....	120
1.8. SDS- PAGE and Western blot.....	121
1.9. Complementation assay on agar plates.....	122
1.10. Prodigiosin production, extraction and quantification.....	122
1.11. High Pressure Liquid Chromatography (HPLC).....	122
1.12. Mass spectrometry.....	123
1.13. Antimicrobial assays.....	124
1.14. Anticancer activity.....	125
1.15. Thermal shift assay.....	126
1.16. CD spectra.....	126
1.17. NAD(P)H assay.....	126
1.18. Ninhydrin assay.....	127
1.19. Ehrlich's assay.....	127
1.20. Bacterial strains and plasmid.....	128
2. Synthesis.....	130
2.1. General considerations.....	130

Preface

2.2. Synthesis of H ₂ MAP analogues	131
2.3. Synthetic route toward other analogues of H ₂ MAP.....	138
2.4. Racemic resolution of H ₂ MAP	142
2.5. Tetrazine coupling.....	143
2.6. Synthesis of PigE potential substrates	144
2.7. Synthesis of potential substrate of PigD.....	149
References	153
Appendix.....	172
1. Bioinformatic of PigE	172
1.1 Phyre alignment	172
1.2 BLAST.....	173
2. Bioinformatic of PigD	174
3. Vector sequences.....	176
4. NMR Spectras	177

List of abbreviations

A	Adenylation domain
ACN	Acetonitrile
ACP	Acyl Carrier Protein
ACT	Artemis comparaison tool
ATP	Adenosine triphosphate
BCL	B-cell lymphoma
BGC	Biosynthetic gene cluster
BLAST	Basic local alignment search tool
Boc	tert-Butyloxycarbonyl
CD	Circular Dichroism
CoA	Coenzyme A
CuTC	Copper (I) thiophene-2-carboxylate
DCM	Dichloromethane
DIBAL-H	Diisobutylaluminium hydride
DMAP	4-Dimethylaminopyridine
DMBN	Dimethyl benzyl amine
DME	Dimethyl ether
DMF	Dimethyl formamide
DMSO	Dimethyl sulfoxide
DNA	Deoxyribonucleic acid
EDC	1-Ethyl-3-(3-dimethylaminopropyl)carbodiimide
ERK	Extracellular Signal-regulated Kinase
ESS	<i>E. coli</i> β -Lactam super-sensitive indicator strain
FAD	Flavin adenine dinucleotide
FDA	Food and drug administration
GI ₅₀	Concentration required for 50% inhibition of growth
H ₂ MAP	5-Methyl-4-pentyl-3,4-dihydro-2H-pyrrole
HBC	4-Hydroxy-2,2'-bipyrrole-5-carbaldehyde
HBM	4-Hydroxy-2,2'-bipyrrole-5-methanol
HEPES	4-(2-Hydroxyethyl)-1-piperazineethanesulfonic acid
HPLC	High pressure liquid chromatography
IC ₅₀	Concentration required for 50% inhibition
IPTG	Isopropyl- β -D-thiogalactoside
IR	Infra-Red
JNK	C-Jun N-terminal kinase
KS	Ketosynthase
LB	Luria-Bertani medium
LBS	LB+0,25 M sorbitol
LC-MS	Liquid chromatography-mass spectrometry
LD ₅₀	Half Lethal Dose
LSD ₁	Lysine specific histone demethylase 1b
MAP	2-Methyl-3-amylpyrrole
MAPK	Mitogen activated Protein Kinases
MBC	4-Methoxy-2,2'-bipyrrole-5-carboxaldehyde

Preface

MH	Mueller-Hinton medium
MIC	Minimal inhibitory concentration
MOMP	Mitochondria Outer Membrane Permeabilization
MS	Mass Spectrometry
NAC	N-acetyl-cysteamine
NAD(P)H	Nicotinamide adenine dinucleotide (phosphate), reduced form
NBSH	Nitrobenzensulfonylhydrazine
NHS	N-hydroxysuccinimide
nmr	Nuclear magnetic resonance
NRPS	Non-ribosomal peptide synthetase
OAS	α Oxoamine Synthase
OD	Optical Density
PAGE	Polyacrylamide gel electrophoresis
PBS	Phosphate-buffered saline
PCP	Peptide carrier protein
PGM	Peptone glycerol medium
PKS	Polyketide synthase
PLP	Pyridoxal phosphate
PMP	Pyridoxamine phosphate
PPDK	Pyruvate-phosphate di-kinase
pTSA	para Toluene sulfonic acid
Py ₂ Tz	3,6-Di(pyridin-2-yl)-1,2,4,5-tetrazine
RNA	Ribonucleic acid
<i>S39006</i>	<i>Serratia</i> sp, ATCC 39006
SAR	Structure activity relationship
SDS	Sodium dodecyl sulphate
<i>Sma</i>	<i>Serratia marcescens</i>
TBAF	Tetra-n-butylammonium fluoride
TBHP	tert-Butyl hydroperoxide
THF	Tetrahydrofuran
TLC	Thin layer chromatography
TMS	Trimethyl silyl
TPP	Thiamine pyrophosphate
TR	Thioester Reductase
TRIS	Tris(hydroxymethyl)aminomethane
UV	Ultra-Violet
WT	Wild type

Chapter 1. Prodigiosin: structure, synthesis and biosynthesis

Chapter 1. Prodigiosin: structure, synthesis and biosynthesis

1. Structure of prodiginines

All through human history, natural products have shown numerous applications. For instance, indigotin extracted from plants has been used as a dye for centuries.¹ Traditional medicines and the use of active products from plant extracts are other examples of applications of natural products. With the rise of the pharmaceutical industry in the 19th century, their importance was once again confirmed: one of the most well-known and commonly used drugs, aspirin, derives from salicylic acid found in willow trees.² Between 1981 and 2014, 25% of the drugs approved by the FDA were either natural products or modified natural products.³ If we include synthetic molecules mimicking natural products, that number rises to 45%. Therapeutic areas covered by natural products are also very diverse: almost half of the molecules accepted for cancer treatment since the late 40s derived from natural products³ and 90% of the antimicrobials used clinically today come from microorganisms.⁴ Considering that cancer occurrence has increased by more than 10% in the UK over the last 20 years⁵ and the fast emergence of antibiotic multiresistant strains,⁶ discovery of new medicines is crucial and natural products represent a large pool of potential candidates.

In bacteria, the genes coding for the proteins involved in the production of secondary metabolites are usually gathered in clusters (called biosynthetic gene clusters, BGCs). In some species, such as some *Actinobacteria*, more than a dozen such clusters can be present, and the understanding of these clusters and the biological assessment of their products are a potential source of new drugs.

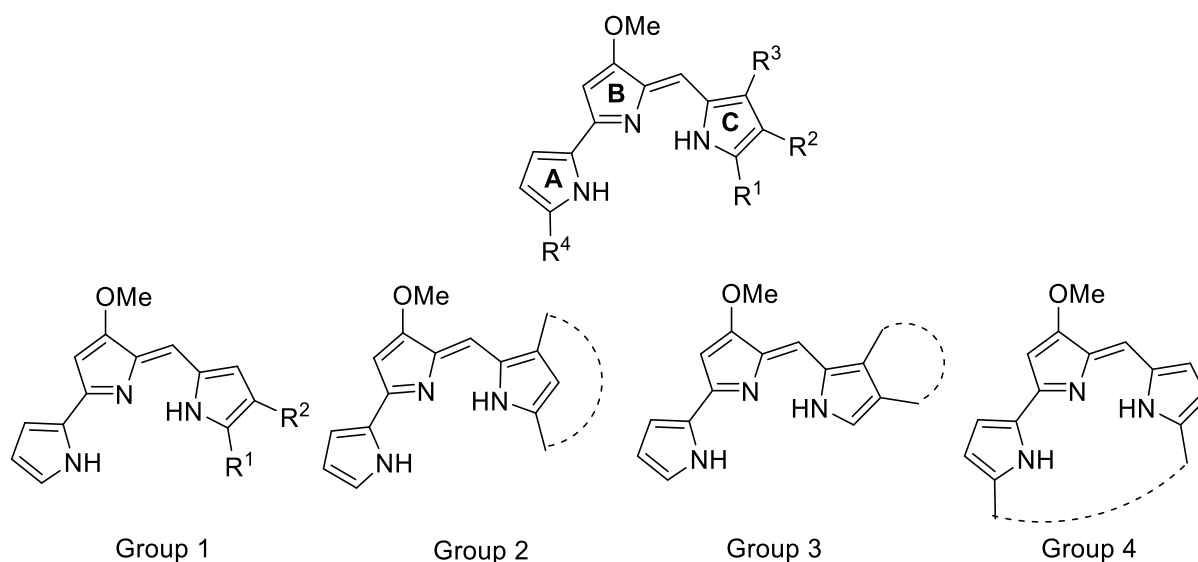


Figure 1.1: The four groups of prodiginines

Prodiginines are a family of secondary metabolites with a 2-pyrrolyldipyrromethene skeleton (**Figure 1.1**) and a methoxy group on ring B. The conjugated π -system containing seven double bonds gives them a bright red colour. Prodiginines are divided into 4 groups, depending on the substituents on ring C (**Figure 1.1** and **1.2**).⁷ Group 1 prodiginines have only linear alkyl chains as illustrated by prodigiosin **1a** from *Serratia marcescens* (*Sma*) and undecylprodigiosin **2** from *Streptomyces coelicolor* A(3) (**Figure 1.2a**).⁸ *S. coelicolor* also produces streptorubin B **3**, which, like metacycloprodigiosin **4** from *Streptomyces longisporus ruber* (**Figure 1.2b**),⁹ is an example of a prodiginine from group 2, where position 1 and 3 of ring C are connected. An example of a group 3 prodiginine, with a cyclic structure between positions 2 and 3 of ring C, is given by cycloprodigiosin **5** produced by *Alteromonas rubra*.¹⁰ Finally, in group 4, a macrocycle connects rings A and C, as illustrated in **Figure 1.2d** by *Actinomadura madurae*'s cyclononylprodigiosin **6** and methylcyclodecylprodigiosin **7**.¹¹

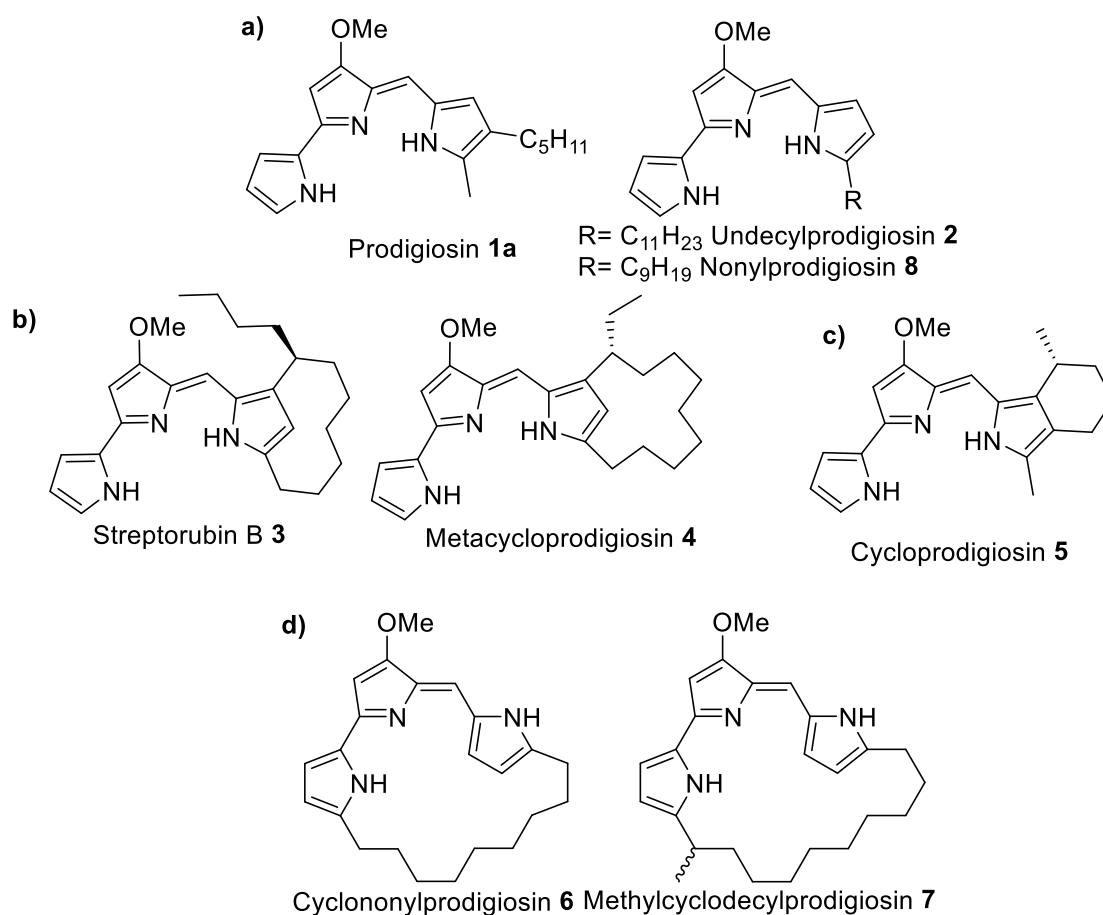


Figure 1.2: Examples of prodiginines from the four groups

2. Discovery and elucidation of the structure of prodigiosin



Figure 1.3:
Bleeding bread

Prodigiosin **1a** is probably the most well-known example of a prodiginine. Indeed, it is famous for its alleged involvement in a number of “miracles” – hence its name – and it was the first prodiginine to be characterised. Observation of bleeding food, especially in starch rich material such as polenta or bread (see **Figure 1.3**), even religious bread, has been documented since the middle ages and up to the 20th century and was often attributed to either witchcraft or divine intervention. In the early 19th century, recurring occurrences of this phenomenon in northern Italy triggered a scientific investigation and botanist Pietro Melo, pharmacist Bartolomeo Bizio and physician Vincenzo Sette independently concluded that the red coloration was due to fermentation and achieved the first isolation of *Sma*.¹² This microorganism was at the time thought to be a fungus but was quickly reclassified as a bacterium. However, the molecule responsible for the pigmentation remained unknown for decades. The first isolation of prodigiosin was performed by Wrede and

Hetche in 1929.¹³ Using degradation studies, they were able to show the presence of three pyrroles and a methoxy group and proposed three possible structures (**Figure 1.4**).¹⁴

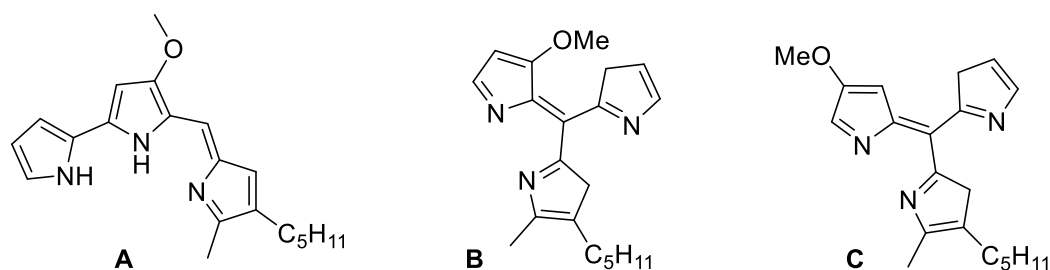


Figure 1.4: The three potential structures for prodigiosin proposed by Wrede and Hetche

Another 30 years passed before Vogel and Wasserman used biochemical tools to rule out incorrect structures. In the early 50s, it was observed that some mutant strains of *Sma* could not produce prodigiosin on their own but could cross complement each other (the pigment was produced when the two strains were cultured together). Santer and Vogel¹⁵ hypothesized that an intermediate in prodigiosin production accumulated in such strains. They were able to isolate a compound consistent with the chemical formula $C_{10}H_{10}O_2N_2$ and to show it contained at least one pyrrole with a hydrogen on one of the carbons α to the nitrogen. Wasserman and coworkers¹⁶ were then able to show that prodigiosin resulted from the condensation of the compound isolated by Vogel and 2-methyl-3-amylpyrrole (MAP) **9**, a compound that Wrede and Rothlaas¹⁴ had observed during their degradation studies. They also were able to demonstrate that Vogel's compound was a bipyrrrole with an α, α' linkage and with a methoxy on the C3 position of one ring and an aldehyde on the C2 or C4 position of the same ring (**Figure 1.5c**). This ruled out two of the three initial proposed structures.

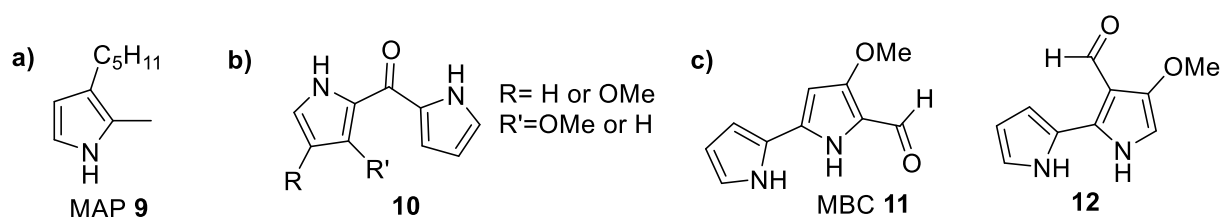


Figure 1.5: Intermediates in prodigiosin structure elucidation a) MAP **8**, isolated by Wrede and Rothlaas, b) synthetic precursor for structure B and C c) potential structures for the intermediate isolated by Santer and Vogel

Definitive proof of prodigiosin structure was reported by Rapoport and Wilson in 1962, when they synthesised a molecule whose optical properties matched perfectly the ones of natural prodigiosin. In a series of papers^{17,18} they first synthesised a methoxypyrrrole **10**¹⁷ that would have been the precursor of structure B, and showed it was inconsistent with the intermediate isolated by Vogel. They then synthesised the two possible regioisomers of the precursors (**11** and **12**)

proposed by Wasserman *et al.*¹⁶ and condensed them with MAP. By comparing the UV absorbance of the two products with natural prodigiosin¹⁸ they were able to conclude that the structure of prodigiosin is the one presented in **Figure 1.2**. This also suggested that the final step for prodigiosin biosynthesis was the condensation of MAP **9** and 4-methoxy-2,2'-bipyrrole-5-carboxaldehyde (MBC) **II**.

Hence, almost 150 years after the first isolation of a bacterium producing prodigiosin, the structure of the pigment was finally known. Yet, two configurations of the compound are possible (**Figure 1.6**). Considering the variety of biological activities that prodigiosin displays (see Section 5), structure activity tests and prediction are important for the design of new potential drugs and it is hence crucial to know which conformation is predominant. Rizzo *et al.*¹⁹ addressed this issue and showed that the two conformational isomers always exist in equilibrium and the rates of interconversion – and consequently the ratio – depended heavily on the pH of the solution. Indeed, the α -conformer is able to form an extra hydrogen bond when protonated, leading to a difference of pKa between the two forms. As a result, prodigiosin is almost purely in its α form at low pH and in its β form at high pH (**Figure 1.6**).

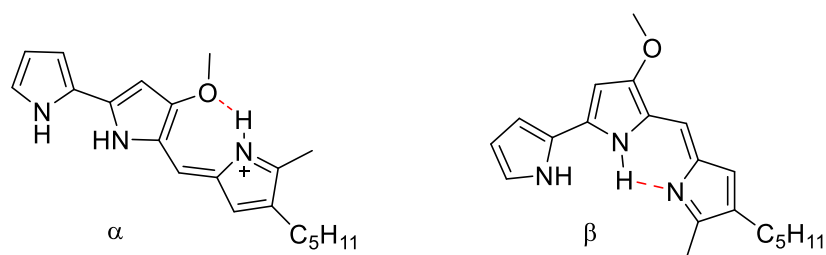


Figure 1.6: The two conformations of prodigiosin

3. Elucidation of prodigiosin biosynthetic pathway

One of the first investigations into prodigiosin biosynthetic pathway was conducted by Williams and his group by isotopic labelling²⁰ as well as by trying to enhance the production of pigment by adding single amino acids to the culture broth²¹. This showed that proline, alanine, histidine, acetate and serine were likely to be involved in the formation of the secondary metabolite.

As mentioned above, Wasserman and co-workers¹⁶ showed in the 60's that prodigiosin resulted from the condensation of MAP and MBC, suggesting a bifurcated pathway. However, the molecular biology tools necessary for a complete elucidation of the pathway were not available before the early 2000s when the complete sequence of *S. coelicolor* became available. This allowed Cerdeño *et al.*²² to attribute a function to each of the 23 genes present in the BCG (noted *red*) by sequence comparison (**Figure 1.7**). They were then able to support their predictions

through complementation experiments with knockout mutants. They concluded that two genes coded for regulators, six were involved in the formation of MBC **II** (**Figure 1.8**), eight in the biosynthesis of 2-undecylpyrrole **B** (**Figure 1.9**) and that two were involved in housekeeping functions. One gene was also predicted to code for the enzyme catalysing the condensation of **II** and **B** into undecylprodigiosin **2** and another gene was forecasted to code the enzyme involved in the conversion to Streptorubin B **3**.

A few later years later, Salmond and co-workers^{23,24} managed to clone and express the prodigiosin BGC in an heterologous host. Whilst investigating carbapenem production by *Serratia* sp. ATCC 39006 (*S39006*) by cloning its genome library into *E. carotovora* ssp. *carotovora*, they observed production of prodigiosin in strains transformed with cosmid pNRT104.^{23,25} By comparing *Sma*'s and *S39006*'s genomes, they located the *Sma* cluster, cloned it and expressed it in *E. coli*.²⁴ The clusters of the two *Serratia* species showed a good conservation of 14 genes (*pigA-N*), which were believed to be responsible for the biosynthesis. An additional gene, *pigO*, was present in the *Serratia 39006* operon, but knocking it out did not prevent the production of pigment, suggesting a regulatory role.²⁴

Williamson *et al.*²⁶ then prepared mutants of *S39006* with in-frame deletions or insertions in every biosynthetic gene. For each mutant, the accumulation of intermediates was checked by Liquid Chromatography-Mass Spectrometry (LC-MS) and the order of many of the enzymes was determined by cross-feeding (**Figure 1.8**).

As mentioned earlier, prodiginines can be produced by a variety of micro-organisms. In addition, a given prodiginine can be found in different strains. For example, prodigiosin **1a** is produced not only by *Sma* and *S39006* but also by other strains of *Serratia* (*nematodiphila* and *plymuthica* for instance), *Vibrio gazogenes* ATCC 43942,²⁷ *Hahella chejuensis* KCTC 2396 (*H2396*)²⁸ and *Janthinobacterium lividum* *BR01*.²⁹ Interestingly, the BGC, noted *pig*, is remarkably well conserved among those organisms (see **Figure 1.8**).³⁰ *S39006* was originally believed to be a strain of *Sma*, but deeper genetic analysis contradicted this assessment.²⁴ *H2396* is a marine bacterium isolated from the South Korea sea and produces prodigiosin using the *hap* cluster. This cluster contains 15 genes, one more than *Sma*: the sequence of the homologue of *pigB* (*hapB*) contains a stop codon, leading to a gene coding for the N terminal domain and one for the rest (see Chapter 2).²⁸ *Janthinobacterium lividum* *BR01* is a psychrophilic bacterium found in Alaskan soil. Although all the other examples of prodigiosin producer are γ -proteobacteria, this one is a β -proteobacterium. In addition, in this strain, the genes coding for PigB and PigC are fused, leading to gene *pigBC*.²⁹

Although the biosynthetic pathways followed are similar with *red* and *pig*, the organisation of the BCG are different: the order of the genes is not the same and they are arranged in three operons in *red* instead of one in *pig* (**Figure 1.7**).³⁰ A recent study showed that the *pig* cluster and its homologues in γ -proteobacteria descended from a common ancestor, whereas the *red* cluster shared most analogy with other actinobacterial clusters coding for pyrrole formation in other secondary metabolites, hinting horizontal gene transfer and convergent evolution.³⁰ Nevertheless, all but three genes in the *pig* cluster show strong homology with enzymes coded by the *red* cluster.²⁴ The three 'missing genes' are *pigB*, *pigD* and *pigE*, suggesting a strong conservation of MBC biosynthesis from one prodiginine to another whereas the biosynthesis of the monopyrrole involves more variation.

Combining results obtained with *S. coelicolor*³¹ and *S39006*, a complete biosynthetic pathway for prodigiosin **1a** was proposed by Williamson *et al.* (**Figure 1.8**).²⁶

3.1. Biosynthesis of MBC^{24,31}

The initial precursor of bipyrrole MBC is L-proline. In *Serratia*, PigI activates L-proline using adenosine triphosphate (ATP) and transfers it to the thiol group of a peptidyl carrier protein (PCP), PigG. PigA then catalyses the oxidation of the pyrrolidine moiety, leading to the corresponding pyrrole (see **Figure 1.8**). In a process similar to that of polyketide synthases (PKS), the thioester is then transferred to the active site of PigJ. A decarboxylative coupling of a malonyl unit carried by an acyl carrier protein (ACP) domain of PigH onto the pyrrole-2-carboxyl thioester then yields a pyrrolyl- β -ketothioester attached to PigH. A pyridoxal phosphate (PLP) dependent α -oxoamine synthase domain in PigH then catalyses a decarboxylative condensation of serine with the pyrrolyl- β -ketothioester to release the 4-hydroxy-2,2'-bipyrrole-5-methanol (HBM) **14**. According to Williamson *et al.*²⁶, no accumulation of any of the intermediates before HBM could be detected by mass spectroscopy (MS), which is consistent with protein-bound intermediates.

Flavin dependent PigM then catalyses the oxidation of HBM into 4-hydroxy-2,2'-bipyrrole-5-carbaldehyde (HBC) **15**. Interestingly, this intermediate can be accepted by the condensing enzyme PigC, leading to the formation of norprodigiosin **16**. Finally, MBC is obtained by methylation of HBC by PigF, possibly in complex with PigN. A *pigF* knock out strain only produces norprodigiosin, whereas in the absence of PigN prodigiosin is produced but in lower amounts, which suggests that PigN is not essential for the methylation but does facilitate it.²⁶

Chapter I. Prodigiosin: structure, synthesis and biosynthesis

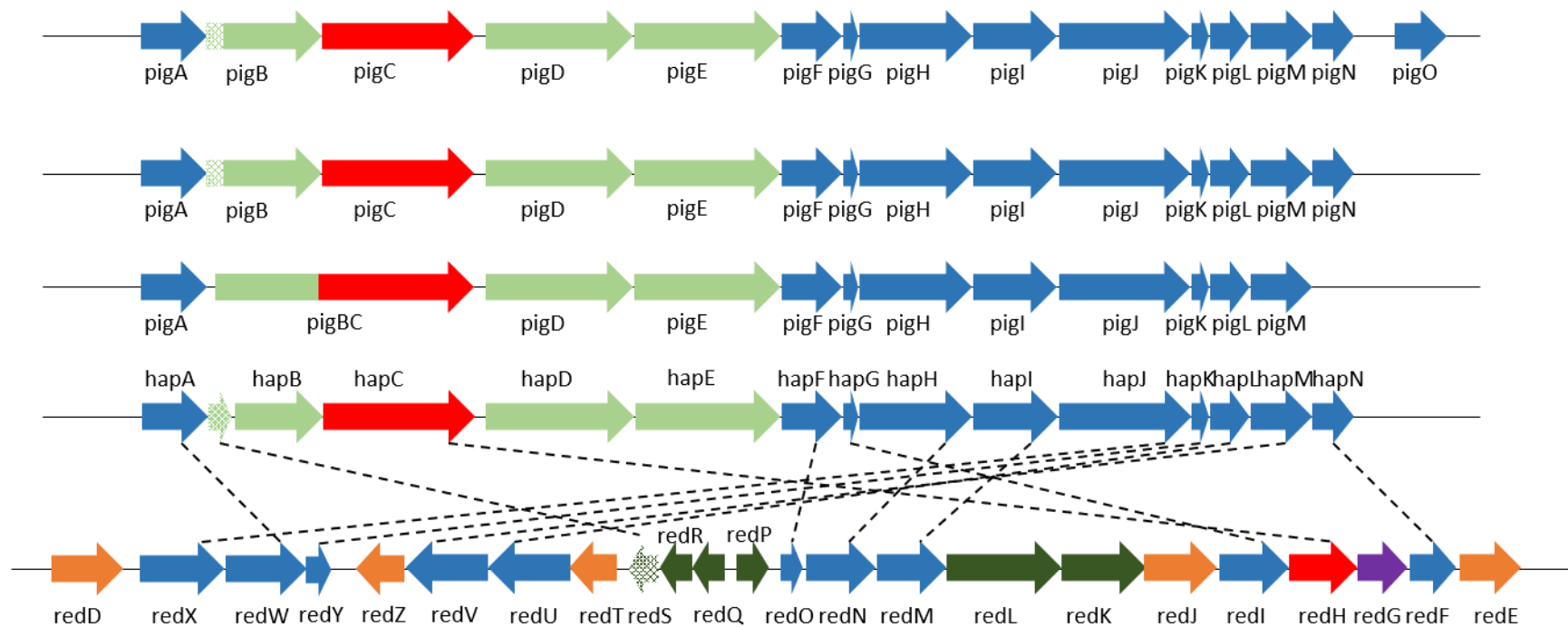


Figure I.7: Examples of prodiginines BGCs; from top to bottom: *S39006*, *Sma*, *Janthinobacterium lividum BR01*, *H2396*, *S. coelicolor*. Blue: synthesis of bipyrrole MBC; green: synthesis of monopyrrole; red: condensation; purple: cyclisation; orange: no known function. The transmembrane domain of PigB and the corresponding gene in *H2396* are green and white. Genes with the same function in the *pig/hap* clusters and the *red* cluster are connected.

PCPs such as PigG need to be phosphopantetheinylated after translation to be active. Sequence comparisons and knock out experiments indicated that PigL was responsible for this step of the pathway.³¹ The function of the last enzyme involved in MBC biosynthesis, PigK, is still not clear: knock out mutants were still able to produce prodigiosin, but the ratio between prodigiosin and norprodigiosin was changed compared to the wild type, which suggested that PigK is involved in MBC formation.³² Comparison with similar proteins suggested that PigK could be an oxygenase taking HBC as a substrate.³³

3.2. Biosynthesis of MAP 9

MAP biosynthesis relies on three enzymes: PigD, PigB and PigE. They have been less extensively studied than the proteins involved in MBC formation because they are specific to prodigiosin whereas the formation of MBC occurs in a similar fashion in the biosynthesis of other prodiginines. 2-Octenal **17**, potentially formed by the action of a thioester reductase on octenoyl ACP, an intermediate in fatty acid biosynthesis, was originally presumed to be the starting point of the pathway.^{26,34,35} However, Dresen *et al.*³⁶ showed that thiamine pyrophosphate (TPP)-dependent PigD, when presented with an aldehyde substrate such as 2-octenal, catalyses a direct attack of an acetyl anion equivalent at the carbonyl carbon instead of the β position. Yet, with less reactive carbonyls (ketones or thioesters) the required attack at the β -carbon was observed.³⁶ It is therefore now proposed that PigD catalyses the decarboxylative coupling of pyruvate with octenoyl ACP (or CoA) to give the corresponding 3-acetyloctanoyl thioester.

PigE is known to be responsible for the formation of 3-(2-aminoethyl)octan-2-one **18** (which cyclises to give dihydroMAP **19**), but its exact substrate and activity are yet to be demonstrated. A crystal structure,³⁵ sequence analysis and feeding studies²⁶ are all consistent with the C-terminal half of PigE being a PLP-dependent transaminase, catalysing the transformation of 3-acetyloctanal **20** into **18**. Bioinformatic analysis of the N-terminal half of PigE, suggests that it might be a reductase which releases the aldehyde, possibly from a thioester (see Chapter 4).

H₂MAP **19** is then oxidised to MAP by PigB. Previous work in the group showed that PigB was a FAD dependent oxidase and that the reaction requires O₂ and releases H₂O₂.³⁷

Chapter 1. Prodigiosin: structure, synthesis and biosynthesis

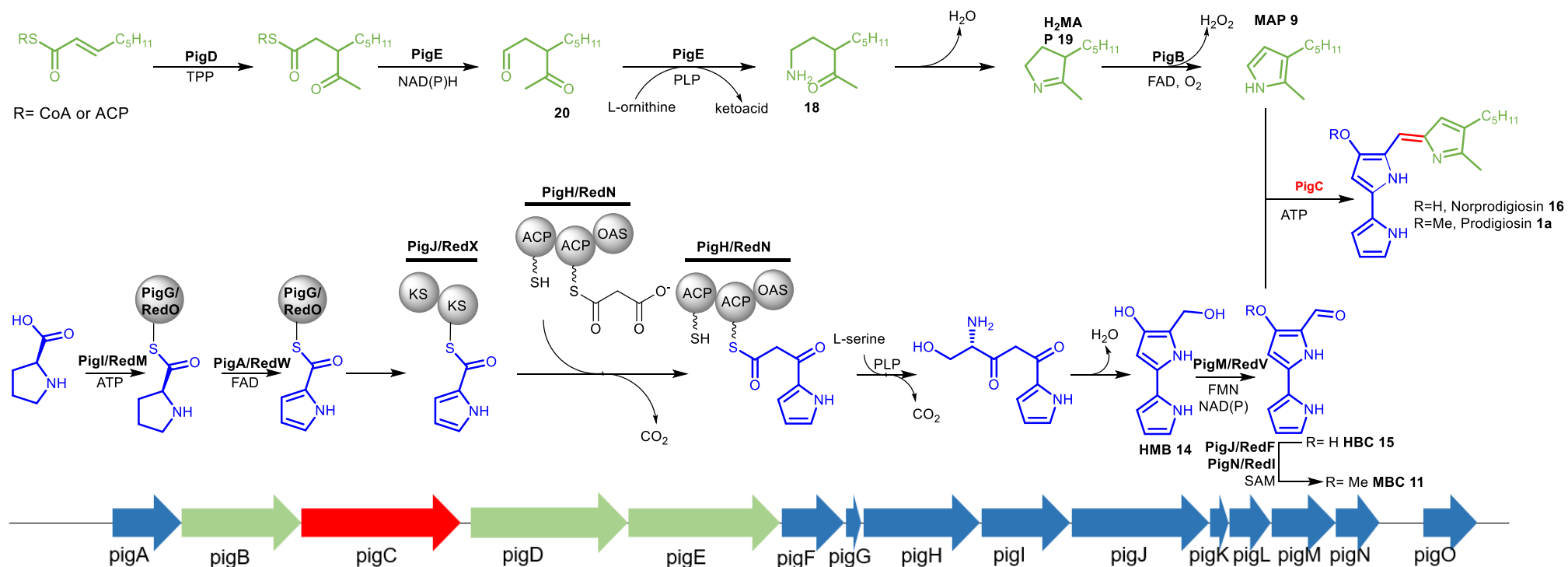


Figure 1.8: Prodigiosin biosynthesis in *S39006* Top: biosynthetic pathway; Bottom, biosynthetic gene cluster; in green: biosynthesis of monopyrrole MAP, in blue: biosynthesis of bi-pyrrole MBC, in red: condensation. KS: ketosynthase, ACP: acyl carrier protein, OAS: α -oxamine synthase; Pig enzymes are involved in the formation of prodigiosin 1a by *S39006*; Red enzymes are involved in the formation of undecylprodigiosin 2 by *S. coelicolor*

3.3. Biosynthesis of 2-undecylpyrrole **13**

As expected from genome analysis, the biosynthesis of 2-undecylpyrrole **13** is very different from that of MAP **9**.³⁸⁻⁴⁰ It appears that at least 6 genes are involved in the biosynthesis of this pyrrole unit (**Figure 1.10**). It has been proposed that the biosynthesis starts with the loading of a malonyl group on the ACP RedQ. The malonyl group would then undergo a decarboxylative condensation with acetyl-CoA, perhaps catalysed by the ketosynthase RedP.³⁸ The acetoacetyl-RedQ would then be reduced, probably by enzymes normally involved in the fatty acid biosynthesis as no genes encoding enzymes fulfilling these functions have been found in the cluster. The chain would then be elongated by translocation onto RedR followed by decarboxylative condensation with malonyl-RedQ, keto-reduction, dehydration and enoyl reduction four times, leading to dodecanoyl-RedQ. Thioesterase RedJ then releases dodecanoic acid **21**. Sequence analysis of the remaining enzymes, combined with LC-MS analysis of knock out mutants, suggested that the dodecanoic acid was then loaded on an ACP domain in RedL by the adjacent adenylation (A) domain. The ketosynthase (KS) domain could then catalyse the condensation of the malonyl group loaded on the next ACP domain with the dodecanoyl thioester, leading to the corresponding β -ketotetradecanoyl thioester. Finally, condensation of the thioester with glycine, catalysed by the PLP dependent α -oxoamine synthase (OAS) domain, would release an α -oxoamine, which could spontaneously cyclise and form 5-undecylpyrrolin-3-one **22**. The final reduction is believed to be catalysed by RedK, before dehydration leads to **13**.

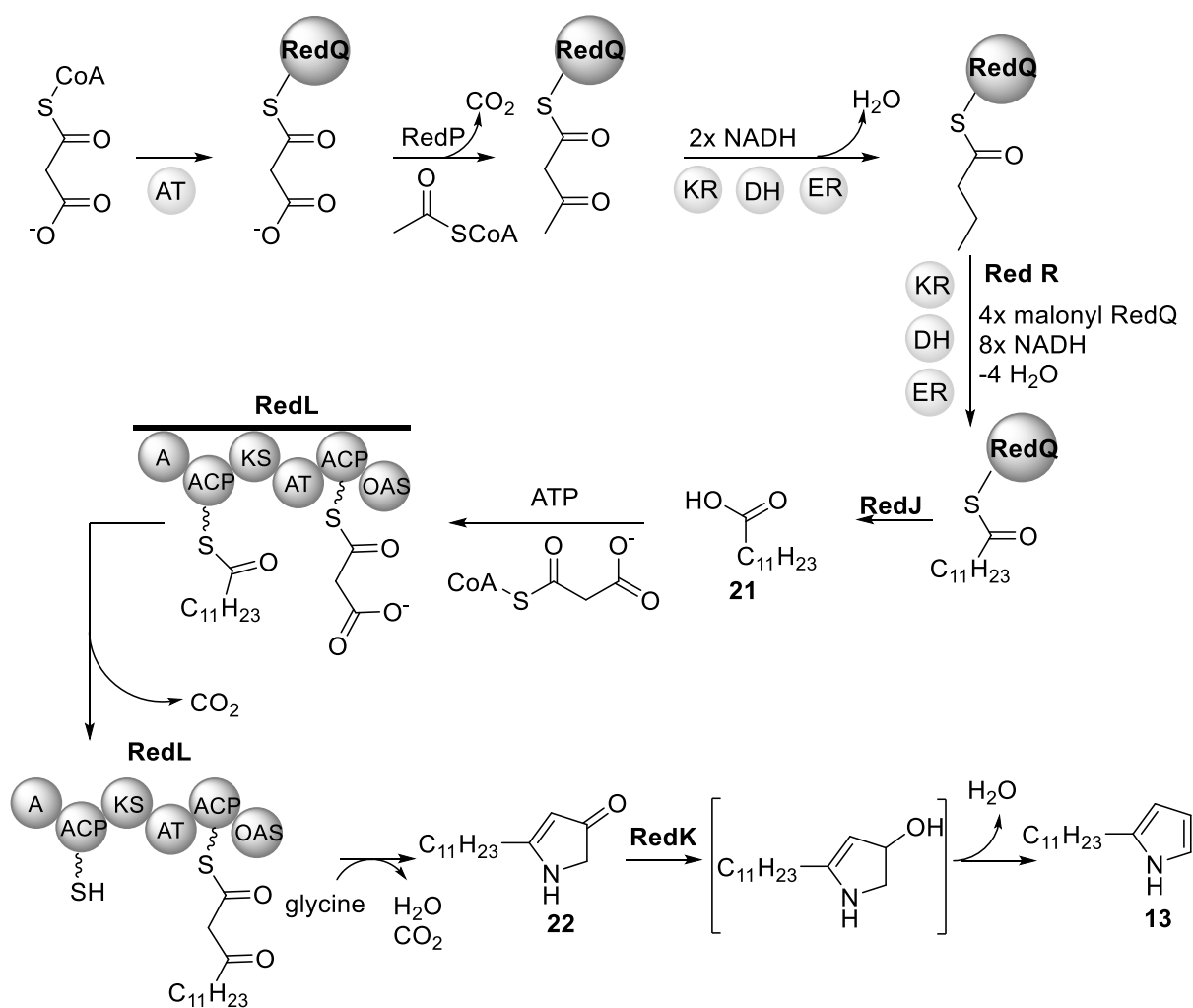


Figure 1.9: Proposed biosynthetic pathway of 2-undecylpyrrole

3.4. Condensation: PigC

Mutants of *S39006* with an in-frame deletion in *pigC* (*S39006 ΔpigC*) showed accumulation of both MBC and MAP. Furthermore, this strain was able to complement mutants with a knockout either in the MAP pathway or in the MBC pathway, indicating that ATP-dependent PigC was responsible for the condensation into the final pigment.²⁶ Interestingly, the reaction can occur spontaneously under acid catalysis, but the bacterial internal pH is not low enough for the reaction to occur uncatalyzed.⁴¹ Two regions of PigC have a strong homology with pyruvate phosphate di-kinase (PPDK): the N-terminal domain of PigC is similar to the ATP binding domain of PPDK, whilst the C-terminal domain of PigC is similar to the phosphoryl transfer domain.³² The central domain of PigC has no strong homology and is presumed to bind MBC and MAP and to catalyse the reaction, probably *via* the phosphorylation of the oxygen atom of MBC's aldehyde group, followed by nucleophilic attack by MAP and release of the phosphate. PigC has also displayed a remarkable substrate flexibility for MBC as well as for MAP units (see Chapter 2). In undecylprodigiosin biosynthesis, the condensation step is catalysed by PigC

homologue RedH.⁴² Interestingly, both PigC (see chapter 2) and RedH can accommodate variations of ring A of MBC, leading to analogues of prodigiosin and undecylprodigiosin.^{42,43}

3.5. Formation of cyclized prodiginines

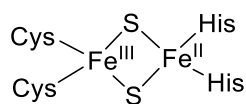


Figure 1.10: Rieske center

For group 2 prodiginines, cyclisation occurs after the condensation step.

For instance, in *S. coelicolor*, it has been shown that RedG (in purple in **Figure 1.7**) catalyses the conversion of undecylprodigiosin **2** to streptorubin B **3** (see **Figure 1.2b**). Similarly, in *S. longisporus*,

metacycloprodigiosin results from the action of McpG, a homologue of RedG on **2**.⁹ These enzymes have been shown to belong to the family of Rieske Non-Heme Iron-Dependent Oxygenases.⁹ This family of enzymes relies on sulphur-iron complexes (**Figure 1.10**) to oxidise a variety of functionality.⁴⁴

The formation of cycloprodigiosin **5** follow a similar mechanism: Keasling and co-workers showed that it resulted from an oxidative cyclisation of prodigiosin **1a** by the alkylglycerol monooxygenase-like enzyme PRUB680 in *P. rubra*. Yet, PRUB680 is different from the other enzymes catalysing the cyclisation of prodiginines as far as it is not a member of a Rieske oxygenase family. It is also noteworthy that this enzyme has no equivalent in *Serratias*' genomes which explain why cycloprodigiosin could not be observed in those prodigiosin producers.⁴⁵

Similarly, the formation of the macrocycle in group 4 prodiginines is still to be explained.

4. Related compounds

Comparison of prodiginine BGCs against all genomes shows some genes of these pathway have homologues in the BGC of a wide range of other secondary metabolites. For instance, *pigA*, *pigI* and *pigJ* have shown homology with genes in *Pseudomonas aeruginosa*'s *plt* cluster, which is involved in the formation of the monopyrrole pyoluterin.³⁰ Whilst this is noteworthy as the use of proline to produce pyrrole is relatively uncommon among γ -proteobacteria, those three gene represent only a small proportion of the cluster. Other natural products share a much stronger analogy with prodiginines.

4.1. Marineosin

Marineosins A (**23**) and B (**24**) (**Figure 1.10**), have been isolated and characterised by Fenical and coworkers⁴⁶ from marine actinomyces.

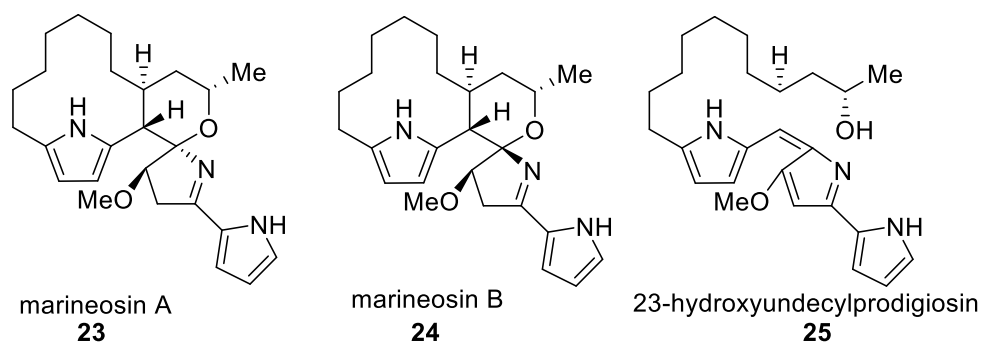


Figure 1.11: Structure of marineosins and their intermediate 23-hydroxyundecylprodigiosin

Despite having a structure much more complex than most prodiginines, it has been shown that their BGC (*mar*) is highly homologous with the *red* cluster, apart from an additional gene, *marA*.⁴⁷ Interestingly, knock-out of the *redG* homologue in the *mar* cluster led to the accumulation of a group I prodiginine, 23-hydroxyundecylprodigiosin **25**, which suggested those compounds derived from a biosynthetic pathway similar to undecylprodigiosin and that MarA performs a final reduction.

4.2. Roseophilin

Roseophilin **26** (Figure 1.12) was first isolated from *Streptomyces griseoviridis* in 1992⁴⁸ and its structure⁴⁹ and stereochemistry^{50,51} were fully elucidated a few years later. Even though it looks very prodiginine-like, its hydrocarbon side-chain is linked to the conjugated system by more C-C bonds than in any other prodiginine. In addition, ring B is a furan in the case of roseophilin, whereas it is a pyrrole in the prodiginines. Yet, the roseophilin BGC (*rph*) from *S. griseoviridis* shows a strong analogy with the *red* cluster.⁵² The similarity between the two pathways was confirmed when prodigiosin RI **27** was isolated from *S. griseoviridis*⁵²: it is believed that its precursor II'-dimethylundecylprodigiosin **28** plays a role in the formation of dechlororoseophilin **29**, which has been shown to be an intermediate in roseophilin biosynthesis.⁵³ Challis and co-workers proposed that after the formation of intermediate **30** through two oxidative cyclisations catalysed by a Reiske oxygenase-like enzyme, ring B could open *via* the deprotonation of the hydroxyl (**31**). After a prototropy, the oxygen could perform a nucleophilic attack on the imine (**32**). Loss of ammonia would then lead to the furan which is characteristic of roseophilins (Figure 1.12b).⁵⁴

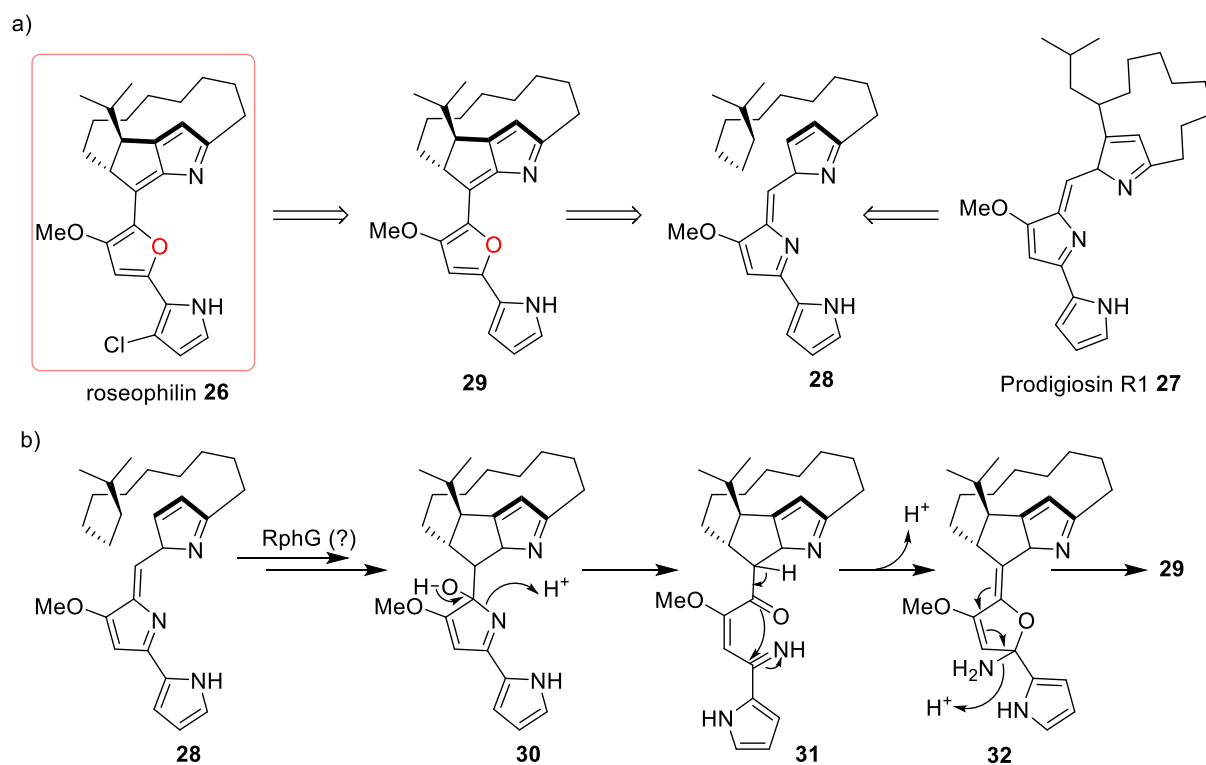


Figure 1.12: Roseophilin: a) structure and potential biosynthetic intermediates; b) proposed mechanism, adapted from Withall *et al.*⁵⁴

4.3. Tambjamines

Tambjamines (**Figure 1.12**) are a family of yellow secondary metabolites which shares the bipyrrrole moiety (rings A and B) of the prodiginines, but where the cycle C is replaced by a substituted imine. They were first isolated from marine invertebrates but in the last decade several compounds from this family have been isolated from soil and marine bacteria such as *Pseudomonas tunicata*. The BGC for tambjamine YPI **33** was elucidated by Burke *et al.*⁵⁵ and it seems the bipyrrrole structure results from a similar pathway to the one leading to the formation of MBC in a prodiginine biosynthesis. The analogy between the two pathways goes further: very recently, analysis of the cluster of cyclic tambjamine MYPI **34** showed the presence of a gene similar to *redG* which could play the same role in the final cyclisation of the molecule.⁵⁶

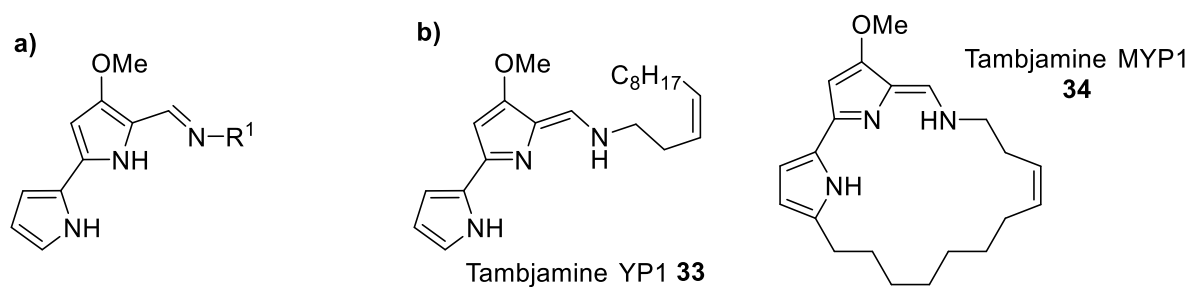


Figure 1.B: Tambjamins a) General structure, b) Examples

5. Biological properties of prodiginines

Interest in prodiginines has been renewed in the past 20 years as their biological activities and potential therapeutic applications were discovered. Some of these properties are described here along with proposed mechanisms of action.

5.1. Antimalarial

Papireddy *et al.*⁵⁷ conducted *in vitro* tests of prodigiosin along with three other natural prodiginines and a range of synthetic ones against the malaria parasite *P. falciparum* pansensitive D6. They concluded that they were all extremely potent with IC₅₀ value between 8 and 1.7 nM for the natural compounds and were more active than their reference drug, chloroquine. The best value was obtained with metacycloprodigiosin. This was consistent with the finding of Isaka *et al.*⁵⁸: they reported an IC₅₀ of 12 nM for metacycloprodigiosin against *P. falciparum*. Finally, Kim *et al.*⁵⁹ investigated cycloprodigiosin and reported a similar IC₅₀ value. These promising *in vitro* assays can be translated into animal models: prodigiosin has for instance been shown to effectively treat monkeys infected with malaria.⁶⁰ Castro also managed to double the survival time of mice infected by *Plasmodium berghei* by injecting them with 40 mg/kg of prodigiosin.⁶¹ This quantity was much lower than the toxicity threshold as no death due to toxicity seemed to appear before 160 mg/kg. Most studies, with the exception of Papireddy *et al.*,⁵⁷ reported no toxicity against mammalian cells at antimalarial dosage.^{58,59} Interestingly, structure-activity relationship (SAR) studies showed that ring C had little influence on the activity, which might explain why metacycloprodigiosin and cycloprodigiosin had similar IC₅₀ values.⁶² This also meant that tambjamins shared prodiginines' potential against malaria.⁶² In conclusion, these studies suggested that prodiginines seem an interesting lead in the fight against malaria. Interestingly, prodigiosin has recently been shown to be able to affect *Trypanosoma cruzi*, another protozoan.⁶³

5.2. Antifungal

Although less common than viral and bacterial infections, fungal infections are also an important risk both for human health – *Cryptococcus sp.* leads to 600,000 mortalities every year⁶⁴ – and the environment. The fungal disease aspergillosis is responsible for wiping out sea fan coral.⁶⁵ This highlights the importance and the urgency to find methods to prevent fungal propagation.

Prodigiosin has been shown to enhance fungicidal effect of other compounds.^{66–68} Moreover, *Sma* has been used by itself on several occasions to control fungal proliferation. It has also been shown that the supernatant from prodigiosin producing *Serratia sp.* had a growth inhibitory effect against *Pythium myriotylum*, *Rhizoctonia solani*, *Sclerotium rolfsii*, *Fusarium oxysporum* and oocycete *Phytophthora infestans*.⁶⁹

5.3. Anti-bacterial

Emergence of multi resistant strains makes the development of novel classes of antibiotic a priority. The activities of prodiginines, in particular prodigiosin **1a**, have been tested against a number of bacteria, both Gram-positive and Gram-negative.^{63,70–72} Prodigiosin showed growth inhibition against *Staphylococcus aureus*, *Enterococcus faecalis*, *Streptococcus pyogenes*⁷¹, *Salmonella typhimurium*, *E. coli*, *C. albicans* and *Bacillus subtilis*.⁷³ The activity of prodigiosin against oxacillin resistant *S. aureus*⁷¹ is noteworthy as those strains are a growing concern in health care facilities where they are responsible for many hospital infections.⁷² *Borrelia burgdorferi* is another strain of interest inhibited by prodigiosin. This strain, responsible for Lyme disease, is resistant to multiple antibiotics but is affected by prodigiosin both in its stationary phase and when it is actively growing.⁷⁴

Besides its growth inhibition capacity, prodigiosin is also able to induce programmed cell death in *Bacillus cereus*, *Pseudomonas aeruginosa*, *S. aureus* and *E. coli* and to reduce the motility of *B. cereus* and *E. coli*.⁷⁵

These studies tend to show that prodigiosin is able to affect both Gram-positive and Gram-negative bacteria, but some discrepancies are to be noted. For example, Lapenda *et al.* did not observe any effect on Gram-negative strains.⁷¹ Different mechanisms of actions have also been proposed: Stopar and co-workers⁷⁰ claimed that prodigiosin affected growth, cell division, protein and RNA synthesis and overall metabolic activity whilst cytoplasmic membrane and chromosomal DNA remained intact; whereas Suryawanshi *et al.*⁷⁶ suggested a chaotropic behaviour, with disruption of the plasma membrane and loss of essential metabolites responsible for the activity. In addition, it is possible that mechanisms of action of prodigiosin

on cancer cells (proton transport, DNA cleavage, see section 1.5) would also contribute to the antibacterial effect. It is worth noting that no information on the mechanism could be gathered from the analysis of a resistance gene as none has been found to date.

Recently, Klein *et al.* tested prodigiosin along with a range of group 3 prodiginines (See **Figure 1.1**) against *E. coli*, *B. subtilis*, *Corynebacterium glutamicum*, *Saccharomyces cerevisiae* and *Komagataella phaffii*. It appears that the size of the chain between the C2 and C3 position of the ring C has little influence on the antibacterial activity.⁷⁷ Interestingly none of the compounds showed activity against the producing organism, *P. putida*.

5.4. Immunosuppressive

As mentioned above, prodiginines, like most secondary metabolites were first screened for their antimicrobial activity. More recently, the interest shifted toward their immunosuppressive properties,⁷⁸ leading to promising results against some auto-immune diseases. This is of importance as the existing treatments, cyclosporin A, rapamycin or FK-506 are known for their toxicity and low efficacy.⁷⁸ Undecylprodigiosin **2** is probably the prodiginine which has been the most extensively investigated.⁷⁹⁻⁸² These studies revealed that, in mice, **2** was able to inhibit T cell proliferation⁸¹ without affecting antibody production⁸² or cell death. It appeared that **2** inhibits both Ca²⁺ dependent and Ca²⁺ independent mitogens, with a preference for cytotoxic T lymphocytes, hence preventing their proliferation. Interestingly, results about its effects on B lymphocytes were contradictory from one study to another: Tsuji *et al.*⁸¹ observed a selective inhibition of T-cells whereas Songia *et al.*⁷⁹ observed effects on B-cells. This could be of importance as B-cell lymphoma is a major side-effect in immunosuppressed patients treated with cyclosporin A. However, the toxicity observed in mice makes **2** a very unlikely drug candidate.⁷⁹

Cyclic prodiginines have also been investigated.⁸³⁻⁸⁵ Despite being slightly less potent than **2**, metacycloprodigiosin **3** showed a good specificity to inhibit T cell proliferation *in vitro*. A massive drawback was its severe toxicity *in vivo*.⁸⁵ Similarly, cycloprodigiosin **8** salts showed inhibition of murine T cell proliferation⁸³ and helped prevent graft rejection in rats.⁸⁴ However, it displayed important side effects in rats⁸⁴ and led to cell death at inhibition concentration,⁸³ which renders modifications necessary to make the compound druggable.

A few studies on prodigiosin **1a** have also been conducted.⁸⁶⁻⁸⁸ Han *et al.*⁸⁷ isolated prodigiosin from culture broth of *Sma B* and showed that it could inhibit the proliferation of T-cells efficiently at 30 nM *in vitro*, whereas cell death could not be induced at concentration lower than 100 nM. They also demonstrated a strong specificity: B-cell proliferation was not affected

at all by prodigiosin.⁸⁷ Prodigiosin inhibits interleukin 2R α receptor expression, which disturbs the interleukin 2 signalling pathway and prevents the proliferation of the cells.⁸⁸ These *in vitro* results were applied *in vivo*: prodigiosin showed promising results to delay the progression of autoimmune diabetes and collagen induced arthritis.⁸⁸ Moreover, it also has a positive effects against graft-versus-host disease and can enhance the effects of current drugs such as cyclosporin A.⁸⁶ Interestingly, and contrary to the other bacterial prodiginines, none of the studies reported toxicity against rats.

To overcome the limitation presented by natural prodiginines' toxicity at inhibition concentrations, a number of synthetic analogues were also screened for immunosuppressive effects.⁸⁹ It resulted in a lead compound, PNU 156804 **35** (Figure 1.14), which suppressed T cell activation as well as **2**, but with a decreased toxicity.⁹⁰ Further *in vivo* studies showed it was as efficient as the reference cyclosporin A to extend rats' lives after a heart transplant.⁹¹ Interestingly, **35** did not seem to affect the same target as prodigiosin but instead inhibited Janus kinase 3, a cytoplasmic tyrosine kinase associated with the γ chain of the interleukin 2 receptor.⁹¹ As of today, this molecule still seems to be the most promising candidate for an immunosuppressive drug with a prodiginine scaffold.

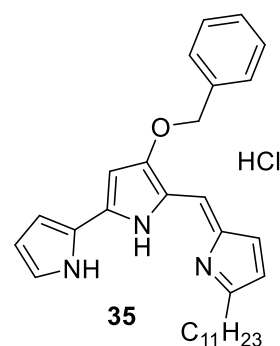


Figure 1.14: PNU 156804

5.5. Antitumour

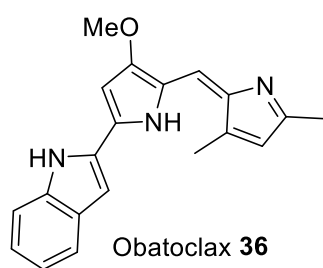


Figure 1.15: Structure of anticancer agent obatoclax

The potential of prodiginines in the fight against cancers has been widely explored. For instance, prodigiosin **1a** has been tested by the National Cancer Institute against more than 60 cell lines and showed an average inhibitory concentration (IC₅₀) of 2.1 μ M.⁹² **1a** gave particularly promising results against breast cancer⁹³ and neuroblastoma cell lines⁹⁴ and was potent enough to be tested a preclinical trial against pancreatic cancer.³² However, a number of other analogues have also been tested. Undecylprodigiosin **2** was effective against human breast carcinoma⁹⁵ whereas cycloprodigiosin **5** induced apoptosis in rat liver cancer.⁹⁶ Besides their activity against cancer cell lines, prodiginines do not seem to be toxic against noncancerous cells.^{78,97} Moreover, none of the multidrug resistance mechanisms examined up to now seem to affect prodiginines.^{96,98} Those interesting properties of prodiginines led to the development of obatoclax **36** (Figure 1.15), which was tested against multiple types of cancer. For instance, it has reached phase II against different blood cancer (leukemia⁹⁹ and lymphoma¹⁰⁰) and was in combination with other drugs against lung cancer.^{101,102}

Prodiginines seem to have several modes of action against cancer cells (**Figure 1.16**). They have been shown to prevent cell invasion and migration, which is key against metastasis. For instance, **1a** decreases the expression of RhoA, a GTPase regulating transduction pathways involved in cell adhesion and migration and inhibits matrix metalloproteinase-2, an enzyme playing a key role in invasion as it degrades extracellular matrix proteins.⁹⁸ More recently, Wang *et al.*⁹³ obtained very good results using **1a** and **36** to treat breast cancer: by acting on the Wnt/ β -catenin signalling pathway, the two prodiginines not only reduced the amount of migration but also triggered apoptosis. This could explain how **1a** and **5** increase the survival in pulmonary metastasis melanoma.⁹⁶ Prodiginines also can prevent proliferation by arresting the cell-cycle. This has been particularly well studied in the case of lymphocytes: T lymphocytes are blocked before entry into S phase but do not die. Treatment with prodigiosin leads to a decrease in known cell-cycle regulatory genes expression such as *cyclin A*, *cyclin D2*, *cyclin E*, *cdk2* and *cdk4*, leading to an arrest in mid-late G1.^{78,79,90} Yet, the predominant effect of prodiginines against cancer cells is the triggering of apoptosis. Li *et al.*¹⁰³ recently illustrated this phenomenon by showing that **1a** up-regulated the production of apoptosis related proteins such as Caspase 9 and Bax in human carcinoma and prostate cancer cell lines. The mechanisms leading to programmed cell death can be divided in three main categories.

5.5.1. Mitogen- activated Protein Kinases (MAPKs)

Studies have shown that prodigiosin could induce apoptosis both in a caspase dependent¹⁰³ and independent manner.¹⁰⁴ MAPKs control many physiological processes and are divided into three families: JNKs, p38 MAPKs and ERKs.⁷⁸ All three can be targeted by prodiginines. For instance, metacycloprodigiosin **4** activated a JNK, leading to the increase of an apoptotic signal.⁸⁵ Prodigiosin **1a** can target p38 MAPKs, but not JNKs.^{105,106} Phosphorylation of ERKs by prodigiosin has not been observed but prodigiosin-induced apoptosis can be prevented by adjusting this pathway.¹⁰⁷ Prodiginines can target other crucial cellular cascades. The Wnt/ β -catenin cascade⁹³ was mentioned above, but Hong *et al.*¹⁰⁸ also shown that prodigiosin could rescue p53 deficient cells by up-regulating p73. The diversity of cascades that prodiginines can affect could be related to their ability to inhibit the specificity of some tyrosine phosphatases.¹⁰⁹

5.5.2. pH regulation

It is essential that pH in cells and specialised organelles remains in an appropriate range. Changes in the intracellular pH can trigger apoptosis.¹¹⁰ Many examples of prodiginines disturbing this equilibrium have been reported.¹¹¹ Prodiginines can act as ionophores and help the symport of H⁺ and Cl⁻ across membranes. This leads to a decrease in pH without changing the membrane potential.¹¹² An indirect consequence of the relocalisation of H⁺ by prodiginines is an ATPase uncoupling effect, either in bacteria and mitochondria (F₀F₁-ATPases)¹¹¹ or in eukaryotes (V-ATPases).¹¹²⁻¹¹⁷ Structure-activity relationship on H⁺/Cl⁻ transport concluded that the presence of the three pyrroles rings^{118,119} as well as the alkyl chain on the C2 position of the C ring¹²⁰ are necessary to observe the activity. It is likely that this chain helps in getting the prodiginine into the membrane.

5.5.3. DNA cleavage

In the presence of copper, prodiginines are able to bind and cleave dsDNA.⁹² Melvin *et al.* studied extensively the interaction between prodigiosin and dsDNA and were able to show that prodigiosin intercalates in the minor groove via hydrogen bond, electrostatic and van der Waals contacts.¹²¹⁻¹²³ In terms of mechanism, prodigiosin binds in a 1:1 ratio to Cu(II) and gets into the dsDNA.¹²⁴ A Cu(I)-Cu(II) cycle then generates the H₂O₂ responsible for DNA cleavage.¹²² Even though DNA cleaving activity has been demonstrated, its influence on the cytotoxicity remains unclear. Indeed, dsDNA cleavage does not lead to anticancer activity with all prodiginines.¹²⁵ Yet, Cu concentration being higher in cancer cells than in healthy ones, this activity could explain why prodiginines have a stronger cytotoxic effect on cancer cells than healthy ones. Actual cleavage is not necessary to observe apoptotic activity. Indeed, prodigiosin has been shown to bind to DNA G-quadruplexes,¹²⁶ which can prevent telomerase from working efficiently. Studies on the effect of substituents on the C-ring on the DNA-binding effect showed that a methylation on the C4 position was not detrimental. In addition, when the C3 position was substituted with different esters and amino groups, a loss of activity was observed with amino groups whereas esters retained their activity. Yet, no clear relationship between the structure and the activity has been established.¹²⁷

5.5.4. Mitochondrial induced apoptosis

Mitochondria outer membrane permeabilization (MOMP) is a central event in apoptosis: apoptosis signals trigger a conformational change in proteins such as Bax which result in the formation of a channel in the mitochondrial membrane, leading to the release of cytochrome c in the cytosol.¹²⁸ Prodiginines can affect different aspects of this process. For instance, prodigiosin **1a** can trigger a conformational change in Bax.¹⁰³ In addition, obatoclax **36** has been

shown to antagonise several member of the B-cell lymphoma (BCL) protein family, such as BCL-2, BCL-X_L, BCL-W and MCL-1.¹²⁹⁻¹³¹ These proteins are found on the mitochondrial membrane and prevent MOMP.¹³²

It is difficult to establish which of these mechanisms is primarily responsible for the apoptosis. Location studies of prodiginine did not lead to an answer to that question: in some studies prodiginines have been shown to accumulate in the cell nucleus, which would suggest that the DNA cleavage is the predominant mechanism, while other reports claimed that it was most concentrated in the cytoplasm or in mitochondria membrane, which would indicate a prevalence of the pH deregulation and the MAPKs mechanisms.

In conclusion, prodiginines have shown anticancer properties against a variety of cell lines, whilst being relatively harmless for non-malignant cells at the same concentrations. Yet, effects vary from one prodiginine to another and from one cell line to another. Prodiginine have been shown to affect many biological targets and it is likely that a combination of all the mechanisms described above is responsible for the overall biological effect.

6. The role of thioester in biosynthesis

Thioesters are common intermediates in many biosynthetic pathways, including the one of prodigiosin. As this project was particularly focused on demonstrating the existence of thioester intermediate in the formation of MAP (see section 7 and Chapter 4), this section aims to give a few notions about the role of these compounds in biosynthesis.

Nature has used the fact that thioesters are less stabilised by resonance than their oxygen ester and carboxylic acid counterparts to drive reactions in many biosynthetic pathways. This is illustrated, for example, by the building of carbon-carbon bonds through Claisen condensation by the use of coenzyme A (CoA) acyl thioesters (**Figure 1.17**). This phenomenon plays a crucial role in terpene and steroid biosynthesis.

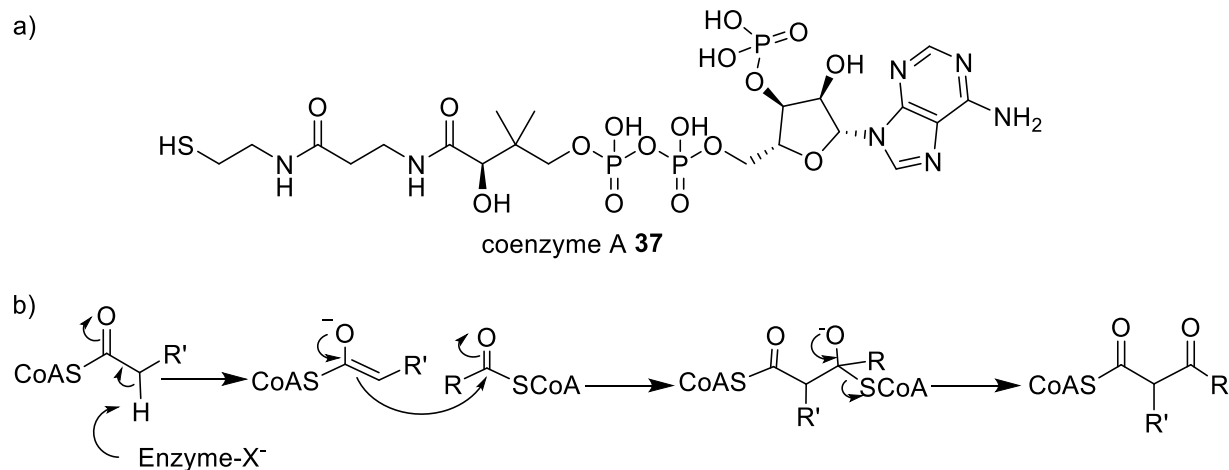


Figure 1.17: Coenzyme A a) structure; b) example of biosynthetic step where CoA is involved

Fatty acid and polyketide biosynthesis are further biological processes where thioesters play a crucial role (**Figure 4.2**). In the first step, the thiol of the 4-phosphopantetheine moiety of an acyl carrier protein (ACP) is charged with a malonyl unit, derived from malonyl CoA, and an active-site cysteine residue of the β -ketoacyl synthase is similarly charged with an acyl unit. The β -ketoacyl synthase then catalyses a decarboxylative Claisen condensation of the malonyl unit with the acyl unit, giving a β -keto-butanoyl ACP thioester. In fatty acid biosynthesis the ketone carbonyl is then reduced by action of NADPH. The (*E*)-unsaturated thioester obtained after dehydration can then undergo further reduction through NADPH, leading to the saturated thioester. This intermediate is then reloaded on the β -ketoacyl synthase active site cysteine residue ready for condensation with a further malonyl unit brought by the ACP.¹³³ The Claisen condensation, the ketone carbonyl reduction, the dehydration and the enol reduction are then repeated and the chain gains two carbons at every cycle. It is worth noting that octenoyl-ACP, the proposed precursor of MAP in the prodigiosin biosynthetic pathway, is formed by this process. The cycle ends when the chain reaches 14 to 18 carbons and a thioesterase hydrolyses the thioester of the acyl-ACP (see Section 1.1.3).

Polyketide biosynthesis involves the same steps as fatty acid biosynthesis except some of the reduction/dehydration steps are omitted, so that each two-carbon chain-extending unit can be left as the ketone or the alcohol or the C=C double bond instead of the fully reduced -CH₂-CH₂-

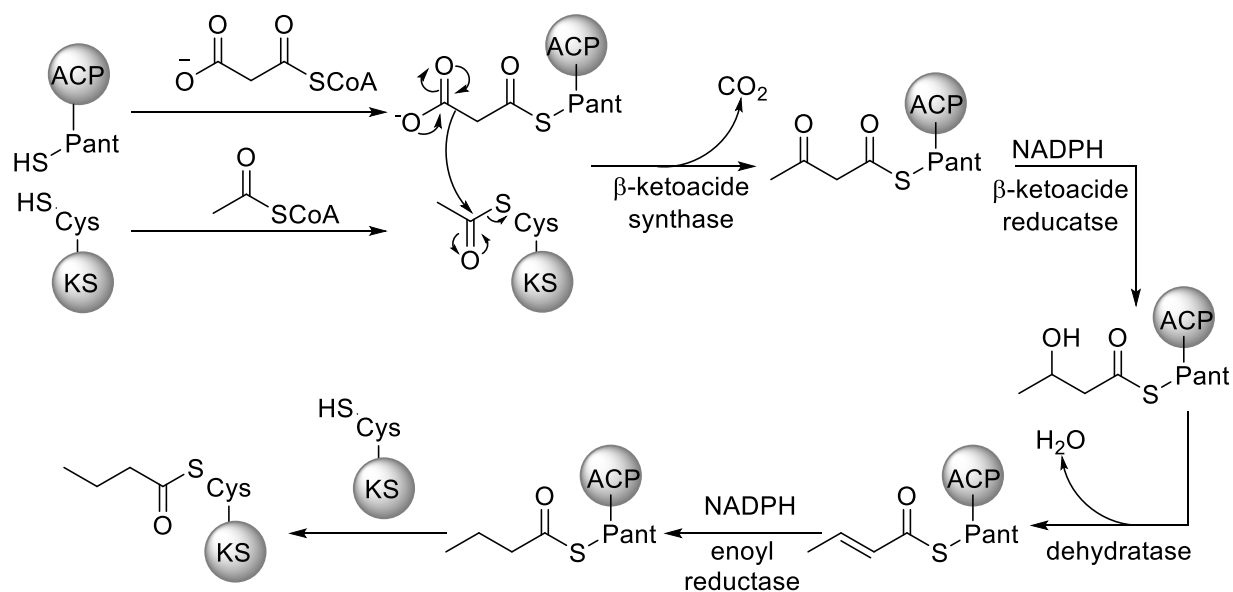


Figure 1.18: Fatty acids biosynthesis, pant= phosphopantothine

7. Aims of the project

This project aimed to study the three enzymes – PigD, PigE and PigB – involved in the formation of MAP. As mentioned earlier, these enzymes have been less extensively characterised than the ones involved in the formation of MBC and little is known about their substrate specificity, enantioselectivity, or kinetics.

Here, the substrate flexibility of PigB and its homologue HapB was investigated through protein- and cell-based assays with analogues of its natural substrate with various alkyl substituents. The substrate flexibility was then applied to the formation of novel prodiginines whose biological properties were then explored.

Out of the three enzymes, PigE is the one that has been characterised the least. In particular, its ability to reduce a thioester substrate to an aldehyde and then to catalyse the transamination of the aldehyde is still uncertain. This project aimed to use a cell-based assay to demonstrate the thioester reductase activity and protein assays to determine the cofactors involved and the kinetic parameters of PigE.

Finally, a demonstration of PigD's capacity to catalyse the acylation of α,β -unsaturated thioesters was attempted.

Chapter 2. Mutasynthesis of new prodiginines by exploiting the substrate flexibility of dihydropyrrole oxidase PigB

1. Objectives

Total synthesis is a powerful tool but also has many drawbacks. For instance, a high number of steps and the use of harsh conditions are not always compatible with large scale reactions. Mutasynthesis provides an alternative to this method. The technique relies on the ability of a strain unable to produce the natural product of interest, often because of a mutation in a gene coding for a protein responsible for the formation of a biosynthetic intermediate, to accept a synthetic intermediate later on in the biosynthetic pathway.¹³⁴ Furthermore, if the enzymes present some substrate flexibility, this can give access to analogues of the natural product with a minimum of synthetic steps.

Since Vogel's¹⁵ work, it is known that some *Serratia* mutants unable to produce prodigiosin can have their pigment production restored by adding an intermediate to the culture broth. Furthermore, some mutant strains can cross-complement, which means that one strain produces and releases an intermediate that the other strain can use to produce prodigiosin (and *vice versa* in some cases). As mentioned earlier, this property was exploited by Salmond and co-workers for the elucidation of the biosynthetic pathway to prodigiosin²⁶ as well as in their study of the substrate flexibility of the condensing enzyme PigC.⁴³ In the latter study, a *S39006* mutant with an in frame deletion in PigH was constructed, hence presenting a white phenotype as MBC could not be produced (see **Figure 1.9**).²⁶ This strain was fed with analogues of MBC having variations in ring A (**Figure 2.1b**). Considering the structure of anticancer agent obatoclax **36**, modifications in those positions had the potential to lead to biologically active compounds. New prodiginines were obtained with all analogues with only one ring. The enzyme was less flexible toward bigger structures, but the indole substrate was accommodated, leading to the formation of **36**.

Chapter 2: Mutasynthesis of new prodiginines by exploiting the substrate flexibility of dihydropyrrole oxidase PigB

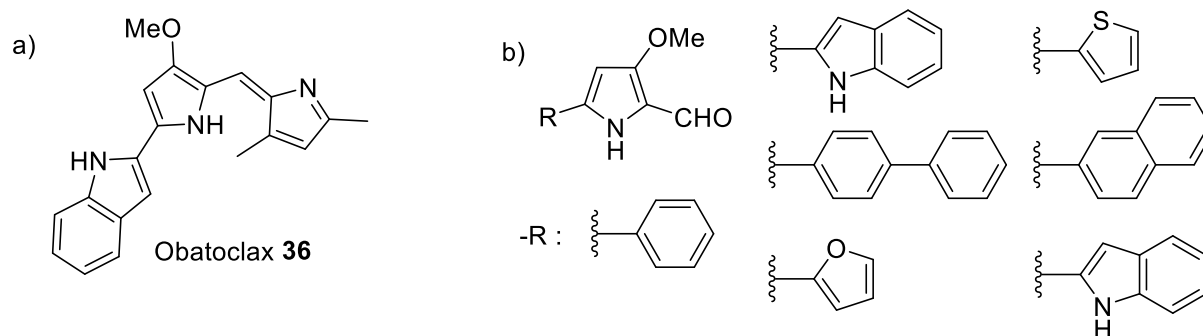


Figure 2.1: Modifications on prodiginosin ring A a) Obatoclax; b) MBC analogues; adapted from Chawrai *et al.*¹³⁵

Recently, the specificity of PigC for its other substrate, MAP, was explored by Klein *et al.*^{136,137} They worked on a *Pseudomonas putida* strain which had been engineered to heterologously express the *Sma pig* gene cluster and constructed a strain with an in frame deletion in *pigD* (*P. putida* Δ *pigD*), the first enzyme involved in MAP biosynthesis (see **Figure 1.9**). After showing that this strain could still produce MBC,¹³⁶ they investigated the flexibility of PigC for analogues of MAP with different alkyl chains on the C2 and C3 positions (**Figure 2.2b**). It appeared that modifications in the C3 position were well accommodated whereas the size of the chain on the C2 position could not be changed without a loss of activity. It is worth noticing they obtained most of the precursors, including MAP **9**, using the Trofimov reaction. This reaction leads to the formation of disubstituted pyrroles from an oxime precursor, meaning that MAP and its analogues could be obtained in a one-pot two-step reaction from the appropriate ketone (**Figure 2.2a**).¹³⁸ However, analogues with hydrogen in either C2 or C3 position could not be obtained this way and the use of hydroxylamine limits the range of the substituents. In addition, regioselectivity problems are observed with unsymmetrical ketones when R¹ is larger than a methyl group. Despite these limitations, Klein *et al.*⁷⁷ managed to use this method to prepare analogues of MAP with rings of five to twelve carbons between the C2 and the C3 positions (**Figure 2.2c**). They were all accommodated by PigC and led to the formation of group 3 prodiginines in just two synthetic steps and one fermentation step with *P. putida*. This method was more efficient than classic isolation and shorter than total synthesis of the compounds, but limitations remain: isolation and purification of the prodiginosin from the culture broth can be difficult and the yields are often lower than chemical synthesis.

Chapter 2: Mutasynthesis of new prodiginines by exploiting the substrate flexibility of dihydropyrrole oxidase PigB

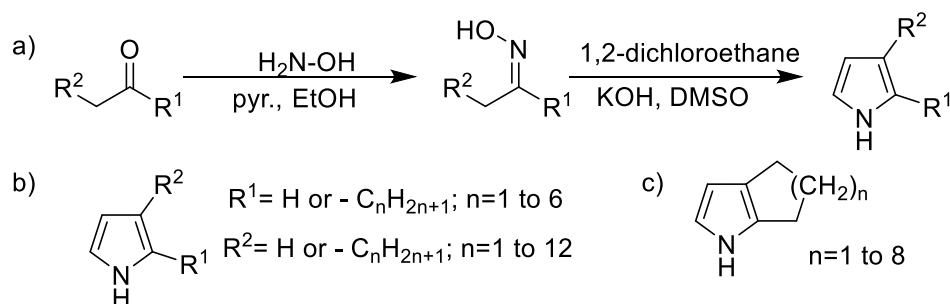


Figure 2.2: Analogues of MAP tested by Klein *et al.* a) Trofimov synthesis of pyrroles; b) analogues with alkyl substituents; c) bi-cyclic analogues of MAP

This project aimed to prepare prodiginines by feeding analogues of **19a** into a *S39006* mutant. To do so, it intended to extend previous work in the group that had identified which regioisomer of H₂MAP is the substrate for PigB. The substrate flexibility and the enantioselectivity of PigB and its homologue HapB were also to be investigated. In addition, the synthesis of new analogues of **19** was explored.

2. Elucidation of the structure of PigB's substrate

As mentioned in Chapter 1, Williamson *et al.*²⁶ showed that PigB and its homologues were responsible for the last step in MAP **9** biosynthesis (see **Figure 1.9**). However, they were not able to determine which of the two possible regioisomers (**Figure 2.3**, compound **19a** and **38**) was the natural substrate.

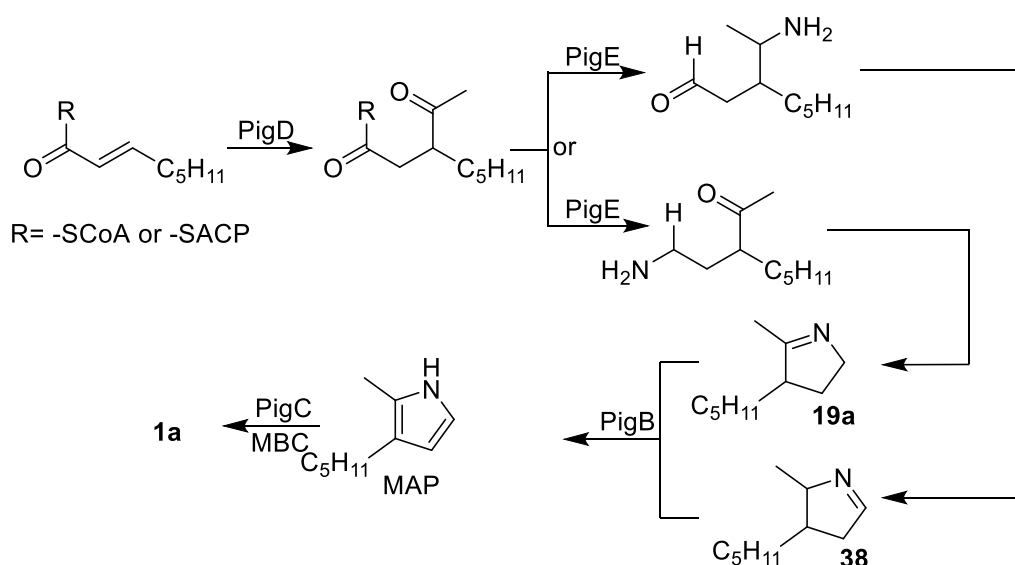


Figure 2.3: Formation of two possible substrates for PigB

Chawrai subsequently synthesised both **19a** and **38** and showed that only **19a** could be taken in as a substrate by a mutant of *S39006* with an in-frame deletion in *pigD* (*S39006 ΔpigD*) (Figure 2.4a).¹³⁹

In the course of this project, bacterial H₂MAP was analysed to corroborate this finding: extracts were prepared from a 200 ml culture of *S39006* with an in-frame mutation in *pigB* (*S39006 ΔpigB*) and its LC-MS chromatogram was compared to one of synthetic **19a** (Figure 2.4 b).

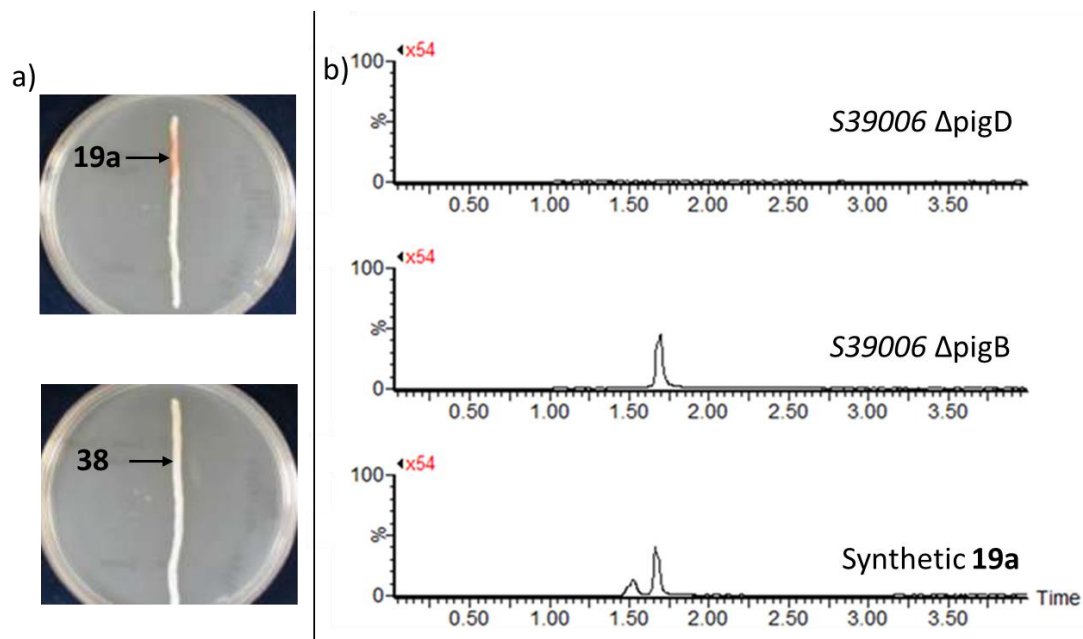


Figure 2.4: Study of PigB regioselectivity a) top: *S39006 ΔpigD* + **19a**, bottom *S39006 ΔpigD* + **38**; b) Extracted chromatograms at 154.16 (**19a** + H⁺), top to bottom: *S39006 ΔpigD* extract, *S39006 ΔpigB* extract, synthetic **19a**

A small peak at 1.50 min was noticed in the chromatogram of the synthetic sample. The experiment was repeated several times at different concentrations, but two peaks were always obtained. The NMR spectrum of the sample though showed a good purity. It is possible that this second peak is due to one of the enamines in equilibrium with **19a** (see Figure 2.5). Because the LC-MS experiment was conducted in a mixture water/acetonitrile, these products can be more stable than in the CDCl₃ used for NMR analysis.

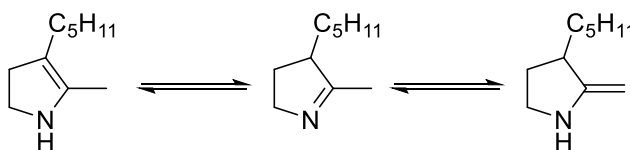


Figure 2.5: Imine/enamine equilibrium of 19a

The chromatograms showed the accumulation of an intermediate in *S39006 ΔpigB* with a mass consistent with H₂MAP and with the same retention time as synthetic **19a**. As expected, no such peak was seen with *S39006 ΔpigD*. This is consistent with Chawrai's results and confirms that **19a** is the natural substrate of PigB.

3. Synthesis of novel analogues of H₂MAP

3.1. Modifications in the C2 and the C3 position

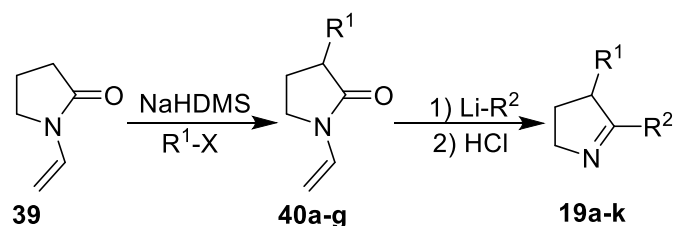


Figure 2.6: Synthesis of H₂MAP analogues with modification on the C2 and C3 positions

In Chawrai's work, H₂MAP **19a** was obtained in two steps from N-vinyl-pyrrolidinone **39** (Figure 2.6). After formation of the enolate of **39** by treatment with NaHDMS, it was alkylated with 1-iodopentane at low temperature, giving intermediate **40a**. MeLi was then added to attack the carbonyl, and, after a couple of hours, the mixture was acidified, triggering deprotection of the amine and dehydration (Figure 2.7).¹³⁹

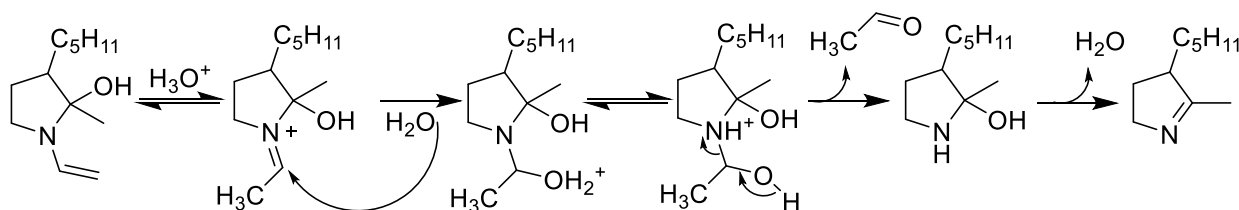


Figure 2.7: Mechanism of acid-catalysed deprotection of the vinyl amine.

A similar method could be used to get analogues with modifications either on the C3 or C2 positions (Table 2.1). For modifications on the C3 position, another halogenoalkane than 1-iodopentane could be used in the first step (compounds **19b-g**). These six analogues of H₂MAP were previously made by Hiral Bhalara in the group²⁰ but were all resynthesized in the current work. Similarly, other organolithium

Compound	R ¹	R ²	Yield (%)
19a	C ₅ H	Me	58
19b	Et	Me	52
19c	Pr	Me	42
19d	Ally	Me	45
19e	C ₆ H	Me	47
19f	C ₇ H	Me	47
19g	<i>i</i> Pr	Me	47
19h	C ₅ H	Et	20
19i	C ₅ H	Pr	7.5
19j	C ₅ H	C ₄ H	25
19k	C ₅ H	Ph	55

compounds were used in the second step to change the

Table 2.1: Analogues of H₂MAP

substituent in the C2 position (compounds **19h-k**). For 2-propyl-dihydroMAP **19i**, propyl-lithium (which is not commercially available) was generated *in situ* by addition of an excess of *t*-BuLi to 1-iodopropane at -80°C followed by stirring at room temperature in Et_2O . This allowed the consumption of *t*-BuLi through a deprotonation of the solvent, leading to the formation of isobutane, ethylene and lithium ethoxide,¹⁴⁰ hence avoiding side reactions. Indeed, despite being less nucleophilic than other organolithium reagents, *t*-BuLi is a strong base and a reducing agent, which led to side products. The drawback of this approach is the loss of some of the newly formed propyl-lithium, decreasing the yield. An excess of **19a** was then added and the reaction could proceed as for commercial alkyl lithiums, leading to the isolation of the desired H₂MAP analogue.

Another issue with this procedure is the formation of side products during the first step. For instance, 3,3-dipentyl-N-vinylpyrrolidin-2-one **41** (see **Figure 2.8**) could be isolated from the reaction mixture during the preparation of **40a**. Yet, such double addition products could be easily separated by column chromatography with an eluent of low polarity.

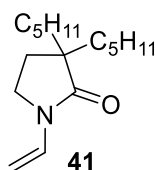


Figure 2. 8: An example of by-product obtained during the synthesis of analogues of 19a

Even though this synthetic route is compatible with a number of different alkyl substituent, it suffers important scope limitations. For instance, hindered organolithium reagents are poor nucleophiles and may reduce **40** instead of nucleophilically attacking it. Furthermore, addition of an aromatic moiety on the C3 position would generally not be possible as S_N2 reactions do not work on aryl halides, preventing the formation of compounds like 3-phenyl-N-vinylpyrrolidin-2-one with this method. However, activated aromatic rings can undergo a S_NAr. Thus, the enolate of **39** successfully reacted with 2-bromopyridine. The analytical data of the resulting product were consistent with the formation of the adduct. However, minor peaks were visible in the NMR spectrum, suggesting that the presence of the aromatic ring β to the carbonyl stabilised the enol tautomer **42** enough that it represents 20% of the mixture. The exchange between the two tautomers (**Figure 2.9**) could explain why the proton next to the aromatic ring was not visible in the NMR spectrum. MeLi was added to the compound in a similar fashion as for the synthesis of **19a-h**, but no reaction was observed. It is likely that the proton next to the

carbonyl is more acidic than in **40a-g**, and MeLi here behaved as a base instead of a nucleophile. However, time did not permit any options to circumvent this to be explored.

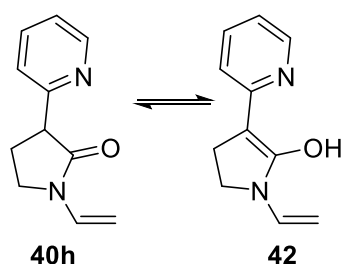


Figure 2.9: Putting an aromatic ring in the C3 position of H₂MAP analogues a) enol equilibrium of **103h**; b) A possible way to circumvent and get the wanted enamine

3.2. Preliminary study of modifications of the substituent on the C4 position

These analogues could be interesting to study the enantioselectivity of PigB regarding the C4 position. These analogues can theoretically be obtained by adapting the method described above with variations on the starting material. Furthermore, the nitrogen atom can be protected by any protecting group stable in basic conditions and labile in acid. As such compounds are not necessary commercially available, a small scale “proof of concept” synthesis of the Boc-protected lactam with a 4-ethyl group **43** was attempted (Figure 2.10)

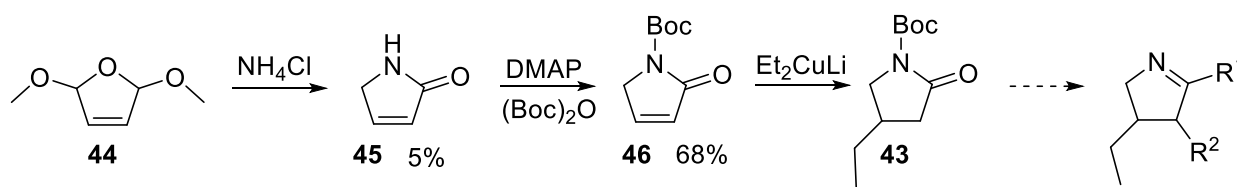


Figure 2.10: Synthetic route toward analogues of H₂MAP with substituents on the C4 position

Oxidation of pyrrole with hydrogen peroxide in the presence of barium carbonate¹⁴¹ was carried out as a first attempt to prepare 1,5-dihydro-2H-pyrrol-2-one **45**, but after several hours at reflux no reaction was observed. Amide **45** was finally prepared *via* the conversion of 2,5-dimethoxy-2,5-dihydrofuran **44** in the presence of ammonium chloride.¹⁴² Even though the yield of that step was very low, enough of **45** was isolated so the Boc protection could be performed, giving **46**. This was then treated with diethyl copper lithium. Monitoring the reaction by TLC showed the appearance of a number of new spots. ¹H NMR analysis of the crude mixture was consistent with the formation of **43**, but it was only a minor component and the scale was too small to isolate the desired product. This process would require optimisation, in particular for the first step, but

it presents an interesting way to prepare precursors of H₂MAP analogues with substituents on three positions of the pyrrole.

3.3. Toward a general methodology

The methods described above suffer strong limitations on the substituents as they need to be compatible with the final organolithium addition, hence preventing the incorporation of most electrophilic or acidic groups.

A route (**Figure 2.II**) overcoming these limitations was investigated.

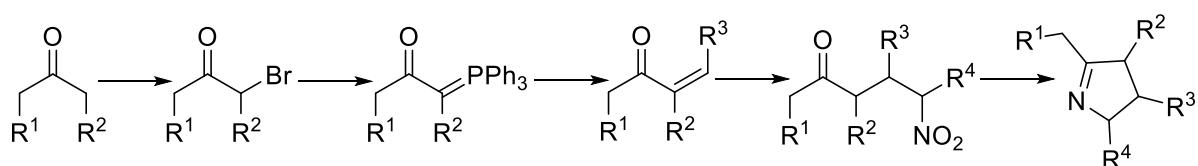


Figure 2.II: Synthetic route giving analogues of H₂MAP with substituents on all four positions

This synthesis would also give the possibility to change the substituents on all four positions of the ring. This would allow a larger understanding of PigB, but only compounds where R⁴ is a hydrogen atom could be converted to a prodiginine.

As illustrated in **Figure 2.12a**, 2-octanone **47** was chosen as the starting material as it would allow us to get the same C2 and C3 substituents as in H₂MAP. Numerous procedures for α-bromination of carbonyls using N-bromosuccinimide (NBS) can be found in the literature.^{143,144} An acid catalyst activates the carbonyl, leading to the formation of an enol, which then quickly attacks NBS. The problem with most of the procedures is a lack of regioselectivity as they are usually performed on symmetrical ketones. Hence a few conditions were attempted (**Table 2.2**). This is particularly relevant because the polarities of the two regioisomers are very close, making separation by flash column chromatography too difficult.

Solvent	Catalyst	Temperature	Time	Selectivity (1-bromo:3-bromo)	Yield (% reacted carbonyl)
CHCl ₃	pTSA	0 °C then r.t.	16 h	3:4	70%
CCl ₄	NH ₄ OAc	80 °C	1 h	1:3	53%
CHCl ₃	NH ₄ OAc	80 °C	16 h	1:9	27%

Table 2.2: Conditions for α-bromination of ketones

It appeared that the best regioselectivity was obtained with NH₄OAc as a catalyst and chloroform as a solvent, but this was accompanied with an important decrease in the yield. This could be due to ammonium acetate being a weaker acid than pTSA, leading to a slower activation

of the carbonyl. As a result, the formation of the enol was under thermodynamic control, leading to the desired regioselectivity, but the yield was decreased. Considering the importance of the regioselectivity for the rest of the route and the fact that the starting materials can be recovered and are cheap, the third set of conditions was preferred. Yet, about 10% of the product was still 1-bromooctanone **48b**, which reacts faster than the 3-bromooctanone **48a** for downstream reactions, leading to the formation of unwanted products such as phosphorane **49b**. Fortunately, this kinetic property could be used to remove this regioisomer: the crude product was reacted for 2 h with dimethyl malonate **50** and potassium carbonate at 60 °C. In these conditions, the malonate addition only occurs on the 1-bromooctanone, leading to the formation of **51** and pure 3-bromooctanone, which could be recovered by flash column chromatography.

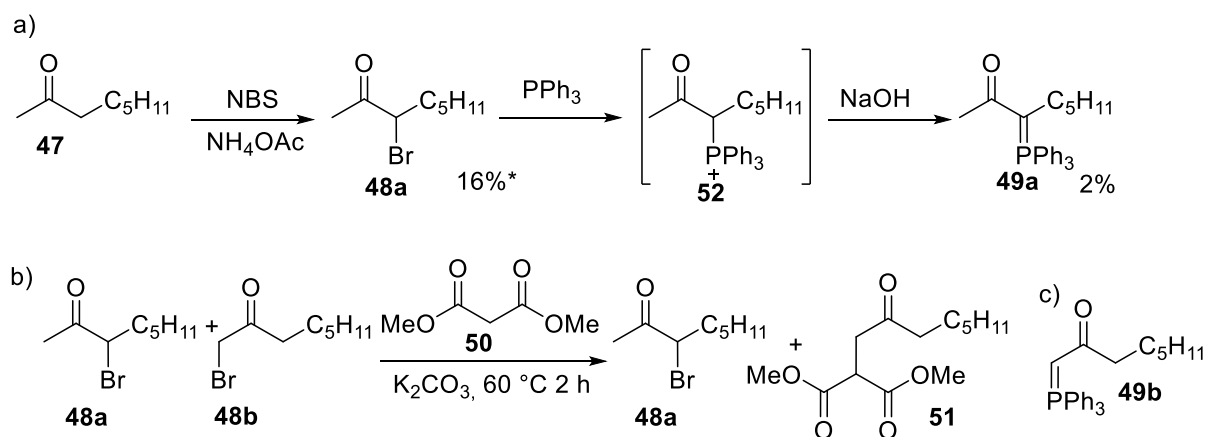


Figure 2.12: Initial steps in the general methodology a) Conversion of 2-octanone **47** into phosphorane **49a**; *the yield for the first step represents the conversion in **48a** and **48b**; b) kinetic resolution of regioisomers of **48**; c) phosphorane obtained by reacting **48b** with PPh₃

48a was reacted with triphenylphosphine to form the phosphonium salt **52**. The precipitate was collected and placed in basic conditions. The resulting ylid **49a** was stabilized by the presence of the carbonyl and could hence be isolated. The yield of this reaction sequence was very low, probably partly because the phosphine oxidised very readily and, despite our best attempts, a lot of it did not participate the reaction. The pentyl chain might also make the phosphonium salt more soluble in toluene and EtOAc than anticipated and a lot of it may have been lost during the washing of the salt.

Before trying to scale up or to screen for different conditions, the Wittig reaction was attempted with another stabilized ylid **53** (Figure 2.13).

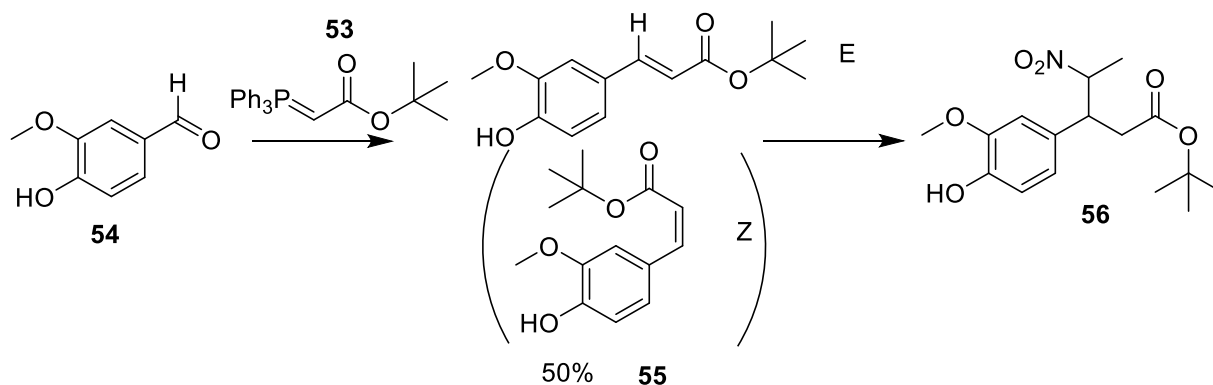


Figure 2.13: Preliminary study for Wittig reaction and Michael addition of a nitroalkane

Vanillin **54** was chosen as the substrate for the reaction because as it is more reactive than a ketone. After 16 h at r.t. in THF, a mixture 3:1 of E and Z isomers ((E)-**55** and (Z)-**55**) was obtained. The two isomers were separated by column chromatography, allowing the testing of the addition of nitroethane on a pure sample of (E)-**55**. The (E)-**55** was stirred with nitroethane and DBU in acetonitrile at r.t. and the reaction was monitored by TLC. After 24 h a new spot was visible under UV, but the starting materials were still predominant in the reaction mixture. After an acidic wash to remove DBU, an NMR of the crude confirmed that (E)-**55** was still the main component of the mixture, but 10% of the mixture was consistent with **56**. More work needs to be done to improve the reaction rate (changing the concentrations, the temperature, the reaction time or the base) before going forward with this reaction.

4. *In vitro* characterisation of PigB homologue, HapB

4.1. Comparison between HapB and PigB

As explained in Chapter 1, proteins fulfilling the same function in prodiginosin biosynthesis in different organisms share a high level of homology. Here, direct comparison using Artemis ACT¹⁴⁵ and EBI's Clustal Omega¹⁴⁶ between PigB and its homologue in *H2396*, HapB, indicated that the two proteins share 41% identity. BLAST analysis showed they both presented a strong homology with flavin-dependent amine oxidases. This was supported by Phyre¹⁴⁷ analysis of HapB (Figure 2.14): the structure of the protein could be modelled based on its homology with the FAD dependent lysine specific histone demethylase 1b (LSD1).¹⁴⁸ This result was in agreement with the role Williamson *et al.*²⁶ attributed to the protein. Furthermore, HapB and PigB presented a high degree of identity in residues 53-65 of HapB (166-178 of PigB), which are predicted to be the FAD binding site (in orange in Figure 2.14). Two other regions (residues 266-307 and 528-544 of HapB) are also highly conserved, which could mean they form part of the active site (in red in Figure 2.14). Interestingly though, alignment with LSD1 showed that

Chapter 2: Mutasynthesis of new prodiginines by exploiting the substrate flexibility of dihydropyrrole oxidase PigB

only one of the residues aligned with amino acids involved in the catalytic pocket of LSDI is found in these regions (in blue in **Figure 2.14**). This could be explained by a difference of function between the two proteins and by the fact that LSDI has extra domains that form part of the active site.¹⁴⁸ A major difference between HapB and PigB is to be noted though: the first 113 residues of PigB have no equivalent in HapB. They are predicted to be a transmembrane domain. A protein homologous to this transmembrane domain is found in *Hahella*'s genome (gene *HCH_06023*), located at the 5' end of *hapB*.

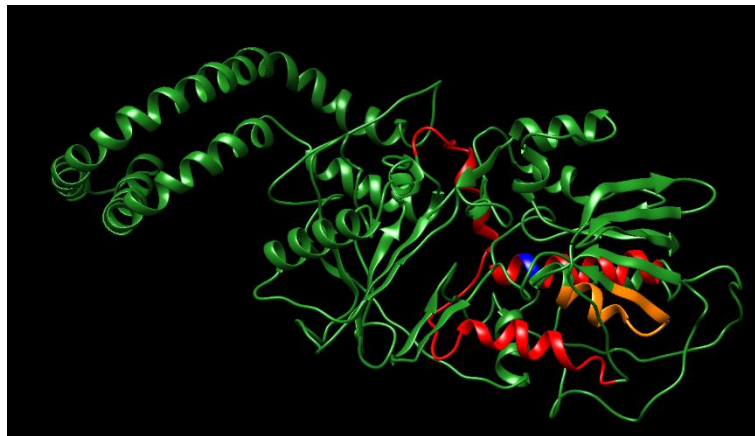


Figure 2.14: Predicted structure of HapB (Phyre) orange: predicted FAD binding site; red: other highly conserved regions, blue: catalytic residue from LSDI.

Bhalara expressed both *hapB* (plasmid pHDB1) and *pigB* (plasmid pHDB4) in *S39006 ΔpigB* and pigmentation was observed in both cases (**Figure 2.15a**), suggesting both proteins could catalyse the oxidation of H₂MAP into MAP. The expression of the two genes could be induced with IPTG.²⁰

Chapter 2: Mutasynthesis of new prodiginines by exploiting the substrate flexibility of dihydropyrrole oxidase PigB

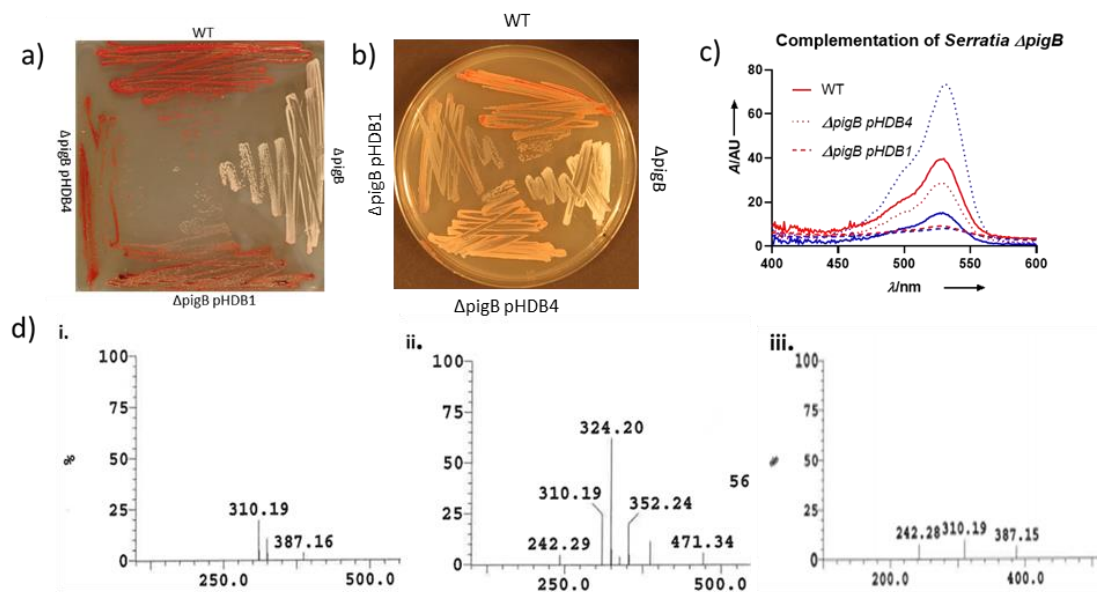


Figure 2.15: Comparison of HapB and PigB activity a) growth on PGM, b) growth on LB, c) UV spectra of prodigiosin culture extracts; Red: No IPTG, Blue: IPTG (1 mM), d) MS analysis of the prodigiosin extracts (i) S39006, (ii) S39006 $\Delta pigB$ pHDB4, (iii) S39006 $\Delta pigB$ pHDB1; Norprodigiosin I_6+H^+ : 310.19; Prodigiosin I_a+H^+ : 324.21. For a) and b), the labels are on the pictures

We noticed that the colonies with the plasmids presented a more purple aspect than the red wild type when cultured on LB (**Figure 2.15b**). Therefore, in the current work, we decided to check that the pigment obtained with the complemented strains was authentic prodigiosin. Prodigiosin extracts were prepared from liquid cultures of S39006, S39006 $\Delta pigB$ pHDB1 and S39006 $\Delta pigB$ pHDB4, with and without IPTG induction. UV spectra of the extracts were measured (**Figure 2.15c**) and they were also analysed by MS (**Figure 2.15d**).

All six extracts had the same UV profile, indicating that the pigments in the samples were similar. Pigment production in S39006 $\Delta pigB$ pHDB4 was significantly enhanced by adding IPTG: without IPTG, the pigment level was slightly below the WT, whereas with IPTG it was more than twice as much. This suggests a by-pass of the regulatory mechanism of pigment production in that strain. On the other hand, the production of pigment in S39006 $\Delta pigB$ pHDB1 was low and unaffected by the presence of IPTG. Several explanations are possible for this phenomenon: HapB is a heterogeneous protein, and hence may not interact properly with S39006's proteins. It also might have solubility issues and overexpression could lead to the formation of inactive inclusion bodies. Finally, HapB activity might be lower in those circumstances because of the absence of the transmembrane domain corresponding to the N terminal domain of PigB. MS results showed the extracts contained mixtures of prodigiosin and norprodigiosin. Norprodigiosin results from the same biosynthetic pathway but instead of using MBC, PigC catalyses the condensation of MAP with HBC, the preceding intermediate which

lacks the O-methyl group. This confirmed that both PigB and HapB catalysed the oxidation of H₂MAP into MAP. This means that characterisation results obtained for one are likely to be similar for the other.

4.2. Substrate flexibility of HapB

Bhalara isolated soluble HapB but, probably because of the transmembrane domain mentioned above, active PigB could not be purified. She then characterized its kinetic parameters *in vitro* (Figure 2.16b), using an Ehrlich's assay: pyrroles with a free α -position quantitatively react with p-dimethylaminobenzaldehyde 57, also known as Ehrlich's reagent to form a red complex 58 (Figure 2.16a). She also demonstrated this enzyme was FAD and O₂ dependent and produced H₂O₂ as a by-product.²⁰

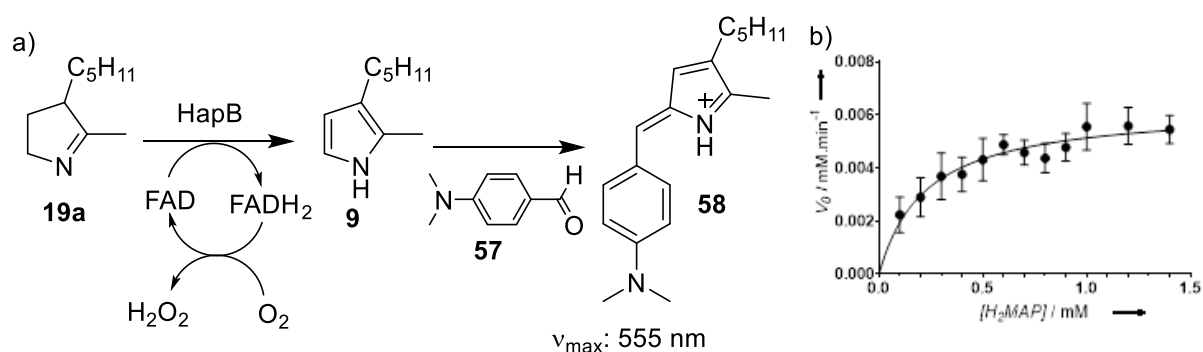


Figure 2.16: a) Principle of the Ehrlich's assay used to measure the activity of HapB b) Michaelis-Menten curve of HapB (work performed by Dr Bhalara)

As changing the alkyl chains on the C2 and C3 positions has little influence on the Ehrlich's assay, it can be used to assess the specificity of HapB for analogues 19b-k. HapB was incubated with each of the ten potential substrates for 15 min before stopping the reaction and assessing the presence of pyrrole. The assays with modification in the C3 (compound 19b-g, Figure 2.17a) position were performed by Bhalara¹⁴⁹ whereas modifications in the C2 position (compounds 19 h-k, Figure 2.17b) were assessed in this study.

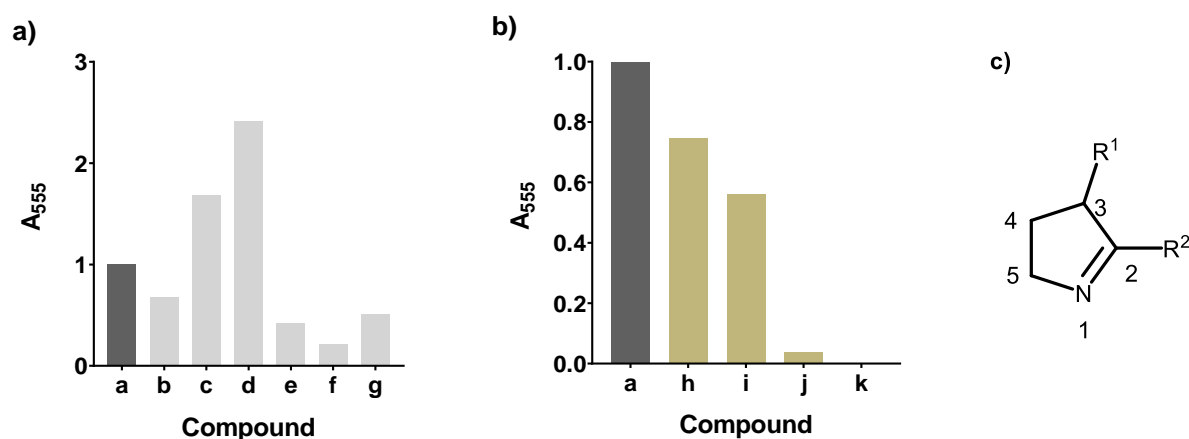


Figure 2.17: Results of Ehrlich's assays with H₂MAP and analogues 19a-k. a) modifications in the C3 position (performed by Dr Bhalara), b) modifications in the C2 position. Each absorbance value is normalised with respect to the absorbance obtained in the parallel experiment with H₂MAP 19a. c) Positions on H₂MAP analogues

It appeared that all modifications in the C3 position could be accommodated. Chains up to three carbons could be accommodated in the C2 position, but longer chain length lead to very little if any pyrrole formation.

5. Mutasynthesis

5.1. Qualitative results of complementation assay

Growing *S39006* on low phosphate media has been shown to enhance prodigiosin production.¹⁵⁰ Hence, two streaks of *S39006* Δ *pigD* were grown on peptone glycerol agar (**Figure 2.18a**). Next to the streaks, 5 μ l of H₂MAP and analogues at 0, 10 or 100 mM in DMSO were spotted. The bacteria were incubated for a further 16 h and the presence of pigment was assessed (**Figure 2.18b**). As expected, H₂MAP led to strong pigmentation as did all analogues with modification on the C3 position. High concentrations of **19h** and **19i** gave some pigmentation, even though it remained very faint with the latter. Other modifications on the C2 position gave no observable pigment. These results, which are testing the substrate flexibilities of both PigB and PigC were in good agreement with the *in vitro* results obtained with HapB. This suggests that PigB and HapB have similar substrate specificities.

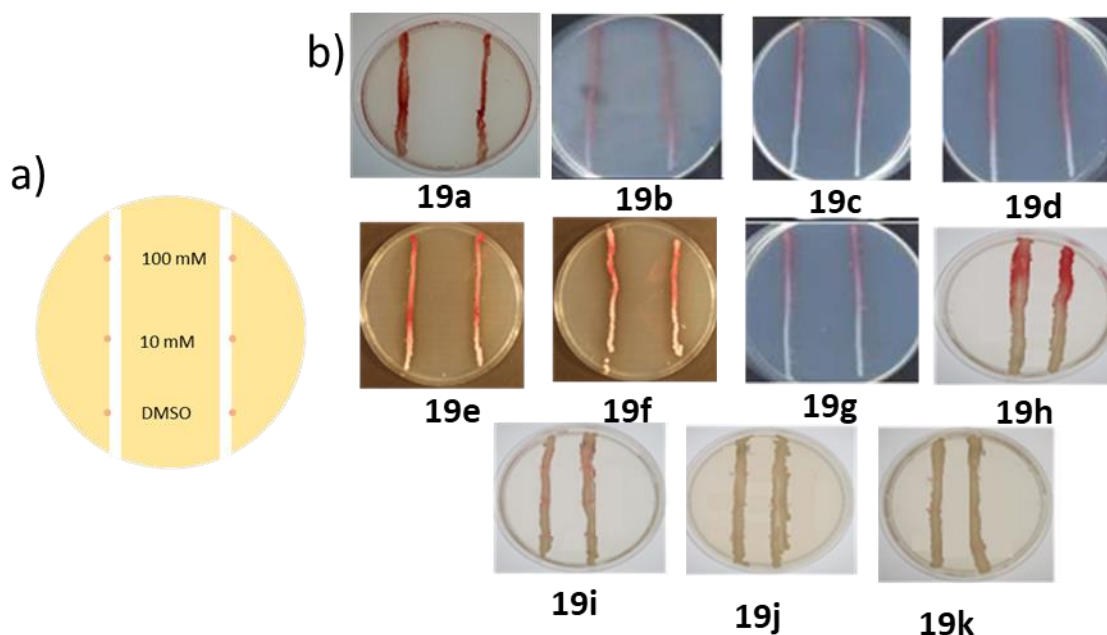


Figure 2.18: Chemical complementation assays on agar plates a) scheme of the plate; b) Results with H₂MAP analogues. Assays with compounds **19b**, **19c**, **19d** and **19g** were performed by Bhalara.²⁰

5.2. Quantitative results

Pigment production by bacteria in liquid culture can be quantified by centrifuging the cells and extracting the pigment from the cell-pellet by vortexing in acidified (4% HCl) EtOH and, after further centrifugation, measuring the quantity of prodigiosin by recording the absorbance at 535 nm (see **Figure 2.15**).¹⁵⁰

Strains with in-frame deletions in *pigD* and *pigE* are both potential candidates for the mutasynthesis experiments. Hence a complementation assay was performed by feeding H₂MAP to strains *S39006* Δ *pigD* and *S39006* Δ *pigE*. The quantity of prodigiosin recovered is presented in **Figure 2.19**.

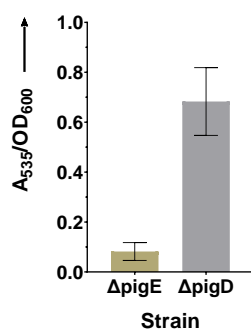


Figure 2.19: Complementation assay of *S39006* Δ *pigD* and *S39006* Δ *pigE* with H₂MAP

It appeared that complementing *S39006 ΔpigD* led to a higher pigmentation than complementing with *S39006 ΔpigE*. These results were consistent with qualitative observations: when complemented on agar, the red colour appeared in a matter of minutes with *S39006 ΔpigD* whereas hours were necessary in the case of *S39006 ΔpigE*. There is no clear explanation for this phenomenon, but it is possible that PigE and PigB form a complex and that the absence of PigE decreases the activity of PigB.

A range of H₂MAP concentrations were also tested with *S39006 ΔpigD*, leading to **Figure 2.20**.

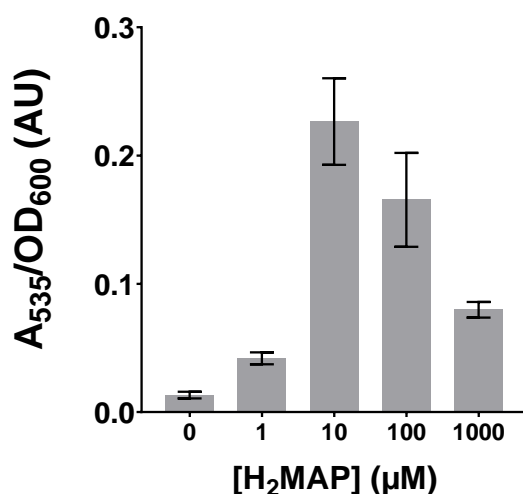


Figure 2.20: Complementation assay of *S39006 ΔpigD* with a range of concentrations of H₂MAP.

Restoration of pigmentation could be observed for concentrations of H₂MAP as low as 1 μM. Yet the highest pigmentation we observed was with 10 μM. Interestingly, increasing the concentration further led to a decrease of the final pigmentation. This is consistent with the inhibition of PigC in presence of excess MAP observed by Chawrai *et al.*¹³⁵

Following these two experiments, it was decided to conduct the *in vivo* flexibility assays of PigB with *S39006 ΔpigD* at 10 μM of substrate. Using the same process as previously, pigment was extracted from *S39006 ΔpigD* fed with the four analogues of H₂MAP with a modification on the C2 position and the five with a modification on the C3 position. Because of equipment limitation, five distinct experiments had to be performed to cover all the substrates. Variations from one experiment to another were compensated by normalising the results to the reading obtained with the positive control H₂MAP for each experiment. As the final compounds only differ in their alkyl chain, it was assumed that the λ_{max} of the prodiginine was not significantly affected by the change in the structure. Furthermore, once the culture reached a certain optical density, ethanolic extracts of uncomplemented *S39006 ΔpigD* were visibly coloured, leading to

background absorbance at 535 nm. This was probably due to the production of carotenes or other such compounds so the value of prodigiosin absorbance was corrected by subtracting the baseline (see experimental). The results are shown in **Figure 2.21**.

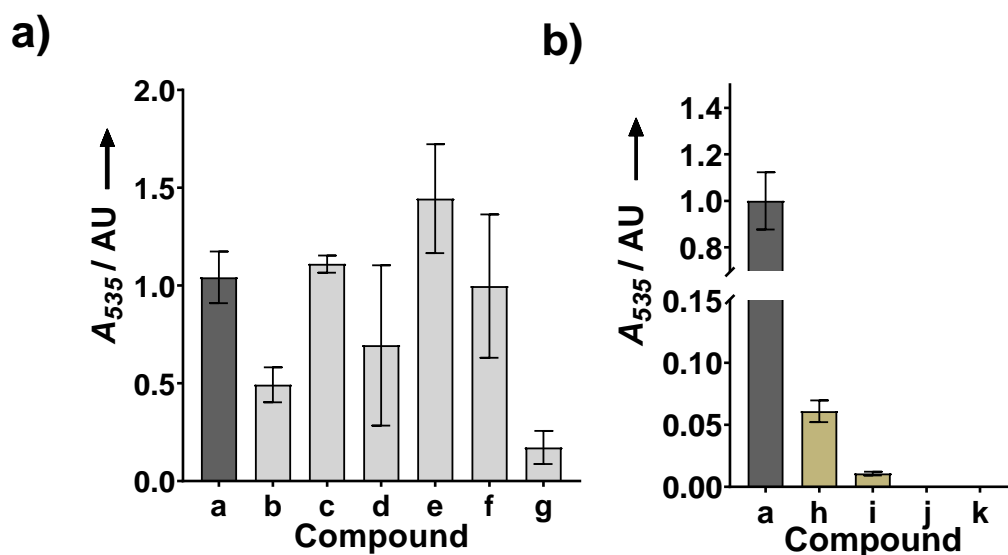


Figure 2.21: Complementation of *S39006* $\Delta pigD$ with H_2MAP and its analogues a) Analogues with modification on the C3 position; b) Analogues with a modification on the C2 position

The results were congruent with the *in vitro* experiments and the qualitative tests. Pigments could be recovered with all analogues with a modification in the C3 position whereas only chains up to 3 carbons on the C2 positions led to pigmentation. Furthermore, the pigmentation obtained with the latter two compounds (**19h** and **19j**) was much weaker than with natural substrate.

The fact that **19g-i** gave lower than expected pigmentation, considering their *in vitro* results, can be explained by compatibility issues with PigC. Indeed, to get to the final pigment, the substrate needs to be accommodated both by PigB and PigC. As mentioned earlier, it has been shown that modifications in the C2 positions led to a significant decrease in PigC activity.¹³⁷ Similarly, it is likely that **9g**, with an isopropyl chain on the C3, cannot be accommodated well by the condensing enzyme.

This experiment also demonstrated the possibility of using analogues of H_2MAP for mutasynthesis of new prodiginines (compounds **1b-i**), whereas all mutasynthesis methodologies to date have relied on analogues of the PigC substrates. This is particularly important as, to the best of our knowledge, **1g** is the first example of a group I prodiginine with a branched side chain on ring C.

6. Enantioselectivity of PigB

PigD has been shown to favour the formation of the S product.³⁶ However, the asymmetric centre introduced by PigD is adjacent to an imine bond in H₂MAP. Hence, it may racemise through an imine/enamine equilibrium (**Figure 2.22**).

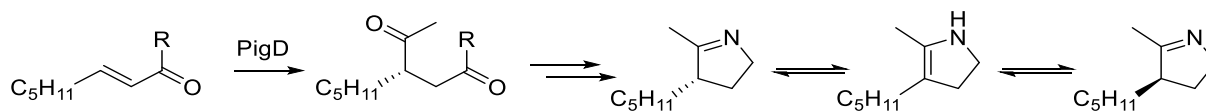


Figure 2.22: Racemisation of H₂MAP

The question of the enantioselectivity of PigB is only relevant if the rate of racemisation of H₂MAP is slower than the enzymatic reaction. When in solution in deuterated water, H₂MAP would incorporate deuterium as a result of the imine-enamine equilibrium, and this can be monitored by NMR spectroscopy. This experiment was run at pH 4 with a phosphate buffer and at pH 7 in pure D₂O. The main difficulty with the experiment was the low solubility of H₂MAP in water, leading to poor sensitivity compared to spectra recorded in CDCl₃ as well as shifting of most of the peaks compared to reference spectra. The proton of interest was associated with the peak at 2.8 ppm and the integral of this peak was monitored. In parallel, the integral of the peak at 3.5 ppm, associated with the protons of the CH₂ next to the nitrogen, and the signals due to the protons of the methyl group at 2.0 ppm were also monitored. The peak at 3.5 ppm was not expected to change during the experiments and hence its integral was set as for two protons in all spectra, whereas protons corresponding to the peak at 2.0 ppm may also be involved in an imine/enamine equilibrium (**Figure 2.23**) and thus the integral of this peak might decrease.

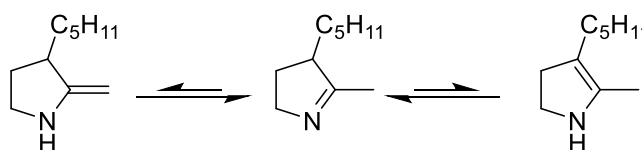


Figure 2.23: Two possible imine/enamine equilibria

Surprisingly, the peak at 2.8 ppm did not seem to change in the course of the experiments, whereas the one at 2.0 ppm showed a slight decrease. It is interesting to note that similar results were obtained at both pH values (**Figure 2.24**). This result was supported by the comparison of spectra acquired 24 h apart: H₂MAP was dissolved in D₂O along with a few drops of d₆-DMSO to help the solubilisation and spectra were recorded just after dissolution and 24 h later. Again, the experiments were conducted at pH 4 and 7. In both cases, the peak at 2.0 ppm underwent a large decrease whereas the 2.8 ppm area was barely affected (**Figure 2.25**). It can be concluded

that H₂MAP was indeed in slow equilibrium with an enamine form. However, this equilibrium does not affect the asymmetric carbon, probably for steric reasons, and racemisation of an H₂MAP solution is not a problem. The enantioselectivity of PigB was hence investigated.

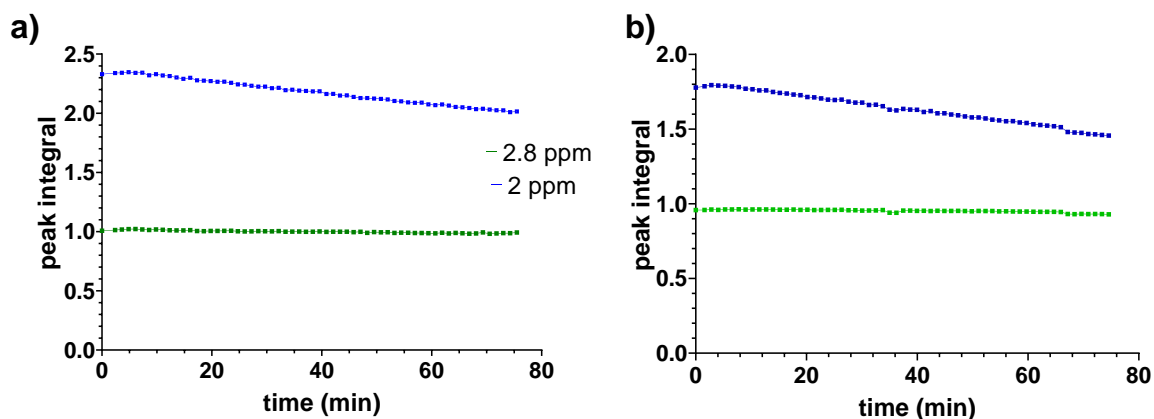


Figure 2.24: evolution of the NMR signal of the protons involved in imine/enamine equilibrium a) pH=4, b) pH=7; Green: 2.8 ppm, Blue 2 ppm

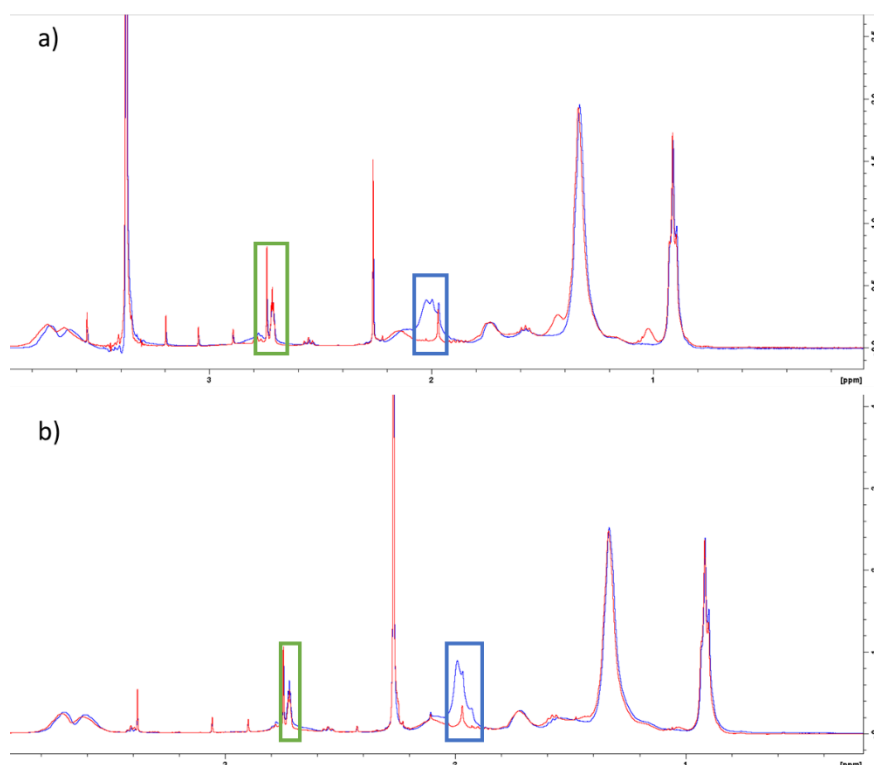


Figure 2.25: Evolution of the NMR spectra of H₂MAP in D₂O over 24 h, a) pH=4, b) pH=7; in blue: t=0, in red t=24 h, square in blue peak corresponding to the proton of the methyl group, squared in green: peak corresponding to the proton of the stereocenter

H₂MAP does not have any chromophore. However, an absorbance maximum can be observed at 275 nm. This is presumably due to a $n \rightarrow \pi^*$ transition – promotion of one of the non-bonding (lone pair) electrons on the nitrogen to the π^* orbital. Contrary to most UV absorbances which

are due to $\pi \rightarrow \pi^*$ transitions, this $n \rightarrow \pi^*$ transition is formally forbidden by quantum mechanics, and hence the absorbance is weak. A relatively high concentration of H₂MAP is therefore necessary to observe it (Figure 2.26).

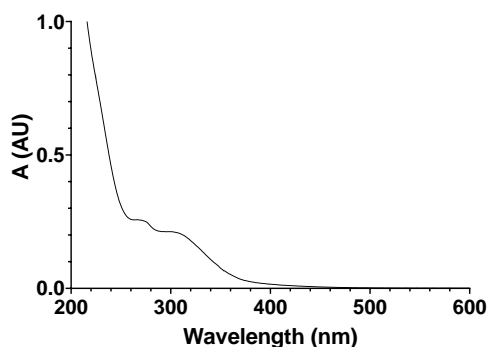


Figure 2.26: UV spectrum of H₂MAP at 100 mM in MeOH

The synthesis of H₂MAP, as described in section 3, leads to a racemic mixture. The isolation of each enantiomer by HPLC was attempted with a Supleco Analytical Chiral column. As illustrated in Figure 2.27, two peaks (retention time: 5 min 50 s and 6 min 45 s) were visible at 210 nm and 275 nm, but the first one looked weaker at 275 nm. A TLC of the collected fraction showed that the first contained a product with the same R_f as H₂MAP whereas the second one looked empty. This suggested that the second peak was actually an impurity: a mixture of only isopropanol and hexane was run on the HPLC in the same conditions and this peak was still present, indicating that those conditions were not suitable to separate H₂MAP enantiomers. Consequently, the polarity of the eluent in the HPLC method was decreased, but the two peaks were only shifted: the impurity was still there whereas the enantiomers of H₂MAP still coeluted. It was concluded that the available column was impractical for the separation of H₂MAP enantiomers. However, even if conditions to separate the two enantiomers by HPLC had been found, the UV absorption of H₂MAP is very weak and the quantity of H₂MAP that can be extracted from *S39006* Δ *pigB* is very low, so detection of the compound by HPLC would have been very challenging.

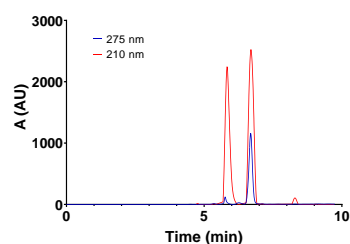


Figure 2.27: HPLC trace of synthetic run on a chiral column

This led to the investigation of a method to enhance H₂MAP detectability by addition of a chiral chromophore (**Figure 2.28**). This should also facilitate the analysis as the diastereoisomers thus obtained should have different retention times on an achiral HPLC column.

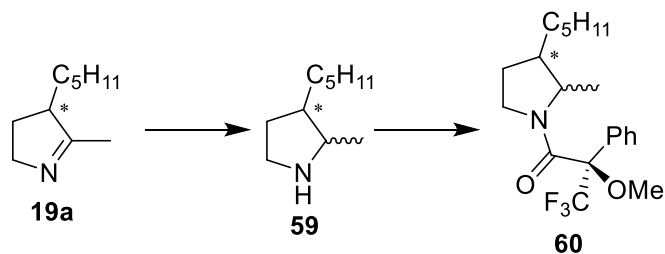


Figure 2.28: Enhancement of H₂MAP detectability

A diastereoselective reduction of the imine would be preferable for the first step because it would lead to only one pair of diastereoisomers after the second step. First a hydrogenation catalysed by palladium-on-charcoal was tried. H₂MAP in EtOH was stirred with fresh Pd/C under H₂ at room temperature. Unfortunately, after 4 days, no formation of the product was observed.

As a consequence, other approaches were investigated. For instance, the use of DIBAL as a reducing agent was investigated: a test reaction with 2 eq. of DIBAL at -10 °C for 15 min produced a mixture of the desired amine and starting material. Purification of the amine by silica chromatography was impossible as a 2D TLC showed that **59** degraded on silica. However, the difference of pK_a between the amine and the imine could be exploited to purify **59** by extraction with a solution of adapted pH (8-9). ¹H NMR analysis of **59** showed a characteristic doublet at 1.15 ppm (see experimental and appendix), but a smaller doublet at 0.99 (ratio 5:1) ppm. In the ¹³C spectra as well, a set of small peaks were observed alongside the main peaks. This indicated the presence of two diastereomers, but, surprisingly, they were not formed in a 1:1 ratio. It is likely that steric hindrance of the pentyl group favours attack from the opposite face, leading to the *cis* isomer (R,R and S,S) preferentially. Test reactions with a large excess of DIBAL and different reaction times were conducted (**Table 2.3**) in the prospect of using it on a biological extract where an excess of DIBAL would compensate for remaining traces of water and where the actual quantity of H₂MAP would be hard to estimate.

Time	Conversion (% amine)
30 min	70%
45 min	75%
1 hrs	100%

Table 2.3: Stirring time with an excess of DIBAL

As illustrated in **Table 2.3**, this resulted in an improvement of the conversion. Interestingly, the ratio *cis/trans* also remained similar from one experiment to another.

Unfortunately, removing the water from biological extracts can be challenging and is likely to lead to some loss of H₂MAP as it is volatile. Furthermore, variability between one bottle of DIBAL and another was observed. NaBH₄ could provide a viable alternative, especially because it can be used in a MeOH/H₂O solvent system.¹⁵¹ Some diastereoselectivity was observed with NaBH₄, but the ratio between the *cis* and *trans* isomers suffered a lack of repeatability, probably because NaBH₄ is less sterically hindered than DIBAL. In addition, changes in the chemical shift of the methyl doublet in the ¹H NMR spectrum were observed from one experiment to another. In conclusion, these approaches were promising and led to the formation of enough **59** to investigate the amine coupling, but they require optimisation.

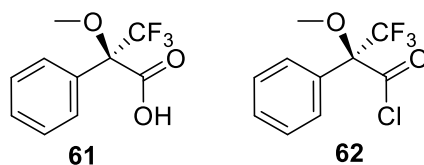


Figure 2. 29: Mosher's acid and the equivalent acyl chloride

Amide coupling with Mosher's acid was then investigated. Activation of (R)-Mosher's acid **61** (**Figure 2.29**) with EDC and DMAP prior to the addition of **59** was tried but without success. Instead, activation of the carboxylic acid by formation of the acyl chloride **62** was investigated.¹⁵² Excess thionyl chloride could be removed under reduced pressure and the amine dissolved in DCM could then be added. It was observed that a poor yield was obtained when the initial activation was only performed for two hours. Therefore, the reaction between Mosher's acid and thionyl chloride was investigated using NMR spectroscopy. In the proton NMR spectrum, the hydrogen of the methoxy group underwent a shift from 3.57 to 3.77 ppm whereas in the ¹⁹F NMR spectrum the CF₃ peak is shifted from -71.77 to -70.68 ppm. An NMR tube was charged with 0.4 ml CDCl₃, 0.3 ml SOCl₂ and 17 mg (R)-Mosher's acid and heated at 80°C. Spectra were recorded over an 18 h period, leading to **Figure 2.30**.

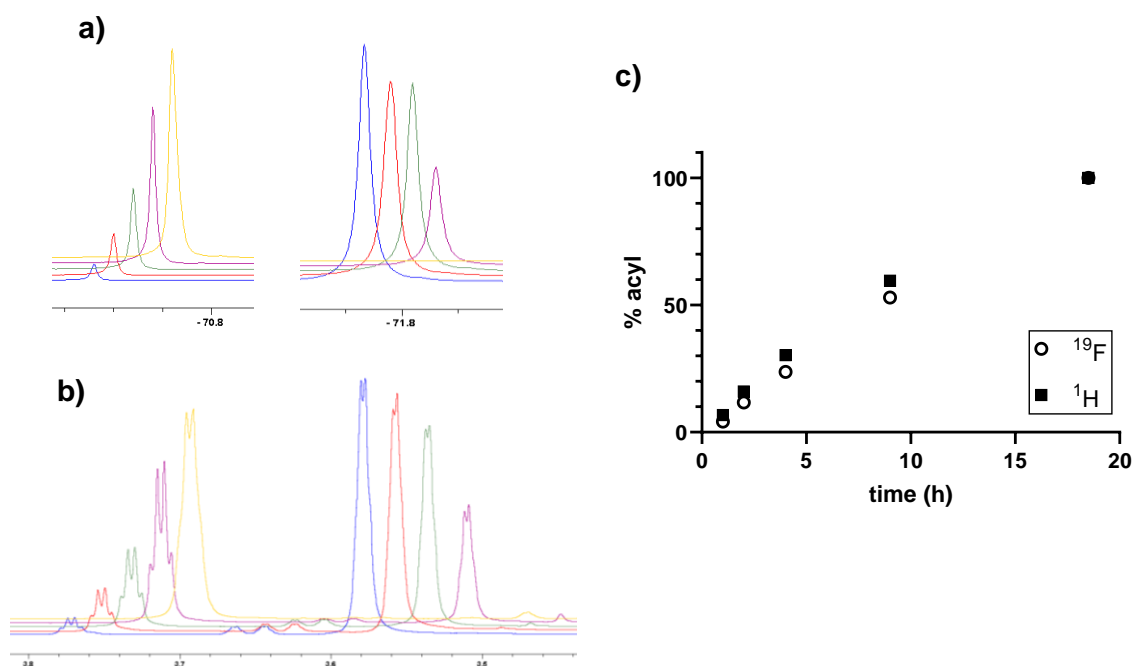


Figure 2.30: Formation of the acyl chloride of Mosher's acid 62 a) Evolution of the ^{19}F NMR spectrum, b) evolution of the ^1H NMR spectrum, c) Monitoring of the acylation Blue: 1 h, red 2 h, green; 4 h, purple 9 h, yellow, 18 h

It was hence decided to do the acylation overnight instead of in 2 hr as stated in the original procedure.

The final amide **60** was obtained, and its UV spectrum was recorded (**Figure 2.31**).

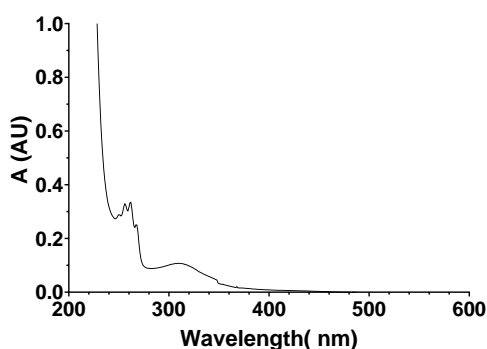


Figure 2.31: UV spectra of 60

60 showed an absorbance maximum at 260 nm. Hence, different HPLC conditions were investigated to separate the 4 diastereomers present in the mixture. Even though the reduction was stereoselective to some extent, the *trans* isomers of the amine were still present, leading to a total of 4 diastereomers after coupling with (R)-Mosher's acid. It appeared that the best results were obtained with a gradient of ACN (0.1% formic acid) from 50 to 90% in water with a Phenomenex Jupiter 5μ C18 300A analytical column (**Figure 2.32**).

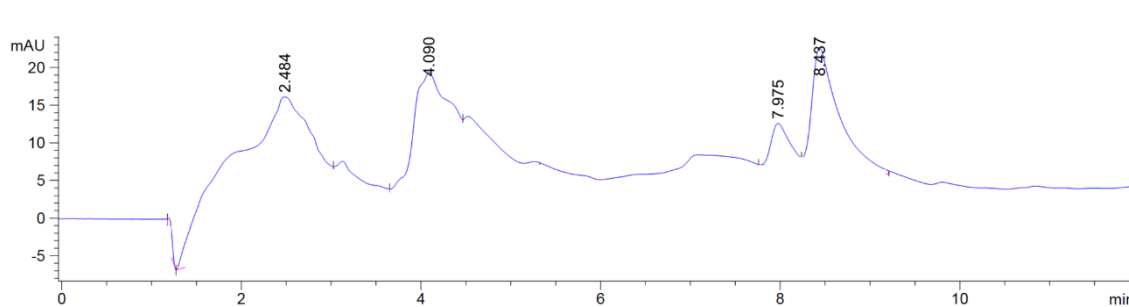


Figure 2.32: HPLC trace of a mixture of isomers of 60

Two major peaks could be observed at 2.48 and 4.09 min, probably related to the *cis* isomers while two smaller peaks were observed at 7.98 and 8.34 min.

7. Conclusion and future work

Comparison of the LC-MS traces of extracted H₂MAP and synthetic standards confirmed the structure of H₂MAP. We also established that the equilibrium between the imine and enamine form of H₂MAP is slow enough compared to an enzymatic reaction to make the investigation of the stereoselectivity of PigB and its homologue relevant. The methodology for this investigation still requires optimisation, in particular, the conditions for the reduction need to be improved whilst more procedures should be tried for the amide coupling. A repeatable process with a good yield must be achieved before trying the procedure on a biological extract.

The flexibility of H₂MAP oxidases PigB and HapB around the C2 and C3 positions was studied, leading to the formation of analogues of prodigiosin by mutasynthesis. This study could be completed by trying side chains with heteroatoms and aromatic rings as well as substitution on other positions. The synthetic route described in section 3.2 gave promising results, but the final steps of the sequence are yet to be confirmed and its scope must be explored.

Chapter 3. Antimicrobial activity of prodigiosin analogues

Chapter 2 described how 8 analogues, compounds **1b-i**, of prodigiosin **1a** were obtained by mutasynthesis. Here, we aimed to assess their biological potential and in particular their antimicrobial activity, both against Gram-positive and Gram-negative bacteria.

1. Construction of a prodigiosin producing strain suitable for antibiotic assays

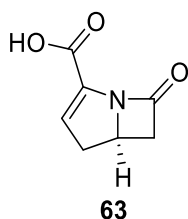


Figure 3. 1: Carbapenem

S39006 is known to produce not only prodigiosin but also the antibiotic carbapenem **63** (**Figure 3.1**). As a result, extracts for *S39006* Δ *pigD* complemented with H₂MAP contain a mixture of two antibiotics. The possibility that carbapenem effect was small enough to be masked by prodiginines activity was investigated through the preparation of extracts containing **1a-i** and from *S39066* Δ *pigD* without complementation. The samples were concentrated to the same concentration and the uninduced sample was concentrated to the minimal possible volume. Discs were then charged with the extracts and placed on a lawn of *S. aureus* (in triplicate). The plate was then incubated at 37°C, and inhibition halos were observed leading to **Figure 3.2**.

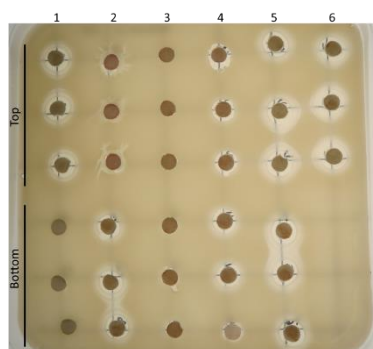


Figure 3.2: Antibiotic activity of S39006 extracts Top three rows: column 1: uninduced, 2: **1a**, 3: **1b**, 4: **1c**, 5: **1d**, 6: **1e**; bottom three rows: column 1: solvent, 2: **1f**, 3: **1g**, 4: **1h**, 5: **1i**

Chapter 3: Antimicrobial activity of prodiginosin analogues

The biggest halos were obtained for the most concentrated samples. This was particularly noticeable for the negative control, which did not contain any prodiginines. It meant that the carbapenem had a more important antibiotic effect than the prodiginines under these conditions and that direct extraction from induced *S39006 ΔpigD* was not suitable for an assessment of prodiginine antimicrobial activity. It was hence decided to construct a *Serratia* strain producing neither PigD nor carbapenem.

Phages are viruses specifically infecting bacteria. They have been the driver of a number of recent biological advancements such as CRISPR-Cas9.¹⁵³ Schematically, a phage infection follows these steps: the phage adsorbs onto its host, injects its DNA which is then replicated by the bacterial machinery, leading to the formation of new phages which finally encapsulate their DNA and exit the cell. During the encapsulation, a phage sometimes acquires bacterial DNA instead of its own. When this phage infects its next host, homologous recombination can happen. This process, called transduction, is a motor of genetic diversity in bacterial populations and can be used to transfer mutations.

Serratia MCA54 (here called *S39006 carA*⁻) was constructed by Thomson *et al.*²³ so that a transposon carrying resistance to kanamycin was inserted in *carA*, a gene coding for an enzyme necessary for carbapenem biosynthesis. A phage lysate was prepared (see experimental) by infecting top lawns of *S39006 carA*⁻ with different concentrations of phage φOT8 and extracting the phages present in plates presenting confluent plaques after an overnight culture. A culture of *S39006 ΔpigD* was then mixed with the resulting lysate for a short time.¹⁵⁴ After washing off the phages, the cells were plated on LB supplemented with kanamycin. Some of the colonies thus obtained were then tested in a carbapenem assay along with *S39006*, *S39006 ΔpigD* and *S39006 carA*⁻ (**Figure 3.3**).

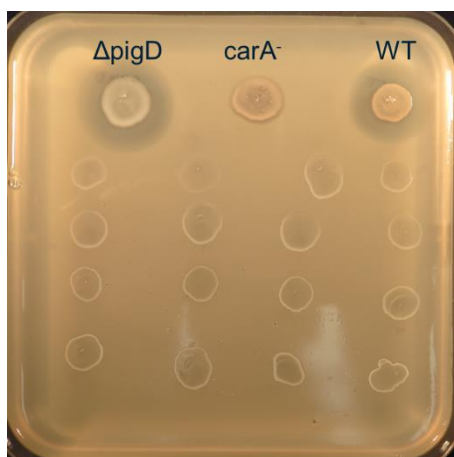


Figure 3.3: Carbapenem assay Δ pigD: *S39006 ΔpigD*, *carA*⁻; *S39006 carA*⁻, WT: *S39006*; the 16 other colonies resulted from the transduction experiment

As expected, large halos were visible surrounding *S39006* and *S39006 ΔpigD*. Interestingly, those halos were also of similar sizes, indicating that prodigiosin had little antibiotic effect compared to carbapenem under these conditions. A small halo was observed around *S39006 carA* which tends to reinforce that the antimicrobial effect of the prodigiosin was present but weaker than that of the carbapenem. No halo could be seen around the 16 colonies resulting from the transduction experiment and they were all white, confirming a phenotype unable to produce prodigiosin or carbapenem. They are noted *S39006 ΔpigD carA*.

2. Antibiotic assay

2.1. Preliminary studies

Prodiginine extracts were prepared with this new strain. Restoration of pigmentation was observed in the same manner as with *S39006 ΔpigD*, indicating that the new mutation did not affect prodigiosin biosynthesis. Cells from 25 ml of cultures inoculated with H₂MAP in LBS (LB+0.25 M sorbitol, see section 5) were extracted with 1 ml of acidified EtOH (**Table 3.1**). The quantity of prodiginine was estimated by measuring the absorbance at 535 nm, with $\epsilon_{535} = 139\,800 \pm 5100 \text{ M}^{-1}\cdot\text{cm}^{-1}$ for prodigiosin.¹³⁶

Compound	1a	1b	1c	1d	1e	1f	1g	1h	1i	Ne
A ₅₃₅ (corr)	1.57	1.71	0.505	2.49	2.18	2.19	2.33	2.87	0.377	0
m _{prod} (μg)	3.611	3.933	1.1615	5.727	5.014	5.037	5.359	6.601	0.8671	0

Table 3.1: Quantity of prodiginine obtained from complementing 25 ml of *S39006 ΔpigD carA*. The absorbances were corrected for non-prodigiosin secondary metabolites by subtracting the value of the negative control

These extracts were concentrated under reduced pressure and redissolved in DMSO so that the concentration was 36 μg/ml in all cases. Filter paper discs were inoculated with the extracts and placed on lawns of *S. aureus*. The plate was incubated overnight at 37 °C leading to **Figure 3.4**.

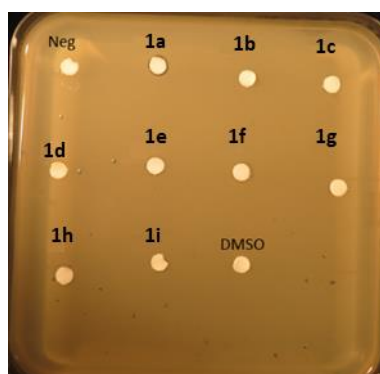


Figure 3.4: Antibiotic assay of prodiginines extracted from 25 ml of *S39006 ΔpigD carA* culture

Only a small halo with prodigiosin **1a** was visible. This indicated that the concentrations of antibiotic were too low to observe any activity. It was hence decided to scale up the production to 400 ml of culture.

Such a culture was inoculated with **19a** and about 80 μg of pigment **1a** were obtained. The sample was then concentrated, and filter paper discs loaded with approximately 7.7 μg of prodiginine. Results of the antibiotic assay against *S. aureus* are shown in **Figure 3.5**.

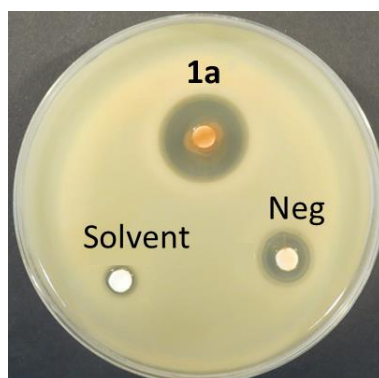


Figure 3. 5: Antibiotic assay of **1a extracted from 400 ml of *S39006 ΔpigD carA⁻* culture** Neg: extract from 400 ml of a *S39006 ΔpigD carA⁻* culture without **19**; solvent: EtOH

Unsurprisingly, a small halo was observed around the disc only inoculated with ethanol. The negative control also displayed a significant halo, which suggest that other secondary metabolites produced by *S39006* could have an antibiotic activity. However, this halo was noticeably smaller than the one obtained with **1a**, which suggests that the effect observed in this case was due to the pigment. This validated the procedure for the preparation of extracts for further antimicrobial experiments.

2.2. Disc diffusion assay

Prodiginine extracts from 400 ml of culture of *S39006 ΔpigD carA⁻* inoculated with H₂MAP analogues were prepared (see experimental). The samples were then evaporated to dryness and resuspended in 0.5 ml of acidified EtOH. Filter paper discs were then charged with 50 μl of extract and placed on an agar plate with a lawn of *E. coli* ESS. This strain displays enhanced susceptibility to some antibiotics¹⁵⁵ and was hence used to obtain halos as big as possible, making the interpretation of the assay easier. A positive control with ampicillin (10 μg) and a negative one with only EtOH were also put on the top lawn. A fourth disc was charged with 0.4 μmol of H₂MAP or the corresponding analogue: this represented the maximum quantity of that could be present on a disc charged with 10% of the total extract. Results after overnight growth at 37°C are presented in **Figure 3.6**.

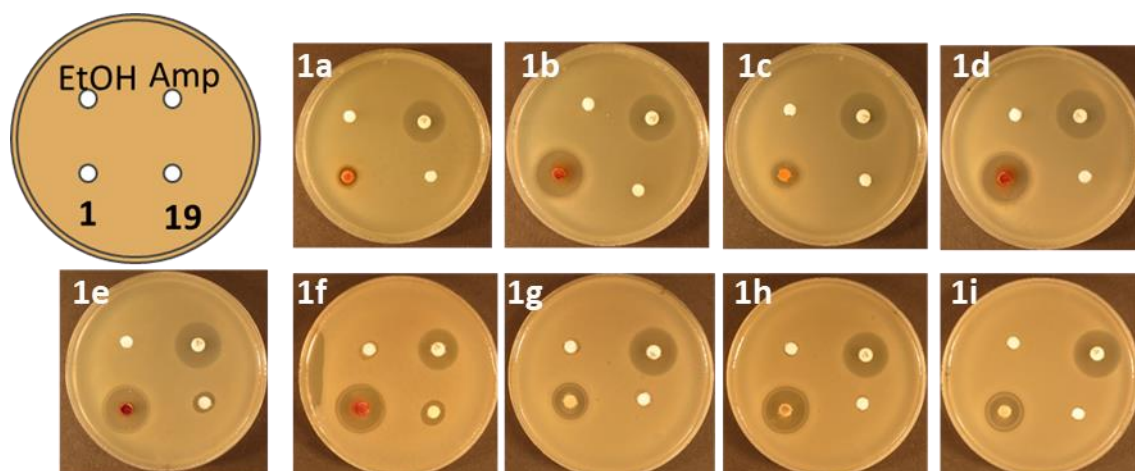


Figure 3.6: Antimicrobial assay of **1a-i** against a Gram-negative bacteria in reading order: scheme of the plate, **1a**, **1b**, **1c**, **1d**, **1e**, **1f**, **1g**, **1h** and **1i**

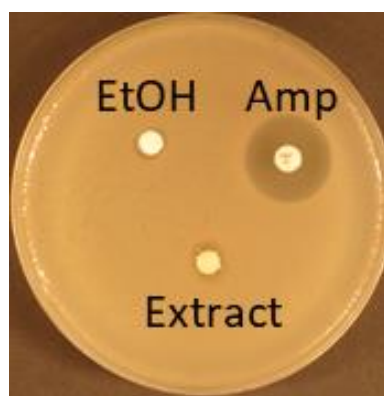


Figure 3.7: Negative control

A negative control was prepared from an extract from *S39006* $\Delta pigD carA^-$ cultured in absence of any H₂MAP **19a** analogues (**Figure 3.7**). As expected, in this plate only ampicillin displayed a halo. In the other plates, both positive and negative controls gave the expected results whilst halos were observed with all the extracts. Interestingly, prodigiosin itself gave the smallest halo whilst extracts that looked barely red gave halos of similar size to ampicillin's (**1h** and **1i**). Most discs impregnated with H₂MAP analogues did not lead to a visible halo. Compounds **19e** and **19f**

did, but the size of these halos was smaller than the size of the ones obtained with the extracts.

Activity against *S. aureus* was also tested (**Figure 3.8**). Here again all prodiginines seemed to have activity. Yet, when the experiment was repeated with a fresh batch in an attempt to imitate **Figure 3.8**, almost no activity could be observed. To rule out the presence of mutations or contamination in the strains used for the assay, the experiment was repeated against bacteria freshly taken out of the glycerol stock, but it gave similar results. The discrepancies could be due to difference of concentration in prodiginine from one batch to another (A_{535} was twice as high in some cases in the original batch) or to the effects of other molecules present in the extract. These variations from batch to batch were also observed with *E. coli*.

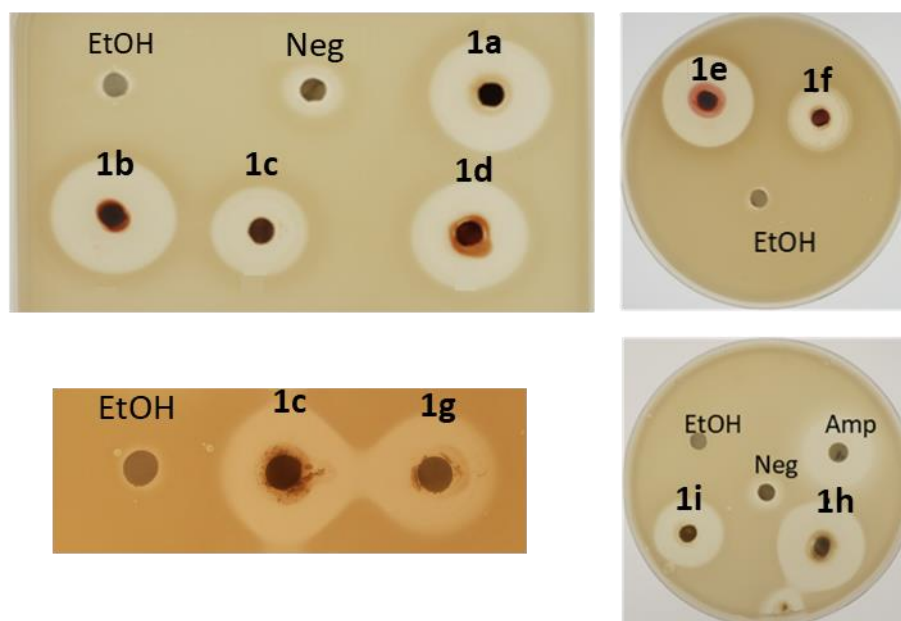


Figure 3.7: Antimicrobial assays of 1a-i against a Gram-positive bacteria

Another limitation of these experiments was the lack of comparability between the compounds as all the discs are charged with a different quantity (Table 3.2).

Compound	1a	1b	1c	1d	1e	1f	1g	1h	1i
A_{535} (corr)	1,57	1,71	0,505	2,49	2,18	2,19	2,33	2,87	0,377
nmol	11.16	12.88	7.62	20.21	14.66	7.87	2.36	1.79	0.72
μg	3.6	3.6	2.5	5.9	4.9	2.6	0.7	0.6	0.3

Table 3.2: Quantity of prodiginine obtained from 400 ml cultures

To get a suitable comparison, the concentration of the prodiginine in all the samples were brought to 0.21 mM (as judged by their A_{535} values). Filter discs were then inoculated with 50 μl of the sample (approx. 3 μg) or 0.4 μmol of the **19** precursors (this represent the maximum quantity of precursor that could have been spotted on the disc from an extract). They were then all placed on a single plate to compare their antibiotic effects (Figure 3.9). The sample used for **1h** was purified by HPLC beforehand.

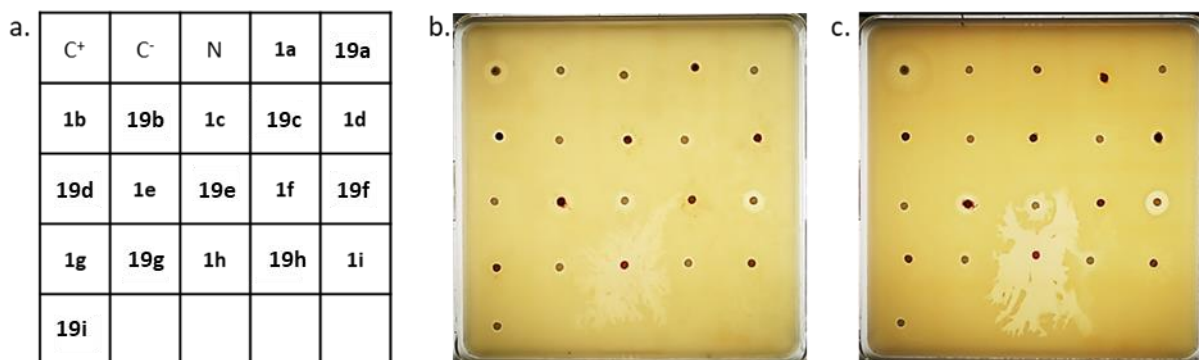


Figure 3.8: comparison of the antibiotic activities of compounds 1a-I a) Scheme of the plate, C⁺: ampicillin, C⁻ EtOH, N: extract from *S39006 ΔpigD carA⁻* cultured without an H₂MAP analogue ; b) Activity against *E. coli*; c) Activity against *S. aureus*

The results for the two strains were similar (**Table 3.3**). The strongest halos were observed with **1e**, but its precursor **19e** gave a similar result. As observed earlier, **19f** also gave halos, but, interestingly, no visible halo was observed with **1f**. Prodiginine **1d** gave halos consistently bigger than its precursor, but they were still small compared to the positive control. Prodiginines **1b** and **1c** also seemed to have some activity against *E. coli*. The purest compound, **1h** had mainly a surfactant effect. However, after the HP-LC purification, the ethanolic solution seemed less viscous than when the cells extracts were directly concentrated and resuspended in ethanol, probably because there were less impurities. It was hence hard to tell if the observed effect was due to antimicrobial activity or surfactant pushing the bacteria away.

Extract	C ⁺	C ⁻	N	1a		1b		1c		1d	
<i>E. coli</i>	4.6 ± 0.5	<1	1 ± 0.0	1.4 ± 0.6	<1	1.5 ± 0.7	<1	1.3 ± 0.1	<1	2 ± 0.9	<1
<i>S. aureus</i>	7.1 ± 0.1	<1	<1	1.3 ± 0	<1	<1	<1	<1	<1	1.8 ± 0.0	<1

Extract	1e		1f		1g		1h		1i	
<i>E. coli</i>	2.9 ± 1.5	3.7 ± 0.4	<1	4.5 ± 0.7	<1	<1	NA	1.0 ± 0.0	<1	<1
<i>S. aureus</i>	3.7 ± 0.7	5.0 ± 0.6	<1	4.1 ± 0.2	<1	<1	NA	NA	1.0 ± 0.0	<1

Table 3.3: Halo sizes C⁺, C⁻ and N as above; left: **1**; right **19**

Considering the results presented in **Figures 3.6** and **3.8**, and even allowing for the fact that less material was used than in some literature reports,⁷¹ the halos were smaller than expected. This could be due to degradation of the samples either during the concentration process or during storage.

The quality of the data as well as the repeatability of these experiments needs to be improved. Using only purified prodiginines in more concentrated solutions so that the discs can be saturated with a higher quantity of compounds whilst minimising the amount of solvent could

be a way to do so. Yet, as a preliminary test, these experiments confirmed the antimicrobial potential of the mutasynthesised prodiginines.

2.3. Half maximal growth inhibition (GI_{50}) experiments

Fresh prodiginines (**1a**, **1e**, **1g** and **1h**) extracts were prepared from 1 L of culture. The ethanolic extracts were sterile-filtered before concentration and resuspension in 1 ml of H₂O/ACN. Prodiginines were then purified by HPLC. The pink fractions were gathered, the solvent removed under reduced pressure, and the residue was resuspended in the minimum volume of EtOH. Unfortunately, the quantity of **1g** – estimated by measuring the A₅₃₅ – hence purified was too low for any downstream applications.

Growth inhibition assays were conducted with maximal concentrations of 1.4 µg/ml (4.3 µM) for **1a** and 7 µg/ml (21 µM) for **1e** and **1h** (Figure 3.10a): 96-well plates were charged with *E. coli* ESS or *S. aureus* (OD₆₀₀ = 0.06) and a serial 2-fold dilution of prodiginine and the plates were incubated at 37 °C for 16 h. Ampicillin was used as a positive control (Figure 3.10a). The plates were then inspected for growth and the OD₆₀₀ was recorded with a plate reader. At **1e** and **1h** concentrations, the absorbance of prodiginines still had to be taken into account when the OD₆₀₀ was measured: the absorbances were hence corrected (see experimental) and normalised by the mean absorbance of wells charged with bacterium but not with antibiotic. The data were finally submitted to a non-linear analysis (Figure 3.10b-f).

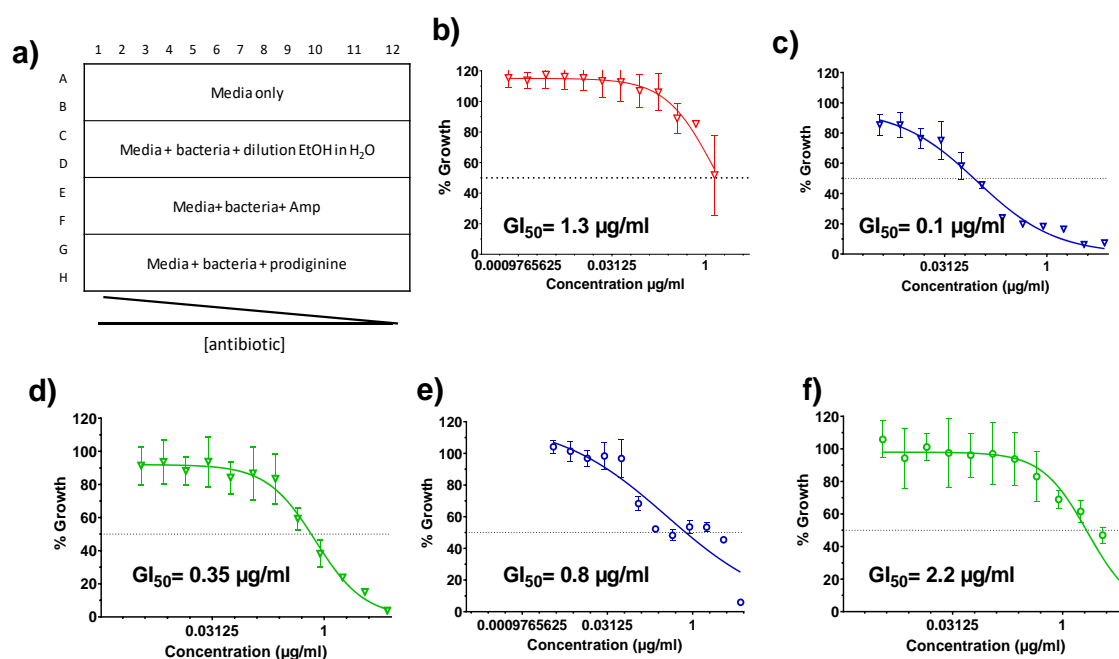


Figure 3.9: GI_{50} assays a) Scheme of the plate, b) **1a** against *S. aureus*; c) **1h** against *S. aureus*; d) **1e** against *S. aureus*, e) **1h** against *E. coli*; f) **1e** against *E. coli*

It appeared that the concentrations were not high enough to see the complete inhibition profiles in some cases. In particular, all the concentrations tested with **1a** were lower than the GI_{50} . Furthermore, the curve obtained for **1h** against *E. coli* did not follow the expected sigmoid and the end growth was sometimes higher than without the antibiotic (**Figure 3.10b** and **e**). Despite these problems, GI_{50} could be estimated in all cases. Interestingly, both **1e** and **1h** are more potent than prodigiosin **1a** against *S. aureus*. It is possible that the extra methyl group on **1e** and **1h** improved the lipophilicity of the molecules, hence enhancing any membrane disturbing effects or cell permeability. The difference between **1e** and **1h** is harder to explain, especially without knowing for certain what the mechanisms of action of prodiginines in the cells are. For both compounds, a better activity against the Gram-positive strain was observed, possibly because of the absence of an outer membrane in that case.

3. Preliminary anti-cancer activity assay

This part of the project was done with the help of Lavinia Dunsmore. Prodiginine **1h** was inoculated to cultures of HeLa cervical cancer cells at concentrations between 1 μM and 62.5 nM with 1% DMSO. The cells were cultured two days and the cell viability was measured and normalised to controls cultured with 1% DMSO only, leading to **Figure 3.11**.

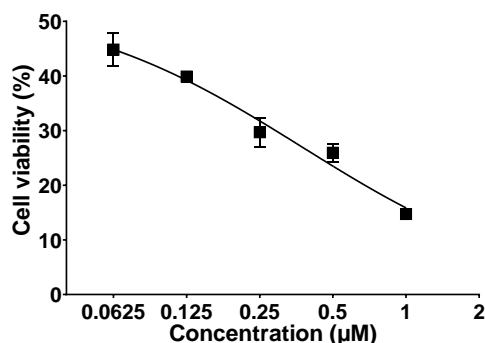


Figure 3.10: Cell viability assay of HeLa cell in presence of **1h (1% DMSO)**

It appeared that the concentrations were higher than the LD_{50} . A non-linear analysis of the data was nevertheless possible, but the confidence interval around the predicted value of the LD_{50} (40 nM) was very wide. Yet, these data indicate that the LD_{50} for **1h** is lower than the reported values for **1a** (about 1 μM).^{156,157} However, it would be necessary to try a wider range of concentrations for precise determination of the LD_{50} . Finally, it would be interesting to also test activity against non-cancer cell lines to assess for cancer cell selectivity.

4. Investigation of a hyper-producing strain for yield improvement

Even with an increased culture volume, the quantity of pigment obtained remained low. The construction of a mutant of *S39006* $\Delta pigD$ with the capacity to produce more prodigiosin was hence investigated. *Serratia rop2* was prepared by Slater *et al.*¹⁵⁰ by transposon mutagenesis. Plasmid pUT-miniTn5 Sm/Sp^{158,159} was used to insert the transposon with resistance to streptomycin and spectinomycin into *pstS*, a gene involved in phosphate transfer during a random transposon mutagenesis experiment aimed to study the regulation of prodigiosin and carbapenem production. The mutant hence obtained was visibly extra-red. Using the same transduction procedure as for the construction of *S39006* $\Delta pigD$ *carA*⁻ (see experimental and section 2), colonies with deletion in *pigD* and the insertion in *pstS* were obtained (strain *S39006* $\Delta pigD$ *rop2*). Resistance to streptomycin and spectinomycin confirmed the presence of the transposon whilst the deletion was checked by colony PCR.

The hyper productivity of the strain was then checked by measuring the quantity of pigment per cell for 11 h after addition of H₂MAP to a culture of *S39006* $\Delta pigD$ *rop2*. The effects of the variations of the media volume – which is reduced by more than half because of the sampling when the experiment is conducted in 25 ml cultures – were first assessed (**Figure 3.12a**), followed by the effect of supplementing the media with sorbitol (**Figure 3.12b**), with the wild type strain.

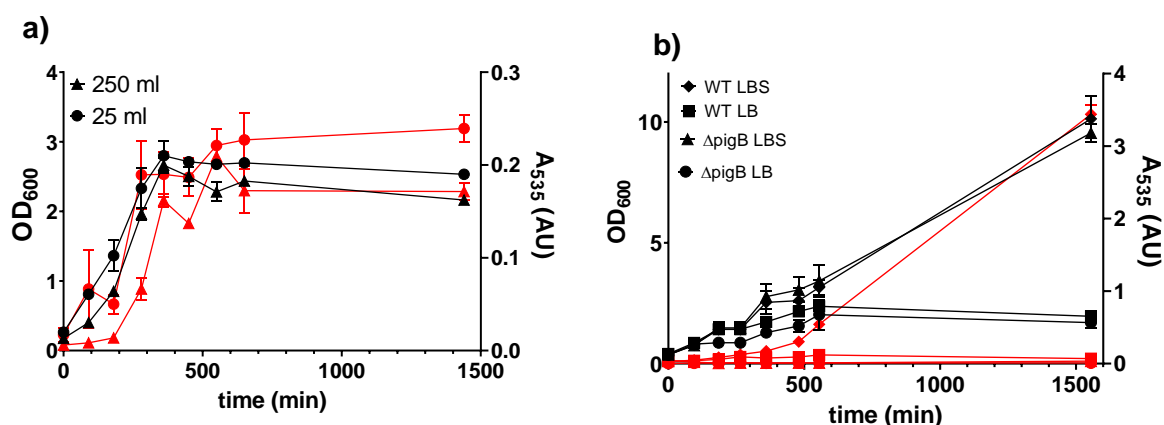


Figure 3.12: Prodigiosin production time curves Black: OD₆₀₀, Red: A₅₃₅, a) influence of the media volume b) Influence of sorbitol supplementation

Growth curve of *S39006* in 25 and 250 ml cultures were similar, even though slightly higher OD₆₀₀ and prodigiosin levels were obtained in 25 ml, probably because of better oxygenation. It was hence decided to perform future growth curves in 25 ml. As expected, the addition of

sorbitol led to a longer exponential phase, and hence a large increase of OD₆₀₀ and of prodigiosin production. Interestingly, the amount of prodigiosin per cell was also six times higher in the presence of sorbitol. This justified the use of sorbitol as a complement for growth curve and complementation assays. A₅₃₅ increased also slightly in *S39006 ΔpigB* in the presence of sorbitol, probably because the higher OD₆₀₀ triggered the formation of other secondary metabolites.

The hyper productivity of pigment in *S39006 ΔpigD rop2* was then assessed and compared to the pigment production in *S39006 ΔpigD* (Figure 3.13) when these strains are cultured in the presence of H₂MAP. Here, H₂MAP was added after 12 h of incubation and the OD₆₀₀ and the pigmentation were monitored for a further 12 h.

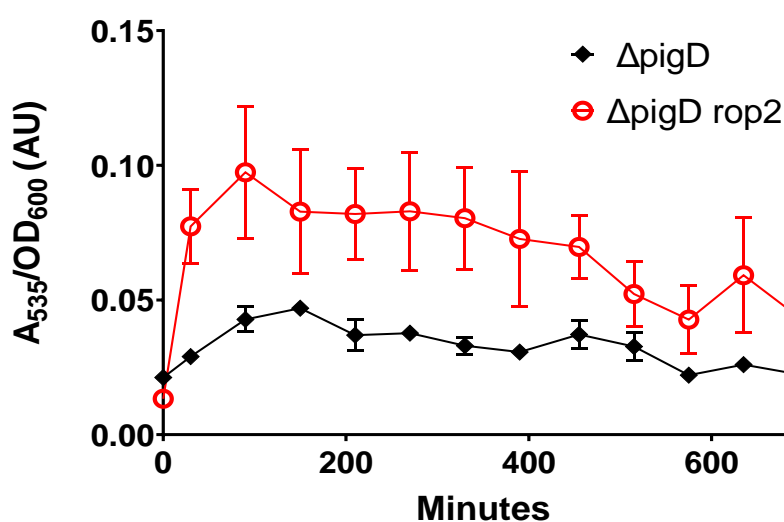


Figure 3.12: Effects of an insertion in *pstS* on pigment production

The amount of pigment per cell was indeed higher with the *rop2* mutation. However, it seemed to decrease as time went on, probably because of the faster consumption of the precursor.

For mutasynthesis and complementation assays, the total amount of pigment is more relevant than the quantity per cell. Because of differences in the growth and in the rate of consumption of the precursor, it was observed that less total pigment was actually obtained with *S39006 ΔpigD rop2* than with *S39006 ΔpigD* after 16 h with H₂MAP (Figure 3.14). Shortening the time would lead to lower OD₆₀₀ and hence decrease the overall pigmentation as well.

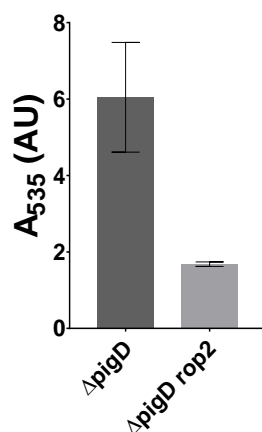


Figure 3.13: Pigment production *S39006* $\Delta pigD$ and $\Delta pigD rop2$ after 16 h of culture with H₂MAP in LBS

In conclusion, even though *rop2* mutation gives a hyperproducer phenotype, optimisation of the feeding assay would be necessary to get a better yield using this strain.

5. Other potential applications of prodigiosin analogues

Indirect applications of these new prodiginines can be imagined. For example, compound **1d** contains an allyl group, which can be used for electrocyclization (as a dienophile in a Diels-Alder reaction for instance), metathesis, and many other things. A potential application could be to follow the prodiginine inside a cancer cell. As mentioned in Section 1.5, studies about the location of prodiginine in cancer cells gave contradictory results. Treating cancer cells with **1d** and then coupling it with a tetrazine attached to a fluorophore would provide a way to conduct this kind of investigation. Coupling between tetrazines and allyl tagged protein have been reported in the literature.¹⁶⁰ In addition, the formation of a coupled product could be observed by LC-MS when 3,6-dipyridyltetrazine (Py₂Tz) **64** was stirred with **19d** in PBS buffer at room temperature (**Figure 3.15**). Even though this is still very far from an imaging process, this illustrates the possibility.

Another idea would be to replace the terminal alkyl group by an alkyne. This would make click reactions with biotin-azide possible and would hence give a way to investigate what protein prodigiosin binds to. In summary, this process to prepare functionalised prodiginine combined with biorthogonal chemistry techniques could lead to a variety of new assays.

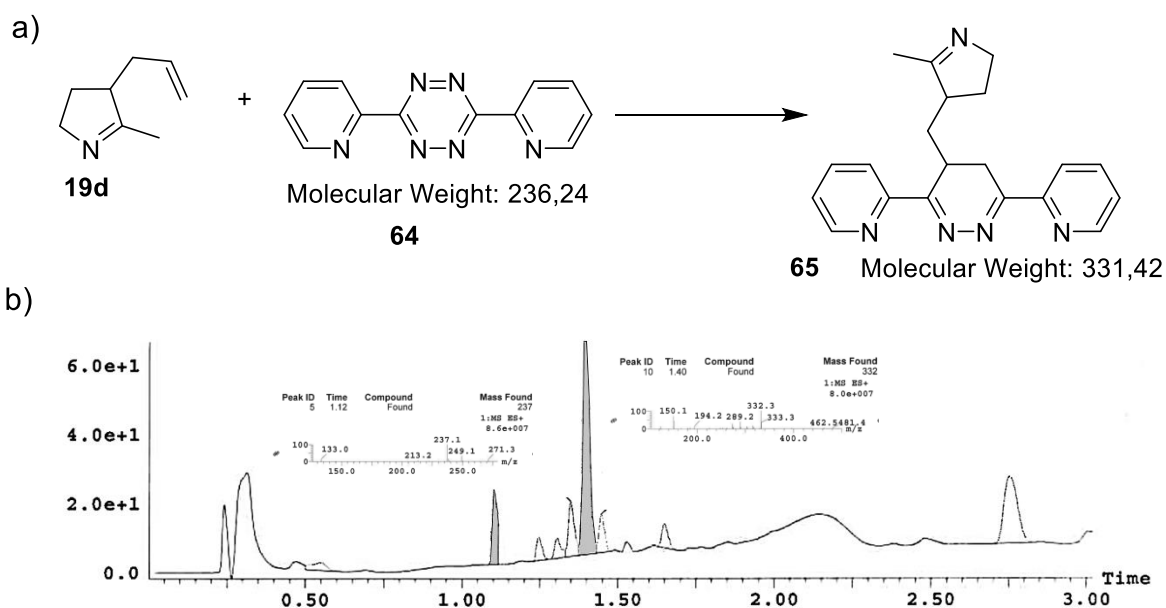


Figure 3.14: Coupling of 19d and a tetrazine a) Reaction scheme of the coupling b) LC-MS chromatogram after 48 h. The peak at 1.12 min has the correct m/z value for $[19d+H]^+$ and the peak at 1.40 min has the correct m/z value for $[65+H]^+$.

6. Conclusion and future work

Initial testing of the prodiginines obtained by mutasynthesis gave promising results. The antimicrobial potential was demonstrated, and two compounds proved more potent than prodigiosin **1a** against *S. aureus* and showed activity against *E. coli*. However, the repeatability of the disc diffusion assays needs to be improved: the surfactant effect observed with **1h** needs to be resolved and the assay should be repeated with purified compounds for more quantitative results. The growth inhibition assays also need to be repeated with higher starting concentrations to get the full inhibition curves and MIC values.

Prodiginines have many biological properties and only two of those have been investigated here. Hence, it would be interesting to assess the antifungal potential of these compounds. More in depth analysis of the anticancer activity would also be interesting: the precise value of the LD_{50} against HeLa cells still needs to be determined and other cell lines could be investigated.

Preliminary experiments also showed that some prodigiosin analogues may have applications beyond their biological properties.

Chapter 4. Characterisation of PigE

1. Overview and aims of the project

1.1. Overview of potential characteristics of PigE

1.1.1. Substrate channelling

PigE is likely to be a bifunctional enzyme (see section 1.2). It might hence be an example of substrate channelling, a phenomenon where the intermediates in an enzymatic sequence are prevented from freely diffusing. Indeed, diffusion of substrates from one active site to another is slow and can lead to the degradation of the intermediate. Different mechanisms preventing diffusion have been observed. The most obvious one is the localisation of the entire reaction cascade in a single organelle – a chloroplast for instance¹⁶¹ – hence reducing the volume in which the diffusion might occur. In bifunctional enzymes and enzymes clusters, structural mechanisms such as intramolecular tunnels, electrostatic guidance or chemical swinging arms have been observed.

As their names indicate, intramolecular tunnels will connect two active sites within a single protein or complex, preventing the intermediates from escaping into the cytoplasm. This is illustrated by the last two steps of catechol degradation: 4-hydroxy-2-ketovalerate aldolase DmpG and acetaldehyde dehydrogenase DmpF form a complex that will catalyse a retro-aldol reaction producing acetaldehyde followed by oxidative thioesterification of the acetaldehyde. Crystal structures of the complex showed that the active sites of the two enzymes are connected by a 29 Å long tunnel, which the acetaldehyde travels along.¹⁶²

If the intermediates are charged, a charged pathway on the protein surface can guide the diffusion from one site to another. This is illustrated by the malate dehydrogenase-citrate synthase complex, where a positively charged surface of the protein guides the diffusion of the negatively charged oxaloacetate intermediate.¹⁶³

Chemical swinging arms, as illustrated by the ACP, are probably the most frequent channelling mechanism as they are used in Type I PKSs as well as in Type I fatty acid synthases. In the case of fatty acid synthesis, the ACP, the β ketoacid synthase, the β ketoacyl reductase, the hydrolase and the enoyl reductase are arranged in a megaenzyme; and the phosphopantetheine moiety of the ACP – or the entire ACP – can translocate to reach the active sites of the different domain.^{161,164}

1.1.2. Thioester reductase (TR)

The most common mechanism for the release of the chain from the ACP domain of PKSs and non-ribosomal peptide synthetases (NRPSs) is thioesterase-catalysed hydrolysis, leading to the formation of a carboxylic acid. Yet, the release can also occur in a reductive manner and, in these cases, it is catalysed by a thioester reductase (TR).^{165,166} All the reported thioester reductase domains are NAD(P)H dependent and present a Rossman fold where the cofactor can bind at

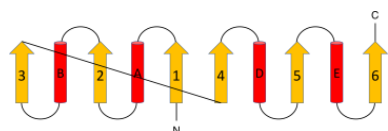


Figure 4.1: Scheme of Rossman fold, red: α helix, yellow: β strand

the N-terminal end (**Figure 4.1**). In addition, threonine, tyrosine, and lysine are always present in the catalytic site.¹⁶⁷

These two features make TRs very similar to short chain dehydrogenases/reductases. Depending on the number of electrons involved (two or four) in the reduction, the TRs are divided into two main classes. When four electrons are involved, the reaction goes all the way to the alcohol, which is the final product in most cases. When only two electrons are involved, the TR gives aldehyde products, but those often undergo further transformations, leading to a variety of functional groups.

TRs catalyse a hydride transfer from NAD(P)H to form a thiohemiacetal intermediate covalently bound to the enzyme and stabilised by H-bonding with tyrosine. Cleavage of the thioacetal then gives the aldehyde (**Figure 4.2**).¹⁶⁸

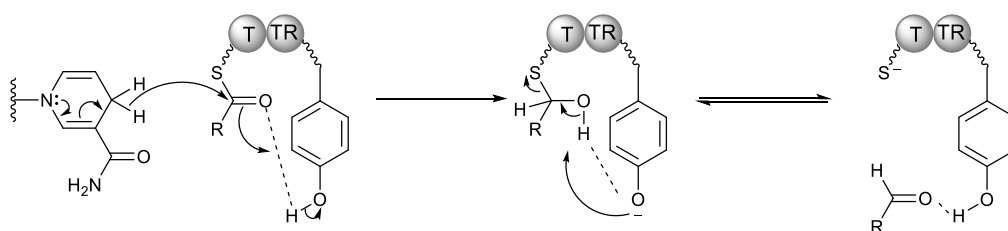


Figure 4.2: Mechanism of action of TR T: ACP or PCP thiolation domain

In some rare instances, the release mechanism of thioester can follow yet another mechanism: in MBC biosynthesis, PigH catalyses the liberation of an α -oxoamine by reaction of a thioester bound to an ACP domain with serine in a PLP-dependent fashion.

1.2. PigE: a potential bifunctional thioester reductase - aminotransferase

As mentioned in Chapter 1, PigE is the second enzyme in MAP biosynthesis (**Figure 4.3**).

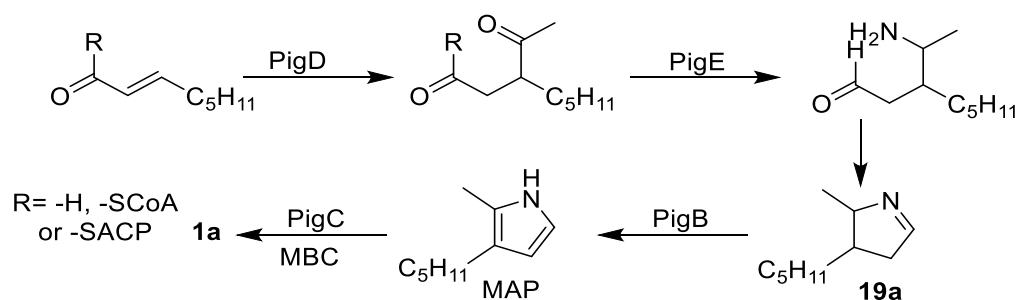


Figure 4.3: Simplified prodigiosin biosynthetic pathway

In their original elucidation of prodigiosin pathway, Williamson *et al.*²⁶ described PigE as a PLP dependent transaminase taking the aldehyde product of PigD and catalysing the transformation of one of the carbonyl groups into an amine, making a spontaneous cyclisation possible. The transaminase activity was investigated by Bhalara, who observed an increase in the absorbance at 330 nm when purified PigE was incubated with L-ornithine, suggesting the formation of a pyridoxamine phosphate (PMP) species (see **Figure 4.4**) and consistent with a PLP-dependent transaminase.²⁰ A crystal structure of the transaminase domain was obtained by Lou *et al.*³⁵ They were also able to show that residue Lys645 binds to PLP, *via* an aldimine (**Figure 4.4**)

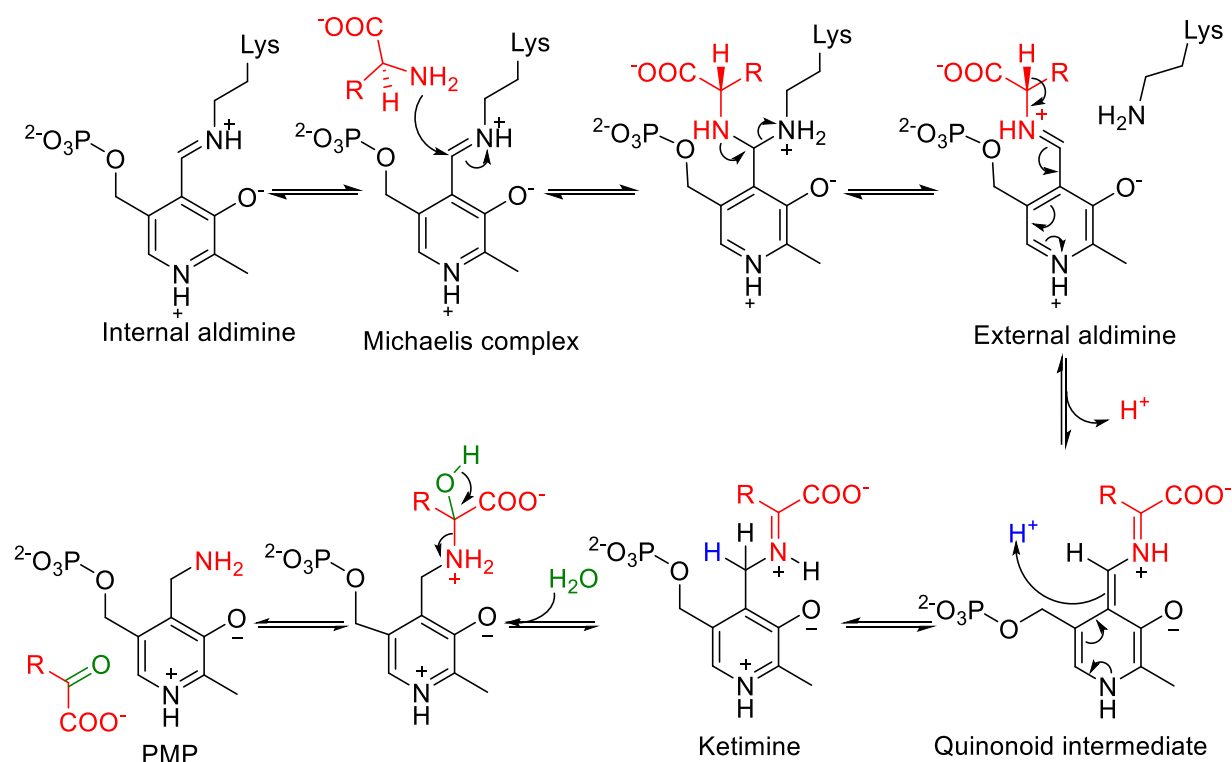


Figure 4.4: Mechanism of transamination by PLP dependent aminotransferase

However, this crystal structure was only partial, no electron density was visible from residue Mat1 to Ala371, probably because of degradation. Consequently, this structure might not be an accurate representation of the native state of PigE.

It is highly unlikely that PigE has only a transaminase activity. Indeed, that would mean that the product of PigD is a free aldehyde. These compounds are very reactive and are known to react with nucleophilic sites in macromolecules,¹⁶⁹⁻¹⁷² for instance the cysteine¹⁷⁰ and lysine¹⁷¹ residues of enzyme active sites, but also DNA.¹⁷² This leads to the formation of adducts impairing the function of essential macromolecules and thus to cytotoxicity.^{169,173} In addition, aldehydes can trigger oxidative mechanisms and the release of free radicals within the cell, causing damage to DNA, proteins and membranes.^{174,175} Furthermore, Dresen *et al.* showed that PigD regioselectivity on aldehyde substrates was not consistent with the rest of prodigiosin biosynthesis (see Chapter 5).³⁶ On the other hand, PigD showed the appropriate regioselectivity with thioester substrates.

We hence hypothesised that the natural substrate of PigE was a thioester, either 3-acetyloctanoyl-CoA **66** or more likely a 3-acetyloctanoyl-ACP **67**.

The aim of this project was to prove that there is a thioester intermediate in MAP biosynthesis, which is reduced to give 3-acetyl octanal **20**. The thioester reductase activity of PigE was to be investigated both in cells and on purified proteins.

2. Bioinformatic analysis of PigE

2.1. NCBI Basic Local Alignment Search Tool (BLAST)¹⁷⁶

When PigE DNA sequence was submitted to blastx (see appendix), the protein sequences matching the best with PigE's were unsurprisingly from prodigiosin producing organisms. To the best of our knowledge, the predicted functions of those protein have never been experimentally established.

Two domains (residue 1 to 335 and 391 to 854) were predicted. The C-terminal domain belongs to the family of acetylornithine PLP-dependent transaminases. This was in agreement with the studies on PigE mentioned earlier. The BLAST results were also consistent with Lou *et al.* and predicted Lys645 to be the residue that formed the Schiff base. It also indicated that residues Gly424, Thr425, Tyr530, His531, Glu583, Asp616 and Gln619 were also likely to be involved in binding with PLP.

The N-terminal domain did not give any specific hits but showed some homology with Acyl ACP reductases, which catalyses the reduction of fatty acyl ACP thioesters to the corresponding aldehyde in cyanobacteria.¹⁷⁷ It also shared some similarity with PRK14982, which is also believed to be an acyl-ACP reductase.¹⁷⁷

2.2. PHYRE¹⁴⁷

Two algorithms can be run with PHYRE software: normal or intensive. The intensive mode uses multiple templates and *ab initio* technique to cover the entire protein. PigE was analysed using both setups.

In both cases, PHYRE first aligned the sequence against other proteins. Here only two proteins that matched the entirety of the sequence (see appendix): HapE, PigE's homologue from *H2396*, and a putative aminotransferase from *Saccharospora erythraea*. The other proteins matching PigE's sequence either matched the N-terminal domain or the C-terminal one. This was an issue because the software uses already solved structures as the basis for the 3D model. As a consequence, the normal algorithm only gave a model based on the best hits, which are, as expected from the BLAST results, covering only the C-terminal domain.

The software was able to predict that PigE C-terminal domain (residues 394 to 848) was most similar to putrescine aminotransferase, a class III PLP dependent aminotransferase.¹⁷⁸ This led to the predicted structure presented in **Figure 4.5**. All but two of the residues predicted by BLAST to interact with PLP (in orange in **Figure 4.5**) were on the outside of a pocket, which was consistent with a cofactor binding site.

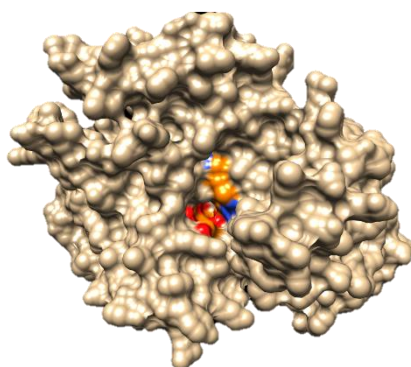


Figure 4.5: Predicted structure of PigE C-terminal domain by PHYRE Orange: residue predicted to be involved in the PLP binding site

However, the intensive algorithm circumvents that limitation: by mixing templates covering both domains of PigE, it was able to model 77% of the structure with more than 90% confidence (**Figure 4.6**). A drawback of this approach was that the prediction about the orientation of one domain compare to the other was unreliable. The template used to model the N-terminal domain was *Methanopyrus kandleri*'s glutamyl tRNA reductase, a V-shaped enzyme catalysing the transformation of glutamyl-tRNA into glutamate-l-semialdehyde through the formation of a thioester intermediate which is then reduced by NADPH.¹⁷⁹

Chapter 4: Characterisation of PigE

With both algorithms, the software predicts the secondary structures for the whole sequence. Estimates from both algorithms were consistent and predicted a structure with approximately 42% of α -helices, 16% of β -strands, 6% of transmembrane domain (TM), and 16% of disordered domains.

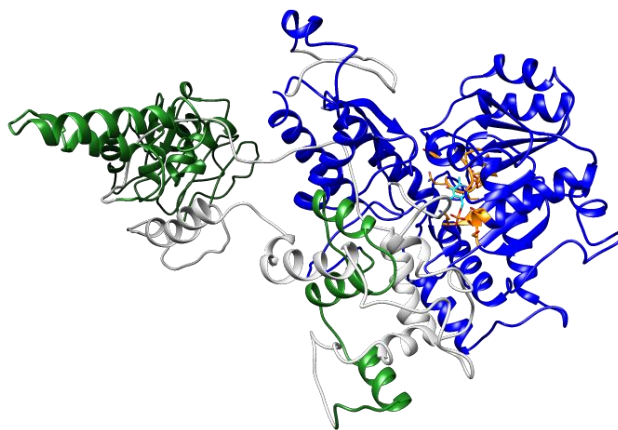


Figure 4.6: Predicted structure of PigE Blue: C terminal domain, Orange: PLP binding site, Light blue: PLP; Green: N terminal domain, White: low level of confidence

In addition, at the end of the pipeline, the model is submitted to 3DLigandSite,¹⁸⁰ a binding site predictor. After the intensive run, a PLP pocket (in orange in **Figure 4.6**) was identified. Its location is in good agreement with the BLAST results, other than Gly424 and Thr425, as observed with the normal run.

A PHYRE analysis of the N terminal domain alone (residue 1 to 426) was performed: the best hit was tRNA glutamate reductase. Other hits included NAD(P)-binding Rossmann fold domains and oxidoreductases, which was consistent with a thioester reductase activity. Unfortunately, most of these proteins have not been crystallised, so despite good alignments (see appendix), they were not used for the modelling. Yet, 63% of the sequence was modelled with more than 90% confidence (**Figure 4.7**). This was not high enough to get reliable results from 3DLigandSite. Interestingly, the model hence obtained differed significantly from the one obtained with the whole protein (**Figure 4.7**). This could be due to the inability for the software to predict the orientation of disordered domains.

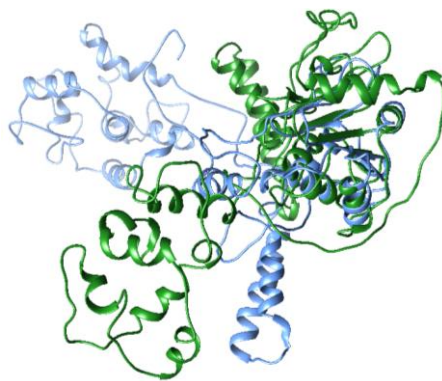


Figure 4.7: Superposition of the PHYRE predicted model for PigE N terminal domain only (green) and the N terminal domain of the predicted structure of the complete PigE (blue)

2.3. Comparison with TamH

In tambjamine biosynthesis, TamH has the same function as PigE in prodigiosin biosynthesis, but with a β,γ -ene substrate instead of a β -acetylated one.⁵⁵ Unfortunately, the sequence of TamH from *Pseudomonas tunica* was not readily available for comparison.

PigE protein sequence was blasted against *Pseudomonas tunica* whole genome, leading to 7 hits, 6 of whom were aminotransferases of approximately 400 amino acids, whereas the last was 941 amino acid long. The entire prodigiosin biosynthetic gene cluster was then compared with this gene's surrounding using Artemis Comparison Tool (ACT), showing homologues of genes involved in MBC formation, confirming that it belongs to tambjamine's biosynthetic cluster (see appendix).

Comparison of TamH and PigE sequences via BLAST and ACT showed (see **Figure 4.8**) that both displayed two domains: one predicted transaminase region and one putative reductase. Interestingly, the order of the domains was the reverse. This suggests some flexibility in the region between the two domains.

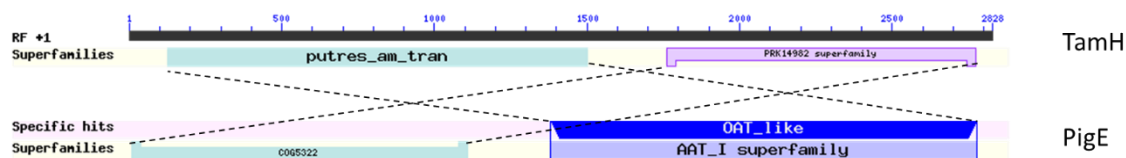


Figure 4.8: Comparison of TamH and PigE sequences. The comparison of the orientations was done using ACT

3. Synthesis of PigE potential substrate(s)

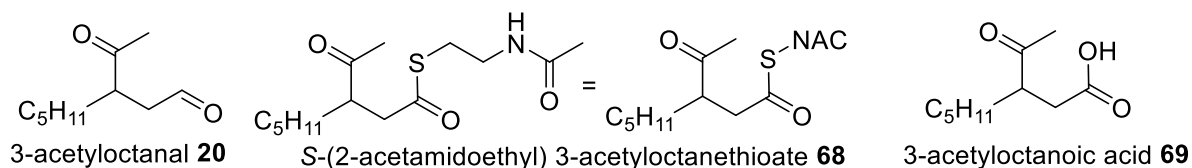


Figure 4.9: Potential substrates of PigE

The synthesis of three different molecules (**Figure 4.9**) was necessary for the study of PigE. 3-Acetyloctanal **20** was the most likely substrate and it was important to make so it can play the role of positive control. 3-Acetyloctanoyl-CoA **66** and 3-acetyloctanoyl-ACP **67** could be synthesised, but they were unlikely to get into the cells, making complementation assays impossible. Hence, the synthesis of mimic **68** was undertaken. Interestingly, this compound has previously been made by PigD-catalysed reaction of thioester octenoyl-S-NAC **70** and pyruvate *in vitro*.³⁶ Finally, thioesters are labile and can hydrolyse in culture broth. Consequently, it was important to prepare carboxylic acid **69**, which is the result of the hydrolysis of **68**. If the hypothesis on the function of PigE is correct, **69** should not be accepted as a substrate. The three molecules share the same carbon skeleton and only differ in one functional group. Once one of the three has been synthesised, the other two can be obtained by functional groups manipulation.

3.1. Method A: from ethyl acetoacetate to 3-acetyloctanal

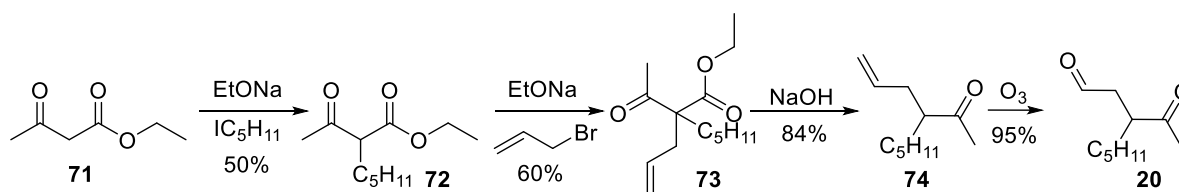


Figure 4.10: Chawrai's synthesis of 20

This method (**Figure 4.10**) was adapted from Williamson *et al.* who synthesised **20** and showed it could complement a *S39006* Δ pigD mutant.²⁶ After formation of the enolate of ethyl acetoacetate **7** by treatment with sodium ethoxide, it was alkylated with 1-iodopentane at reflux to give intermediate **72**. As often with this kind of procedures, double-addition product **72b** could sometimes be observed but could easily be removed by column chromatography.

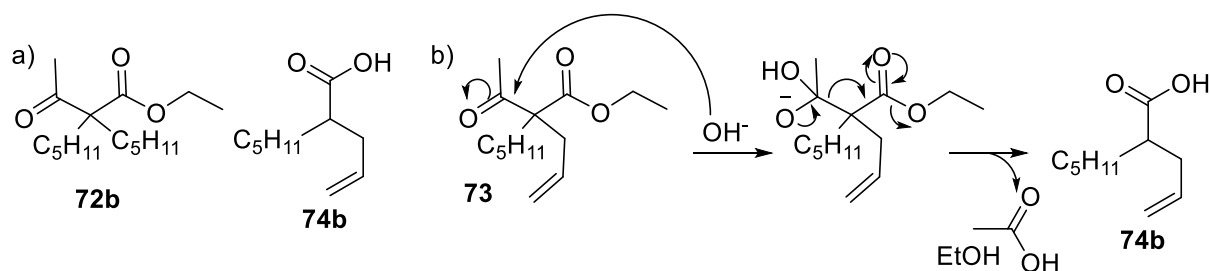


Figure 4.11: Side products observed during the synthesis of **20** a) Structures, b) Mechanism of formation of **74b**

The second step followed the same principle: after formation of the enolate, alkylation was performed with allyl bromide at reflux, leading to **73**. A few conditions were tried before getting the hydrolysis-decarboxylation product **74**. When the reaction was conducted in MeOH/H₂O 1:4 and 5% NaOH at 80 °C overnight, no product at all could be detected. Changing the base for KOH did yield some **74** but the main product of the reaction was a side product **74b**, the product of a retro-Claisen condensation followed by hydrolysis (**Figure 4.11b**). Finally, doing the reaction in MeOH/H₂O 4:1 instead of 1:4 gave the desired product. In these conditions the retro-Claisen reaction was less likely to happen as the available quantity of hydroxy anion was decreased. Alkene **74** could be converted to **20** by ozonolysis.

Several procedures were attempted to convert **20** into **68** and **69** (**Figure 4.12**). Carboxylic acid **69** was obtained directly by oxidising **20** in presence of sodium chlorite and H₂O₂.¹⁸¹ A direct synthesis of the thioester from the aldehyde was attempted following a procedure developed by Huang *et al.*:¹⁸² **20** was dissolved in water along with *tert*-butyl hydroperoxide (TBHP) and *N*-acetylcysteamine (H-SNAC) **75** before pouring on catalyst FeBr₂. After stirring at 110 °C for 1 h, no trace of the thioester could be detected. A more classic way to get thioester is through the coupling of a carboxylic acid and a thiol. In a first two-step attempt, synthesis of the activated species **76** was tried by coupling carboxylic acid **69** and NHS, and DMAP and EDC as coupling agents. Unfortunately, this intermediate could not be isolated. In a one-step approach, the same reaction was tried with H-SNAC instead of NHS, this time successfully, giving the last wanted product **68**.

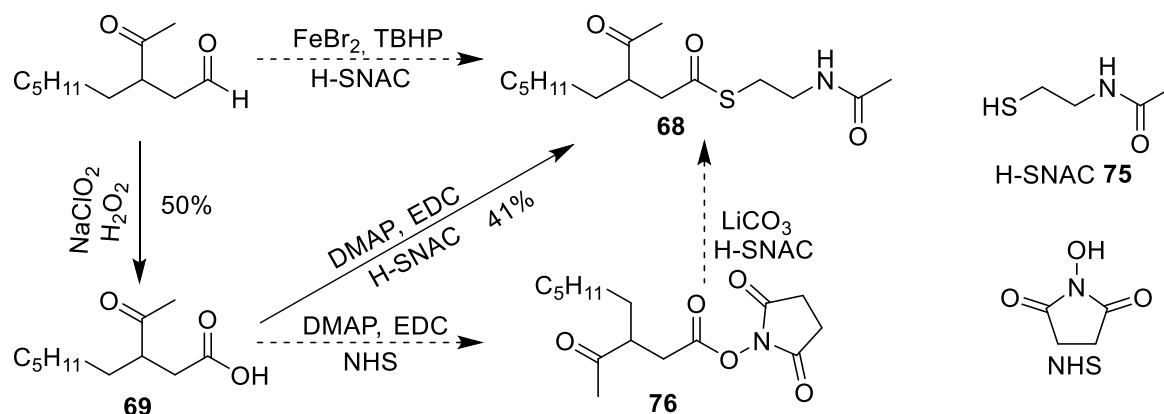


Figure 4.12: Conversion of 20 into 68

3.2. Method B: From 2-octanone to 3-acetyloctanoic acid

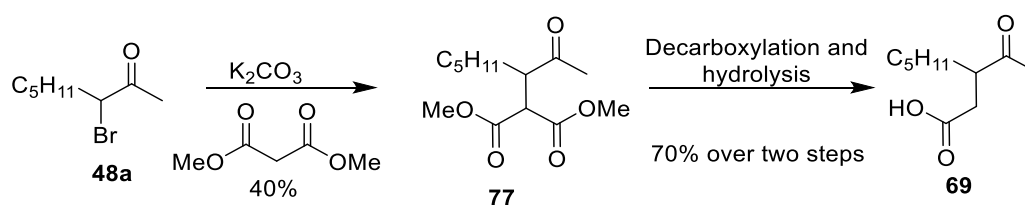


Figure 4.13: Formation of 69 from 3-bromo-octanone

A shorter approach to **69** was also investigated (**Figure 4.13**). Focusing the synthesis on the carboxylic acid allowed us to get either the thioester with the coupling reaction or the aldehyde through a redox process without having to make one to get the other.

3-Bromo-octan-2-one **48a** was obtained from 2-octanone following the method developed in Chapter 2. Dimethyl malonate addition could then be carried out on **48a** at 60 °C overnight, leading to the formation of **77**.

The synthesis of **69** then required hydrolysis of **77** and decarboxylation. To avoid incomplete hydrolysis, a large excess of KOH in MeOH/H₂O 4:2 was added to **77**, leading to diacid **78** (**Figure 4.14**).

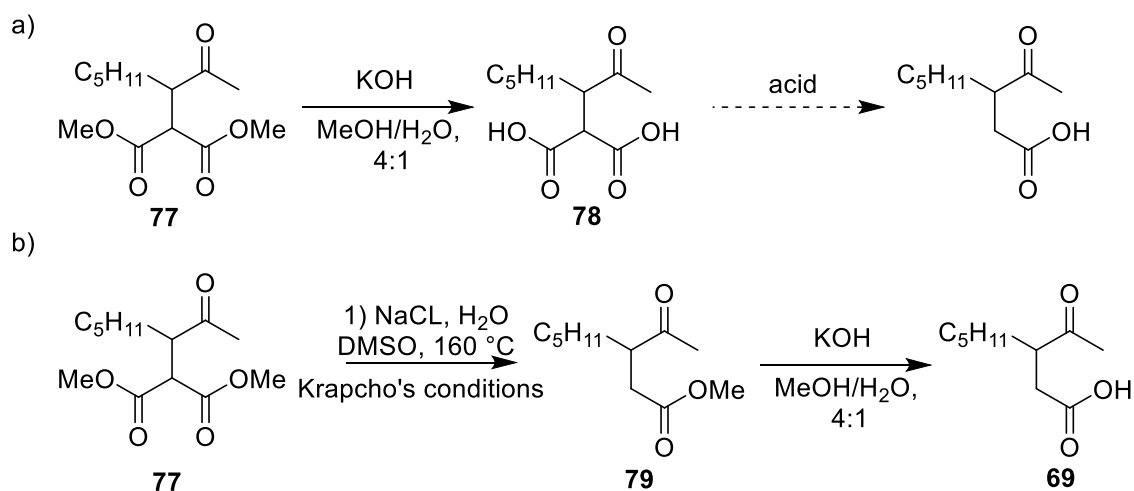


Figure 4.14: Methods investigated to convert 77 into 69; a) saponification followed by decarboxylation in acidic conditions (second step unsuccessful) b) Krapcho decarboxylation followed by saponification

However, even upon acidification of the reaction mixture, no decarboxylation was observed. A few conditions were tried (Table 4.1) but **69** could not be isolated in any cases. The formation of **69** was assessed by NMR spectroscopy by looking for doublets of doublet at 2.39 ppm and at 2.76 ppm (proton α to the carboxyl group). In some cases, proton NMR only showed peaks around 0.8 and 1.2 ppm, which suggests degradation of the products as none of the expected peaks of **69** or **78** were present.

Acid	Time	temperature	Results
H ₂ SO ₄	5 min	r.t.	Degradation
HCl	4 h	r.t.	Diacid 78
HCl	6 h	60°C then 80°C	Degradation
HCl	16 h	60°C	Traces of 69 but mainly degradation
acetic acid	3 h	60°C	Partial degradation; 69 present but could not be isolated

Table 4.1: Screen of decarboxylation conditions

Hence it was decided to perform decarbomethoxylation first, followed by hydrolysis. Following Krapcho's conditions,¹⁸³ **77** was dissolved in wet DMSO with NaCl and the mixture was heated up at 160°C overnight. DMSO was then washed away, leading to the intermediate **79** which could then be used without further purification. Carboxylic acid **69** could then be obtained by hydrolysis (see experimental).

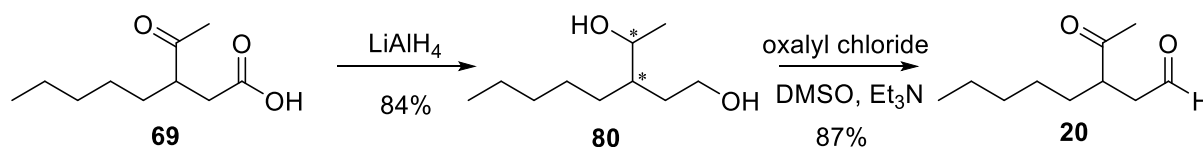


Figure 4.15: Two steps conversion of 69 into 20

68 was then synthesised following the same procedure as in section 3.2. Mild reduction conditions were tested to transform carboxylic acid **69** into aldehyde **20** without affecting the ketone. Carboxylic acid **69** was reacted with TMSCl before addition of DIBAL-H at $-78\text{ }^\circ\text{C}$ ¹⁸⁴ but after workup, no aldehyde could be detected. A two-step procedure was hence investigated, with first the reduction of both functional group to the alcohol followed by a mild oxidation to the dicarbonyl compounds. Test reactions were conducted with borane-dimethyl sulphide (BMS) as a reducing agent and pyridinium chlorochromate as an oxidant¹⁸⁵ as well as with LiAlH_4 as a reducing agent and Swern conditions for the oxidation.¹⁸⁶ The latter gave the most promising results and was investigated further. After treatment with LiAlH_4 , NMR spectroscopy analysis of the crude mixture was consistent with a mixture of diastereomers of diol **80** with very little impurities, confirming that it could be used without direct purification (**Figure 4.15**). The most noticeable impurity was BHT, a solvent stabiliser which fortunately does not significantly affect the reactions. Swern oxidation could be performed on the diol leading to the formation of the desired aldehyde **20**.

4. Complementation experiments

4.1. Qualitative assay

Similarly to the qualitative assays performed with H_2MAP analogues in Chapter 2, the capacity of aldehyde **20** and thioester **68** to restore pigmentation in *S39006* ΔpigD was first assessed. Two lines of the bacterium were streaked on Peptone Glycerol Media (PGM, see experimental for the composition) agar and cultured for two days. Aldehyde **20** or thioester **68** ($2\mu\text{l}$, 1M in DMSO) were then spotted next to the streaks and the plate was incubated a further 16 h at $30\text{ }^\circ\text{C}$. As illustrated in **Figure 4.16**, red colour was obtained in both cases, meaning that both compounds could be accepted as substrates.

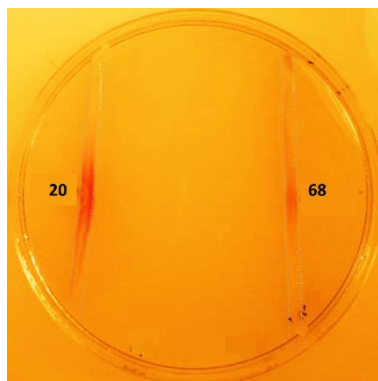


Figure 4.16: Chemical complementation of *S39006* Δ *pigD* with aldehyde 20 (left) and thioester 68 (right) Colour and contrast were digitally enhanced for better visualisation

4.2. Conditions for quantitative complementation assay with PigE substrate

Due to the position of the PigE-catalysed step in prodigiosin biosynthesis, chemical complementation with potential substrates of this enzyme can only be done on *S39006* Δ *pigD*.

4.2.1. Influence of the media

As shown in Chapter 3, culture in LBS supplemented with 0.25 M sorbitol (LBS) leads to an increase in pigment production. However, low phosphate media have also been shown to induce prodigiosin production¹⁵⁰ which explains why complementation assays on agar are performed with PGM. To compare the results with these two broths, prodigiosin produced by *S39006* was extracted in both cases (**Figure 4.17**):

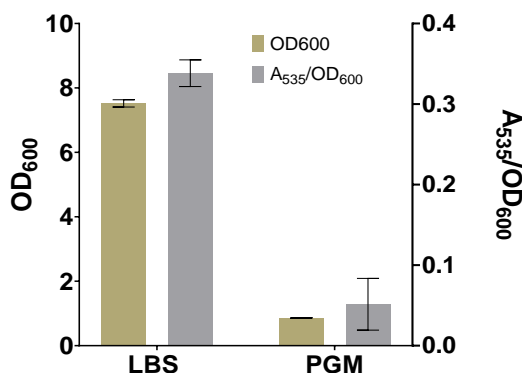


Figure 4.17: Prodigiosin production in different media

PGM is far less rich than LB, especially when an additional sugar like sorbitol is present. It was hence unsurprising that the final OD₆₀₀ would be lower in the case of PGM. The total pigmentation was lower as well (data not shown), but even the quantity of pigment per cell was about ten times lower in PGM than in LBS. The following experiments were therefore performed in LBS.

4.2.2. Influence of the substrate concentration

Uptake of molecules from the culture medium by the cells can vary a lot from one compound to another. Hence, before hoping to see pigmentation with **68**, it was important to determine what concentration was best with its aldehyde analogue **20**, which is known to be accepted as a substrate of PigE. The importance of this test was reinforced by the weakness of pigmentation obtained during agar qualitative complementation experiments (see **Figure 4.16**).

Pigment extracts were prepared from cultures of *S39006 ΔpigD* supplemented with different concentrations of **20** (**Figure 4.18**). For these experiments, the aldehyde was added to the culture at the same time as the inoculation with bacteria.

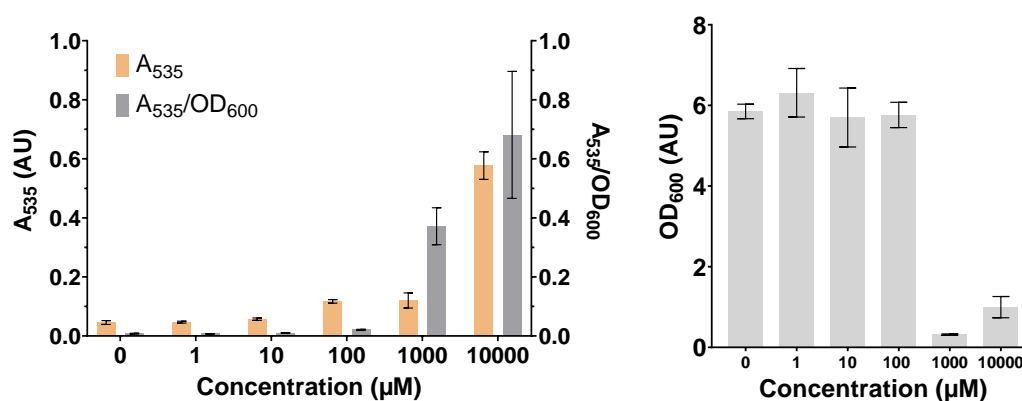


Figure 4.18: Effect of **20** concentration on growth (right) and pigment production (left) of *S39006 ΔpigD*

No effect was visible for concentrations lower than 100 μM . Yet, even at this concentration, both the total pigmentation and the quantity of pigment per cell remained relatively low. The real threshold was at 1 mM: at this concentration the pigmentation per cell was 10 times higher. However, the total pigmentation remained quite low. At 10 mM, both quantities were higher. It is important to make the distinction between these two quantities as the overall pigmentation needs to be high enough for good detection, whereas the pigmentation per cell indicated if the concentration was high enough for prodigiosin to be produced. In conclusion, both need to be high for a successful complementation assay. **Figure 4.18** (right) shows the final OD_{600} obtained with the different concentrations of **20**. The threshold observed for prodigiosin production was also visible here: from 1 mM the final OD_{600} was 10 times lower than in normal circumstances. This could be due to toxicity induced by the aldehyde **20**.

4.2.3. Influence of the OD₆₀₀ at the time of inoculation

As **20** seemed to prevent the growth of *S39006* at concentrations of interest, a “pre-culture” approach was investigated. The growth curve (see chapter 3, **Figure 3.12**) indicated that once OD₆₀₀ was around 4, the quantity of prodigiosin that can be expected was enough for satisfactory detection. LBS was inoculated with *S39006 ΔpigD* and cultured until OD₆₀₀ was around 4. Then 1 mM of **20** was added and the cells were cultured a further 16 h. Controls without **20** or where **20** was added at the same time as the bacteria were also prepared. OD₆₀₀ and pigmentation were measured in all three cases (**Figure 4.19**).

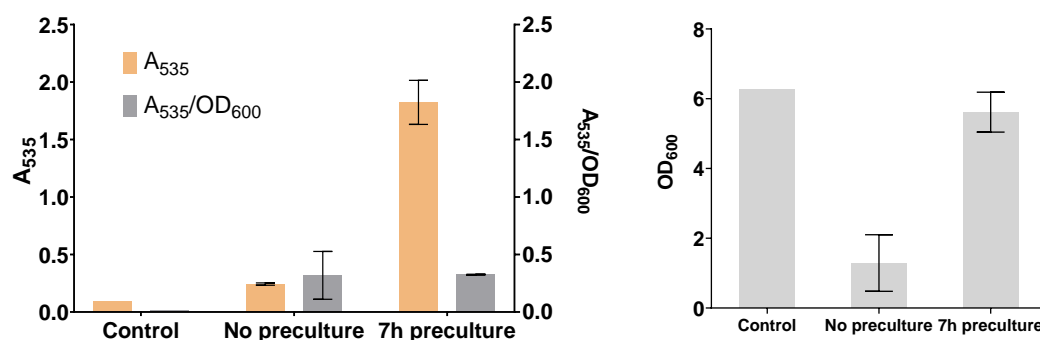


Figure 4.19: Effects of a preculture on pigment production (left) and growth (right) of *S39006 ΔpigD* complemented by **20**

The quantity of pigment per cell was the same in both samples inoculated with **20**, which meant that the uptake of the substrate was barely affected by the OD₆₀₀. However, the final OD₆₀₀ of the culture treated with **20** later was similar to a culture without **20** and much higher than the one treated with **20** at the same time as inoculation. Hence, pre-growing the cells until an OD₆₀₀ of around 4 is reached is a way to overcome toxicity issues and for pigmentation to be easily detectable. These conditions were chosen for further experiments with the other substrates.

4.3. Complementation assays with thioester **68**

4.3.1. Recovery of pigmentation

Following the procedure described above, extracts were prepared from *S39006 ΔpigD* supplemented with aldehyde **20**, thioester **68** and carboxylic acid **69** (**Figure 4.20**).

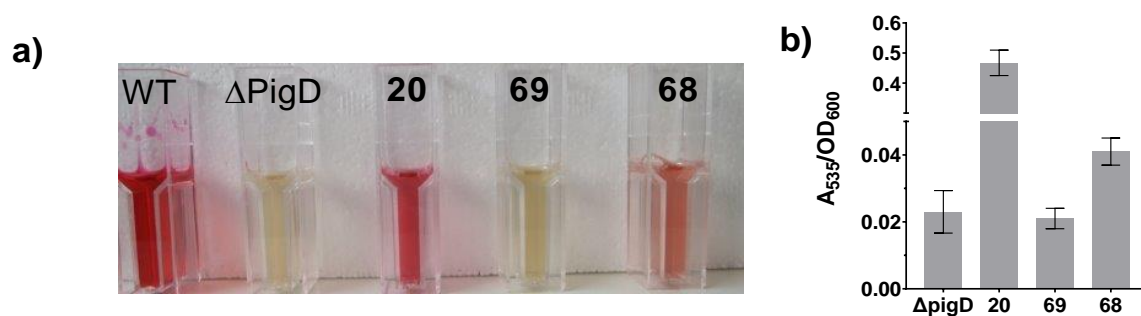


Figure 4.20: Complementation assays a) Pigment extracts, WT: *S39006*, $\Delta pigD$: *S39006 \Delta pigD* (negative control) unsupplemented, the number indicates which substrate were added, b) Pigmentation per cell

As illustrated in **Figure 4.20a**, both **20** and **68** triggered pigmentation, whereas both unsupplemented cultures and the ones supplemented with carboxylic acid **69** remained colourless. The absorbance at 535 nm confirmed this observation, with a quantity 3 times as high with bacteria fed with **68** than with the negative control or the carboxylic acid (**Figure 4.20b**). Yet, the results remained much lower than with the aldehyde. This might be due to a poorer uptake of the thioester or due to partial degradation of the thioester or because the NAC thioester is a poor mimic of the natural thioester. The absence of pigmentation in the case of the carboxylic acid proved that the thioester itself, rather than its hydrolysis product, was responsible for the pigmentation.

The results obtained with the negative control illustrated once again the capacity of *S39006* to produce compounds other than prodigiosin absorbing at 535 nm. As a result, it was necessary to prove that the pigment obtained by feeding with **68** was indeed prodigiosin

4.3.2. Time-course of pigment production

As in Chapter 3, pigment production was monitored after addition of **20** or **68** into 10 ml cultures of *S39006 \Delta pigD* (**Figure 4.21**). Pigment was visible in *S39006 \Delta pigD* fed with **20** after 2 hr, whereas pigment started to appear with the thioester only 12 h after the inoculation and the end level was much lower.

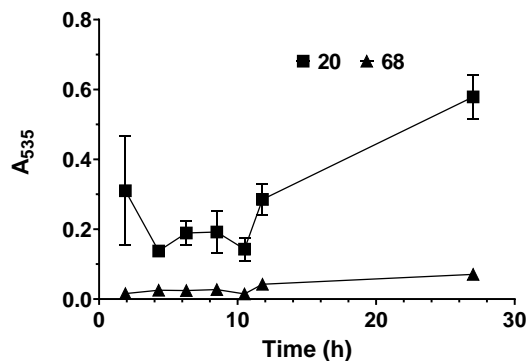


Figure 4.21: Kinetics of pigment production after complementation with 20 and 68.

This could be linked to a lesser capacity of the thioester to get into the cell or a lesser availability of the enzymatic domain responsible for its reduction.

4.3.3. Analysis of the pigment

Unfortunately, extracts of *S39006 ΔpigD* complemented with 68 were too dilute to detect prodigiosin by MS.

4.3.3.1. UV spectrometry

UV spectra of ethanolic extracts from *S39006*, *S39006 ΔpigD* and *S39006 ΔpigD* complemented with 68 were recorded (Figure 4.22). Because the absorbance was too high, the extracts from *S39006* were diluted 100 times. Extracts from *S39006 ΔpigD* complemented with 68 presented a peak at the same wavelength as the one from the wild type (WT). This peak was absent from extracts of unsupplemented *S39006 ΔpigD* and is consistent with prodigiosin.

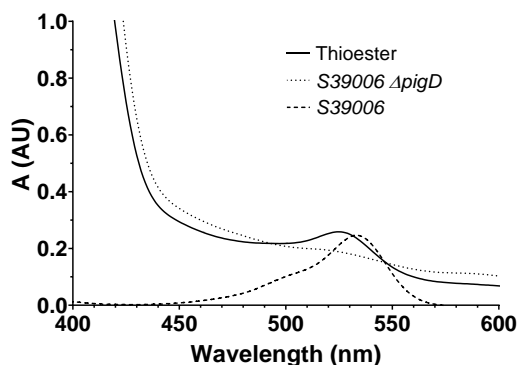


Figure 4.22: UV spectra of pigments extracts

4.3.3.2. HPLC

The pigment is known for its bright colour, and the UV/visible spectra above shows this method is viable to detect it. HPLC instruments usually have UV-Vis detectors, so comparing the HPLC traces at 500 and 535 nm of an extract from *S39006* and one from a complementation assay would indicate if prodigiosin was present in the extract or not.

Chapter 4: Characterisation of PigE

Using the conditions described by Eckeman *et al.* for the purification of pigment from *Sma* on extracts from *S39006* led to two peaks (**Figure 4.26**).¹⁸⁷ This could be explained either by a difference of retention time between prodigiosin's rotamers or the presence of two prodiginines. To discriminate between these two possibilities each peak was collected, concentrated and analysed by HPLC using the same solvent gradient (**Figure 4.27a**).

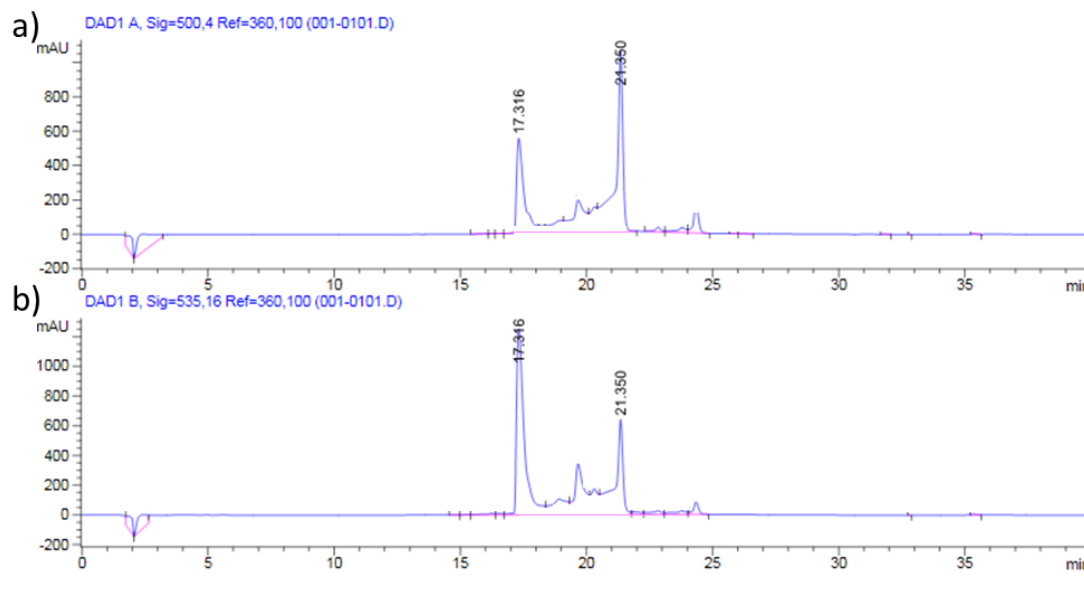


Figure 4.23: HPLC traces of *S39006* extracts a) detection at 500 nm, b) detection at 535 nm

Each peak gave a single peak when re-run on the HPLC (**Figure 4.23a**), which meant they were not rotamers but two distinct prodiginines. MS analysis (**Figure 4.23b**) showed that the first fraction contained a molecule with mass of 310.19, consistent with norprodigiosin **16**+H⁺ (see Chapter 1) while the second fraction had one of mass 324.21, consistent with prodigiosin **1a**+H⁺.

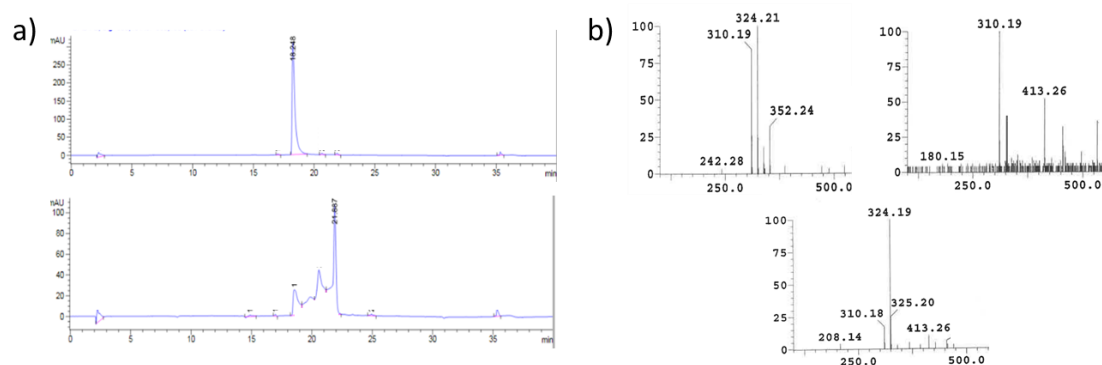


Figure 4.24: Analysis of the prodigiosin extract a) HPLC trace of the two peaks (top, peak at 17.3 min, bottom, peak at 21.3 min, detection at 535 nm); b) MS analysis, top left: crude extract, top right, peak at 17.3, bottom, peak at 21.3)

Pigment extracts from *S39006* Δ *pigB* supplemented with **68** were concentrated to dryness and re-dissolved in H₂O/ACN before being analysed on the HPLC using the method developed above

(Figure 4.25). The two peaks corresponding to the prodigiosin and norprodigiosin were present. This meant that MAP production was restored by the addition of **68**, which proves that *S39006* can reduce the thioester and incorporate it into prodigiosin biosynthesis.

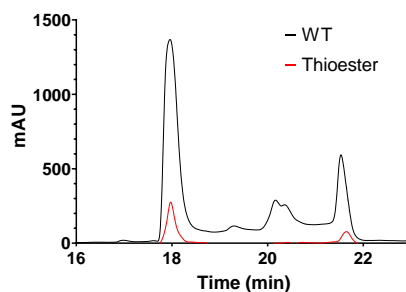


Figure 4.25: Superposition of HPLC traces of prodigiosin extracts from *S39006* (black) and *S39006* Δ *pigB* supplemented by **68** (red).

4.4. Investigation in the role of PigE in the thioester reduction

According to bioinformatics analyse (see Section 2), and previous work, PigE N-terminal domain (PigE-N) should be responsible for the reduction of thioester **68** whereas the C-terminal domain (PigE-C) catalyses the transamination of the resulting aldehyde **20** with ornithine. To demonstrate the role of the N-terminal domain, a strain expressing only PigE-C was constructed. Such a strain should be able to recover pigmentation when complemented with **20** but not with **68**.

4.4.1. Construction of a pQE80L::oriT *pigE*-C (pPigE-C) plasmid

pigE-C (from Met405 to Asp853) was amplified using primers MC01 and MC02 by PCR (see experimental). pBluescript (pBS) (see appendix) contains a multiple cloning site between *lacZ* and its promoter, thus preventing the expression of *lacZ* when a sequence with a stop codon is inserted. *LacZ*, which catalyses the hydrolysis of X-gal, producing a blue pigment, is not normally expressed by *E. coli* DH5 α . This makes the visualisation of successful insertion easier. PigE-C amplicons were cloned into pBS using *SacI* and *PstI* as restriction enzymes (see experimental) and *E. coli* DH5 α was transformed with the ligation mixture, leading to plasmid pBS-PigE-C. Five white colonies were obtained, and in all cases analysis of their plasmids was consistent with the desired construct: the double digested products showed two bands whose size corresponded to the insert (1.4 kb) and the vector (3 kb), while mono-digested product showed a single band whose size was consistent with the size of the vector and the insert ligated together. The sequence of the insert was confirmed by sequencing using primers oBS-F and oBS-R.

The construction of that intermediate plasmid was useful for the next steps, as it allowed us to be sure that the inserts were digested for the following ligations. This was used to clone *pigE*-C into pQE80L::oriT to give pPigE-C, a plasmid coding for PigE-C with a N-terminal His₆ tag which

was then used to transform *E. coli* DH5 α , leading to 14 colonies. Analysis of their plasmids showed that only one was consistent with pPigE-C, which was confirmed by sequencing using primers oQE-F and oQE-R.

4.4.2. Preparation of strain *S39006* Δ *pigE* pPigE-C

Transformation of *S39006* and its mutants is challenging. Attempts to transfer plasmid either by electroporation or chemical transformation were unsuccessful. However, *S39006* has been shown to incorporate plasmids readily by conjugation,¹⁸⁸ i.e. direct transfer of DNA from one bacterium to another. pPigEC was used to transform *E. coli* β 2163 (noted β 2163) leading to the formation of strain β 2163 pPigE-C. β 2163 is diaminopimelic acid (DAPA)-dependent, which drives the selection after the conjugation. Cultures of *S39006* Δ *pigE* and β 2163 pPigE-C were mixed in a LB+DAPA broth and, after an overnight culture, plated on LBA supplemented with ampicillin but without DAPA (see experimental). Sixteen colonies hence obtained were replated on LB with ampicillin and cultured overnight. Their plasmids were then extracted, and digestion and sequencing analysis showed they were all consistent with the desired pPigE-C.

4.4.3. Verification of *S39006* Δ *pigE* pPigE-C

S39006 Δ *pigE* was constructed to have a deletion of nucleotides 9 to 2553 in *pigE* (*pigE* is 2561 bp long).²⁶ Primers MC04 and MC05 were designed to match the sequence 250 bp before and after the deletion. One colony each of *S39006*, *S39006* Δ *pigE* and newly formed *S39006* Δ *pigE* pPigE-C were analysed by colony PCR using these primers (see experimental) (Figure 4.26).

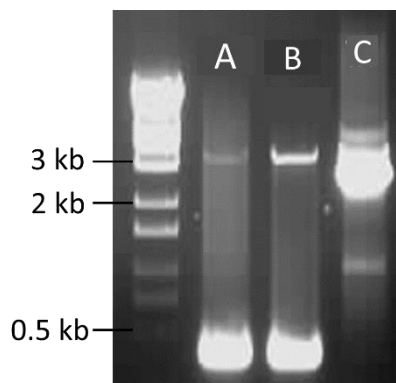


Figure 4.26: Agarose gel of the colony PCR of *S39006* Δ *pigE* pPigE-C (A), *S39006* Δ *pigE* (B) and *S39006* (C) using MC04 and MC05 as primers. Ladder from Henrici *et al.*¹⁸⁹

As expected, the two Δ *pigE* strains showed a strong band at 500 bp whereas the *S39006* strain showed an amplicon around 3 kb. A faint band around 3 kb was also observed in *S39006* Δ *pigE* pPigE-C, but sequencing was inconclusive, meaning this was probably just non-specific amplification. Sequencing of the 500 bp band, on the other hand, was consistent with the

Chapter 4: Characterisation of PigE

sequence on each side of the deletion. This experiment confirmed that the strain is indeed unable to produce full length PigE.

Conditions for efficient protein expression were then investigated: *S39006 ΔpigE* pPigE-C was cultured in LBS at 30°C and was inoculated with different concentrations of IPTG when OD₆₀₀ reached 2. Aliquots were taken before the induction and at the end of the experiment and cell concentrations were equalised before lysing the cells by boiling. The proteins contained in the cell lysates were separated by SDS-PAGE before being analysed by Western blot using a mouse anti His₆ primary antibody (**Figure 4.27**).

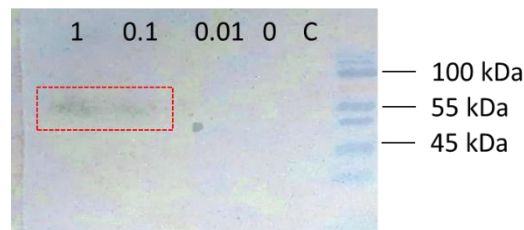


Figure 4.27: Western blot of lysates of *S39006 ΔpigE* pPigE-C induced with different concentrations of IPTG (concentrations shown in μM) C: *S39006 ΔpigE* lysate

Bands could be observed in the Western blot at sizes consistent with PigE-C. It is to be noted that nothing was visible before the induction (data not shown) or at IPTG concentrations lower than 100 μM. The solubility of the protein was also assessed: *S39006 ΔpigE* pPigE-C was cultured at 30°C in LBS to OD₆₀₀ = 1 and 1 mM or 100 μM of IPTG was added. For each concentration, one sample was then cultured at 16 °C whereas the other remained at 30°C. *E. coli* BL21 pPigE-C and, as negative control, *S39006 ΔpigE* were also cultured, with the appropriate IPTG induction. After 16 h cell lysates were prepared. Soluble and insoluble fractions were separated by centrifugation and the insoluble fraction was resuspended in 1 ml of water. Two SDS-PAGE gels of the different fractions were run, and one was used for Western blot whereas the other was directly stained with Coomassie blue (**Figure 4.28**).

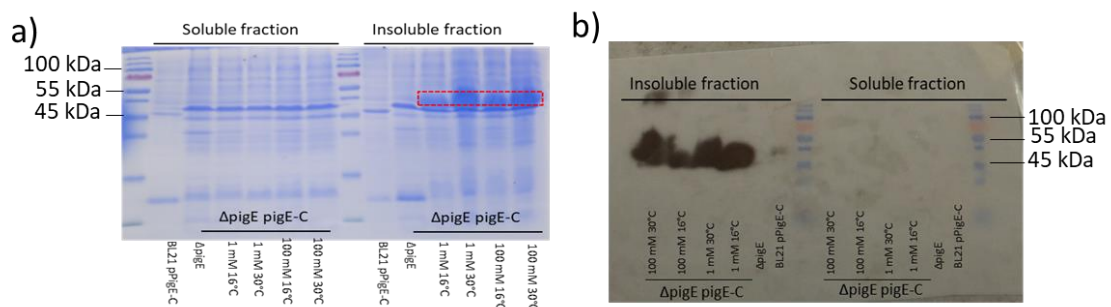


Figure 4.28: SDS-PAGE analysis of PigE-C a) Coomassie staining, b) Western blot

It appeared that PigE-C was mainly in the insoluble fraction, meaning that isolation and purification would be difficult. Hence, it was decided to use the strains primarily for *in vivo* testing. Furthermore, the intensities of the bands were similar with all four conditions tried with *S39006 ΔpigE* pPigE-C, meaning that the temperature of incubation had little importance. This will allow the chemical complementation experiments to be conducted as before. Interestingly, the bands were stronger than when the IPTG was added after OD₆₀₀ had reached 2, suggesting these conditions were more suitable for protein expression. The bands obtained with BL21 were weak, but this might be because the OD₆₀₀ was too high when IPTG was added. This also showed that the formation of insoluble aggregates was not simply due to the high concentration in *S39006*, as no band was visible in the *E. coli* soluble fraction despite the lower concentration.

In conclusion, the strain that was constructed cannot express full length PigE but, when induced with IPTG, can produce the PigE C-terminal domain, although in insoluble form.

4.4.4. Complementation assay with *S39006 ΔpigE* pPigE-C

Qualitative agar assays were conducted with *ΔpigE* and *ΔpigE* pPigE-C and **20** and **68** as substrate (**Figure 4.29**).

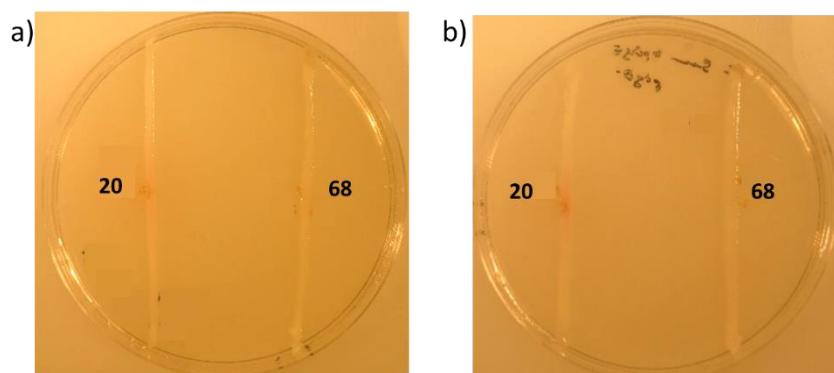


Figure 4.29: Complementation of *S39006 ΔpigE* (a) and *S39006 ΔpigE* pPigE-C (b) with **20 and **68**** Thioester **68** seems unable to trigger pigmentation in either *ΔpigE* or *ΔpigE* pPigE-C strains. Strangely, aldehyde **20** seemed to be accepted by both *S39006 ΔpigE* pPigE-C and *S39006 ΔpigE* despite the absence of the transaminase.

To get quantitative results, prodigiosin extracts were prepared from LBS cultures of the strains mentioned above as well as *S39006 ΔpigD*, inoculated with 1 mM of **20** and **68** (**Figure 4.30**).

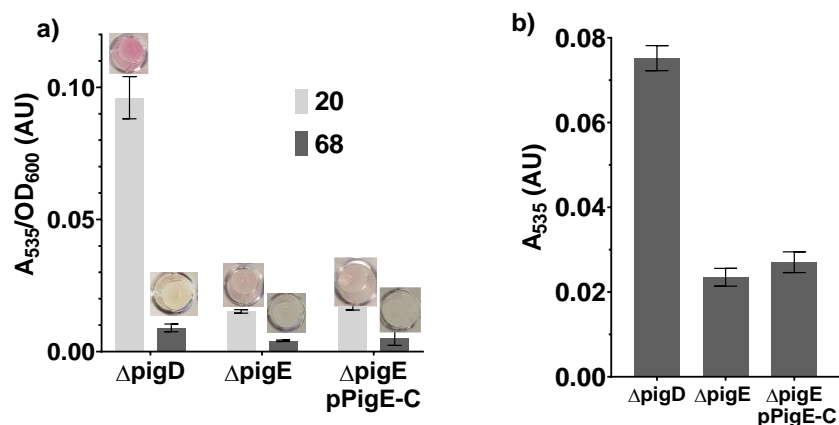


Figure 4.30: Pigmentation of different *S39006* strains supplemented with 20 or 68 a) Results with 20 and 68, a picture of the well is given on top of the bar, b) Focus on the results with 68

The results were congruent with the qualitative assays: as expected pigmentation was observed with both substrates in the case of *S39006* $\Delta pigD$. On the other hand, **68** did not trigger any pigmentation with strains not expressing *pigE*. Finally, **20** restored pigmentation to the same low level in *S39006* $\Delta pigE$ and *S39006* $\Delta pigE$ pPigE-C. It is likely that a non-specific transaminase was responsible for the formation of H₂MAP in both strains. Alternatively, the aldehyde might have been transformed into MAP by action of the ammonia generated during bacterial growth.¹⁹⁰ Unfortunately, this phenomenon hides any potential activity of PigE-C. This preliminary experiment had been run without IPTG as pQE vectors are known to be leaky and at least low levels of PigE-C expression were expected. *S39006* $\Delta pigE$ pPigE-C was fed with **20** in presence of different concentrations of IPTG (Figure 4.31). No significant difference in prodigiosin production was observed, meaning that, even if it expressed, PigE-C was either inactive or at least not as active as the non-specific transaminase.

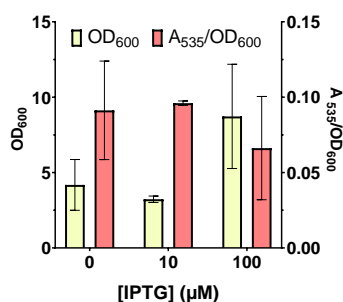


Figure 4.31: Influence of IPTG on pigment production in *S39006* $\Delta pigE$ pPigE-C

Conclusion: a non-specific transaminase hides any potential effect of PigE-C and it is hence impossible to conclude about the transaminase activity of that protein. Thioester **68** did not lead to the recovery of pigmentation with *S39006* $\Delta pigE$ in any of the attempts, but it did with *S39006* $\Delta pigD$, suggesting that PigE was necessary for the reduction of that thioester.

5. *In vitro* characterisation of pigE

In vivo experiments suggested that PigE was a bifunctional protein, responsible for both the reduction of a thioester and the subsequent transamination of the resulting aldehyde. Yet, those experiments have limitations, for instance it is impossible to use them to determine the cofactor involved in the thioester reductase activity with this method. Two approaches were followed to overcome these challenges: isolation and purification of PigE and the use of cell-lysates. Cell lysates are relatively complex mixtures and the quantity of protein of interest cannot be accurately assessed in those conditions. However, proteins in cell lysates are more likely to be active as they undergo less steps between the lysis and the assay. In addition, the activity of transmembrane proteins can be tested in cell lysates. Cell-lysates also give the possibility to perform coupled assays, using several proteins which would have been difficult to isolate together. Using pure proteins, on the other hand, gives a perfect knowledge of the reaction mixture, including the concentration of the protein, which is necessary for kinetic studies.

5.1. Construction of BL21 pPigE and expression of the protein

A similar approach to the construction of plasmid pPigE-C was followed: *pigE* was first amplified by PCR from S39006 gDNA using primers MC01 and MC03. After cloning into pBS and using the resulting vector to transform *E. coli* DH5 α , white colonies had their plasmid extracted and digested (**Figure 4.32**).

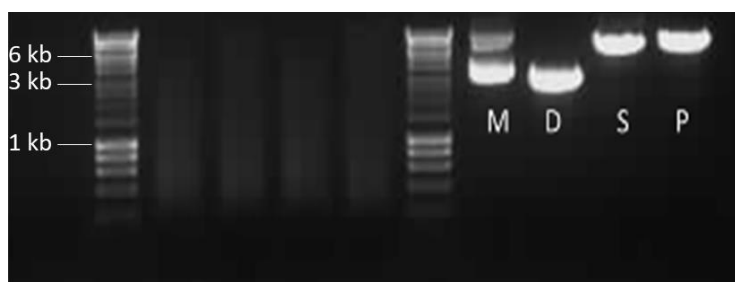


Figure 4.32: Agarose gel of digested plasmids from some white colonies M: miniprep, D: double digest, S: digestion with SacI, P: digestion with PstI

It appeared that a number of colonies were false positive. Yet, some colonies gave results consistent with the desired plasmid: the monodigested samples (S and P in **Figure 4.32**) were bigger than the double digested one and all digested plasmids were different from the miniprep, proving that the restriction enzymes were active. Only one band was visible with the double digest but pBS is 3 kb long whereas *pigE* is 2.5 kb long, so the two bands were supposed to come close to each other and it is likely that, in the settings for this particular gel, they actually superposed. This plasmid was sent for sequencing and the results were consistent with a *pigE* insert, confirming the formation of plasmid pBS-PigE

pBS-PigE was digested by SacI-HF and PstI-HF along with pQE80L::oriT, and the digested products were run on an agarose gel until a clear separation of the pBS and *pigE* bands was observed. The relevant bands were extracted and used for ligation. After transformation, plasmids were extracted from colonies resistant to ampicillin and plasmids consistent with pPigE were sent for sequencing with primers specific for pQE (oQE-F and oQE-R) and *pigE* (MCO1 and MCO3), which confirmed they had a pQE vector with a *pigE* insert. This plasmid was then used to transform *E. coli* BL21.

5.2. Protein expression and purification

Preliminary experiments to determine expression conditions were conducted. On the one hand, BL21 cells were grown in LB until $OD_{600} = 1$ and 10 mM of IPTG was added before growing the cells for a further 1 h at 37 °C. On the other hand, IPTG was added at $OD_{600} = 0.8$ and the cells were grown a further 16 h at 16 °C. Aliquots were taken before the addition of IPTG and at the end of the experiment. Quantities of cell were normalised, and the samples boiled to lyse the cells. They were analysed on an SDS-PAGE gel (**Figure 4.33**). Bands at a size corresponding to PigE (95 kDa) could clearly be seen in the second set of conditions and not in the first.

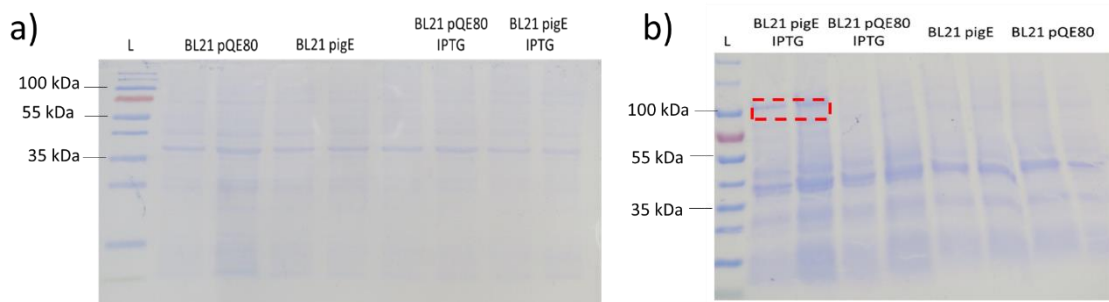


Figure 4.33: SDS-PAGE of cell lysates obtained with different protein production conditions a) Incubation for 1 h, b) incubation 16 h; the gels are Coomassie stained

pPigE codes for the expression of PigE with an N-terminal His₆-tag, it can therefore be purified by affinity column with a Ni-NTA resin. PigE was hence isolated from one litre of culture. The proteins in the different fractions were analysed by SDS-PAGE (**Figure 4.34**). **Figure 4.34a** confirmed that the protein expression was successful. It also indicated that PigE seemed to partly be in the insoluble fraction, either because of the formation of aggregates, the presence of a transmembrane domains or simply because of a poor cell lysis. Yet, the soluble fraction showed a band in the proper region and some elution fractions also showed a band at the proper size, indicating that some of PigE still goes into the soluble fraction and could be purified. Excess imidazole was then removed by dialysis.

Chapter 4: Characterisation of PigE

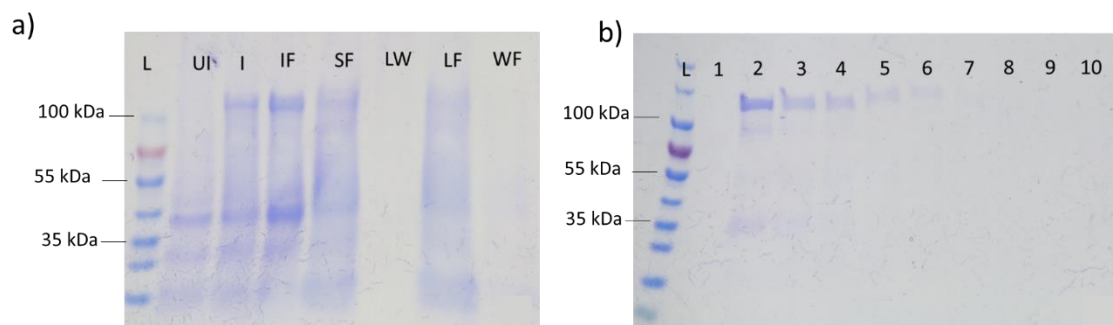


Figure 4.34: SDS-PAGE of fractions from purification of PigE by affinity column a) L: Molecular weight markers, UI: uninduced sample, I induced sample, IF: insoluble fraction, SF: soluble fraction, LW: Lysis wash, LF: lysis flow through, WF: wash flow through, b) elution fractions

Bio-Rad DC protein assay showed that 0.4 mg of protein had been isolated. A UV spectrum was also recorded (**Figure 4.35**). The characteristic absorbance peak of proteins (280 nm) was present; but no peak was visible between 300 and 800 nm.

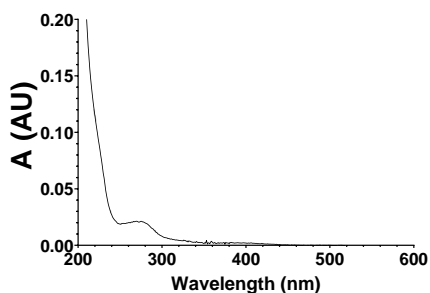


Figure 4.35: UV spectra of PigE purified without PLP in the buffers

As PigE is a PLP-dependent transaminase, it should absorb at 410 nm because of the Schiff's base it forms with its cofactor (see Section 1). It seemed that PLP was not incorporated in this batch. To circumvent this problem, 0.05% pyridoxine HCl was added to culture media and 1 mM of PLP was added to all purification buffers. PigE was purified under those conditions and its UV/Visible spectrum was measured after a dialysis removed the excess pyridoxine (**Figure 4.36**): it indicated the presence of PLP.

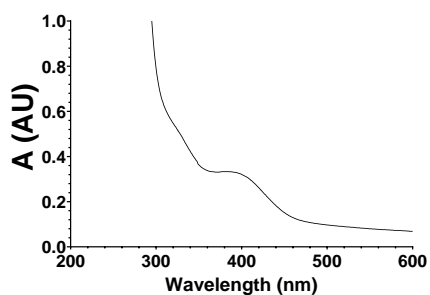


Figure 4.36: UV spectra of PigE (1 mg/ml) purified with additional PLP in the buffers

Yet, only 1 mg of protein was obtained from 1 L of culture, so other conditions were explored to improve the yield: different concentrations of IPTG were tested, as well as the addition of 1% Triton X100 in the lysis buffer. As illustrated in **Figure 4.37**, no obvious differences could be seen between the soluble fractions arising from these conditions.

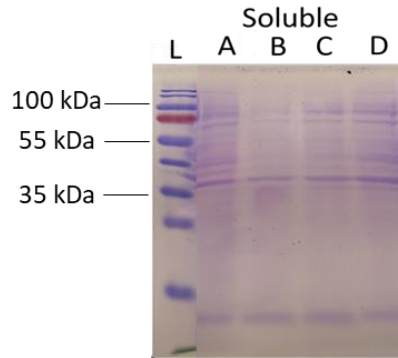


Figure 4.37: SDS PAGE of soluble fraction obtained with different PigE production conditions A: pQE80L, [IPTG]= 1 mM (negative control), B: pPigE [IPTG]=1 mM, C pPigE [IPTG]= 0.1 mM, D: pPigE, [IPTG]= 1 mM, 1% Triton X100

Triton X100 is supposed to affect mainly the efficiency of the lysis and the solubility of proteins, which should result in an increase of concentration of the soluble fraction, confirmed by DC assay. Unfortunately, when purification was carried all the way in those conditions, two bands at 35 kDa and 70 kDa appeared, suggesting a degradation of the protein. To investigate this phenomenon, two samples were lysed, one with Triton X100 (T⁺) in the buffer and the other without (T⁻). Furthermore, 2 tablets of protease inhibitor were added to T⁺. Analysis of the elution fraction after the Ni-NTA column on SDS-PAGE (**Figure 4.38**) showed that, in both cases, these extra bands were present, but their intensity compared to the band of interest was very low.

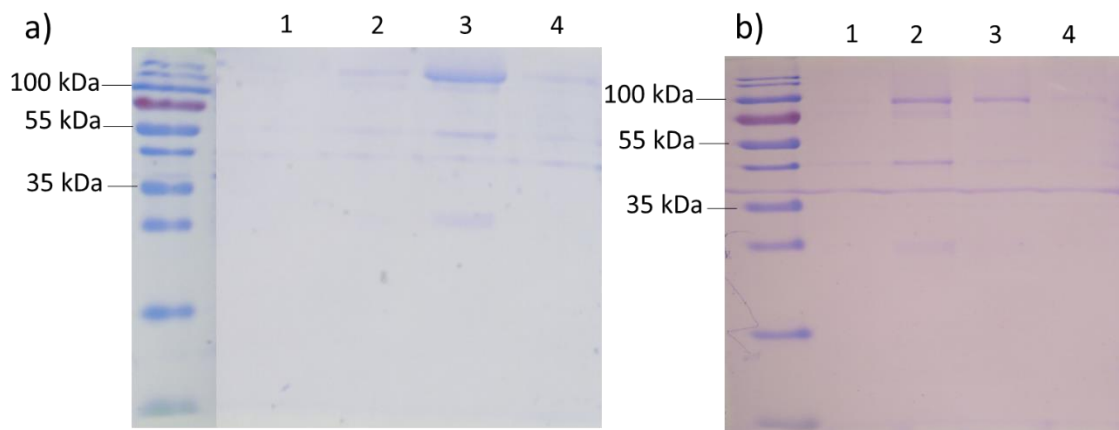


Figure 4.38: Elution fraction when Triton X was used for lysis a) T⁻, b) T⁺

Furthermore, a Western blot showed that only the band corresponding to PigE had the His₆ tag. Purification of PigE with addition of Triton X100 in the lysis buffer and proteases inhibitor tablet in the elution buffer worked, but the improvement in the total quantity of protein obtained was marginal. To get more protein, the purification process was scaled up four-fold. The amount of resin had to be increased accordingly: as more protein was loaded on the Ni-NTA column with this approach, some unspecific binding occurred and the resin could saturate, leading to the loss of some PigE when the soluble fraction was flowed through the column. Using a gradient during the elution was a way to tackle unspecific binding: by increasing the concentration of imidazole progressively, most of the impurities were washed off before the desired protein, justifying the use of mixtures of wash buffer/elution buffer. Using this method, 14 mg of PigE was isolated. The yield was similar to the previous smaller scale culture, but the total quantity of protein obtained was enough for downstream applications.

5.3. Protein characterisation

5.3.1. Circular dichroism¹⁹¹⁻¹⁹³

Circular dichroism (CD) measures the difference in absorbance of the two directions of circularity of circularly polarised light. In proteins, secondary structures such as α helices and β sheets have signature CD profiles in the far UV. Hence recording such a spectrum allows the proportion of the different secondary structures in the overall folding to be estimated and indicates if the proteins are correctly folded.

CD spectra of a fresh batch of PigE and an older one were recorded. This confirmed the impression given by SDS-PAGE gels, that PigE was not stable enough to be kept any extended period of time, even at 0°C. The results were much better with the fresh batch (**Figure 4.39**).

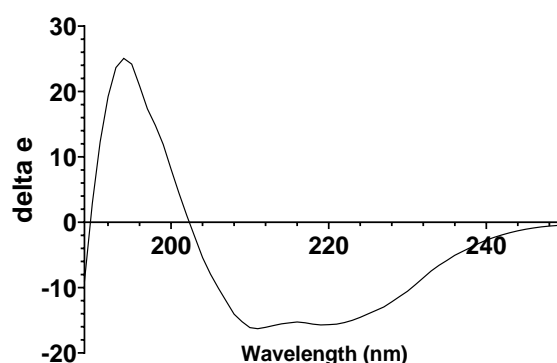


Figure 4.39: PigE CD spectra

This proved that the purification process does give a folded protein. Further analysis using Dichroweb website gave the following results (**Table 4.2**):

Algorithm	Set	Helix 1	Helix 2	Strand 1	Strand 2	Turns	Unordered
Selcon 3 ¹⁹⁴	4	0.607	0.211	-0.017	-0.002	0.097	0.125
Contin ¹⁹⁵	4	0.549	0.156	0.009	0.009	0.075	0.202

Table 4.2: Fitting of PigE CD spectra

Fitting with the Contin algorithm match the data best, but the values were in the same range with the two algorithms. The values extracted from the CD spectra did not match PHYRE predictions (see section 2) exactly, but were relatively close, and both PHYRE predictions and curve fitting results present some uncertainty. The high percentage of α -helixes is noteworthy as it is consistent with a folded protein.

5.3.2. Thermal shift assay

This assay monitors the stability of a protein as a function of temperature. A fluorescent dye, here SYPRO orange, binds to the hydrophobic regions of the protein. When the protein starts to unfold because of temperature elevation, more hydrophobic regions become exposed, leading to an increase of fluorescence. As the temperature continues to increase, vesicles start to form, decreasing the exposed surface of the protein and the fluorescence decreases. The inflexion point in the increase of the fluorescence (or the maximum of the derivative curve) corresponds to the melting temperature (T_m) of the protein. The presence of ligand often increases the stability of a protein, leading to an increase of T_m . Thermal shift is hence a quick way to characterise the stability of a protein and to screen for potential ligands.

PigE was subjected to this assay (see experimental) against a range of potential substrates: **68**, NADH, NADPH and a number of amino acids (**Figure 4.40**).

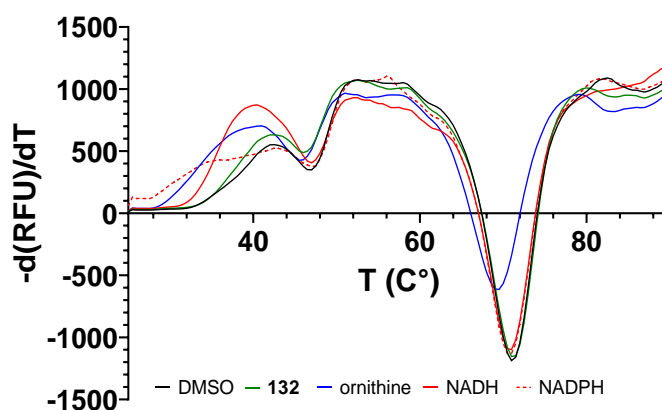


Figure 4.40: Examples of the derivative of the thermal shift curves obtained with PigE. The substrates represented here are the one which were most likely to bind

The profile of the curve obtained was unusual: most proteins have their T_m around 40-50°C, whereas here a T_m around 71.25 °C was obtained. An inflexion at 47 °C was visible, which would be more consistent with a protein T_m , but its intensity was much lower than the one at 71.25 °C. Another unusual aspect was that the fluorescence decreased before the increase leading to the melting point. These observations might have been the result of different phenomena: for instance, PigE is rather unstable and even though the quality of the sample was checked shortly before the assay, degradation cannot be excluded. It is also possible the two domains of PigE have different melting points, the first one unfolding at 47 °C, leading to the formation of vesicles which explains the decrease in fluorescence until the second very stable domain unfolds at 71 °C.

Compound	Control DMSO	Control buffer	68	NADH	Ala	Asn	Cys	Glu	Gln	Gly	Ser
ΔT_m 47°C	0	-0.25	-0.50	-0.25	-0.75	0.25	-0.5	-1.5	-0.5	0	-1
ΔT_m 71.25°C	0	-0.5	0	-0.5	-1.25	-0.5	-1.25	-1.75	-1.38	-0.88	-1.25

Compound	Tyr	His	Orn	Ile	Lys	Phe	Thr	Val	NADPH
ΔT_m 47°C	-0.25	-1.25	-2.5	-1.5	NA	-1.75	-0.75	-0.5	0.5
ΔT_m 71.25°C	-1.25	-2	-1.88	-0.88	-0.88	-1.75	-1.75	-1	-0.75

Table 4.3: Thermal shifts

No significant thermal shifts at 47 °C or at 71 °C were observed with the added ligands (Table 4.3) and none of them led to an increase of T_m . The thioester reductase activity necessitates binding of either NADH or NADPH whereas the transaminase domain requires the presence of an amino acid, ornithine according to previous studies. This casts some doubt on the validity of this assay.

5.3.3. NAD(P)H monitoring

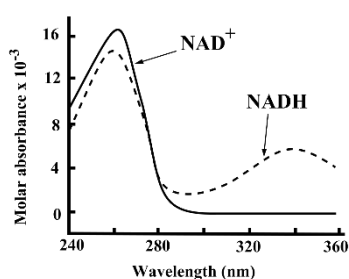


Figure 4.41: UV absorbance spectra of NAD^+ and $NADH$ ¹⁹⁶

NAD(P)H absorbs at 340 nm whereas its oxidised counterpart does not (Figure 4.41).¹⁹⁶ Monitoring the absorbance of a mixture hence allow one to follow the quantity of reduced and oxidised cofactor. Interestingly, NAD(P)H present the same profile in TRIS, KPi, citric acid and HEPES buffers.

Stock solutions of NADH and NADPH at 2 mM in 0.02 M aqueous NaOH were prepared following Sigma's recommendations. These solutions were supposed to maximise the stability of the reduced cofactor. After checking that NAD(P)H was still in its reduced form,

the different components - including at least the thioester substrate **68**, NAD(P)H and ornithine (see experimental)- were mixed and the absorbance at 340 nm was monitored (**Figure 4.42**).

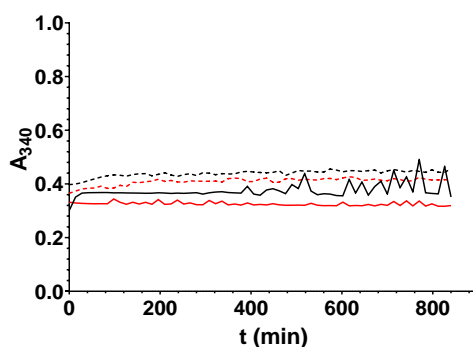


Figure 4.42: Evolution of A_{340} Black: NADH, Red NADPH, plain: control, dotted: Complete mixture, [PigE] = 1 μ M.

Two different concentrations of enzyme were tried (1 μ M and 10 μ M), but the evolution of the absorbance did not seem to be different from the control with cofactor only in any of the cases. NAD(P)H monitoring experiments were carried with and without metal ions in the mixture, but no difference could be observed. Even though the concentrations of protein were relatively low, they were in the same range as some literature examples.⁴⁰ Hence it appeared that no thioester reductase activity could be observed under these conditions. Similar results were obtained when the experiment was performed in other buffers (KPi, citric acid and HEPES).

This set of experiments was disappointing: either NAD(P)H was not the cofactor involved in the thioester reduction, or PigE was simply inactive under the conditions chosen for the experiment. It is also possible that the kinetics of PigE were slower than NAD(P)H atmospheric oxidation either because the concentrations were too low or because the N-acetylcysteamine thioester **68** was a poor mimic of the natural substrate. It is also possible that PigE forms a complex with some other protein(s) or ligand(s) that are removed in the purification process and hence it loses its activity. Finally, it was mentioned that PigE was visible in the insoluble fraction and it is possible that it needs to be inserted in a membrane to be active.

5.4. Cell extracts assays

By choosing carefully the strain used to prepare a cell extract, a wide variety of assays can be performed. For instance, PigE activity can be assessed indirectly, by monitoring the activity of enzymes further down the line in prodigiosin synthesis. PigE thioester reductase activity could also be monitored using the NAD(P)H technique described above.

5.4.1. Coupled assays

5.4.1.1. Following MAP production

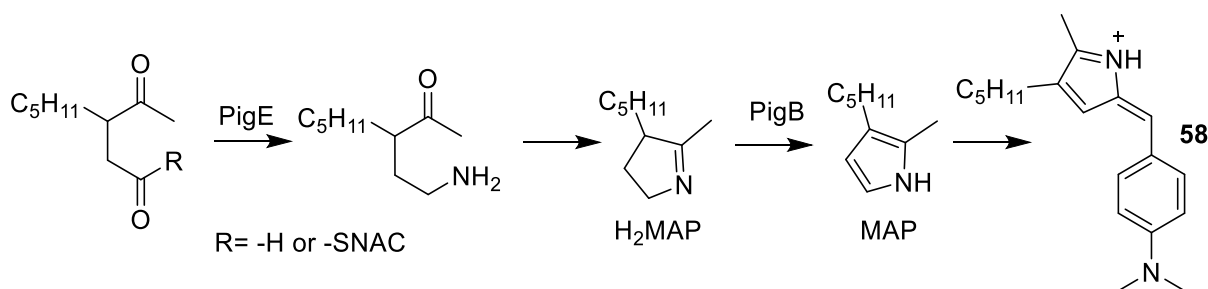
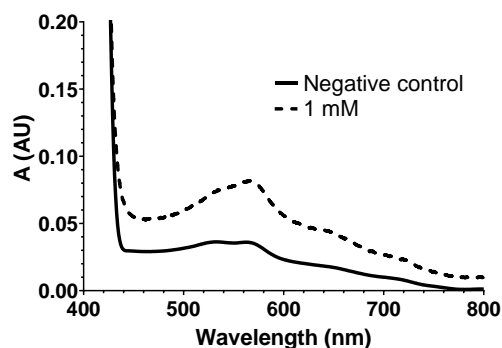


Figure 4.43: Method to follow MAP formation using Ehrlich's assay

In Chapter 2, we described a way to quantify the formation of MAP (or an analogue) by reacting it with the Ehrlich's reagent (*p*-N,N-dimethylbenzaldehyde **57**), leading to the formation of a red compound **58** with a maximum absorbance at 555 nm. This allowed to measure the activity of HapB in presence of different analogues of H₂MAP. As illustrated in **Figure 4.43**, the aim here is to use MAP as an indirect indicator of PigE activity. The cell extracts contained both PigE and PigB, hence it was hypothesised that, in those conditions, the product of PigE could be accepted by PigB and transformed into MAP.

To make sure that no substrate of PigE would be present in the lysate, the extracts were prepared from *S39006 ΔpigD*. The procedure to prepare the lysates was very similar to protein purification, but without the purification step (see experimental).

The activity of PigB in the soluble fraction was checked before going forward with the coupled assay. The extract was diluted in MES buffer and H₂MAP was added (1 mM) before incubating for 10 min. The reactions were then stopped, and Ehrlich's reagent was added. UV/Vis spectra of the samples were recorded, leading to **Figure 4.47**.

Figure 4.44: UV/Vis spectra of cell extract reacted with H₂MAP and Ehrlich's reagent

After 10 min, it appeared that when the extracts and H₂MAP were incubated together, the mixtures turned pink after the addition of Ehrlich's reagent, whereas, in the control without

protein the sample remained colourless. However, the increase of absorbance remained low. Nevertheless, this shows that, despite it being mainly insoluble, PigB activity could be observed in this sample.

As complementation assays were consistent with PigE transaminase activity, the coupled assay was tested by incubating the extract with a mixture of **20**, ornithine and PLP before performing Ehrlich's assay (**Figure 4.45**).

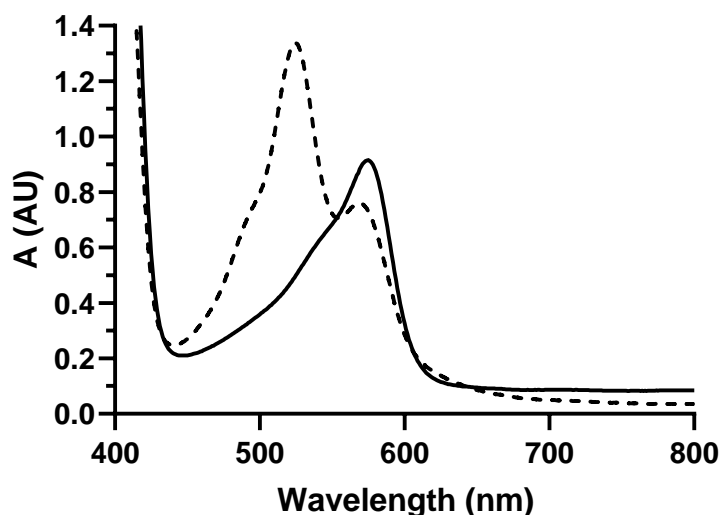


Figure 4.45: Two replicates of coupled assays using Ehrlich's reagent

The results obtained were extremely variable. In particular, the UV/Vis spectra often showed two peaks at 530 and 570 nm. Ornithine can react directly with **20** without enzyme catalysis, leading to the formation of amine **81** (**Figure 4.46**). Then, in presence of strong acid such as perchloric acid, **81** can be converted into pyrrole **82**, which would react with Ehrlich's reagent. This might be the cause for the second peak that was observed during the coupled assay. This side reaction, combined with the observed lack of repeatability of the test, made this assay a poor solution to study PigE.

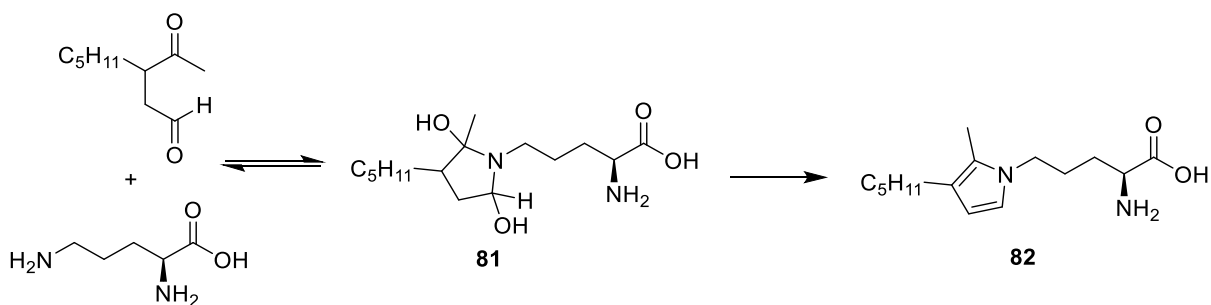


Figure 4.46: Ornithine can lead to a false positive with the Ehrlich's reagent

5.4.1.2. Following prodigiosin production

Cell extracts have been used to study PigC by measuring the production of prodigiosin.¹³⁷ Furthermore, cofactors needed by PigE, PigB or PigC have a strong absorbance in the near UV but almost none at 535 nm, making the monitoring of even very a small quantity of pigment possible. Another advantage of this approach was the very low risk of false positive as it relies on a direct measurement of prodigiosin.

The method to prepare the cell lysate was slightly different from the one described above. Protein production was induced for 16 h in *S39006 ΔpigE* pPigE and *S39006 ΔpigE* before freezing the cell pellets until the assay. The pellets were then thawed and resuspended in a phosphate buffer before lysis (see experimental). Because of the opacity of the suspension hence obtained, only the soluble fraction was used. A 96-well plate was charged with the soluble fraction, thioester **68**, ornithine, PLP, MBC, ATP and FAD (see experimental). A_{535} was monitored for 200 min (**Figure 4.47**).

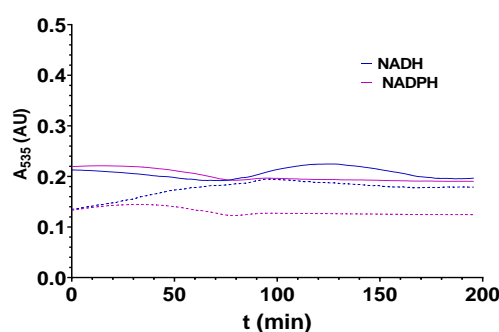


Figure 4.47: Monitoring of prodigiosin formation Plain extract from *S39006 ΔpigE*, Dotted: extracts from *S39006 ΔpigE* pPigE

The curves shown in **Figure 4.47** were smoothed as the noise was substantial, making the results unreliable. The plate was kept overnight at room temperature and a deposit was present in some wells: supernatant was pipetted out and the deposit resuspended in acidified EtOH to be compared with prodigiosin, but none of them showed a peak at 535 nm.

It is possible that this assay failed because some of the enzymes involved in the process are transmembrane proteins and were not in the soluble fraction or were in an inactive form. Hence, microcentrifuge tubes were charged with cell lysates containing both the cell debris and the soluble fractions as well as the substrates and cofactors listed above and incubated overnight at 30 °C. The mixtures were then centrifuged and the pellets extracted with EtOH. The supernatants were discarded because they were visibly not red and prodigiosin has a very low solubility in water. The UV/Vis spectra of the ethanolic extract obtained from the cell pellets were recorded, but once again no peak at 535 nm could be observed.

It seems prodigiosin could not be produced in these conditions. This might result from an inappropriate ratio of protein/cofactor, too low a concentration of the necessary proteins, or simply one of the three enzymes required to transform **68** into prodigiosin was inactive in the assay conditions.

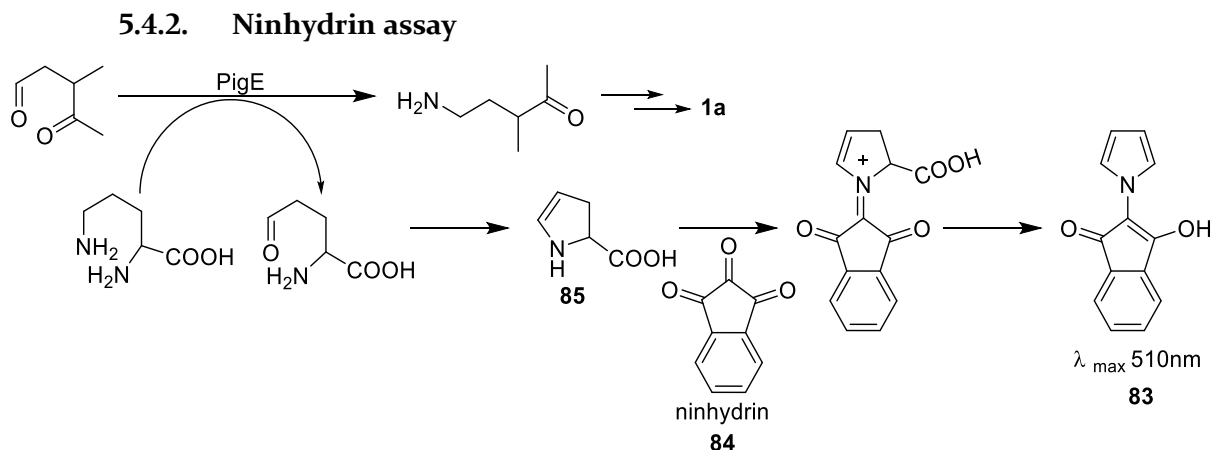


Figure 4.48: Principle of the ninhydrin assay.

Ninhydrin is a common indicator for amines because when they react a purple product is formed. In addition, the transaminase activity of PigE is supposed to generate enamine **85**, which has a nitrogen susceptible to react with ninhydrin. Hence, as illustrated in **Figure 4.48**, this assay relies on the formation of a coloured product **83** when ninhydrin **84** reacts with the by-product of PigE transamination.¹⁹⁷ To check that side-reactions would not lead to product also absorbing at 510 nm, PigE's product H₂MAP and ornithine were submitted to the assay (see experimental) (**Figure 4.49**).

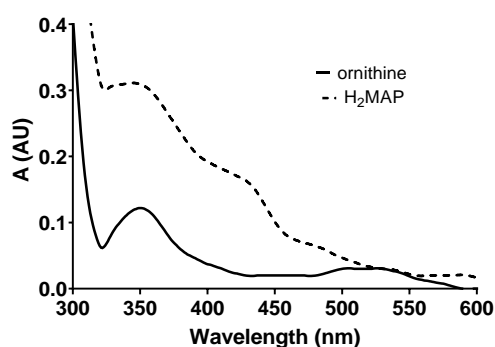


Figure 4.49: UV spectra of the reaction mixture of ornithine and H₂MAP with ninhydrin

In both cases, the absorbance at 510 nm remained low. Interestingly a small increase at that wavelength was visible with ornithine. Perchloric acid was present in the reaction mixture as it was to be used to stop the enzymatic reaction. This might have led to the oxidation of ornithine into **85**, which could then react with ninhydrin. However, this effect remained low.

The assay was then conducted on lysates of *S39006 ΔpigB* and *S39006 ΔpigD* incubated with **20**, PLP and ornithine. A control without **20** was also performed (**Figure 4.50**).

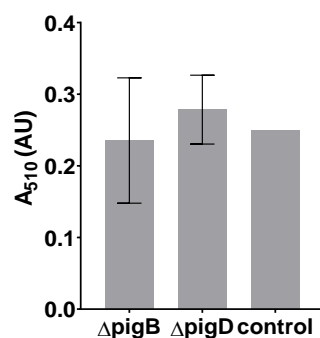


Figure 4.50: Results on the ninhydrin assay on different cell extracts

Unfortunately, the results obtained with both extracts were close to the control, probably because of the reaction between ornithine and perchloric acid mentioned above.

As a conclusion, this assay lacked reliability and could not be used to study the thioester reductase activity of PigE. No further optimisation was attempted and assays giving insights in both activities of PigE were investigated.

5.4.3. NAD(P)H monitoring

Two different conditions were investigated for monitoring NAD(P)H disappearance with cell extracts from *S39006*. The cells extracts were both lysates but in one they were in lysis buffer (A) and in the other they were in phosphate buffer (B). Furthermore, with A the samples were diluted in a Tris buffer and the mixture was supplemented with metal ions, whereas in B no additional buffer nor metal ions were used and some PLP was added (see experimental).

In both conditions the concentrations of the different mixture components were in a similar range. In conditions B, PLP concentration was chosen to be 0.125 mM because any higher concentration led to a significant increase in absorbance at 340 nm and prevented any monitoring at that wavelength. Cell debris were removed from the mixtures for a similar reason.

In both cases the absorbance at 340 nm was recorded at 30°C (**Figure 4.51**). Conditions B were tried not only on *S39006* and *S39006 ΔpigE* but also with *S39006 ΔpigE pPigE*.

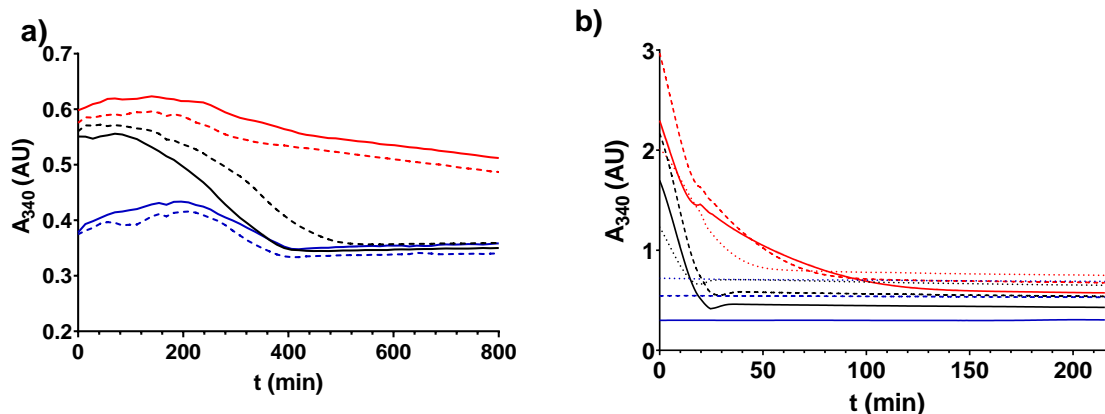


Figure 4.51: NAD(P)H monitoring with *S39006* extracts a) conditions A; b) conditions B; Black NADH, Red: NADPH, Blue: no cofactor, Plain: *S39006* Δ *pigE*, Dashed: *S39006*, Dotted *S39006* Δ *pigE* pPigE

In conditions A, NADH seemed to decrease whereas NADPH did not. However, this decrease happened both in extracts from *S39006* and *S39006* Δ *pigE*, meaning that PigE was probably not responsible for that effect. The experiment was done again without adding thioester **68** and a similar curve was obtained (data not shown). It could hence be deduced that, in these conditions, another reductase uses NADH but PigE thioester reductase activity could not be observed.

In conditions B, decrease of A_{340} can be observed in all cases, without significant variation of the rate. As above, this effect was present in the strains expressing PigE but also in the strain not expressing it, indicating that the consumption of NAD(P)H was not due to PigE. As before, performing the experiment without **68** gave similar results. Yet, here again, the oxidation was faster than if it was only caused by atmospheric oxygen, implying the involvement of another NAD(P)H dependent enzyme.

It is interesting to notice that modifications of the conditions caused a major change in the shape of the absorbance evolution. It might be because the proteins responsible for NAD(P)H consumption in conditions B were not the same as in conditions A as both NADPH and NADH are affected. These experiments highlighted one of the main limitations of cell extracts assays: the lack of control on the composition of the mixtures. Here the desired phenomenon was observed, but it was not caused by the protein we were investigating.

PigE was also overexpressed in *E. coli* BL21 and cell lysates in phosphate buffer were prepared. The same process was applied to BL21 without plasmid as a control and these two extracts were analysed by Western Blot (**Figure 4.52a**) and submitted to the NAD(P)H assay following conditions B (**Figure 4.52b**).

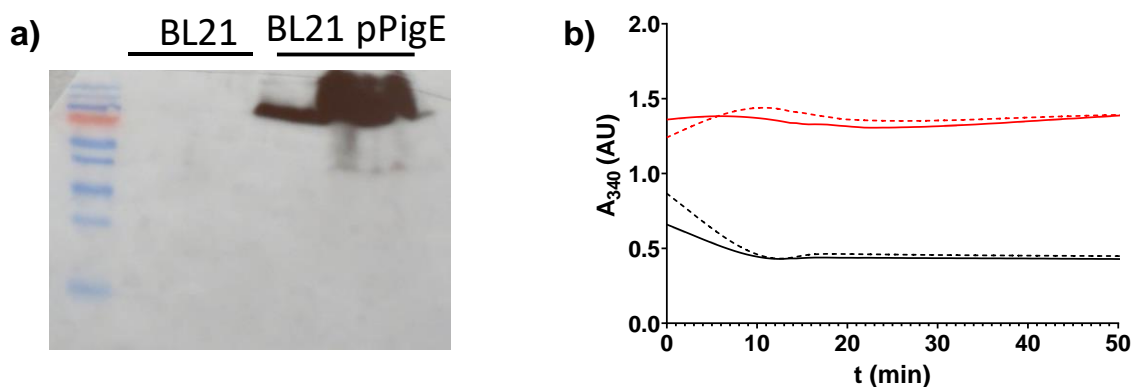


Figure 4.52: BL21 extracts with PigE a) Western blot of the cell extract (left lane= soluble fraction, right lane: insoluble fraction); b) NADPH monitoring Black NADH, Red: NADPH, Plain: BL21, Dashed: BL21 pPigE

The evolution of the NAD(P)H absorbance was very different here than with *S39006* extracts. This suggested that one or more active reductases are present in the *S39006* extract but not in the *E. coli* samples. Both strains behaved the same with NADH, with a fast decrease followed by a plateau. With NADPH, in both cases a slow decrease started after a transition period. The rate of decrease from $t = 80$ min was slightly higher in BL21 pigE than in BL21 ($1.2 \times 10^{-3} \pm 15 \times 10^{-6} \text{min}^{-1}$ against $0.9 \times 10^{-3} \pm 18 \times 10^{-6} \text{min}^{-1}$). This difference could suggest that NADPH was consumed faster in the presence of PigE but the rate remains extremely low and there is only a 25% difference between the two rates. In addition, the behaviour before $t = 80$ min was not consistent with a continuous oxidation of NADPH.

In conclusion, PigE contained in cell extracts did not trigger decrease in NAD(P)H over the course of the experiments. For opacity reasons, the experiments were conducted only with the soluble fraction of the lysate. Furthermore, protein purification experiments showed that the concentration of PigE in such extracts was low. Hence it is possible that the protein was active but that the rate of the reaction could not be distinguished from the O_2 driven oxidation.

5.5. LC-MS

Following the lack of success in monitoring PigE activity by spectrophotometry and the difficulties encountered to develop coupled assays, a MS method was investigated.

Cell lysates of *S39006* ΔpigE , *S39006* ΔpigE pPigE, *E. coli* BL21 and BL21 pPigE were prepared in a KPi buffer, and the cell debris were kept in suspension. Microcentrifuge tubes were charged with this mixture along with ornithine, thioester **68**, NAD(P)H and PLP before being incubated overnight at 30°C (see experimental). Debris were centrifuged down and the supernatant analysed by LC-MS (**Figure 4.53**).

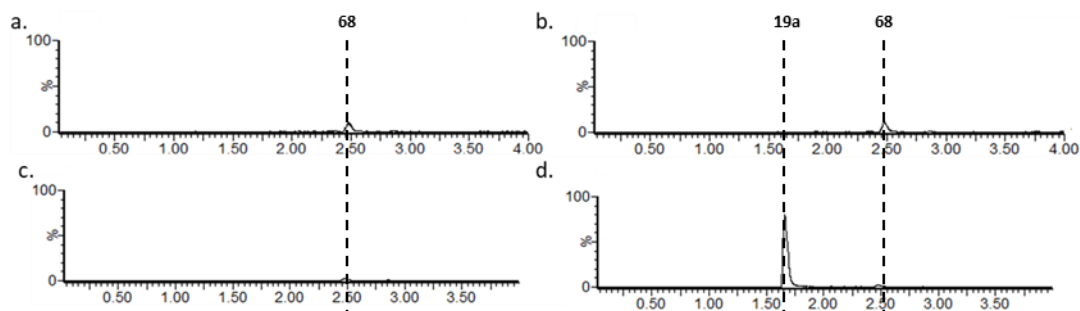


Figure 4.53: Extracted ion chromatograms (154.16+288.16) from the overnight mixtures a) *S39006* $\Delta pigE$ extracts; b) *S39006* $\Delta pigE$ pPigE extracts, c) BL21 extract, d) BL21 pPigE extract; Retention times corresponding to **19a** and **68** are shown

The extracted chromatograms at 288.16 (**68**+H⁺) and 154.16 (**19a**+H⁺) all looked the same for *S39006* extracts (see appendix): only a small peak at 2.50 min was observed. Analysis of the ion's mass as well as comparison with synthetic **68** chromatogram (**Figure 4.54**) showed it was the unreacted thioester.

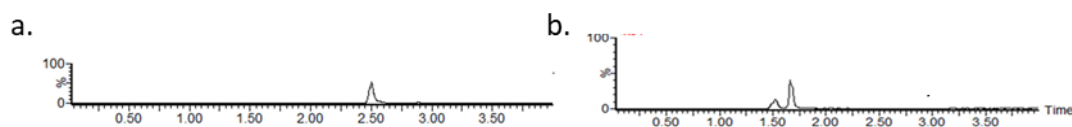


Figure 4.54: Extracted ion chromatogram from LC-MS analysis of synthetic a) **68** (at $m/z=288.16$, **68**+H⁺); b) **19a** (at 154.16 **19a**+H⁺)

As expected, extracts from BL21 also only showed the peak corresponding to **68**. However, H₂MAP was observed in the mixture with BL21 pPigE extracts. Interestingly, the presence of added cofactors to the mixture did not seem to impact the formation of H₂MAP. This was probably due to the presence of NAD(P)H in the extracts themselves. It indicates that the protein was active, but it did not allow to discriminate between the two potential cofactors.

The protein purification method described previously was adapted to isolate PigE from the soluble fraction and the membrane fraction of BL21 pPigE. After lysing the cells, the debris were submitted to ultracentrifugation where three layers were visible: the soluble fraction was collected and further purified by Ni-NTA affinity chromatography whereas the membrane fraction was resuspended in phosphate buffer and used directly. The rest of the cell debris was discarded. SDS-PAGE showed that the membrane fraction (MF) contained one main band at 180 kDa, which was too high for PigE. This was unexpected as the insoluble fraction of the cell lysate did seem to contain PigE (**Figure 4.55**).

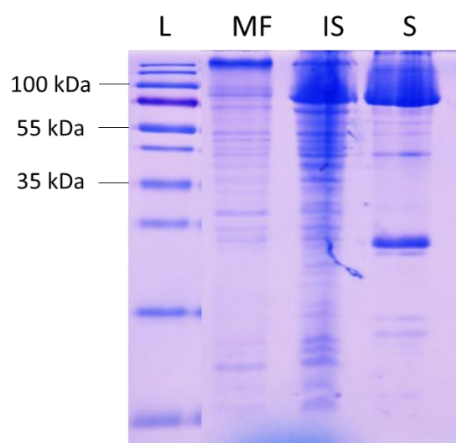


Figure 4.55: SDS-PAGE gel of samples of interest in PigE purification MF: membrane fraction, IS: insoluble fraction, S: soluble fraction

Like for the cell extracts assay, protein (S or MF) were mixed with **68**, ornithine and NAD(P)H in a phosphate buffer for 16 h at 30 °C before analysing the sample by LC-MS.

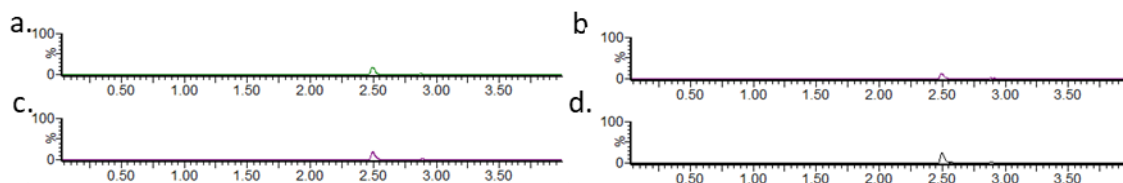


Figure 4.56: Extracted chromatograms (at $m/z=154.16+288.16$) from the LC-MS analysis of the reaction mixtures after a 16 h incubation at 30 °C with purified PigE a) MF, NADH; b) MF, NADPH, NAH; c) S, NADH d) S, NADPH

As illustrated in **Figure 4.56**, no peaks corresponding to H₂MAP was observed. The experiment was then repeated but instead of resuspending PigE and the other reagents in the phosphate buffer, they were resuspended in the flow-through obtained when the soluble fraction was loaded on the Ni-NTA column (**Figure 4.57**). H₂MAP was observed with the soluble protein but not with the MF. This meant that nothing in the buffer was able to catalyse both the reduction of **68** and the subsequent transamination. In addition, *E. coli* is a heterologous host and does not seem to have close homologues of either domain of PigE. Thus, this experiment showed that the soluble fraction of PigE was active, but that it required more than just NAD(P)H and ornithine to carry out the transformation. A screening of conditions with metal ions, different amino acids and possibly other hydride generators than NAD(P)H would be the next steps in the study of PigE.

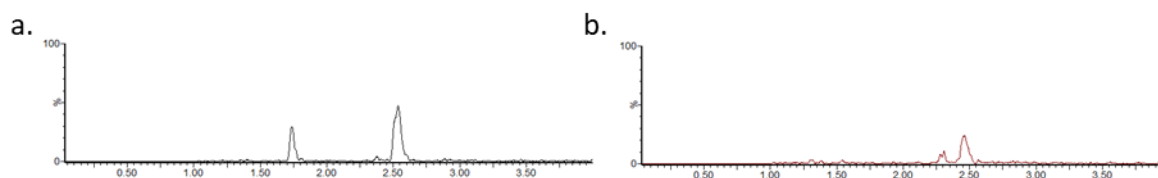


Figure 4.57: Extracted chromatograms (at $m/z=154.16+288.16$) from LC-MS analysis of the reaction mixtures after a 16 h incubation at 30 °C in presence of cell extracts a) S, b) MF

6. Conclusions and perspective

Complementation assays have been designed and support our hypothesis that PigE is a bifunctional enzyme. This was the first time that the thioester reductase activity had been demonstrated through complementation assays.

It was possible to purify PigE with an N-terminal His₆ tag and LC-MS experiments showed that the enzyme could mediate the transformation of thioester **68** into H₂MAP **19a**.

Screening of different conditions would be the next step, with in particular the study of the influence of metal ions and other reducing cofactors. LC-MS analysis seems promising for the screening of the conditions, but an assay needs to be developed to study the kinetics of the reaction. The construction of a plasmid expressing PigE with a C-terminal His₆ tag could also be a way to improve the activity.

It might be difficult to isolate PigE-C terminal domain as it is mainly insoluble (section 4.3). However, the construction of a strain only expressing PigE-N terminal domain would be interesting so as to determine the activity of each domain individually.

Chapter 5. Toward an *in vivo* characterisation of PigD

1. Overview and aim of the project

PigD is the first enzyme involved in MAP biosynthesis. This thiamine diphosphate (TDP) dependent enzyme catalyses the transfer of an acetyl group from a pyruvate to an octenoyl thioester through a Stetter-type reaction (**Figure 5.1**).

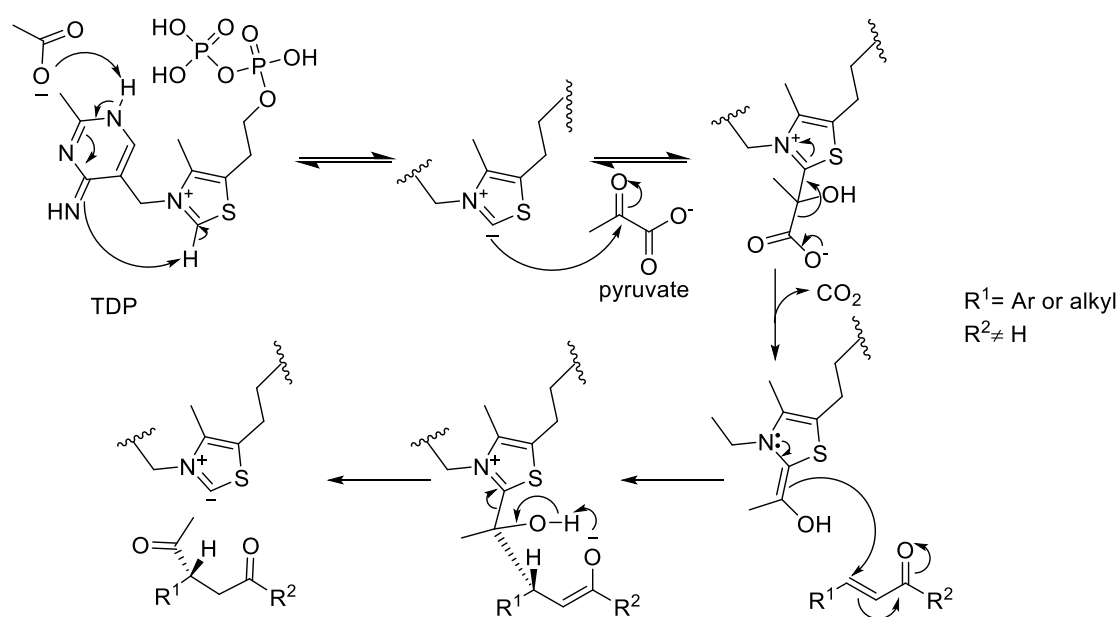


Figure 5.1: Mechanism of TDP dependent 1,4-addition of an acetyl group on an α,β -unsaturated carbonyl compound

Whilst looking for an enantioselective catalyst for Stetter reactions, Dresen *et al.* purified PigD and characterised its regioselectivity and enantioselectivity.³⁶ The Stetter reaction uses an umpolung mechanism, converting the carbon atom of a carbonyl group from an electrophile to a nucleophile. In most cases, this requires the addition of cyanide or a thiazolium ylide to form the Breslow intermediate, which can then carry out a nucleophilic attack. As illustrated in **Figure 5.1**, TDP dependent acylations follow a similar mechanism, but the enzyme scaffold imparts higher enantioselectivity.

Dresen *et al.* first used PigD on α,β -unsaturated aldehyde substrates, but they only obtained 1,2-addition products – where the attack occurs on the carbonyl carbon of the aldehyde. However, when they moved to less reactive species such as α,β -unsaturated ketones and thioesters, they

only observed 1,4-addition products. Interestingly, conversion could be obtained for a wide range of R¹ and R² groups, including alkyl chains, aromatic groups, and heteroatoms. The worst yields were obtained for branched chains whereas the best one was obtained for a thioester **70**, a mimic of octenoyl-ACP (**Figure 5.2**).



Figure 5.2: PigD catalysed acetylation of a mimic of octenoyl-ACP

Finally, they confirmed that the reaction was stereoselective with ee > 95% for all the tested substrates. The *R/S* configuration of the product depends on the order of priority of R²: with **70** as starting material the reaction gives the (*S*) product (**(S)-68**).

In this project, we aimed to probe PigD substrate specificity *in vivo*. Because PigD is the first enzyme in the biosynthetic pathway, a chemical complementation approach as in Chapter 2 and Chapter 4 could not be followed. It was hence decided to feed *S39006* with deuterium labelled compounds **86** and **87** and analyse the pigment produced by MS, where the deuterium labels should induce a shift of two mass units (**Figure 5.3**).

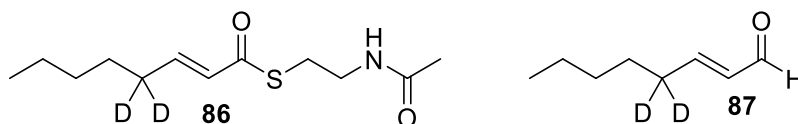


Figure 5.3: Deuterated potential substrates for PigD

2. Bioinformatics analyses

PigD amino acid sequence was submitted to BLAST¹⁷⁶ and PHYRE¹⁴⁷. BLAST showed that residues 373-803 were consistent with a TDP dependent enzyme and predicted that Met681, Gly704, Asp705, Gly706, Ala707, Asn740 and Gly742 (orange in **Figure 5.4**) are involved in the PLP binding site. Interestingly, the N-terminal region of the protein did not seem to belong to any family (see appendix).

Similarly, none of the sequences aligned with PigD in PHYRE covered the first 240 amino acids. The best hit was an acetolactate synthase, another TPP dependent enzyme which reacts two pyruvate molecules together at the beginning of the biosynthesis of valine, leucine and isoleucine. Despite the lack of a homologue for the N-terminal region, the software was able to model the entire structure, with 90% of confidence for 71% of the residues (in Green in **Figure 5.4**).



Figure 5.4: Model of PigD as predicted by PHYRE. Green: structure modelled at > 90 % confidence, Orange: residue involved in the TPP binding site

The structure was submitted to 3Dligand, which predicted a unique binding site containing TPP but also Mg^{2+} and Ca^{2+} . In addition, Dresen *et al.*³⁶ used buffers containing $MgSO_4$ when they assessed the activity of PigD activity, which is consistent with a metal ion binding site. The residues involved in the binding site were consistent with the BLAST prediction, with the addition of Leu680, Ser744, Val745 and Ile 746.

3. The PigD product is not secreted

Cross feeding assays were used extensively to determine the prodigiosin biosynthetic pathway.^{15,26} Strains with one of the enzymes in the pathway inactivated usually accumulate the intermediate that was supposed to be transformed by the said enzyme. Through secretion or diffusion, if the molecule is small and non-polar enough, the intermediate may escape into the culture medium and be taken up by another strain blocked earlier in the biosynthetic pathway. Hence if two white strains are grown together, one with an inactive enzyme further on in the biosynthetic pathway than the other, then pigmentation can be recovered. However, this only works if the intermediate can get out of the cells. Cross-feeding experiments were conducted with *S39006 ΔpigD*, *S39006 ΔpigE* and *S39006 ΔpigB* in pairwise co-culture in LB supplemented with sorbitol. Pigment was extracted and quantified, leading to **Figure 5.5**.

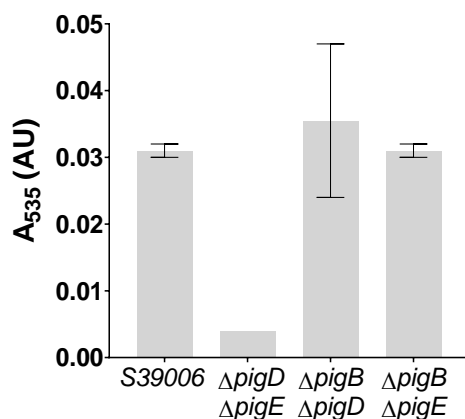


Figure 5.5: Pigment production in cross feeding assays.

It appeared that, unlike the products of PigE and PigB (H₂MAP and MAP respectively), the product of PigD either cannot get out of the cell or cannot be incorporated again. It is hence unlikely that it is a small non-polar molecule such as aldehyde **20**. It is already known from feeding experiments that *S39006* Δ*pigD* can take up aldehyde **20** from solution and use it to complete the biosynthesis of prodigiosin (see Chapter 4). This strongly supports the product of PigD being a CoA or ACP thioester not an aldehyde. CoA thioesters, although small molecules, are sufficiently polar that they cannot diffuse through membranes.

4. Synthesis of the unlabelled potential substrate

Before trying a synthesis involving deuterated material, a synthesis of **70** and the non-deuterated 2-octenal **17** was attempted. Hexanal **88** was chosen as the precursor as the enol/aldehyde equilibrium offered a way to replace the α-hydrogen atoms with deuterium atoms (see section 5).

4.1. Knoevenagel condensation

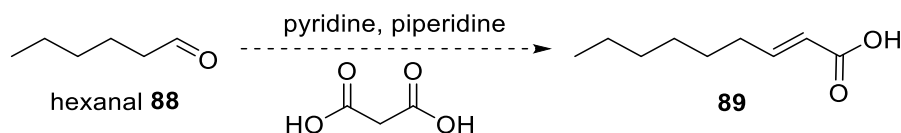


Figure 5.6: conversion of **182** into α,β-unsaturated acid **183** using a Knoevenagel condensation.

As illustrated in Figure 5.6, hexanal was mixed with malonic acid in the presence of base to trigger the malonic addition. The mixture was then acidified, leading to the dehydration and the decarboxylation. However, after purification, no 2-octenoic acid **89** was obtained, but 3-octenoic acid **89b** (Figure 5.8a) was isolated instead. The experiment was repeated, and the acidification

was performed at 0 °C dropwise, but it did not alter the regioselectivity of the reaction. Another route was hence investigated.

4.2. Wittig reaction

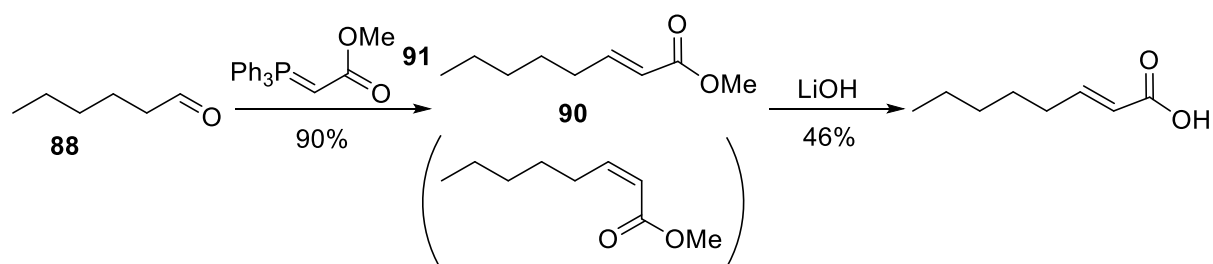


Figure 5.7: conversion of **88** to **89** via a Wittig reaction

A small-scale test reaction showed that (E)-**90** could be obtained by reacting **88** with the commercial stabilised ylid **91** in water, at r.t. for one hour. However, the yield was low, probably because of partial oxidation of the starting ylid. Consequently, the ratio of ylid was doubled for the scale up, leading to a significant increase in the conversion yield but also to the formation of (Z)-**90**. The two stereoisomers could then be separated by column chromatography.

Ester **90** being very insoluble in water, it was necessary to conduct the hydrolysis in a mixture of solvents. However, when the reaction was carried in a mixture containing methanol, a Michael addition of the alcohol on **90** happened, leading to the formation of **89c** (Figure 5.8b). An attempt to perform the hydrolysis in a mixture $\text{H}_2\text{O}/\text{THF}$ only gave the starting ester back and decreasing the amount of base was not enough to prevent the formation of **89c**. More sterically hindered alcohols were tried: with $i\text{PrOH}$, traces of a Michael addition product were still detected, whereas $t\text{BuOH}$ gave the desired carboxylic acid as the only product, but at a slower rate.

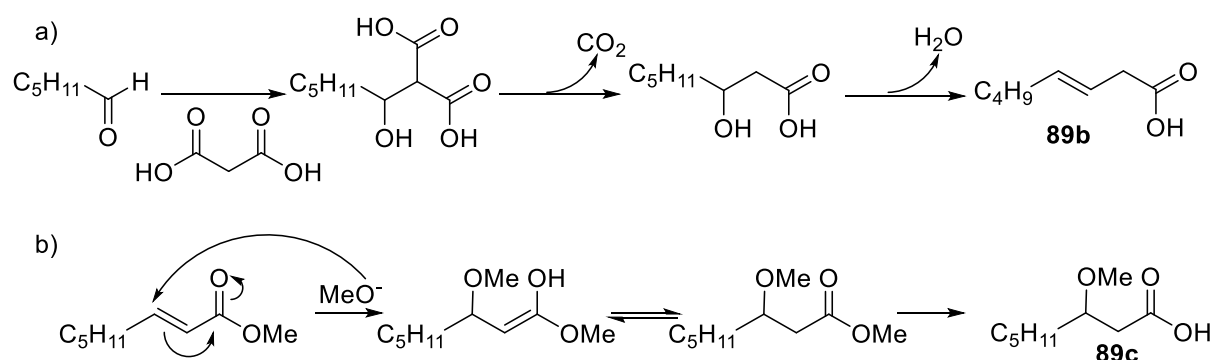


Figure 5.8: Formation of undesired products in the synthesis of **70** a) formation of **89b**, b) formation of **89c**

Conversion to the desired thioester **70** was then performed using the same coupling conditions as for **68**.

4.3. Formation of the aldehyde **17**

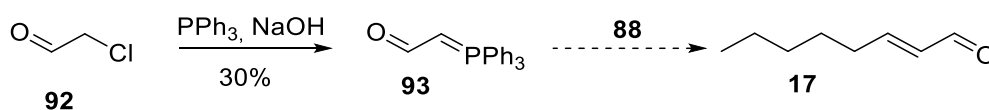


Figure 5.9: Route toward **17**

To prevent polymerisation, chloroacetaldehyde **92** is sold in solution at 50% in water. But the first step of the preparation of the ylid was done in chloroform, so **92** was diluted in chloroform and the water removed by distillation of the azeotrope. Triphenylphosphine was then added and the mixture refluxed for 16 h. The phosphonium salts were recovered by filtration and the ylid **93** was obtained after treatment with NaOH.

Unfortunately, performing the Wittig reaction under the same conditions as above did not lead to the formation of any **17** and only the starting materials were recovered. Before investigating other conditions for this reaction, conditions for the deuterium labelling were explored (Section 5).

5. Deuterium labelling

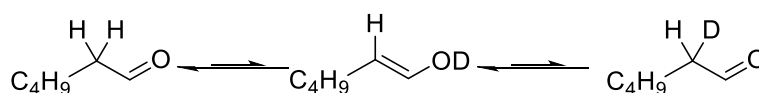


Figure 5.10: Principle of deuterium labelling of hexanal

As illustrated in **Figure 5.10**, the deuterium labelling of hexanal relied on the enol/aldehyde equilibrium and the exchange of protons with the solvent.

In a first attempt, hexanal was diluted in MeOD and spectra were recorded two hours and a day after the dissolution (**Figure 5.11**).

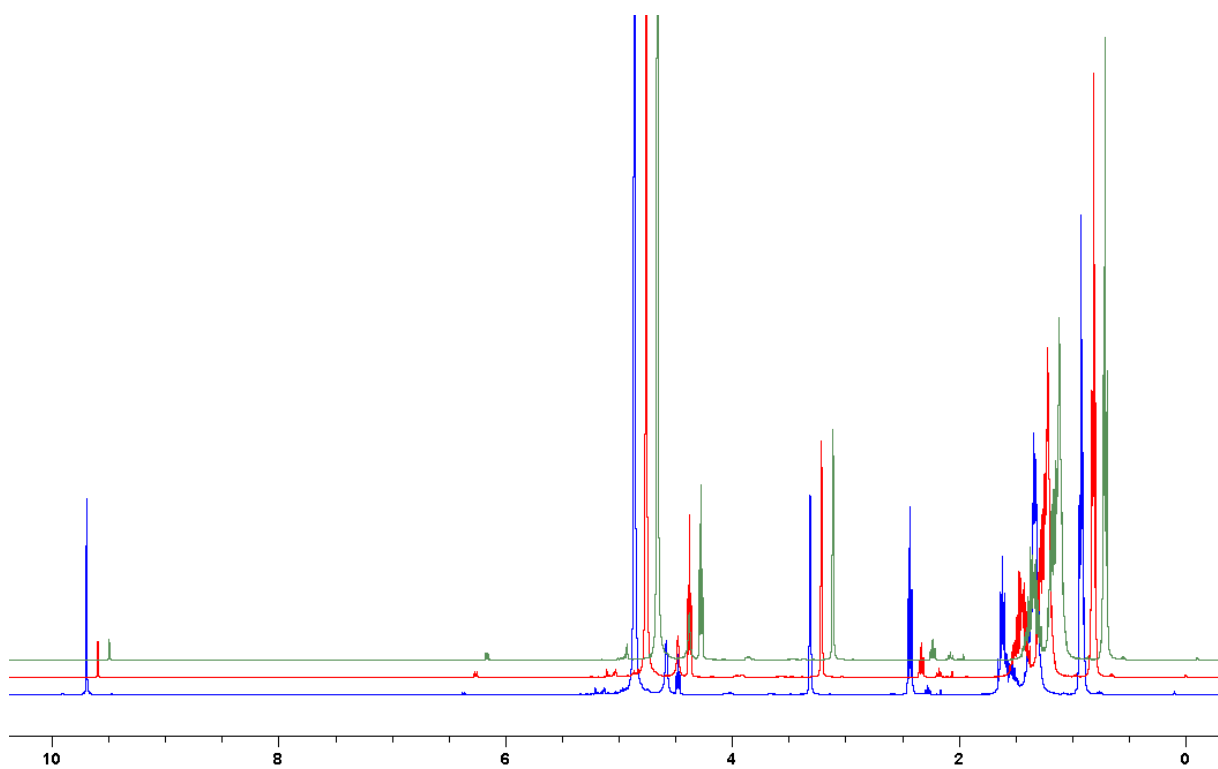


Figure 5.11: Hexanal in MeOH Blue: t=0, Red: t=2h, Green: t=48h

The peak corresponding to the protons α to the carbonyl group (2.4 ppm), showed a large decrease in the first two hours and then remained constant. Interestingly, the proton on the carbonyl carbon atom (9.7 ppm) followed a similar evolution. In addition, the total number of protons in those spectra remained constant, and a triplet at 4.47 ppm appeared after two hours. This suggested that the evolution of the spectra was due to the formation of the hemiacetal **94** (Figure 5.12) and the labelling was too slow to be observed in those conditions.

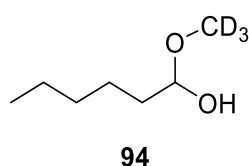


Figure 5.12: Hemiacetal **94**

To increase the rate of the labelling, Et_3N was added to the mixture. Despite the formation of the hemiacetal, a decrease of the integral of the peaks corresponding to the proton α to the hemiacetal (1.6 ppm) could be observed after one week at r.t. or 16 hr at 60°C (Figure 5.13). Unfortunately, after removing MeOD under reduced pressure, the NMR spectrum taken in chloroform was consistent with **94**. An attempt to hydrolyse the hemiacetal by treating with 1M HCl only led to degradation.

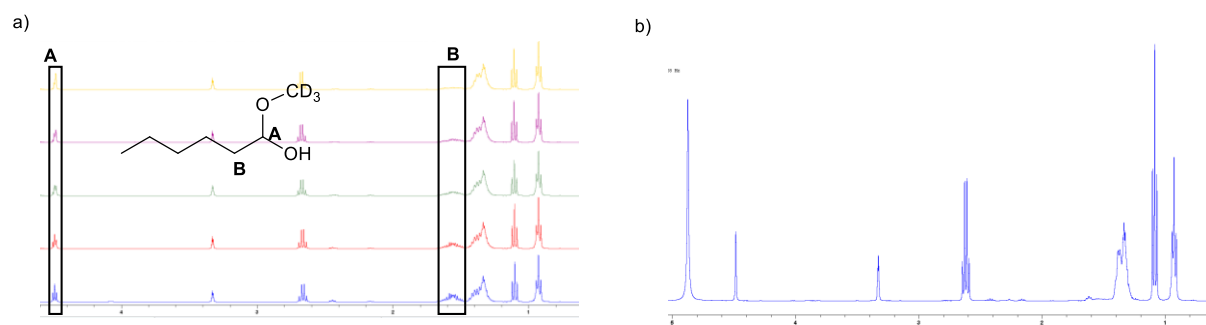


Figure 5.B: Evolution of hexanal NMR spectrum in MeOD in presence of Et₃N a) r.t., Blue t=0, Red= t=1 d, Green t=2 d, Purple, t= 3 d, Yellow t)5d; b) After 16h at 60°C

KOH was tried as an alternative base: it seemed that the signal for the protons in α to the carbonyl disappeared before the recording of the first spectrum. However, the intensity of several signals in the ¹³C NMR spectrum were also affected which suggest other reaction(s) might be involved.

Finally, the reaction was tried in D₂O, but led to the formation of the hydrate.

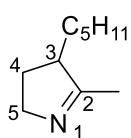
These methods gave promising results but still need optimisation: the recovery of hexanal still has to be optimised. Acid catalysis could also be explored. The formation of labelled hexanal will also have to be confirmed by MS as well as NMR. Unfortunately, none of the equipment available at that stage could record a mass spectrum for a compound with a molecular weight of 102.

In conclusion, this work showed that the synthesis of a thioester substrate of PigD from hexanal was possible and explored a route for deuterium labelling of **88**. The proton exchange with the solvent was observed but it was coupled with the formation of acetal and hexanal could not be recovered. Out of the three enzymes involved in MAP synthesis, PigD has been characterised the best. It was hence decided to focus our efforts on PigB and PigE.

Chapter 6. Conclusions and future work

As mentioned above (see Chapter 1), prodigiosin results from the condensation of the monopyrrol MAP and a bipyrrrole MBC. In the course of this project, the three enzymes involved in the formation of MAP - PigD, PigE and PigB - have been studied.

PigD being the first enzyme of the pathway, a synthesis of deuterated substrates to monitor its activity in cell (see Chapter 5) was attempted. It was shown that the synthesis of the wanted substrates from hexanal was possible. Unfortunately, the deuteration of hexanal still requires optimisation.



Four new analogues with variations in the C2 substituents (see **Figure 6.1**) of PigB substrate (H_2MAP) were synthesised. The capacity of PigB's homologue HapB to use these compounds as substrates was established *in vitro*. In addition, a $\Delta pigD$ mutant of *S39006* was fed with these analogues as well as compounds with variations on the C3 position of H_2MAP (see Chapter 2). It appeared that the quantity of prodiginine hence obtained correlated well with the *in vitro* results, showing that PigB and HapB share similar flexibility and that substrates tolerated by PigB were also accepted by the condensing enzyme PigC. It appeared that both longer and shorter chains could be tolerated on the C3 position, whereas alkyl chains of more than 3 carbons were not accepted on the C2 position.

Eight analogues of prodigiosin were obtained when *S39006* $\Delta pigD$ was fed with analogues of H_2MAP . Activity both against Gram-positive and Gram-negative bacteria was assessed, and in both cases all the prodiginines displayed some antibiotic activity in the disc diffusion assay. IG_{50} experiments indicated that some of these compounds could inhibit the growth of *E. coli* and *S. aureus* in the low micromolar range. In addition, a preliminary experiment with HeLa cells showed that some of the new prodiginines could be more potent than prodigiosin against cancer cells (see Chapter 3).

However, a more detailed analysis of antibiotic and anticancer activity of the derivatives would be useful. In particular, the GI_{50} experiment needs to be repeated with all the analogues of prodigiosin rather than just two. For the anticancer activity, more analogues need to be tested and the proper concentration range to measure the activity is still to be determined. In addition, the prodiginines tested here were all issued from analogues of H_2MAP with variation on the C2

or C3 position. It would be interested to test other analogues of H₂MAP, which would require the optimisation of some of the potential synthetic route explored in Chapter 2.

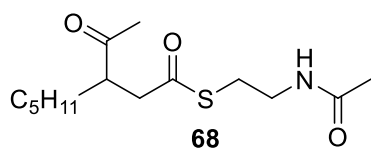


Figure 6.2: Mimic of potential natural thioester substrate of PigE

Finally, using feeding experiments, we demonstrated that thioester **68** (Figure 6.2) could be accepted as a substrate in the prodigiosin biosynthetic pathway (see Chapter 4). This proved the existence of a thioester intermediate, probably either 3-acetyloctanoyl-CoA **66** or, more likely, a 3-acetyloctanoyl-ACP **67**. LC-MS experiments with lysates of *E. coli* expressing PigE showed that PigE could catalyse the transformation of **68** into H₂MAP proving that PigE plays the role of thioester reductase for the thioester substrate. However, a number of unknowns about this reaction remain: what are the cofactors? Can PigE perform substrate channelling between the thioester reductase the aminotransferase active sites? What are the kinetic parameters of the thioester reduction and of the transamination? The first question can probably be answered by screening conditions to see in which cases H₂MAP can be detected by LC-MS when purified PigE is incubated with **68** and various cofactors. It will only be possible to design experiments to answer the other questions once all the reagents involved in the transformations catalysed by PigE are known.

Chapter 7 Materials and methods

1. Biological chemistry

1.1. General considerations

Chemicals and media were purchased from Sigma Aldrich, Insight Biotechnology LDT, Fluka, Formedium, Fisher Scientific, Tetanal, Difco, and Biorad. Commercial enzymes and kits were purchased from New England Biolab (NEB), Sigma, Thermo Fisher, and Gibco. Sequencing was performed by Eurofins Genomics (formerly GATC).

All media were prepared in deionised water and sterilised at 121 °C for 20 min. Glassware used for bacterial culture was sterilised at 121 °C.

HPLC purification and analysis were performed on an Agilent 1100 Series system fitted with a autosampler and a UV/Vis detector. Eluents were supplemented with 0.1% formic acid.

1.2. Media and buffers

1.2.1. Culture media

Media	Component	Quantity (g/L)
Luria-Bertani medium (LB)	Tryptone	10
	Yeast extract	5
	NaCl	10
LB agar (LBA)	LB	As above
	Agar	15
LB+ sorbitol 0.25M (LBS)	LB	As above
	sorbitol	45.5
Marine broth	Difco™ Marine Broth 2216	37.4
Marine agar	Marine broth	As above
	Agar	18
Peptone Glycerol Media (PGM)	Peptone	5
	Glycerol	10 ml
	Agar	15
Mueller Hinton (MH)	Infusion from dehydrated beef	300.0

Casein hydrolysate	17.5
Starch	

1.2.2. Buffers for protein purification (pH = 8)

Lysis	NaH ₂ PO ₄ , (H ₂ O) ₂	7.8
	Imidazole	0.68
	NaCl	17.54
Wash	NaH ₂ PO ₄ , (H ₂ O) ₂	7.8
	Imidazole	1.36
	NaCl	17.54
Elution	NaH ₂ PO ₄ , (H ₂ O) ₂	7.8
	Imidazole	17
	NaCl	17.54

When relevant the buffers were supplemented by 1 mM of PLP

1.2.3. Buffer for SDS-PAGE and Western blot

Running gel buffer	Tris	50.86
	HCl (1 M)	To pH 8.3
Stacking gel buffer	Tris	30.3
	HCl (1 M)	To pH 6.8
Electrode buffer (stock x 10)	Glycine	150
	Tris	30
Transfer buffer	Glycine	14.4
	Tris (base)	3.03
	MeOH	150 ml
Wash buffer	PBS	
	Tween 20	20

1.2.4. Selection

Supplement	Concentration
Ampicilin (Amp)	0.1 mg/ml
Erythromycin (Erm)	0.2 mg/ml
Kanamycin (Kn)	50 µg/ml
Spectinomycin (Sp)	50 µg/ml
DAPA	0.3 mM

1.2.5. Buffer for heat shock competent cells preparation

Solution A	1 M MnCl ₂	9.9 ml
	1 M CaCl ₂	49.5 ml
	50 mM MES	198 ml
	dH ₂ O	742.6 ml
Solution A + glycerol	Solution A	350 ml
	Glycerol	150 ml

1.2.6. Miscellaneous

Buffer	Component	Quantity
TAE IX	Tris base	40 mM
	Acetic acid	20 mM
	EDTA (sodium salt dihydrate)	1 mM
Sodium fluoride	NaF	4.1 g/L
	NaH ₂ PO ₄	7.8 g/L
	NaOH	To pH 8
Phosphate (Kpi)	KH ₂ PO ₄	6.8 g/L
	KOH	To pH 7
Tris	Tris HCl	10 mM
HEPES		50 mM
Citric acid		0.1 M

pH in Tris, HEPES and citric acid buffer was adjusted to 7.5

1.3. PCR

Polymerase Chain Reaction (PCR) was performed using a Veriti® 96-Well Thermal Cycler. For 25 µl standard PCR reactions the following mixture was used.

	Compound	Quantity (µl)
Standard PCR	gDNA template	1
	Oligonucleotide 1 (10 µM)	2.5
	Oligonucleotide 2 (10 µM)	2.5
	DMSO	0.75
	dNTP (10 µM)	2
	5x HF Buffer	5
	Phusion® Hi-Fidelity DNA polymerase	0.2
	SD-H ₂ O	Up to 25 µl
Colony PCR	DNA template*	1
	Oligonucleotide 1 (10 µM)	2.5
	Oligonucleotide 2 (10 µM)	2.5
	dNTP (10 µM)	0.5
	DMSO	0.75
	5x GC Buffer	5
	Phusion® Hi-Fidelity DNA polymerase	0.25
	SD-H ₂ O	Up to 25 µl

*1 colony resuspended in 100 µl of H₂O

PCR cycling parameters included 6 minutes of initial denaturation at 98°C, following 35 cycles of denaturation (10 seconds at 98 °C), annealing (15 second at 55 °C) and extension (5 to 7 minutes at 72 °C), and a final extension for 10 minutes at 72 °C. The amplified PCR products were analysed by agarose gel electrophoresis. 1% (w/v) agarose gel containing ethidium bromide was run at 90 V in 1xTAE buffer (section 1.2.6).

Name	Sequence 5'-3'	Restriction enzyme	Usage
oQE-F	CCCGAAAAGTGCCACCTG		pQE8o-L and pQE8o-L: <i>oriT</i> sequencing - forward
oQE-R	GTTCTGAGGTCATTACTGG		pQE8o-L and pQE8o-L: <i>oriT</i> sequencing - reverse
oBS-F	GTAAAACGACGGCCAGT		pBlueScript Sequencing - Forward
oBS-R	AGCGGATAACAATTCACACAGGA		pBlueScript Sequencing - Reverse
MC01	GGCTGCAGTTACTCTAAAAATGTTGATAGC	<i>PstI</i>	<i>pigE</i> amplification -reverse
MC02	GAGAAAGAGCTCATGATGGTGGAAATTTCTCAA ACTG	<i>SacI</i>	<i>pigE</i> C-terminal domain amplification - forward
MC03	GAGAAAGAGCTCATGAAGTTTGGATTTATCGC TC	<i>SacI</i>	<i>pigE</i> amplification- forward
MC04	AATGCGGCCATCTGTTTA		<i>pigE</i> + 250 F
MC05	TTGGCGGCATCAATACC		<i>pigE</i> + 250 R

1.4. Cloning

1.4.1. Plasmid construction

Genes of interest were amplified using the conditions described above and the appropriate primers (see above). Amplicons were extracted from the agarose gel and digested for 1 hr at 37 °C following the conditions described below by the appropriate restriction enzymes. In parallel the vector was digested with the same restriction enzymes and 0.5 µl of CIP were added 15 min before the end of the incubation. The digestion products were analysed by agarose gel electrophoresis and the digested products were purified using a PCR purification kit. Instead of a PCR amplicon, a plasmid with the insert could be digested with the appropriate restriction enzymes and the digested insert was then extracted from the agarose gel. Ligation mixtures were prepared following the conditions described below and the mixtures were incubated at 22°C. After 30 min, 5 µl of the mixtures were used to transform competent cells. The remaining mixture was incubated a further 16 h at 22°C and then used for transformation.

	Compound	Quantity (µl)
Digestion	Restriction enzyme 1	1
	Restriction enzyme 2	1
	CutSmart® Buffer	2
	Plasmid/ PCR amplicon	5 /16
	SD-H ₂ O	Up to 20 µl
Ligation	Linear vector	5
	Insert	5 or 12.8

10x T4DNA ligase buffer	2
Thermo Scientific T4 DNA Ligase	0.2
SD-H ₂ O	Up to 20 µl

1.4.2. Preparation of heat shock competent cells and transformation

25 ml LB in 250 ml conical flask containing 375 µl 1 M MgCl₂ (final conc. 15 mM) were inoculated with 500 µl of an overnight culture (OD₆₀₀~3). The cells were grown at 37°C, 300 rpm until OD₆₀₀=0.4-0.6. The cultures were transferred to a pre-chilled universal flask and kept on ice for 1 h. The cells were pelleted by centrifugation, the supernatant was discarded and the cells resuspended in 10 ml of cold solution A. After 20 min on ice the cells were pelleted (4500 rpm, 10 min, 4°C), the supernatant discarded and the cells resuspended in 2 ml of cold solution A + glycerol. 5 µl of DNA were added to 50 µl of cell and the mixture was incubated on ice for 1 h. the mixture was put at 42°C for 2 min, resuspended in LB and allowed to recover for 45 min at 37 °C. The cells were then plated on LBA with the appropriate selection.

1.5. Conjugation

Overnight cultures of the donor strain (DS) and recipient strain (RS) were prepared. OD₆₀₀ were recorded and cells were pelleted and resuspended at the same concentration. The cells were mixed in a 1:3 ratio (DS/RS) and 20 µl were spotted on LBA appropriately supplemented. The plate was incubated overnight (at 30 °C for *S39006* and related strains) and the spot was resuspended in 1 ml of LB. The mixture was diluted 100-fold and 1000 fold and the two resulting suspensions were plated on LBA with appropriate selection.

1.6. Transduction

1.6.1. Preparation of the phage lysate

A 10-fold serial dilution of a φOT8 lysate was prepared (10⁻¹ - 10⁻⁴). 10 µl of each dilution was added to 4 ml of top agar (0.35%) inoculated with 200 µl of an overnight culture of the DS. The top lawn was then pured on LBA, and after solidification, the plates were incubated overnight (at 30 °C for *Serratia*). The top lawn from plate with congruent plaques were then resuspended in 3 ml of LB and 0.5 ml of CHCl₃ saturated with NaHCO₃, vortexed for 30 s and incubated at r.t. for 30 min. The mixture was then centrifugated and the supernatant was used as phage lysate.

1.6.2. Testing the phage lysate

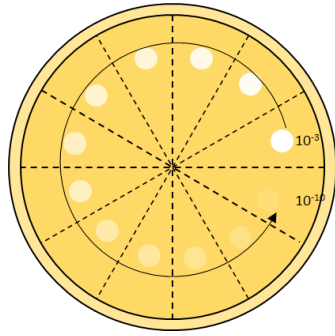


Figure 7.1: Phage lysate assessment

10 fold serial dilutions from 10^{-3} to 10^{-10} of the phage lysates were prepared. 10 μ l of each dilution were then spotted on a top lawn infected with a strain susceptible to the phage (**Figure 7.1**). After an overnight growing the cell at an appropriate temperature, the p.f.u./ml was estimated.

1.6.3. Transduction

2 ml of an overnight culture of RS were inoculated with 50 μ l of lysate, vortexed and incubated for 1 h at r.t. The cells were then pelleted and resuspended in 0.3 ml of LB three times to remove the phage. 150 μ l were then plated on LBA with the appropriate selection.

1.7. Protein expression and purification

1.7.1. Preparation of cell lysates

Cells expressing the desired protein were grown at an appropriate temperature (37 °C for *E. coli*, 30 °C for *S39006*) on a shaker at 250 rpm to obtain an OD₆₀₀ of approximately 0.6. Cultures were then induced with 1 mM isopropyl- β -D-thiogalactopyranoside (IPTG) at 16 °C for 14-16 h. This step was skipped for strains expressing the protein from their genomic DNA. Aliquots were collected before and after the induction by IPTG to monitor the expression of protein and analysed by Sodium Dodecyl Sulphate-Polyacrylamide Gel Electrophoresis (SDS-PAGE). Cells were harvested by centrifugation at 4500 rpm for 20 min at 4 °C. The cells were incubated 15 min on ice and resuspended in 20 ml of lysis buffer including lysosyme (20 mg/g of cell) (Method A) or phosphate buffer (Method B). After a further 30 min on ice, the cells suspensions were sonicated (6 x 20 s with 30 s breaks). The lysate could then be used directly for assay, or the soluble and insoluble fractions could be separated by centrifugation (see below)

1.7.2. Protein purification from soluble fraction

The above lysate was centrifuged at 4500 rpm at 4 °C for 1 h. The clarified lysate was loaded onto a Ni-NTA (Ni²⁺-nitrilotriacetate) column (Qiagen) for affinity purification and the flow through was collected for SDS-PAGE analysis. The column was washed twice with wash buffer and the bound protein was eluted: 6 fractions of 2 ml with a gradient of elution buffer (0 to 100%, increase of 20% at each fraction) in wash buffer were collected. The fractions containing purified protein were pooled and dialyzed against storage buffer.

1.7.3. For protein isolation as membrane fraction

Cell lysates were prepared as described in Section 1.7.2. The lysates were submitted to ultracentrifugation (4 °C, 1 h, 25000 rpm, SW32 Ti rotor, Beckman Coulter OPTIMA L-100XP ultracentrifuge). The soluble fraction was discarded, and the membrane fraction was separated from the cells debris and resuspended in phosphate buffer.

1.8. SDS- PAGE and Western blot

Once the running gel has polymerised, the stacking gel is poured on top of it with a comb. After polymerisation the gel was transferred to the running buffer, the protein loaded and approximately 90 V are applied for 2 h.

Running gel	Running gel buffer	5 ml
	Acrylamide 30%	5 ml
	APS (80 mg/ml)	100 µl
	SDS 20%	50 µl
	TEMED	5 µl
Stacking gel	Stacking gel buffer	1 ml
	Acrylamide 30%	2 ml
	APS (80 mg/ml)	100 µl
	SDS 20%	50 µl
	TEMED	5 µl
	H ₂ O	7 ml
Coomassie stain	MeOH	10 ml
	Acetic acid	20 ml
	H ₂ O	70 ml
	Coomassie	A few mg

The gel was removed and either stained with Coomassie or equilibrated in transfer buffer for the Western Blot. The transfer unit was then prepared, with, in that order, the negative base, a sponge, wet filter paper, the gel, activated PVDF membrane, filter paper, another sponge and the positive base. 250 mA are then applied for 90 min at 0 °C. The membrane was blocked with milk and incubated with the primary antibody for 1 h. After washing, the secondary antibody was added for 1 h. the membrane was then developed using a Millipore kit and X-Ray film.

1.9. Complementation assay on agar plates

Two colonies of the strain of interest were picked and plated as two parallel streaks on a PGM agar plate. The plate was incubated for two days at 30 °C and 5 µl of the potential substrate in DMSO were spotted next to the streaks. The plate was incubated for a further 16 hr at 30 °C.

1.10. Prodigiosin production, extraction and quantification

1.10.1. Strains producing pigment.

A solution of LBS was inoculated with an overnight culture of the strain (5 ml of overnight culture for 20 ml of LBs, the final concentration of sorbitol is 0.25M). The culture was incubated at 30 °C, 250 rpm for 16 h. 25 ml of cells were then pelleted (2219 g, 20 min, 4 °C) and the supernatant was discarded. The pellets were vortexed for 1 min in acidified EtOH (4% 1 M HCl). After centrifugation the supernatant gave the desired prodiginine extract.

1.10.2. Strain not producing prodigiosin.

The strain of interest was grown in LBS at 30 °C, 250 rpm until OD₆₀₀ reached 4. A potential substrate was added (10 µM for H₂MAP and its analogues, 1 mM for PigE putative substrates) was then added and the cells were grown for a further 16 h. Cells were then pelleted and prodiginine extracted as described above.

1.10.3. Prodigiosin quantification

A spectrum of the extract described above was recorded on a Cary 300-Bio UV-visible spectrophotometer. If the A₅₃₅>2, the sample was diluted 10 times in EtOH (4% 1 M HCl), and the recorded absorbance was subsequently multiplied by 10. Prodigiosin's maximum absorbance is at 535 nm, but to correct for the absorption of other extracted compounds, A₅₃₅ was corrected using the formula

$$A_{535}^{corr} = A_{535} - \frac{85 \times A_{570} + 35 \times A_{450}}{120}$$

1.11. High Pressure Liquid Chromatography (HPLC)

1.11.1. Achiral analytical

1.11.1.1. Analysis of prodiginines

Samples obtained following the procedures described in Section 1.9 were concentrated to dryness and resuspended in ACN/ H₂O 1:1 (15 ml for strain producing prodigiosin, 1 ml otherwise). They were then run on the HPLC equipped with Phenomenex Jupiter 5µ C18 300A

with an acetonitrile gradient (5 to 100% in 30.5 min, then back to 5% in 30 s and constant 5% for 9 minutes). The absorbances at 500 and 535 nm were monitored.

1.11.1.2. Analysis of 60

Amide **60** was diluted in ACN/H₂O at 0.1 mg/ml. The sample was then run of the HPLC equipped as above with an acetonitrile gradient (50 to 90% in 12 min). The absorbance was monitored at 260 nm.

1.11.2. Chiral analytical

H₂MAP was diluted in hexane (50 mg/ml). 20 µl were injected in the HPLC equipped with Supleco Analytical Astec cellulose DMP column and submitted to a gradient of *i*PrOH in hexane (15 to 50% in 30 min). The absorbance was monitored at 210 nm and 280 nm.

1.11.3. Semi preparative column-prodiginine purification

S39006 ΔpigD in 1 L of LBS were supplemented with **19a**, **19e**, **19g** or **19h** (10 µM) at OD₆₀₀ around 4. The cultures were grown a further 16 hr and the cells were pelleted by centrifugation (25 min, 4500 rpm, 4 °C). Prodigiosin was extracted in 150 ml of acidified EtOH (4% 1 M HCl). After removing the cells by centrifugation, the extract was sterile-filtered (22 µm pores) and concentrated to dryness under reduced pressure. The solid deposit was then resuspended in 1 ml of ACN/H₂O with a few drops of MeOH. After filtration of solid residues, the mixture was purified on the HPLC equipped with an Agilent Zorbax SB-C18 column with a gradient of ACN in H₂O (5 min at 5% then 5 to 100% in 30.5 min, then back to 5% in 30 s and constant 5% for 9 min). The absorbance was monitored at 500 and 535 nm.

1.12. Mass spectrometry

1.12.1. Sample preparation for MS

1.12.1.1. H₂MAP from S39006 ΔpigB

200 ml of LBS in a 2 L flask were inoculated with a 5 ml of an overnight culture of *S39006 ΔpigB* (or *ΔpigD* for negative control). The cells were cultured at 30 °C for 16 h. The cultures were centrifuged, and the cell pellets extracted with 100 ml of acetone/Et₂O 4:1. The extracts were concentrated to 5 ml under reduced pressure. 300 µl were taken and diluted to 1 ml in CH₃CN/H₂O 1:1

1.12.1.2. Analysis of PigE effect on 68

Eppendorf tubes were charged with 1 mM of **68**, 1.25 mM of ornithine and PLP, and 1.25 mM of NAD(P)H. For negative control, no NAD(P)H was added. The solution contained PigE (cell lysates or purified protein) or the corresponding control was added. The resulting 0.5 ml were

gently shaken overnight at 30 °C. The insoluble fraction was eliminated by centrifugation and the soluble fraction analysed directly.

1.12.1.3. Prodigiosin

20 ml of LBS were inoculated with 5 ml of an overnight culture of *S39006*, $\Delta pigB$ (pHDB4) or $\Delta pigB$ (pHDB1). In the case of $\Delta pigB$ (pHDB1) and $\Delta pigB$ (pHDB4), ampicillin (0.1 mg.ml⁻¹) was added. After growing the cells overnight at 30 °C at 250 rpm, pigment was extracted following the method described above. The solvent was then removed under reduced pressure in a pre-weighed flask. The extracts were redissolved in CH₃CN/H₂O 1:1 at 10 mg/ml. When some solid was still visible after vortexing, the sample was filtered through cotton wool.

1.12.2. MS method

H₂MAP samples were run on a Waters Xevo G2-S. Eluent A: H₂O+ 0.1% formic acid, eluent B: 95% ACN/ H₂O+0.1% formic acid. Gradient: 0-0.38 min, 95% A, 5% B; 0.38-3 min, 95-5% A, 5-95% B; 3-4 min, 5% A, 95% B. The chromatograms at 154.16 (H₂MAP+H⁺) are then extracted.

Prodigiosin samples were run on a Waters LCT Premier. Eluent A H₂O+0.05% formic acid, eluent B ACN. Flow: 50% A, 50% B for 3 min

1.13. Antimicrobial assays

1.13.1. Carbapenem assay

8 ml of top lawn agar (LB+0.7% agar) were inoculated with 400 µl of an overnight culture of *E. coli* Super Sensitive (ESS) and poured on an LBA plate (square, 125 x 125 mm). Once the lawn had set, 5-10 µl of an overnight culture of the strain of interest were spotted on the plate. When the carbapenem productions of different strain were assessed on the same plate, the OD₆₀₀ of the overnight cultures were normalized by dilution in LB. The plate was then cultured at 37 °C overnight and the size of the halo around the spot assessed.

1.13.2. Disc assays

Prodiginine extracts were prepared from 400 ml of *Serratia* $\Delta pigD$ complemented with H₂MAP or one of its analogues using the method described above. The extracts were then concentrated under reduced pressure and resuspended in 0.5 ml of acidified EtOH. Paper-filter discs (diameter: 5 mm) were sterilized and 50 µl of the concentrated extract or 40 µl of 10 mM of **19b** in EtOH were spotted on it. Ampicillin discs (10 µg) were bought from Abtek Biological Ltd. The discs were placed on a top lawn (LB + 0.35% agar) inoculated with *ESS* or *S. aureus*. The plate was incubated overnight at 37°C and the size of the halo around the discs assessed.

1.13.3. Half growth inhibition (IG₅₀)

Prodiginine samples were purified as described in Section 1.10.1.1. Fractions containing prodiginines were then concentrated under reduced pressure and resuspended in 200 µl of acidified EtOH. The presence of prodiginines was checked by MS and UV/Vis spectra were recorded. The samples were diluted to 140 µM and a 2-fold serial dilution in water was prepared. A 96 well plate was then charged with MH broth (100 µl), bacterial culture at OD₆₀₀ 0.063 (10 µl, *ESS* or *S. aureus*), and antibiotic (20 µl). A serial dilution of ampicillin (from 10 µg/ml) was used as a positive control. Wells not inoculated with bacteria nor antibiotic were included to check the sterility of the media and wells with media, bacteria and solvent were included as the negative controls. Two wells were used for each concentration of antibiotic. The plates were gently shaken overnight at 37 °C and the OD₆₀₀ with Biochrom EZ Read 400 Microplate Reader. When no growth was visible in the well with the highest concentration of prodigiosin, the OD₆₀₀ was corrected following the formula: $OD_{600}^{cor} = OD_{600} - (OD_{600}(\text{highest concentration prodigiosin}) - \text{average } (OD_{600}(\text{no bacteria}))) / 2^n$ where n is the number of time the most concentrated solution of prodigiosin solution of prodiginine have been diluted by 2. The percentage of growth was then calculated by dividing by the average OD₆₀₀ of wells without antibiotic.

1.14. Anticancer activity

The prodiginine samples were prepared as described in Section 1.11.3. The solvent was removed under reduced pressure and the pigments resuspended in DMSO at 100 µM. HeLa (HeLa ATCC[®] CCL-2[™]) cells were grown in a humidified incubator at 37 °C under 5% CO₂ with 90% humidity and passaged at approximately 80% confluence using Trypsin-EDTA solution 0.25%. Cells were grown in DMEM supplemented with 10% heat-inactivated FBS, 100 units/mL penicillin and 100 µg/mL streptomycin, 2 mM GlutaMax[™]. When the cell density reached 3.2.10⁵ cells/ml, the media was removed, and the cells resuspended in DMEM supplemented with 2 mM GlutaMax[™] and diluted 4 fold. A serial dilution of the prodiginine in the buffer was prepared. The quantity of DMSO was equalised at all dilutions and controls with just DMSO in the buffer were prepared. In a 96 well plate, wells were charged with 180 µl of the cell culture (15000 cells/well) and 20 µl of prodiginine solution or the control 2 h later. After 48 h the media was removed, and the cells were resuspended in Cell Titer Blue (Promega). After 2 h, the fluorescence at 560_{Ex}/590_{Em} was recorded. Results were normalised to the viability measured for the control.

1.15. Thermal shift assay

A RT-PCR 96 well plate was charged as described below with the following potential ligands: **68**, NADH, Ala, Asn, Cys, Glu, Gln, Gly, Ser, Tyr, His, Orn, Ile, Lys, Phe, Thr, Val and NADPH. It was loaded in the RT-PCR machine and a temperature gradient (25°C to 80°C, 0.5 °C every 30 s) was applied and the fluorescence was recorded.

Component	Volume (µl)
NaF buffer	22.025
Sypro orange (5 M)	0.025
Protein (147 µM)	1.7
Ligand (100 mM)	1.25

1.16. CD spectra

The spectra were recorded on an Aviv Model 410. The apparatus was flushed with N₂ before turning on the lamps, followed by the rest of the device. After running a blank in sodium fluoride buffer, the spectra with PigE in solution in this buffer (0.07 mg/ml) was recorded.

1.17. NAD(P)H assay

Cell lysates were prepared as described in section 1.7.1. UV transparent 96 well plates were charged as described below. A₃₄₀ was then monitored at 30°C with a FLUOstar Omega for a few hr.

	Compound	Final concentration (mM)
Purified protein	68	0.2
	Ornithine	0.2
	NAD(P)H	0.2
	Metal ions cocktail	0.2
	Enzyme	1 or 10 µM
	Buffer	To 100 µl
Cell extracts	68	0.2
Method A	Ornithine	0.2
	NAD(P)H	0.2
	Metal ions cocktail*	0.2
	Extract	1 or 10
	Buffer	To 100 µl

Cell extracts	68	1
Method B	Ornithine	0.125
	NAD(P)H	1.25
	PLP	0.125
	Extract in phosphate buffer	To 100 μ l

The metal ions cocktail contained MgCl₂, MnCl₂, KCl and NiCl₂; at the same concentration.

For the experiment with purified protein and method A, Phosphate buffer, TRIS buffer, citric acid and HEPES buffer were tried.

1.18. Ninhydrin assay

Cell lysates were prepared as described in Section 1.7.1. The mixture described below was incubated 15 min at 30 °C. 0.3 ml of perchloric acid (3 M) was added, followed by 0.3 ml of ninhydrin. The UV spectrum was recorded after a 10-fold dilution to avoid saturating the detector.

Component	Concentration (mM)
129	5
Ornithine	35
PLP	50
Cell lysate	20 μ l
TRIS buffer	To 1 mL

1.19. Ehrlich's assay

Solution A (MES pH 6.0 10 mM, HapB 29 μ g.ml⁻¹ or cell lysate) and B (MES pH 6.0 10 mM, H₂MAP 0.1 to 1.4 mM, DMSO 8%) were prepared and incubated separately for 10 and 5 min respectively. The reaction was then initiated by mixing 25 μ l of each per well in a 96-well plate. The reaction was stopped by addition of 50 μ l of stop reagent (HgCl₂ 100 mM, TCA 10% in H₂O) followed by 100 μ l of Ehrlich's reagent (2% *p*-dimethylaminobenzaldehyde in acetic acid with 16% perchloric acid). The plate was incubated for a further 20 min at r.t. and an absorbance spectrum was recorded. The baseline was subtracted using the formula $A_{555}^{corr} = A_{555} - (A_{460} + A_{650})/2$

1.20 Bacterial strains and plasmid

Strain	Genotype/phenotype	Source
<i>Serratia</i>		
ATCC 39006	Wild type (Car+, Pig+)	Bycroft <i>et al.</i> ¹⁹⁸
NW14 (noted $\Delta pigB$)	In-frame <i>pigB</i> Δ (3270–4773, 501 aa Δ)	Williamson <i>et al.</i> ²⁶
NW13 (noted $\Delta pigD$)	In-frame <i>pigD</i> Δ (7895–9446, 517 aa Δ)	Williamson <i>et al.</i>
NW6 (noted $\Delta pigE$)	In-frame <i>pigE</i> Δ (10321–12865, 848 aa Δ)	Williamson <i>et al.</i>
ROP2	<i>pstS::miniTn5Sm/Sp</i> , Sp ^R	Slater <i>et al.</i> ¹⁵⁰
MCA54	<i>carA::miniTn5lacZl</i> , Km ^R	Thomson <i>et al.</i> ²³
$\Delta pigD$ <i>carA</i> -	In-frame <i>pigD</i> Δ (7895–9446, 517 aa Δ), <i>carA::miniTn5lacZl</i> , Km ^R	This study
$\Delta pigD$ <i>rop2</i>	In-frame <i>pigD</i> Δ (7895–9446, 517 aa Δ), <i>pstS::miniTn5Sm/Sp</i> , Sp ^R	This study
<i>E. coli</i>		
DH5 α	<i>supE44</i> , <i>hsdR17</i> (r _K ⁻ m _K ⁻), <i>thi-1</i> , <i>recA1</i> , <i>gyrA96</i> (Nal ^R), <i>relA1</i> , Δlac (<i>lacIZYA-argF</i>) U169 <i>deoR</i> ($\phi 80 lacZ\Delta M15$)	Grant <i>et al.</i> ¹⁹⁹
BL21 (DE3)	<i>B F⁻ ompT gal dcm lon hsdS_B(r_B⁻ m_B⁻) λ(DE3</i> <i>[lacI lacUV5-T7p07 ind1 sam7 nin5]) [malB⁺]_K</i> <i>l2</i> (λ^S)	Studier <i>et al.</i> ²⁰⁰
C43	<i>F⁻ ompT gal dcm hsdS_B(r_B⁻ m_B⁻)(DE3)</i>	NEB
ESS	β -Lactam super-sensitive indicator strain	Bainton <i>et al.</i> ¹⁵⁵
$\beta 2163$	F-RP4-2-Tc::Mu <i>DdapA::(erm-pir)</i> , Km ^s Em ^s	Ramsay <i>et al.</i> ²⁰¹
<i>S. aureus</i> H	WT	Takebe <i>et al.</i> ²⁰²
Plasmid		
pQE80-L	6xHis fusion expression vector, Amp ^R	Qiagen
pQE80-L:: <i>oriT</i>	6xHis fusion expression vector containing <i>oriT</i> gene for bacterial conjugation, Amp ^R	Monson <i>et al.</i> ¹⁸⁸
pBlueScript-II KS+	ColEI replicon, Amp ^R	Stratagene
pHDB1	1698 bp <i>Bam</i> HI/ <i>Sph</i> I containing N-His ₆ - <i>hapB</i> ligated into pQE80L	Couturier <i>et al.</i> ³⁷
pHDB2	1639 bp <i>Bam</i> HI/ <i>Pst</i> I containing N-His ₆ - <i>pigB</i> ligated into pQE80-L (truncated)	Couturier <i>et al.</i>

pHDB3	2013 bp <i>Bam</i> HI/ <i>Pst</i> I containing N-His ₆ - <i>pigB</i> ligated into pQE80-L:: <i>oriT</i>	Couturier <i>et al.</i>
pHDB4	2013 bp <i>Eco</i> RI/ <i>Pst</i> I containing C-His ₆ - <i>pigB</i> ligated into pQE80-L:: <i>oriT</i>	Couturier <i>et al.</i>
pBS- <i>pigEC</i>	1359 bp <i>Pst</i> I/ <i>Sac</i> I containing <i>pigE</i> C-terminal domain ligated into pBlueScript	This study
pPigEC	1359 bp <i>Pst</i> I/ <i>Sac</i> I containing N-His ₆ tag <i>pigE</i> C-terminal domain ligated into pBlueScript	This study
pBS- <i>pigE</i>	2562 bp <i>Pst</i> I/ <i>Sac</i> I containing <i>pigE</i> ligated into pBlueScript	This study
pPigE	2562 bp <i>Pst</i> I/ <i>Sac</i> I containing N-His ₆ tag <i>pigE</i> ligated into pQE80-L:: <i>oriT</i>	This study

2. Synthesis

2.1. General considerations

Standard solution-phase chemistry was used for the synthesis of the various biosynthetic intermediates and their analogues. All reactions were carried out under N₂ in pre-dried glassware and all organic solvents used were freshly distilled. Solvents and reagents for anhydrous reactions were dried by conventional methods prior to use. Milli-Q deionised water was used in all chemical reactions and biochemical work. High temperature reactions were carried out using a silicone oil bath. Yields refer to chromatographically and spectroscopically pure compounds. Microanalyses were performed by the University of Cambridge Microanalytical Laboratory in the Department of Chemistry, and are quoted to the nearest 0.1% for all elements except for hydrogen, which is quoted to the nearest 0.05%. Reported atomic percentages are within the error limits of $\pm 0.3\%$.

2.1.1. Nuclear Magnetic Resonance spectroscopy

NMR Spectra were recorded in deuterated solvents (as specified) using a Bruker AM/DPX-400 (¹H NMR at 400 MHz, ¹³C NMR at 100 MHz). Chemical Shifts (δ) are quoted in parts per million (ppm) and referenced to solvent peaks. Coupling constants (J) are reported in Hz. The multiplicities and general assignments of the spectroscopic data are denoted as: singlet (s), doublet (d), triplet (t), quartet (q), quintet (quin), double doublet (dd), double double doublet (ddd), double doublet triplet (ddt), double triplet (dt), triple triplet (tt), double quartet (dq), unresolved multiplet (m), and broad (br).

2.1.2. LC-MS

LC-MS analyses were performed with an Waters H-Class UPLC on a Waters Acquity UPLC BEH C18, 1.7 μ m column eluted with a gradient of 10 mM aqueous ammonium acetate containing 0.1% formic acid to 95% acetonitrile over 3 min, coupled to a Waters SQD2 and/or with a Alliance HT Waters 2795 Separations Module on a Waters Atlantis dC18 4.6 x 30 mm, 3 μ m column eluted with a gradient of 10 nM aqueous ammonium acetate containing 0.1% formic acid to 95% acetonitrile over 8 min, coupled to a Waters Micromass ZQ Quadrupole Mass Analyser (using electrospray ionisation (ESI)) with accuracy no greater than 0.4 Da.

2.1.3. High Resolution Mass Spectrometry

Accurate masses were obtained with a Waters LCT Premier high-resolution mass spectrometer and/or a Waters Xevo G2-S.

2.1.4. Infra-Red (IR) Spectroscopy

IR spectra were recorded neat on a diamond/ZeSe plate using a Perkin-Elmer Spectrum One FT-IR Universal Attenuated Transmittance Reflectance (ATR) sampling accessory spectrometer with internal referencing. Characteristic absorption maxima (λ_{\max}) are reported in wavenumbers (cm^{-1}) and the following abbreviations are used: w, weak; m, medium; s, strong; br, broad.

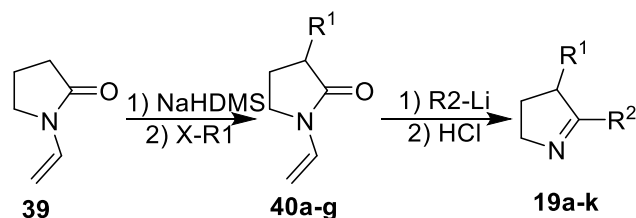
2.1.5. Silica Gel Chromatography

Unless otherwise stated, flash column chromatography was performed using 230-400 mesh Kieselgel 60 silica. Analytical thin layer chromatography (TLC) was performed on commercial silica gel plates (Merck glass- or aluminium-backed plates coated with a 0.20 mm layer of silica gel 60 with fluorescent indicator UV254). These plates were visualised using either ultraviolet light (254 or 365 nm), or by staining the plates with potassium permanganate or vanillin solutions or with Ehrlich's reagent.

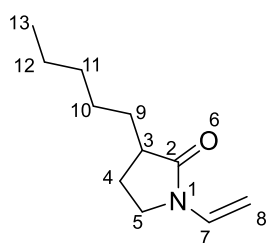
2.1.6. Ultraviolet-Visible (UV-Vis) spectrophotometry

All the UV-Vis spectra for the various compounds were taken on a Helios Zeta UV-Vis with a 6 multicell holder using 1 cm path length using either 1 ml quartz cuvettes or polystyrene disposable cuvettes.

2.2. Synthesis of H₂MAP analogues



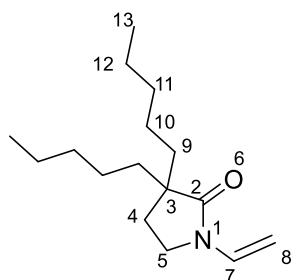
3-Pentyl-1-vinylpyrrolidin-2-one **40a**



A solution of N-vinylpyrrolidin-2-one **39** (5 ml, 50 mmol, 1 eq.) in dry THF (20 ml) was added dropwise to a stirred solution of NaHDMS (2 M in THF, 26 ml, 52 mmol, 1.04 eq.) at $-78\text{ }^{\circ}\text{C}$ under N_2 . After 1 h a solution of 1-iodopentane (7.15 ml, 55 mmol, 1.1 eq.) in dry THF (20 ml) was added dropwise. The mixture was allowed to warm to r.t. (RT), stirred for 16 h, diluted with diethyl ether (20 ml), filtered and evaporated under reduced pressure. Purification by column chromatography (petroleum ether/EtOAc, 85:15) gave **40a** (5.6 g, 30 mmol, 60%) as a colourless oil. ^1H NMR (400 MHz, CDCl_3): δ 0.89 (3H, t, J 7.0 Hz, H_{13}), 1.20-1.40 (7H, m, H_{10} , H_{11} , H_{12} , H_{9a}), 1.74 (1H, m, H_{4a}), 1.87 (1H, m, H_{9b}), 2.28 (1H, m, H_{4b}), 2.50 (1H, m, H_3), 3.38 (1H, m,

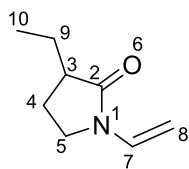
H_{5a}), 3.49 (1H, td, *J* 10.0 & 4.0 Hz, H_{5b}), 4.38 (1H,d, *J* 16.0 Hz, H_{8a}), 4.42 (1H,d, *J* 9.0 Hz, H_{8b}), 7.10(1H, dd, *J* 16.0 & 9.0 Hz, H₇); ¹³C NMR (100 MHz, CDCl₃): δ 14.02 (C₁₃), 22.52 (C₁₂), 24.41 (C₄), 26.83 (C₁₀), 31.11 (C₉), 31.71 (C₁₁), 42.44 (C₃), 42.88 (C₅), 93.97 (C₈), 129.63 (C₇), 175.32 (C₂); IR (neat): ν_{max} 2954m, 2928m, 2858m, 1704s (C=O) cm⁻¹; HRMS: *m/z* calcd for C₁₁H₁₉NO+H⁺: 182.1545; found: 182.1551.

3,3-Dipentyl-1-vinylpyrrolidin-2-one **41**



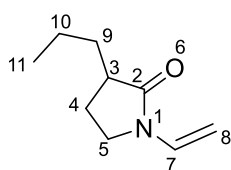
This compound was sometimes formed along **40a**. ¹H NMR (400 MHz, CDCl₃) δ 0.87 (6H, t, *J* 7.0 Hz, H₁₃), 1.1-1.40 (12H, m, H₁₀, H₁₁ and H₁₂), 1.51 (4H, m, H₉), 1.97 (2H, t, *J* 7.0 Hz, H₄), 3.39 (2H, t, *J* 7.0 Hz, H₅), 4.37 (1H, d, *J* 16.0 Hz, H_{8a}), 4.42 (1H, d, *J*, 9.0 Hz, H_{8b}), 7.10 (1H,dd, *J* 9.0 & 16.0 Hz, H₇)

3-Ethyl-1-vinylpyrrolidin-2-one **40b**

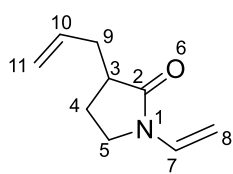


Product **40b** (17 mmol, 70%) was obtained by a similar procedure as for **40a**. ¹H NMR δH (400 MHz, CDCl₃): 0.97 (3H, t, *J* 8.0 Hz, H₁₀), 1.45 (1H, m, H_{9a}), 1.75 (1H, m, H_{4a}), 1.90 (1H, m, H_{9b}), 2.28 (1H, m, H_{4b}), 2.46 (1H, m, H₃), 3.39 (1H, m, H_{5a}), 3.49 (1H, td, *J* 10.0 & 3.0 Hz, H_{5b}), 4.38 (1H, d, *J* 16.0 Hz, H_{8a}), 4.42 (1H,d, *J* 9.0 Hz, H_{8b}), 7.10 (1H, dd, *J* 16.0 & 9.0 Hz, H₇); ¹³C NMR (100 MHz, CDCl₃): 11.40 (C₁₀), 23.80 (C₄), 24.14 (C₉), 42.88 (C₃), 43.78 (C₅), 94.02 (C₈), 129.60 (C₇), 175.13 (C₂); IR (neat): ν_{max} 2954m, 2928m, 2858m, 1704s (C=O) cm⁻¹; HRMS: *m/z* calcd for C₈H₁₃NO+H⁺: 140.1070; found 140.1068.

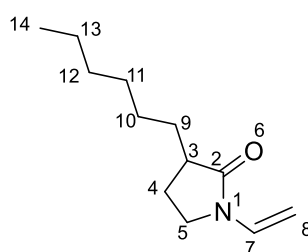
3-Propyl-1-vinylpyrrolidin-2-one **40c**



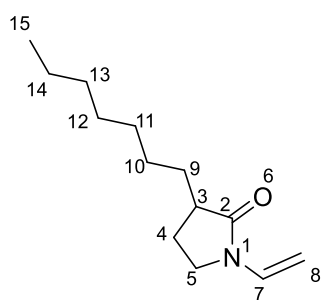
Product **40c** (15 mmol, 60%) was obtained by a similar procedure as for **40a**. ¹H NMR (400 MHz, CDCl₃): 0.94 (3H, t, 7.0 Hz, H₁₁), 1.33-1.46 (3H, m, H₁₀, H_{9a}), 1.74 (1H, m, H_{4a}), 1.86 (1H, m, H_{9b}), 2.28 (1H, m, H_{4b}), 2.51 (1H, m, H₃), 3.37 (1H, m, H_{5a}), 3.49 (1H, td, *J* 10.0 & 4.0 Hz, H_{5b}), 4.38 (1H, d, *J* 16.0 Hz, H_{8a}), 4.42 (1H, d, *J* 9.0 Hz, H_{8b}), 7.10(1H, dd, *J* 16.0 & 9.0 Hz, H₇); ¹³C NMR (100 MHz, CDCl₃): 13.95 (C₁₁), 20.36 (C₁₀), 24.40 (C₄), 33.28 (C₉), 42.21 (C₃), 42.88 (C₅), 93.97 (C₈), 129.62 (C₇), 175.32 (C₂); IR (neat): ν_{max} 2956m, 2928m, 2860m, 1702s (C=O) cm⁻¹; HRMS: *m/z* calcd for C₉H₁₅NO+H⁺: 154.1226; found: 154.1227.

3-Allyl-1-vinylpyrrolidin-2-one **40d**

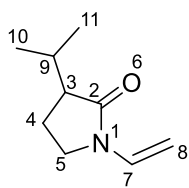
Product **40d** (16 mmol, 64%) was obtained by reacting **39** with allylbromide in the same conditions as for **40a**. ^1H NMR (400 MHz, CDCl_3): δ 1.80 (1H, m, H_{4a}), 2.23 (2H, m, H_{4b} and H_{9a}), 2.61 (2H, m, H_3 and H_{9b}), 3.39 (1H, m, H_{5a}), 3.49 (1H, td, J 10.0 & 4.0 Hz, H_{5b}), 4.38 (1H, d, J 16.0 Hz, H_{8a}), 4.42 (1H, d, J 9.0 Hz, H_{8b}), 5.10 (2H, m, H_{11}), 5.78 (1H, m, H_{10}), 7.10 (1H, dd, J 16.0 & 9.0 Hz, H_7); ^{13}C NMR (100 MHz, CDCl_3): 23.52 (C_4), 35.27 (C_9), 41.90 (C_3), 42.86 (C_5), 94.30 (C_8), 117.20 (C_{11}), 129.54 (C_7), 135.50 (C_{10}); IR (neat): ν_{max} 2954m, 2928m, 2859m, 1700s ($\text{C}=\text{O}$) cm^{-1} ; HRMS: m/z calcd for $\text{C}_9\text{H}_{13}\text{NO}+\text{H}^+$: 152.1070; found: 152.1068.

3-Hexyl-1-vinylpyrrolidin-2-one **40e**

Product **40e** (18 mmol, 70%) was obtained by a similar procedure as for **40a**. ^1H NMR (400 MHz, CDCl_3): δ 0.87 (3H, t, J 6.0 Hz, H_{14}), 1.26-1.42 (9H, m, H_{10} , H_{11} , H_{12} , H_{13} , H_{9a}), 1.73 (1H, m, H_{4a}), 1.88 (1H, m, H_{9b}), 2.28 (1H, m, H_{4b}), 2.49 (1H, m, H_3), 3.37 (1H, m, H_{5a}), 3.49 (1H, td, J 10.0 & 3.0 Hz, H_{5b}), 4.38 (1H, d, J 16.0 Hz, H_{8a}), 4.42 (1H, d, J 9.0 Hz, H_{8b}), 7.10 (1H, dd, J 16.0 & 9.0 Hz, H_7); ^{13}C NMR (100 MHz, CDCl_3): δ 14.07 (C_{14}), 22.60 (C_{13}), 24.40 (C_4), 27.12 (C_{10}), 29.18 (C_{11}), 31.16 (C_9), 31.70 (C_{12}), 42.44 (C_3), 42.88, 93.98 (C_8), 129.62 (C_7), 175.32 (C_2); IR (neat) ν_{max} 2956m, 2928m, 2860m, 1703s ($\text{C}=\text{O}$) cm^{-1} ; HRMS, m/z calcd for $\text{C}_{12}\text{H}_{21}\text{NO}+\text{H}^+$: 196.1696; found 196.1694.

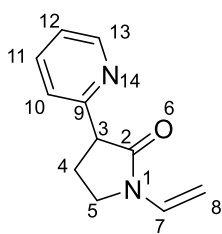
3-Heptyl-1-vinylpyrrolidin-2-one **40f**

Product **40f** (19 mmol, 73%) was obtained by a similar procedure as for **40a**. ^1H NMR (400 MHz, CDCl_3): δ 0.88 (3H, t, J 7.0 Hz, H_{15}), 1.20-1.40 (11H, m, H_{10} , H_{11} , H_{12} , H_{13} , H_{14} , H_{9a}), 1.74 (1H, m, H_{4a}), 1.87 (1H, m, H_{9b}), 2.28 (1H, m, H_{4b}), 2.49 (1H, m, H_3), 3.38 (1H, m, H_{5a}), 3.49 (1H, td, J 9.7 & 3.2 Hz, H_{5b}), 4.38 (1H, d, J 16.0 Hz, H_{8a}), 4.42 (1H, d, J 9.0 Hz, H_{8b}), 7.10 (1H, dd, J 16.0 & 9.0 Hz, H_7); ^{13}C NMR (100 MHz, CDCl_3): δ 14.07 (C_{15}), 22.64 (C_{14}), 24.40 (C_4), 27.17 (C_{10}), 29.17 (C_{12}), 29.49 (C_{11}), 31.16 (C_9), 31.81 (C_{13}), 42.44 (C_3), 42.88 (C_5), 93.97 (C_8), 129.62 (C_7), 175.32 (C_2); IR (neat): ν_{max} 2954m, 2930m, 2858m, 1705s ($\text{C}=\text{O}$) cm^{-1} ; HRMS: m/z calcd for $\text{C}_{13}\text{H}_{23}\text{NO}+\text{H}^+$: 210.1852; found: 210.1853.

3-Isopropyl-1-vinylpyrrolidin-2-one **40g**

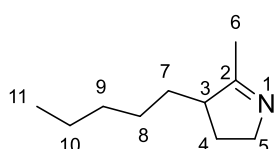
Product **40g** (3.8 mmol, 60%) was obtained by a similar procedure as for **40a**.

^1H NMR (400 MHz, CDCl_3): δ 0.87 (3H, d, J 7.0 Hz, H_{11}), 1.01 (3H, d, J 7.0, H_{10}), 1.87 (1H, m, H_{4a}), 2.10 (1H, m, H_{4b}), 2.23 (1H, m, H_9), 2.50 (1H, m, H_3), 3.38 (1H, m, H_{5a}), 3.46 (1H, td, J 10.0 & 4.0 Hz, H_{5b}), 4.37 (1H, d, J 16.0 Hz, H_{8a}), 4.42 (1H, d, J 9.0 Hz, H_{8b}), 7.11 (1H, dd, J 16.0 & 9.0 Hz, H_7); ^{13}C NMR (100 MHz, CDCl_3): δ 17.71 (C_{11}), 19.32 (C_4), 20.52 (C_{10}), 28.46 (C_9), 43.04 (C_5), 48.20 (C_3), 93.99 (C_8), 129.55 (C_7), 174.65 (C_2); IR (neat): ν_{max} 2954m, 2930m, 2858m, 1704s ($\text{C}=\text{O}$) cm^{-1} ; HRMS: m/z calcd for $\text{C}_9\text{H}_{15}\text{NO}+\text{H}^+$: 154.1226; found: 154.1225.

3-(Pyridin-2-yl)-1-vinyl-4,5-dihydro-1H-pyrrol-2-ol **40h**

Product **40h** (1.817 g, 20%) was obtained by reacting **39** with

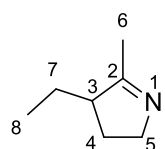
bromopyridine in the same conditions as for **40a**. ^1H NMR (400 MHz, CDCl_3): δ 2.50 (1H, m, H_{4a}), 2.68 (1H, m, H_{4b}), 3.74 (2H, m, H_5), 4.64 (2H, m, H_8), 7.14 (1H, dd, J 9.0 & 16.0 Hz, H_7), 7.26 (1H, m, H_{12}), 7.45 (1H, d, J 8.0 Hz, H_{10}), 7.74 (1H, t, J 8.0 Hz, H_{12}), 8.57 (1H, d, J 5.0 Hz); ^{13}C NMR (100 MHz, CDCl_3): δ 34.0 (C_4), 41.9 (C_5), 79.3 (C_3), 96.2 (C_8), 119.5 (C_{10}), 123.1 (C_{12}), 129.8 (C_7), 137.2 (C_{11}), 148.4 (C_{13}), 172.8 (C_2); IR (neat): ν_{max} 3326br (O-H), 3000w, 2957w, 2893w, 1681s ($\text{C}=\text{N}$), 1635s ($\text{C}=\text{O}$) cm^{-1} ; HRMS: m/z calcd for $\text{C}_{11}\text{H}_{12}\text{N}_2\text{O}+\text{H}^+$: 189.1022 found 189.1024

5-Methyl-4-pentyl-3,4-dihydro-2H-pyrrole (H_2MAP) **19a**

A solution of 3-pentyl-1-vinylpyrrolidin-2-one **40a** (1 g, 5.5 mmol, 1 eq) in Et_2O (2 ml) was added dropwise to a stirred solution of MeLi (1.6 M in Et_2O , 4.5 ml, 7.2 mmol, 1.3 eq.) at -10°C . The mixture was stirred at -10°C for 1 h and at r.t. for 1 h. It was then cooled to 0°C and hydrochloric acid (1 M) was added slowly to pH 2. The mixture was stirred at r.t. for 40 min. The two phases were separated, and the organic phase was extracted with hydrochloric acid (1 M). The combined aqueous phases were washed with DCM. Aq. NaOH (1 M) was added to pH 11 and the mixture was extracted with DCM. The organic layer was dried (MgSO_4) and evaporated. Purification by column chromatography (DCM/MeOH, 9:1) gave **19a** (658 mg, 78%) as an oil. ^1H NMR (400 MHz, CDCl_3) δ 0.87 (3H, t, J 7.0, H_{11}), 1.28 (7H, m, H_{7a} , H_8 , H_9 and H_{10}), 1.50 (1H, m, H_{4a}), 1.65 (1H, m, H_{7b}), 1.94 (3H, s, H_6), 1.98-2.08 (1H, m, H_{4b}), 2.51-2.65 (1H, m, H_3), 3.54-3.66 (1H, m, H_{5a}), 3.67-3.82 (1H, m, H_{5b}); ^{13}C NMR (125 MHz, CDCl_3 , APT used for assignments): δ 13.9 (C_{11}), 18.1 (C_6), 22.6 (C_{10}), 27.3 (C_4), 29.1, 31.8 and 31.9 (C_7 , C_8 and C_9), 50.7 (C_3), 58.8 (C_5), 177.6 (C_2); IR (neat):

ν_{\max} 2955m, 2928s, 2860m, 1649s (C=N) cm^{-1} ; HRMS: m/z calcd for $\text{C}_{10}\text{H}_{19}\text{N}+\text{H}^+$: 154.1596; found: 154.1595.

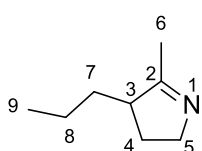
5-Methyl-4-ethyl-3,4-dihydro-2H-pyrrole **19b**



Product **19b** (5.3 mmol, 75%) was obtained by a similar procedure as for **19a**.

Purification by column chromatography was not necessary. ^1H NMR (400 MHz, CDCl_3): δ 0.91 (3H, t, J 7.2 Hz, H_8), 1.28 (1H, m, H_{7a}), 1.52 (1H, m, H_{4a}), 1.73 (1H, H_{7b}), 1.97 (3H, s, H_6), 2.05 (1H, m, H_{4b}), 2.59 (1H, m, H_3), 3.64 (1H, m, H_{5a}), 3.74 (1H, m, H_{5b}); ^{13}C NMR (100 MHz, CDCl_3): δ 11.73 (C_8), 17.96 (C_6), 24.63 (C_7), 28.52 (C_4), 52.20 (C_3), 58.90 (C_5), 177.94 (C_2); IR (neat): ν_{\max} 2957m, 2929s, 2860m, 1649s (C=N) cm^{-1} ; HRMS: m/z calcd for $\text{C}_7\text{H}_{13}\text{N}+\text{H}^+$: 112.1121; found: 112.1121.

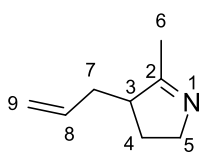
5-Methyl-4-propyl-3,4-dihydro-2H-pyrrole **19c**



Product **19c** (4.6 mmol, 71%) was obtained by a similar procedure as for **19a**.

Purification by column chromatography was not necessary. ^1H NMR (400 MHz, CDCl_3): δ 0.87 (3H, t, J 8.0 Hz, H_9), 1.14-1.42 (3H, m, H_8 , H_{7a}), 1.50 (1H, m, H_{4a}), 1.65 (1H, m, H_{7b}), 1.97 (3H, s, H_6), 2.05 (1H, m, H_{4b}), 2.62 (1H, m, H_3), 3.62 (1H, m, H_{5a}), 3.74 (1H, m, H_{5b}); ^{13}C NMR (100 MHz, CDCl_3): δ 14.10 (C_9), 17.97 (C_6), 20.94 (C_8), 29.12 (C_4), 34.05 (C_7), 50.63 (C_3), 58.78 (C_5), 178.04 (C_2); IR (neat): ν_{\max} 2955m, 2929s, 2862m, 1650s (C=N) cm^{-1} ; HRMS: m/z calcd for $\text{C}_8\text{H}_{15}\text{N}+\text{H}^+$: 126.1217; found: 126.1215.

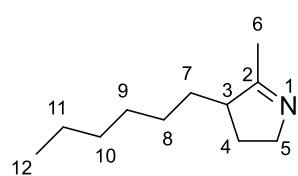
5-Methyl-4-allyl-3,4-dihydro-2H-pyrrole **19d**



Product **19d** (4.5 mmol, 70%) was obtained by a similar procedure as for **19a**.

Purification by column chromatography was not necessary. ^1H NMR (400 MHz, CDCl_3): δ 1.58 (1H, m, H_{4a}), 2.0 (3H, s, H_6), 2.05 (2H, m, H_{4b} , H_{7a}), 2.42 (1H, m, H_{7b}), 2.74 (1H, m, H_3), 3.70 (2H, m, H_5), 5.06 (2H, m, H_9), 5.72 (1H, m, H_8); ^{13}C NMR (100 MHz, CDCl_3): δ 18.07 (C_6), 28.67 (C_4), 36.05 (C_7), 50.09 (C_3), 58.91 (C_5), 116.71 (C_9), 135.74 (C_8), 176.88 (C_2); IR (neat): ν_{\max} 2955m, 2927s, 2859m, 1649s (C=N) cm^{-1} ; HRMS: m/z calcd for $\text{C}_8\text{H}_{13}\text{N}+\text{H}^+$: 124.1121; found: 124.1123.

5-Methyl-4-hexyl-3,4-dihydro-2H-pyrrole **19e**

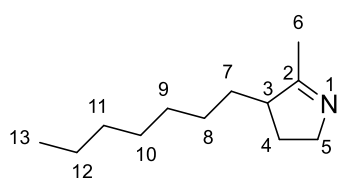


Product **19e** (3.4 mmol, 68%) was obtained by a similar procedure as for **19a**.

^1H NMR (400 MHz, CDCl_3): δ 0.89 (3H, t, J 7.0 Hz, H_{12}), 1.20-1.34 (9H, m, H_{11} , H_{10} , H_9 , H_8 , H_{7a}), 1.50 (1H, m, H_{4a}), 1.67 (1H, m, H_{7b}), 1.97 (3H, s, H_6), 2.05 (1H, m, H_{4b}), 2.62 (1H, m, H_3), 3.63 (1H, m, H_{5a}),

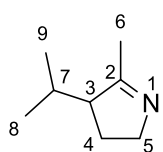
3.76 (1H, m, H_{5b}); ¹³C NMR (100 MHz, CDCl₃): δ 14.07 (C₁₂), 18.01 (C₆), 22.62 (C₁₁), 27.71 (C₈ or C₉), 29.17 (C₄), 29.35 (C₈ or C₉), 31.77 (C₇), 31.86 (C₁₀), 50.83 (C₃), 58.89 (C₅), 177.88 (C₂); IR (neat): ν_{max} 2957m, 2930m, 2861 M, 1649s (C=N) cm⁻¹; HRMS: *m/z* calculated for C₁₂H₂₁NO+H⁺: 196.1696; found: 196.1694.

5-Methyl-4-heptyl-3,4-dihydro-2H-pyrrole **19f**



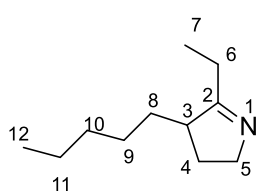
Product **19f** (3.1 mmol, 65%) was obtained by a similar procedure as for **19a**. Purification by column chromatography was not necessary. ¹H NMR (400 MHz, CDCl₃): δ 0.88 (3H, t, *J* 7.0 Hz, H₁₃), 1.20-1.34 (11H, m, H₁₂, H₁₁, H₁₀, H₉, H₈, H_{7a}), 1.50 (1H, m, H_{4a}), 1.65 (1H, m, H_{7b}), 1.97 (3H, s, H₆), 2.05 (1H, m, H_{4b}), 2.61 (1H, m, H₃), 3.63 (1H, m, H_{5a}), 3.75 (1H, m, H_{5b}); ¹³C NMR (100 MHz, CDCl₃): δ 14.08 (C₁₃), 17.99 (C₆), 22.64 (C₁₂), 27.7 (C₈), 29.14 (C₄), 29.22 (C₁₀), 29.64 (C₉), 31.83 & 31.84 (C₇ and C₁₁), 50.82 (C₃), 58.84 (C₅), 177.96 (C₂); IR (neat): ν_{max} 2955m, 2928s, 2860m, 1650s (C=N) cm⁻¹; HRMS: *m/z* calcd for C₁₂H₂₃N+H⁺: 182.1903; found: 182.1906.

5-Methyl-4-isopropyl-3,4-dihydro-2H-pyrrole **19g**

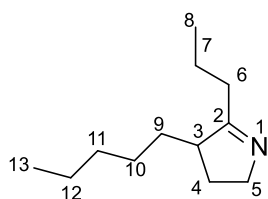


Product **19g** (3.9 mmol, 60%) was obtained by a similar procedure as for **19a**. ¹H NMR (400 MHz, CDCl₃): δ 0.71 (3H, d, *J* 6.0 Hz, H₈), 0.96 (3H, d, *J* 7.0 Hz, H₉), 1.66 (H, m, H_{4a}), 1.84 (1H, m, H_{4b}), 1.97 (3H, s, H₆), 2.10 (1H, m, H₇), 2.69 (1H, m, H₃), 3.69 (2H, m, H₅); ¹³C NMR (100 MHz, CDCl₃): δ 16.3 (C₈), 18.2 (C₆), 21.7 (C₉), 22.9 (C₄), 28.0 (C₇), 57.2 (C₃), 59.54 (C₅); IR (neat): ν_{max} 2956m, 2928s, 2860m, 1650s (C=N) cm⁻¹; HRMS: *m/z* calcd for C₈H₁₅N+H⁺: 126.1217; found: 126.1216.

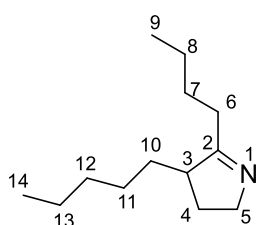
5-Ethyl-4-pentyl-3,4-dihydro-2H-pyrrole **19h**



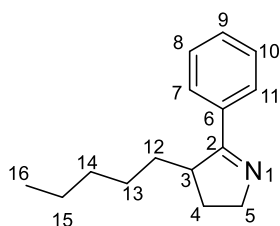
Product **19h** (0.17 mmol, 17%) was obtained by a similar procedure as for **19a**. ¹H NMR (400 MHz, CDCl₃): δ 0.87 (3H, t, *J* 7.0, H₁₂), 1.13 (3H, t, *J* 8.0, H₇), 1.17-1.36 (7H, m, H_{8a}, H₉, H₁₀ and H₁₁), 1.50 (1H, m, H_{8b}), 1.64 (1H, m, H_{6a}), 2.04 (1H, m, H_{6b}), 2.23 (1H, m, H_{4a}), 2.34 (1H, m, H_{4b}), 2.66 (1H, m, H₃), 3.65 (1H, m, H_{5a}), 3.76 (1H, m, H_{5b}); ¹³C NMR (100 MHz, CDCl₃): δ 10.7 (C₇) 14.2 (C₁₂), 22.8 (C₁₁), 25.0 (C₆), 27.7 (C₄), 29.3, 32.0, 32.1 (C₈, C₉ and C₁₀), 49.9 (C₃), 58.9 (C₅), 182.4 (C₂); LC/MS: *m/z* for C₁₁H₂₁N+H⁺: 168.17 ; found: 168.3

5-Propyl-4-pentyl-3,4-dihydro-2H-pyrrole **19i**

To a stirred solution of iodopropane (52 μ l, 0.55 mmol, 1 eq.) dry n-pentane-Et₂O (3:2, 5 ml) under N₂ at -78 °C was added dropwise tBuLi (1.7 M in hexane, 0.7 ml 1.21 mmol, 2.2 eq.). The mixture was stirred at -78 °C for 5 min and at r.t. for 1 h, then cooled again to -78 °C. A solution of **40a** (200 mg, 1.1 mmol, 2 eq.) in dry Et₂O (0.4 ml) was added dropwise. The mixture was stirred for 1 h at -10 °C and then 1.5 h at r.t. Hydrochloric acid (1 M) was then added dropwise to pH 2. After being stirred for 20 min, the organic layer was separated and extracted with hydrochloric acid (0.1 M). The combined aqueous layers were washed with Et₂O. Aq. NaOH (1 M) was then added to pH 10 and mixture was extracted with DCM. The combined extracts were dried (MgSO₄) and evaporated. Purification by column chromatography (DCM/MeOH, 98:2) gave **19i** (10 mg, 55 μ mol, 10%). ¹H NMR (400 MHz, CDCl₃): δ 0.87 (3H, m, H₁₃), 0.93 (3H, t, *J* 7.0, H₈), 1.26-1.39 (11H, m, H₆, H₇ H_{9a}, H₁₀, H₁₁ and H₁₂), 2.13-2.34 (3H, m, H₄ and H_{9b}), 2.63 (1H, m, H₃), 3.57-3.69 (1H, m, H_{5a}), 3.69-3.81 (1H, m, H_{5b}); ¹³C NMR (125 MHz, CDCl₃): δ 14.1 (C₈) 14.1 (C₁₃), 21.1 (C₄), 22.5 (C₁₂), 22.6 (C₇), 27.5, 30.8, 31.7, 31.9 (C₆, C₉, C₁₀ and C₁₁), 40.2 (C₃), 60.2 (C₅), 171.1 (C₂); LC/MS: *m/z* calcd for C₁₂H₂₃N+H⁺:182.19; found 182.3.

5-Butyl-4-pentyl-3,4-dihydro-2H-pyrrole **19j**

Product **19j** (66 μ mol, 33%) was obtained by a similar procedure as for **19a**. ¹H NMR (400 MHz, CDCl₃): δ 0.90 (6H, m, H₉ and H₁₄), 1.13-1.42 (9H, m, H₆, H₈, H_{10a}, H₁₁, H₁₂ and H₁₃), 1.13-1.73 (4 H, m, H₆ and H₇), 2.02 (1H, m, H_{10b}), 2.19 (1H, m, H_{4a}), 2.28 (1H, m, H_{4b}), 2.62 (1H, m, H₃), 3.64 (1H, m, H_{5a}), 3.75 (1H, m, H_{5b}); ¹³C NMR (100 MHz, CDCl₃): δ 13.9 (C₁₄), 14.1 (C₉), 22.6 (C₁₃), 22.7 (C₈), 27.5 (C₄), 28.4, 29.0, 31.4, 31.8 and 31.9 (C₆, C₇, C₁₀, C₁₁, and C₁₂), 49.8 (C₃), 58.8 (C₅), 181.0 (C₂); LC/MS: *m/z* calcd for C₁₃H₂₅N+H⁺:196.21; found 196.3.

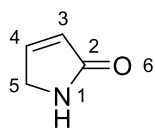
5-Phenyl-4-pentyl-3,4-dihydro-2H-pyrrole **19k**

Product **19k** (1.5 mmol, 75%) was obtained by a similar procedure as for **19a**. ¹H NMR (400 MHz, CDCl₃): δ 0.84 (3H, t, *J* 7.0, H₁₆), 1.19-1.34 (6H, m, H₁₃, H₁₄ and H₁₅), 1.64 (2H, m, H₁₂), 1.82 (1H, m, H_{4a}), 2.14 (1H, m, H_{4b}), 3.33 (1H, m, H₃), 3.92 (1H, m, H_{5a}), 4.03 (1H, m, H_{5b}), 7.39 (3H, m, H₈, H₉ and H₁₀), 7.77 (2H, m, H₇ and H₁₁); ¹³C NMR (100 MHz, CDCl₃): δ 14.0 (C₁₆), 22.6 (C₁₅), 27.5 (C₄), 29.1, 31.8, 32.0 (C₁₂, C₁₃ and C₁₄), 47.3 (C₃), 58.8 (C₅),

127.8 (2C, C₇ and C₁₁), 128.4 (2C, C₈ and C₁₀), 130.0 (C₉) 176.7 (C₂); LC/MS: *m/z* calcd for C₁₅H₂₁N+H⁺:216.17 ; found 216.3.

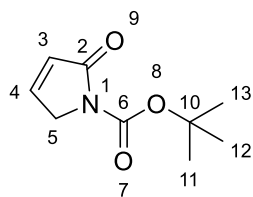
2.3. Synthetic route toward other analogues of H₂MAP

1,5-Dihydro-2*H*-pyrrol-2-one **45**



To a solution of NH₄Cl (6.2g 115 mmol, 5 eq.) in H₂O (18 ml), 2,5-dimethoxy-3,4-dihydrofuran (3 g, 23 mmol, 1 eq.) was added. The mixture was stirred at r.t. for 1 h. NaHCO₃ was added until pH = 7. EtOAc (20 ml) was added and the mixture was filtered. The aqueous layer was extracted with EtOAc (2 x 20 mL). The extracts were concentrated under reduced pressure to give 1.4 g of a brown liquid. Column chromatography was performed (EtOAc then EtOAc/ MeOH 9:1) to give **45** (0.7 mmol, 3%). ¹H NMR (400 MHz, CDCl₃) δ 4.02 (2H, m, H₅), 6.13 (1 H, m, H₃), 7.14 (1H, m, H₄); LC/MS: *m/z* calcd for C₄H₅NO: 83.04; found 83.1.

tert-Butyl 2-oxo-2,5-dihydro-1*H*-pyrrole-1-carboxylate **46**

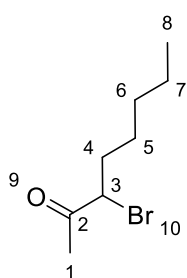


To a solution of **45** (40 mg, 0.48 mmol, 1 eq.) in THF (0.69 ml), DMAP (4.3 mg, 0.04 mmol, 0.1 eq.), dissolved in THF (0.1 mL), was added followed by (Boc)₂O (152mg, 0.69 mmol, 1.5 eq.). The mixture was stirred for 20 min at r.t. It was concentrated under reduced pressure, diluted in EtOAc (2 mL), washed with NH₄Cl sat. (2x5mL) and water (2 x 5 mL). The aqueous layers were extracted with EtOAc (2 x 10 mL). The organic layers were gathered, dried (MgSO₄) and concentrated under reduced pressure to give **46** (0.32 mmol, 68%) as a black oil. ¹H NMR (400 MHz, CDCl₃) δ 1.48 (9H, s, H₁₁, H₁₂ and H₁₃), 4.28 (2H, t, *J* 2.0, H₅), 6.09 (1 H, dt, *J* 3. & 2.0 Hz H₄), 7.15 (1H, dt, *J* 3.0 & 2.0 Hz H₃); ¹³C (100 MHz, CDCl₃), δ 28.0 (C₁₁, C₁₂ and C₁₃), 52.0 (C₅), 82.8 (C₁₀), 128.2 (C₃), 145.4 (C₄), 149.7 (C₆), 169.2 (C₂).

tert-Butyl 4-ethyl-2-oxopyrrolidine-1-carboxylate **43**

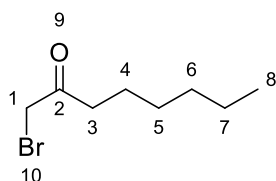
CuI (62 mg, 0.33 mmol, 1 eq.) was suspended in dry THF (0.6 ml) under N₂ and cooled at -78°C. EtLi (0.5 M in benzene, 1.3 ml, 0.65 mmol, 2 eq.) was added and the mixture was stirred for 1 h. **46** (60 mg, 0.33 mg, 1 eq.) dissolved in dry THF (0.18 ml) was then added. The mixture was stirred for 1 h at -78 °C and 2 h at 0 °C. Hydrochloric acid (1 M; 0.6 ml) was added. The aqueous layer was extracted with hexane and the combined organic layers were washed with water, dried (MgSO₄) and concentrated under reduced pressure. No pure product could be isolated.

3-Bromooctan-2-one **48a**

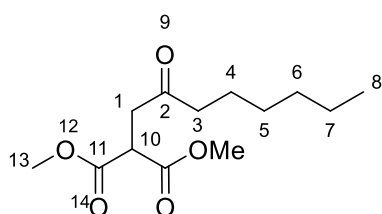


A RBF was charged with 2-octanone (5 g, 39 mmol) **47** and CHCl_3 (40 ml). NH_4OAc (300 mg, 0.1 eq.) was added, followed by N-bromosuccinimide (NBS) (7g, 39 mmol). The mixture was heated at 80 °C and stirred for 24 h. Hexane (40 ml) was added and the mixture was filtered. The filtrate was washed with sat. aq. NaHCO_3 and brine. The organic layer was dried (MgSO_4) and the solvent removed under reduced pressure. The mixture was purified by flash column chromatography EtOAc/hexane, 1:9 leading to a mixture 9:1 MC21/1-bromooctanone **48b**. (1.285 g, 6.2 mmol, 16%). Pure **48a** was recovered from kinetic resolution. ^1H NMR (400 MHz, CDCl_3): δ 0.90 (3H, t, J 7.0 Hz, H_8), 1.27-1.40 (5H, m, $\text{H}_7, \text{H}_6, \text{H}_{5a}$), 1.5 (1H, m, H_{5b}) 1.85-2.08 (2H, m, H_4), 2.37 (3H, s, H_1), 4.24 (1 H, t, J 7.0 Hz, H_3); ^{13}C NMR (100 MHz, CDCl_3 , HMQC and HMBC used for assignments): 13.9 (C_8), 22.4 (C_7), 26.0 (C_1), 26.9 (C_5), 31.1 (C_6), 33.5 (C_4), 54.4 (C_3), 202.19 (C_2) IR (neat): ν_{max} 2929m, 2860m, 1716s (C=O) LC-MS: m/z calcd for $\text{C}_8\text{H}_{15}\text{BrO}+\text{H}^+$: 209.04; found: 209.08

1-bromooctanone **48b**



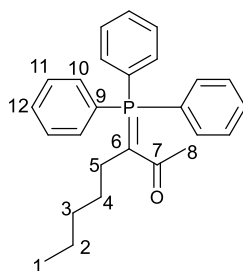
^1H NMR (400 MHz, CDCl_3) δ 0.88 (3H, t, J 7.0 Hz, H_8), 1.27-1.36 (6H, m, H_5, H_6 and H_7), 1.61 (2H, m, H_4), 2.65 (2H, t, J 7.0 Hz, H_3), 3.88 (2H, s, H_1)



Kinetic resolution: A mixture of **48a** and **48b** (approximately 9:1, 1 g, 4.8 mmol, 1 eq.) was dissolved in acetone (5 ml) along with K_2CO_3 (0.5 g, 3.6 mmol, 0.75 eq.) and dimethylmalonate (300 μl , 2 mmol, 0.4 eq.). The mixture was stirred at 60 °C for 2 h. DCM (15 ml) was added and the mixture was washed with

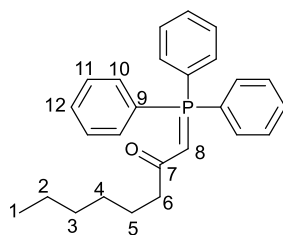
brine. The organic layer was dried (MgSO_4), concentrated under reduced pressure and purified by flash column chromatography, giving pure **48a** (846 mg, 4 mmol, 90% recovery). **51** was isolated, but it was not quantified. ^1H NMR (400 MHz, CDCl_3) δ 0.88 (3H, t, J 7.0 Hz, H_8), 1.25-1.29 (6H, m, H_5, H_6 and H_7), 1.58 (2H, m, H_4), 2.45 (2H, t, J 7.0 Hz, H_3), 3.04 (2H, d, J 7.0 Hz, H_1), 3.7 (6H, s, H_{13}), 3.90 (1H, t, J 7.0 Hz, H_{10})

3-(Triphenyl- λ^5 -phosphanilydene)octan-2-one **49a**



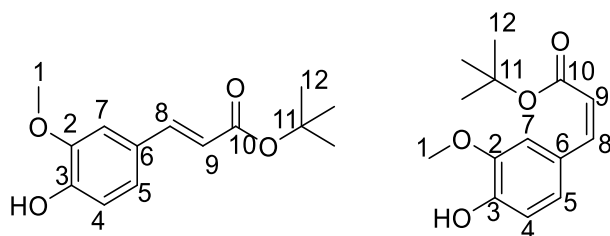
To a solution of **48a** (500 mg, 2.4 mmol) in toluene (5 ml) PPh₃ (650 mg, 2.4 mmol) was added under N₂. The mixture was stirred at 80 °C overnight. After cooling to r.t. the mixture was filtered and the filtrate was concentrated under reduced pressure. The residue was diluted in DCM (20 ml) and stirred vigorously with aq. NaOH (1 M; 5.2 ml) at r.t. for 1 h. The mixture was extracted with DCM and washed with brine. The organic layer was dried (MgSO₄) and concentrated under reduced pressure. After purification by flash column chromatography (PET/EtOAc then MeOH/DCM), **49a** was obtained (17 mg, 2%). ¹H (400MHz, CDCl₃) δ 0.73 (3H, t, *J* 7.0 Hz, H₁), 0.94-1.10 (4H, m, H₂ and H₃), 1.19 (2H, tt, *J* 7.0 & 8.0, H₄), 1.90 (2H, ddd, *J* 8.0 & 10.0 & 22.0 Hz, H₅), 2.13 (3H, s, H₈), 7.40-7.49 (6H, m, H₁₀), 7.50-7.62 (9H, m, H₁₁ and H₁₂); ¹³C (100 MHz, CDCl₃) δ 14.05 (C₁), 21.69 (C₈), 22.14 (C₂), 23.65 (m, C₆), 28.20 (d, *J* 14 Hz, C₅), 31.53 (C₃), 33.74 (C₄), 128.60 (d, *J* 11.0 Hz, C₁₀), 131.62 (C₁₂), 133.57 (d, *J* 8.0 Hz, C₁₁), 174.13 (C₇); ³¹P (160.16 MHz, CDCl₃) 18.18; IR (neat): ν_{max} 3061w, 2925m, 2954m, 1509s (C=O), 1104 (P-Ph) cm⁻¹; LC-MS *m/z* calcd for C₂₆H₂₉OP+H⁺ 389.2, found 389.3

1-(Triphenyl-λ⁵-phosphanylidene)octan-2-one **49b**



A mixture of **48a** and **48b** was submitted to the same conditions as for the formation of **49a**. **49b** was isolated after flash column chromatography (23 mg, 0.06 mmol, 1%). ¹H NMR (400 MHz, CDCl₃), δ 0.87 (3H, t, *J* 13.0 Hz, H₁), 1.25-1.40 (6H, m, H₂, H₃ and H₄), 1.66 (2H, tt, *J* 7.0 & 8.0 Hz, H₅), 2.30 (2H, t, *J* 8.0 Hz, H₆), 7.44 (6H, m, H₁₁), 7.52 (3H, t, *J* 7.0 Hz, H₁₂), 7.64 (6H, dd, *J* 8.0 & 12.0 Hz, H₁₀); ¹³C NMR (100 MHz, CDCl₃) δ: 14.1 (C₁), 22.7 (C₂), 27.2, 29.4, 31.9 (C₃, C₄ and C₅), 41.8 (d, *J* 14.0 Hz, C₆), 51.0 (d, *J* 102.0 Hz, C₈), 127.4 (d, *J* 90.0 Hz, C₉), 128.8 (2C, d, *J* 14.0 Hz, C₁₁), 131.9 (C₁₂), 133.1 (2C, d, *J* 11.0 Hz, C₁₀), 194.3 (C₇)

tert-Butyl 3-(4-hydroxy-3-methoxyphenyl)acrylate (E+Z) **55**

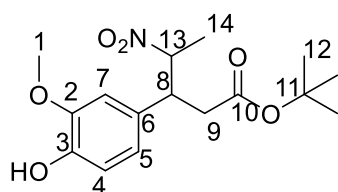


Vanillin (100 mg, 0.67 mmol, 1 eq.) in solution in dry THF (2 ml) was added dropwise to a solution of *tert*-butyl 2-(triphenyl-λ⁵-phosphanylidene)acetate **53** (252 mg, 0.67 mmol, 1 eq.) in THF (2 ml) under N₂. The mixture was stirred at r.t. for 16 h. Solvent was removed under reduced

pressure and a flash column chromatography (hexane/EtOAc) gave (E)-**55** (47mg, 28%) and (Z)-**55** (40 mg, 24%). (E)-**55**: ^1H (400MHz, CDCl_3) δ 1.52 (9H, s, H_{12}), 3.91 (3H, s, H_1), 6.22 (1H, d, J 16.0 Hz, H_9), 6.90 (1H, d, J 8.0 Hz, H_4), 7.00-7.06 (2H, m, H_7 and H_5), 7.51 (1H, d, J 16.0 Hz, H_8); ^{13}C (100 MHz, CDCl_3) δ 28.24 (C_{12}), 55.93 (C_1), 80.29 (C_{11}), 109.23 (C_7), 114.67 (C_4), 117.63 (C_9), 122.89 (C_5), 127.49 (C_6), 143.64 (C_8), 146.75 (C_2), 147.70 (C_3), 166.63 (C_{10}); IR (neat): ν_{max} 3379br, 2977m, 2934m, 1692m (C=O), 1511 M, 1267s, 1204m, 1145s cm^{-1} ; HR-MS m/z calcd for $\text{C}_{14}\text{H}_{18}\text{O}_4$ 273.11, found 273.11.

(Z)-**55**: ^1H (400 MHz, CDCl_3), δ 1.47 (9H, s, H_{12}), 3.90 (3H, s, H_1), 5.75 (1H, d, J 13.0 Hz, H_9), 6.71 (1H, d, J 13.0 Hz, H_8), 6.87 (1H, d, J 8.0 Hz, H_4), 7.07 (1H, dd, J 8.0, 1.9 Hz, H_5), 7.45 (1H, m, H_7); ^{13}C (100 MHz, CDCl_3) δ 28.11 (C_{12}), 55.93 (C_1), 80.36 (C_{11}), 112.51 (C_7), 113.82 (C_4), 119.31 (C_9), 124.84 (C_5), 127.26 (C_6), 141.70 (C_8), 145.87 (C_2), 147.17 (C_3), 166.09 (C_{10}); IR (neat): ν_{max} 3438br, 2977m, 2934m, 1706m (C=O), 1514m, 1276m, 1209m, 1140s cm^{-1}

tert-Butyl 3-(4-hydroxy-3-methoxyphenyl)-4-nitropentanoate **56**

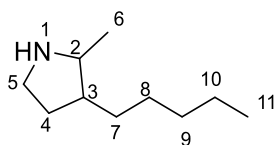


DBU (3 μl , 0.02 mmol, 1 eq.) was added to a solution of nitroethane (2 μl , 0.03 mmol, 1.5 eq.) and **55** (5mg, 0.02 mmol, 1 eq.) in ACN (0.2 ml). The mixture was stirred 24 h at r.t. and water (1 ml) was added dropwise. The mixture was acidified to pH2 with HCl (1 M)

and extracted with DCM. The organic layer was dried (MgSO_4). The crude was mainly consistent with **55** but proton NMR was consistent with a partial conversion (approx. 10%) to **56**. Isolation was unsuccessful. ^1H NMR (partial, 400 MHz, CDCl_3), δ 1.47 (9H, s, H_{12}), 3.0 (1H, m, H_8), 3.5 (3H, m, H_1), 4.1 (1H, q, J 7.0 Hz, H_{13})

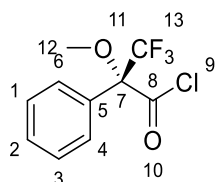
2.4. Racemic resolution of H₂MAP

2-Methyl-3-pentylpyrrolidine **59**



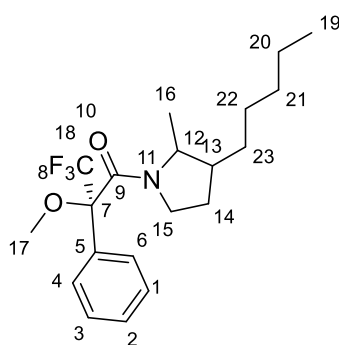
H₂MAP **19a** (100 mg, 0.65 mmol, 1 eq.) was dissolved in MeOH/H₂O (4:1, 15 ml) in a RBF. NaBH₄ (30mg, 0.81 mmol, 1.2 eq.) were added in small quantity with vigorous stirring at r.t. The mixture was stirred at r.t. under N₂ overnight. The mixture was cooled on an ice bath and 1 M HCl was added slowly to pH 2. The mixture was stirred 1 h at r.t. The pH was adjusted to 13 with 3M NaOH and the product was extracted with DCM. The organic phase was dried (MgSO₄) and concentrated under reduced pressure to give **59** (60 mg, 59%). Main diastereomer: ¹H NMR (400 MHz, CDCl₃): δ 0.88 (3H, t, *J* 7.0, H₁₁), 1.15 (3H, d, *J* 6.0, H₆), 1.2-1.5 (10H, m, H_{4a}, H₃, H₇, H₈, H₉ and H₁₀), 1.98 (1H, m, H_{4b}), 2.4 (1H, s, H₁), 2.6 (1H, m, H₂), 2.88 (1H, m, H_{5a}) 3.01 (1H, m, H_{5b}); ¹³C NMR (100 MHz, CDCl₃, HMQC used for assignment): δ 14.26 (C₁₁), 20.05 (C₆), 22.73, 28.35, 32.22, 33.5 (C₇, C₈, C₉ and C₁₀), 32.95 (C₄), 45.29 (C₅), 47.38 (C₃), 60.49 (C₂); Minor diastereomer ¹H NMR (400 MHz, CDCl₃): δ 1.15 (d, *J* 7.0, H₆), 3.23 (1H, m, H₂); ¹³C NMR (100 MHz, CDCl₃): δ 16.25 (C₆), 29.84, 30.74 (pentyl), 42.65 (C₄), 44.70 (C₅), 56.16 (C₂); IR (neat): ν_{max} 2934m, 2923m, 2856m, 1634w (N-H bend), 1457m, 1376m (C-N); LC-MS *m/z* calcd for C₁₀H₂₁N+H⁺ 156.18; found 156.16

(R)-3,3,3-Trifluoro-2-methoxy-2-phenylpropanoyl chloride **62**



(R)-Mosher's acid **61** (30 mg, 0.1 mmol, 1 eq.) and thionyl chloride (0.4 ml, 5 mmol, 50 eq.) were mixed in CDCl₃ (0.4 ml) and heated at 80 °C. The reaction was monitored by NMR. After 24 hr a complete conversion was observed, and volatile species were removed under reduced pressure. ¹H NMR (400 MHz, CDCl₃): δ 3.76 (3H, s, H₁₂), 7.41-7.46 (3H, m, H₂, H₄ and H₆), 7.56, (2H, m, H₁ and H₃); ¹³C NMR (100 MHz, CDCl₃) δ 56.6 (C₁₂), 127.0 (C₄ and C₆), 128.8 (C₁ and C₃), 130.5 (C₂), 171.1 (C₈); ¹⁹F NMR (376 MHz, CDCl₃): δ -71.8; IR (neat): ν_{max} 2953w, 1788m (C=O), 1260m, 1168s (C-F), 706s (C-Cl) cm⁻¹

(2R)-3,3,3-Trifluoro-2-methoxy-1-(2-methyl-3-pentylpyrrolidin-1-yl)-2-phenylpropan-1-one **60**

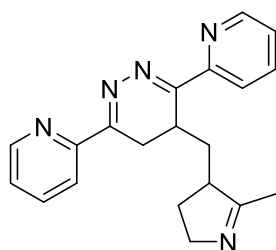


Amine **59** (30 mg, 0.2 mmol, 1 eq.) was dissolved in DCM (2ml) and added to **62** (50 mg, 0.2 mmol, 1 eq.). The mixture was stirred at r.t. overnight. The resulting mixture was diluted in 5 ml of saturated aq. NaHCO₃ and then extracted with DCM. The organic phase was dried (MgSO₄) and the solvent removed under reduced pressure to give **60** (70 mg, 94%). ¹H NMR (400 MHz, CDCl₃): δ 0.89 (3H, t, *J* 7.0, H₁₉), 1.08 (2H, m, H₂₀), 1.14-1.34 (9H, m, H₁₆, H₂₁, H₂₂ and H₂₃), 1.40 (1H, m, H_{14a}), 1.62 (1H, m, H₅), 1.88 (1H, m, H_{14b}), 2.03 (1H, m, H₁₂), 2.99 (2H, m, H₁₅), 3.49 and 3.54 (3 H, 2 x s, H₁₇: not a doublet but one peak for each enantiomer), 7.32, 7.46, 7.66 (H₁, H₂, H₃, H₄ and H₆); ¹³C NMR (100 MHz, CDCl₃, ATP used for assignment): δ 14.02 (C₁₉), 22.53 (C₂₀), 27.70 (C₂₁), 28.49 (C₂₂), 30.64 (C₂₃), 31.69 (C₁₄), 43.00 (C₁₅), 45.24 (C₁₃), 54.88 (C₁₇), 59.96 (C₁₂), 127.75-128.93 (C₁, C₂, C₃, C₄ and C₆), 130.53 (C₁₈), 135.90 (C₅), 170.59 (C₉); UV Peaks at 317 and 263 nm

2.5. Tetrazine coupling

4-((5-Methyl-3,4-dihydro-2H-pyrrol-4-yl)methyl)-3,6-di(pyridin-2-yl)-4,5-dihydropyridazine

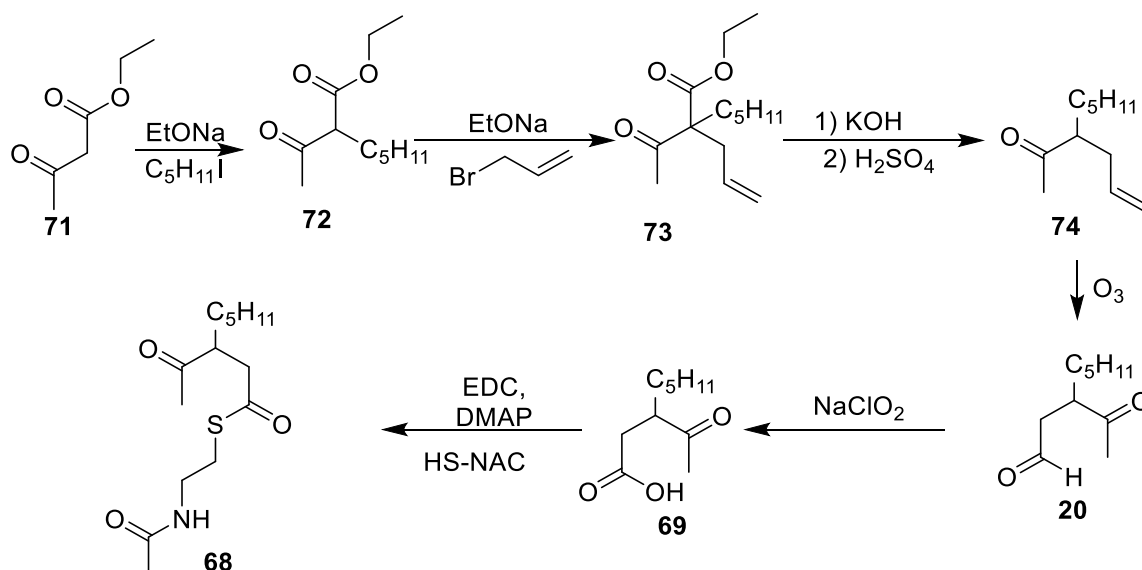
65



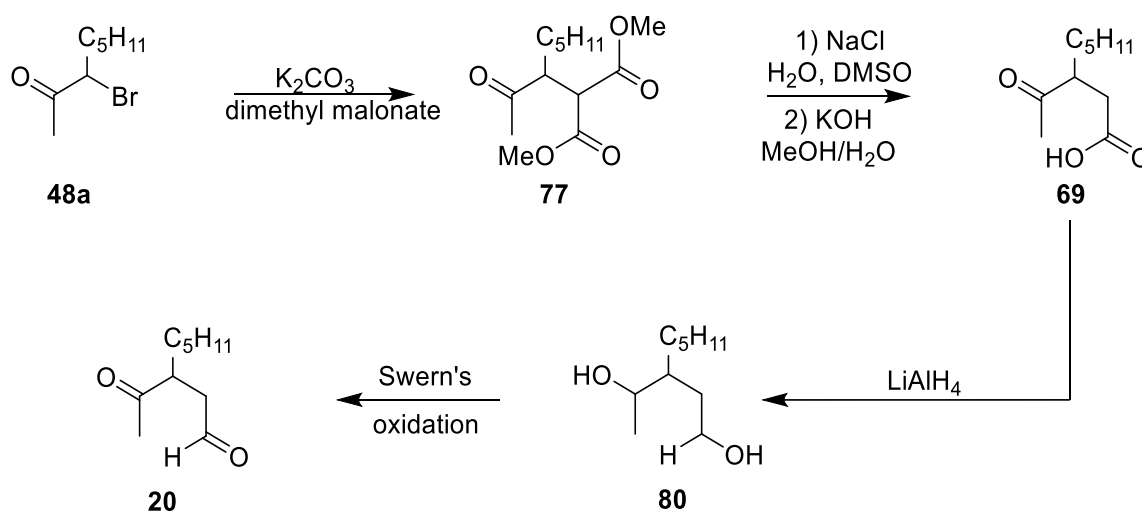
19d (0.2 μmol, 1 eq.) in solution in DMSO (200 μl) was mixed with Py₂Tz **64** (300 μl, 0.4mg/34 μl in DMF, 15 μmol, 70 eq.) in PBS buffer (1 ml). The mixture was stirred at r.t. for 48h and monitored by LC-MS. After 24 hr a colour change was visible. After 48h, LC-MS was consistent with a 70% conversion. The mixture was diluted in EtOAc and washed with brine. The organic layer was dried and concentrated, but **65** could not be isolated pure.

2.6. Synthesis of PigE potential substrates

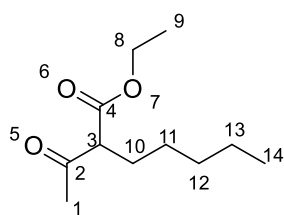
Method A



Method B



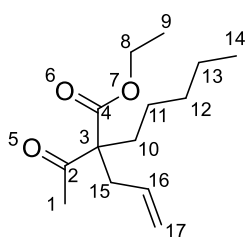
Ethyl 2-acetylheptanoate 72



Dry EtOH (0.6 ml) was added to Na (20 mg, 0.86 mmol, 1.1 eq.) under N_2 . After the first intense reaction, the mixture was heated to 60°C . After the total disappearance of Na, ethyl acetoacetate (100 mg, 0.77 mmol, 1 eq.) was added slowly, followed by 1-iodopentane (182 mg, 0.91 mmol, 1.2 eq.). The solution was heated at reflux (80°C) and stirred for 4 h, cooled and evaporated to dryness. The residue was partitioned between DCM and water. The organic phases were combined, dried (MgSO_4) and evaporated. Purification by flash column

chromatography eluting with EtOAc 3% in hexane gave product **72** (109 mg, 50%). ^1H NMR (400 MHz, CDCl_3): δ 0.87 (3H, t, J 7.0, H_{14}), 1.22–1.31 (9H, m, H_9 , H_{11} , H_{12} and H_{13}), 1.73–1.88 (2H, m, H_{10}), 2.20 (3H, s, H_1), 3.35 (1H, t, J 7.0, H_3), 4.15 (2H, q, J 7.0, H_8); ^{13}C NMR (100 MHz, CDCl_3): 13.3 (C_{14}), 14.1 (C_9), 22.3 (C_{13}), 27.1 (C_{10}), 28.2 (C_1), 28.7 and 31.4 (C_{11} and C_{12}), 60.0 (C_3), 61.2 (C_8), 170.0 (C_5), 203.4 (C_2) δ ; HRMS: m/z calcd for $\text{C}_{11}\text{H}_{20}\text{O}_3+\text{H}^+$: 201.1491; found 201.1487

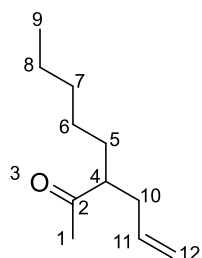
Ethyl 2-acetyl-2-allylheptanoate **73**



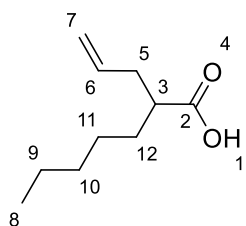
Na (180 mg, 7.74 mmol, 1.3 eq.) were dissolved under N_2 in EtOH (4.8 ml) at r.t. and then heated up to 60°C . **72** (1.2 g, 6 mmol, 1 eq.) was added slowly, followed by allyl bromide (0.75 ml, 8.75 mmol, 1.45 eq.) and the mixture was stirred at 60°C for 2 h. A white precipitate appeared. The mixture was filtered and the solvent removed under reduced pressure. The

residue was partitioned between water and DCM and the organic layer was dried (MgSO_4) and the solvent removed under reduced pressure. Purification by flash chromatography (hexane/acetone 9:1) gave product **73** (870 mg, 60%). ^1H NMR (400 MHz, CDCl_3): δ 0.86 (3H, t, J 6.9 Hz, H_{14}), 1.10 (2H, t, J 7.0 Hz, H_9), 1.21–1.27 (7H, m, H_{11} , H_{12} and H_{13}), 1.75–1.92 (2H, m, H_{10}), 2.11 (3 H, s, H_1), 2.60 (1H, dd, J 8.0 & 15.0, H_{15a}), 2.58 (1H, dd, J 8.0 & 15.0, H_{15b}), 4.19 (2H, q, J 7.0, H_8), 5.03 (1H, d, J 10.0, cis- H_{17}), 5.07 (1H, d, J 17.0, trans- H_{17}), 5.58 (1H, ddt, J 17.0 & 10.0 & 8.0, H_{16}); ^{13}C NMR (100 MHz, CDCl_3 , ATP used for assignments): δ 13.86, 14.04 (C_9 and C_{14}), 22.27 (C_{13}), 23.19 (C_{12}), 26.24 (C_1), 31.25 (C_{10}), 32.10 (C_{15}), 35.8 (C_{11}), 61.2 (C_8), 63.4 (C_3), 118.8 (C_{17}), 132.6 (C_{16}), 172.1 (C_4), 204.8 (C_2); HRMS: m/z calcd for $\text{C}_{14}\text{H}_{24}\text{O}_3+\text{H}^+$: 241.1804; found: 241.1798.

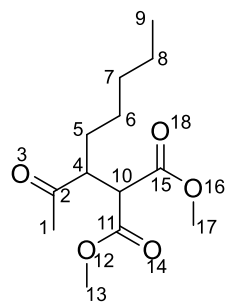
3-Allyloctan-2-one **74**



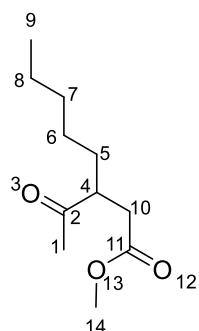
Ester **73** (1.9 g, 7.9 mmol, 1 eq.) was dissolved in MeOH/ H_2O (4:1, 22.8 ml) and 1.3 g of KOH (1.3 g, 23.2 mmol, 3 eq.) was added. The mixture was stirred at 80°C overnight. H_2SO_4 was added until $\text{pH}<5$. Extraction with DCM and the organic layers were washed with aq. NaOH (1 M), dried (MgSO_4) and the solvent was removed under reduced pressure. Purification by flash column chromatography (hexane/EtOAc 5:1) gave **74** (993 mg, 84%). ^1H NMR (400 MHz, CDCl_3): δ 0.87 (3H, t, J 7.0 Hz, H_9), 1.19–1.35 (6H, m, H_6 , H_7 and H_8), 1.42 (1H, m, H_{5a}), 1.53–1.65 (1H, m, H_{5b}), 2.12 (3H, s, H_1), 2.19 (1H, m, H_{10a}), 2.30 (1H, m, H_{10b}), 2.53 (1H, tt, J 6.0 & 8.0 Hz, H_4), 4.97 (1H, d, J 10.0 Hz, cis- H_{12}), 5.03 (1H, d, J 17.0 Hz, trans- H_{12}), 5.70 (1H, ddt, J 17.0 & 10.0 & 7.0 Hz, H_{11}); ^{13}C NMR (100 MHz, CDCl_3): δ 13.94 (C_9), 22.42 (C_8), 26.86 (C_5), 29.10 (C_1), 31.11 (C_6), 31.83 (C_{10}), 35.71 (C_7), 52.70 (C_4), 116.61 (C_{12}), 135.62 (C_{11}), 212.16 (C_2); HRMS: m/z calcd for $\text{C}_{11}\text{H}_{20}\text{O}+\text{H}^+$: 169.1592; found: 169.1592

2-Allylheptanoic acid **74b**

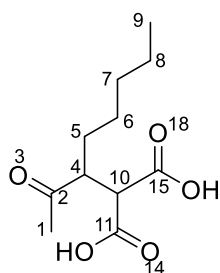
Instead of the decarboxylated product, a deacetylated product was sometimes formed during **74** synthesis. Its formation is the result of a retro Claisen mechanism. ^1H NMR (400 MHz, CDCl_3): δ 0.87 (3H, t, J 7.0 Hz, H_8), 1.19–1.39 (6H, m, H_9 , H_{10} and H_{11}), 1.49 (1 H, m, H_{12a}), 1.61 (1H, m, H_{12b}), 2.24 (1H, m, H_{5a}), 2.30–2.45 (2H, m, H_3 and H_{5b}), 5.01 (1H, d, J 10.0 Hz, cis- H_7), 5.06 (1H, d, J 17.0 Hz, trans- H_7), 5.76 (1H, m, H_6).

Dimethyl 2-(2-oxooctan-3-yl) malonate **77**

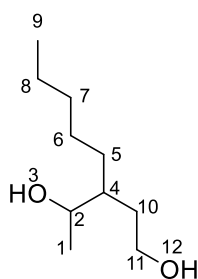
Dimethyl malonate (487 μl , 4.2 mmol, 1 eq.) and K_2CO_3 (750 mg, 13.4 mmol, 3.2 eq.) were added to **48** (1.5 g, 7.2 mmol, 1.7 eq.) in acetone (7.5 ml). The mixture was stirred at 80 $^\circ\text{C}$ overnight. DCM (20 ml) were added and the organic phase was washed with H_2O and brine. The organic phase was dried (MgSO_4) and the solvent removed under reduced pressure. Purification by flash column chromatography (hexane/EtOAc) gave **77** (755 mg, 2.9 mmol, 40%). ^1H NMR (400 MHz, CDCl_3): δ 0.87 (3 H, t, J 6.0 Hz, H_9), 1.2–1.34 (6H, m, H_6 , H_7 , H_8), 1.52 (2H, m, H_5), 2.28 (3H, s, H_1), 3.34 (1H, dt, J 11.0 & 6.0 Hz, H_4), 3.69 (3H, s, H_{13} or H_{17}), 3.75 (3H, s, H_{13} or H_{17}), 3.83 (1H, d, J 11.0 Hz, H_{10}) ^{13}C NMR (100 MHz, CDCl_3 , HMQC and HMBC used for assignments) δ 13.9 (C_9), 22.8 (C_8), 25.6 (C_6), 29.0 (C_5), 30.5 (C_1), 31.8 (C_7), 50.6 (C_4), 52.7 (C_{13} and C_{17}), 53.1 (C_{10}), 169 (C_{11} and C_{15}), 209.9 (C_2); IR (neat): ν_{max} 2955w, 2862w, 1735s ($\text{C}=\text{O}$), 1713 ($\text{C}=\text{O}$), 1265m, 1226m, 1151s ($\text{C}-\text{O}$) LC-MS: m/z calcd for $\text{C}_{13}\text{H}_{22}\text{O}_5+\text{Na}^+$: 281.14; found: 281.14

Methyl 3-acetyloctanoate **79**

77 (191 mg, 0.74 mmol, 1 eq.), NaCl (120 mg, 2 mmol, 2.7 eq.), and H_2O (54 μl , 3 mmol, 4 eq.) in DMSO (12 ml) were stirred at 160 $^\circ\text{C}$ under a condenser for 16 h. The mixture was diluted in EtOAc (20 ml) and washed with water and brine. The aqueous phase was reextracted with EtOAc. The organic layers were dried (MgSO_4) and evaporated under reduced pressure, giving **79** (110 mg, 0.55 mmol, 74%). ^1H NMR (400 MHz, CDCl_3): δ 0.88 (3H, t, J 12.0 Hz, H_9), 1.26 (6H, m, H_6 , H_7 and H_8), 1.41 (1H, m, H_{5a}), 1.60 (1H, m, H_{5b}), 2.23 (3H, s, H_1), 2.35 (1H, dd, J 17.0 & 4.0 Hz, H_{10a}), 2.73 (1H, dd, J 17.0 & 10.0 Hz, H_{10b}), 2.98 (1H, m, H_4), 3.64 (3H, s, H_{14}); ^{13}C NMR (100 MHz, CDCl_3) δ 14.0 (C_9), 22.4 (C_8), 26.6 (C_6), 29.5 (C_1), 31.3 (C_5), 31.7 (C_7), 34.9 (C_{10}), 47.9 (C_4), 51.7 (C_{14}), 173.0 (C_{11}), 211.1 (C_2).

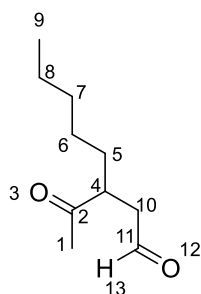
2-(1-Oxooctan-3-yl) malonic acid **78**

KOH (67.2 mg, 1.2 mmol, 15 eq.) in solution in MeOH/H₂O 4:1 (1 ml) was added to **77** (20 mg, 0.077 mmol, 1 eq.) and the mixture was stirred at 60°C overnight. The mixture was washed with DCM, acidified to pH 2 with HCl 1 M and extracted with DCM. The organic layer was dried (MgSO₄) and concentrated under reduced pressure to give **78** (15 mg, 0.065 mmol, 84%)
¹H NMR (400 MHz, D₂O) δ 0.76 (3H, t, *J* 7.0 Hz, H₉), 1.18 (6H, m, H₆, H₇ and H₈), 1.55 (2H, m, H₅), 1.96 (3H, s, H₁), 3.08 (1H, m, H₄), 3.67 (1H, d, *J* 10.0 Hz H₁₀); ¹³C NMR (100 MHz, D₂O) δ 13.1 (C₉), 21.7, 28.2, 30.9 (C₆, C₇, C₈), 25.6 (C₁), 53.5 (C₁₀)

3-Pentylpentane-1,4-diol **80**

LiAlH₄ (1 M in THF, 2.1 ml, 2.1 mmol, 4 eq.) was cooled to 0°C. **69** (100mg, 0.53 mmol, 1 eq.) in THF (1.25 ml) was added dropwise. The reaction was allowed to reach r.t. and stirred o/n. H₂O (75 μl), NaOH (15% in H₂O, 75 μl) and H₂O (225 μl) were added slowly at 0°C. The cold bath was removed, and the reaction stirred for 1 more hr. The mixture was diluted in THF, dried (MgSO₄) and concentrated under reduced pressure to give **80** (80 mg, 0.46 mmol, 87%).

NMR ¹H(400 MHz, CDCl₃) δ: 0.88 (3H, t, *J* 7.0 Hz, H₉), 1.15 and 1.21 (3H, d, *J* 6.0 Hz, H₁), 1.23-1.35 (8H, m, H₅, H₆, H₇ and H₈), 1.46 (1/2H, m, H_{4a}), 1.5-1.58 (1/2H, m, H_{10a1}), 1.6-1.68 (1 H, m, H_{10a2} and H_{4b}), 1.74-1.79 (1H, m, H_{10b}), 3.65 (1H, m, H_{11a}), 3.77 (1.5 H, m, H_{11b}, H_{2a}), 3.9 (m, 1/2H, H_{2b}); ¹³C NMR (100 MHz, CDCl₃) δ 14.1 (C₉), 18.5 and 21.3 (C₁), 22.62 (C₈), 26.9 and 27.4 (C₅), 30.8 and 31.0 (C₆), 32.1 and 32.2 (C₇), 32.4 and 32.6 (C₁₀), 43.2 and 43.3 (C₄), 60.6 and 61.7 (C₁₁), 70.1 (C₂); IR (neat): ν_{max} 3306br (O-H), 2925s, 2857s, 1052s (C-O)

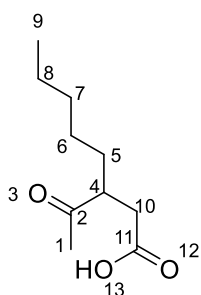
3-Acetyloctanal **20**

Method A: Alkene **74** (990 mg, 5.9 mmol) was dissolved in DCM (15 ml). O₃ was bubbled in the solution until the solution turned blue. The ozonolizer was turned off and O₂ was bubbled in the solution until the blue colour disappeared. The mixture was poured into a suspension of Zn in DCM (15 ml) at 0 °C. Acetic acid (1 ml) was added slowly, and the solution was allowed to reach r.t. and to stir overnight. The mixture was filtered and washed with sat. aq, NaHCO₃ and brine. The organic phases were dried (MgSO₄) and the

solvent was removed under reduced pressure. Product **20** was obtained (955 mg, 95%).

Method B: oxalyl chloride (675 μ l, 7.8 mmol, 4.5 eq.) was added dropwise to a stirred solution of DMSO (755 μ l, 10.6 mmol, 9 eq.), in DCM (10 ml) at -78°C . the mixture was stirred 10 min at -78°C and diol **80** (300 mg, 1.7 mmol, 1 eq.) in solution in DCM (5 ml) were added dropwise. The mixture was stirred a further 10 min at -78°C . Et_3N was added and the reaction was stirred at r.t. for approximately 30 min. The mixture was diluted in Et_2O (20 ml) and washed with brine. The organic layer was dried (MgSO_4) and concentrated under reduced pressure. Purification by flash column chromatography gave **20** (250 mg, 1.5 mmol, 88%) ^1H NMR (400 MHz, CDCl_3): δ 0.87 (3H, t, J 7.0 Hz, H_9), 1.22(6H, m, H_6 , H_7 and H_8), 1.42 (1H, m, H_{5a}), 1.58(1H, m, H_{5b}), 2.20 (3H, s, H_1), 2.45 (1H, dd, J 4.0 & 18.0 Hz, H_{10a}), 2.92 (1H, dd, J 10.0 & 18.0 Hz, H_{10b}), 3.02 (1H, m, H_4), 9.70 (1H, s, H_3); ^{13}C NMR (100 MHz, CDCl_3 , HMQC used for assignments): δ 14.0 (C_9), 22.4 (C_8), 26.6 (C_6), 29.4 (C_1), 31.2 (C_5), 31.7 (C_7), 44.9 (C_{10}), 45.9 (C_4), 200.7 (C_{11}), 210.7 (C_2); IR (neat): ν_{max} 2957m, 2958m, 2857m, 2750w (aldehyde C-H), 1713 ($\text{C}=\text{O}$); LC-MS: m/z calcd for $\text{C}_{10}\text{H}_{18}\text{O}_2+\text{H}^+$: 171.14; found: 171.14

3-Acetyloctanoic acid **69**



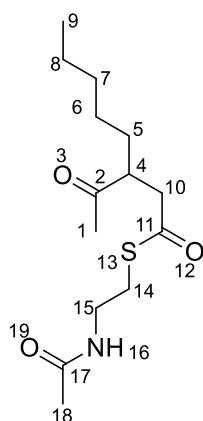
Method A: NaClO_2 80% (180 mg, 1.6 mmol, 1.3 eq.) in solution in water (2.1 ml) was added dropwise to a solution of **20** (200 mg, 1.2 mmol, 1 eq.) in ACN (1.15 ml), buffered with NaH_2PO_4 (35 mg, 0.3 mmol) and 35% H_2O_2 (120 μ l, 1.2 mmol, 1 eq.). The temperature was kept under 10°C . The reaction was stirred under 10°C for two hours and Na_2SO_3 was added to destroy any unreacted oxidant. Aq. HCl (1 M) was added until $\text{pH}=2$. The solution turned green. The

mixture was extracted with DCM. The organic phase was dried (MgSO_4) and the solvent removed under reduced pressure to give **69** (109 mg, 50%).

Method B: **79** (110 mg, 0.55 mmol, 1 eq.) was dissolved in $\text{MeOH}/\text{H}_2\text{O}$ 4:1 (4 ml) and KOH (270 mg, 4.8 mmol, 8.7 eq.) was added. The mixture was heated up to 60°C and stirred for 4 hr. Hydrochloric acid 1 M was added slowly until $\text{pH}<2$. The mixture was extracted with DCM. Analysis of the organic phase showed presence of DMSO from the previous step and unreacted **79** (less than 10% of the mixture). DCM was removed under reduced pressure and the mixture dissolved in NaHCO_3 sat. and washed with DCM. The aqueous phase was then acidified by adding hydrochloric acid (1 M) and extracted with DCM. The organic extract was then dried, and the solvent removed under reduced pressure to give **69** (100 mg, 0.53 mmol, 96%). ^1H NMR (400 MHz, CDCl_3): δ 0.88 (3H, t, J 7.0 Hz, H_9), 1.23-1.34 (6H, m, H_6 , H_7 and H_8), 1.42 (1H, m, H_{5a}), 1.59 (1H, m, H_{5b}), 2.20 (3H, s, H_1), 2.39 (1H, dd, J 17.0 & 4.0 Hz, H_{10a}), 2.76 (1H, dd, J 17.0 & 910.0 Hz, H_{10b}), 2.93 (1H, m, H_4); ^{13}C NMR (100 MHz, CDCl_3 , HMQC used for assignments): δ 14.11 (C_9), 22.57 (C_8), 26.69 (C_7), 29.41 (C_1), 31.27 (C_6), 31.89 (C_5), 35.09 (C_{10}), 47.94 (C_4), 177.55

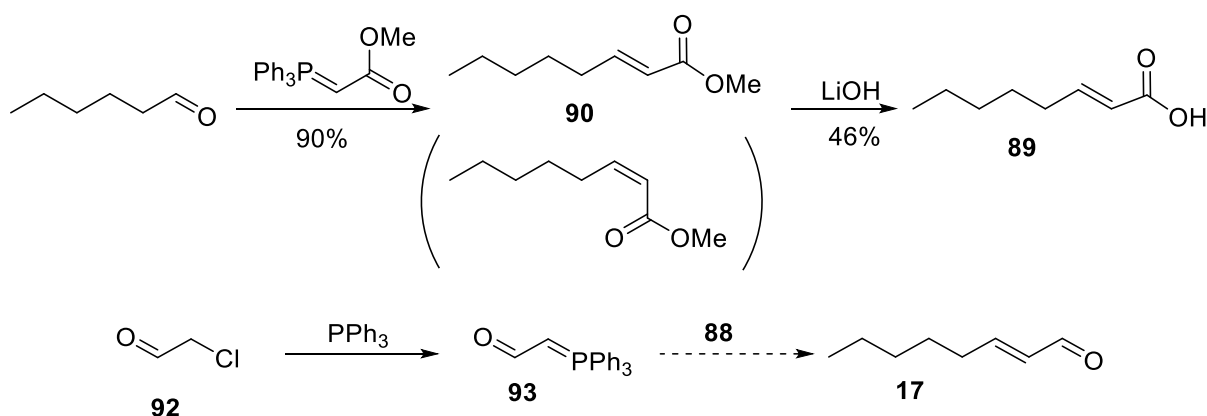
(C₁₁), 210.74 (C₂); IR (neat): ν_{\max} 2958m, 2928m, 2861 M, 1707s (C=O), 1374 (C-O carboxylic acid); UV Absorbance max at 276 nm; LC/MS m/z calcd for C₁₀H₁₈O₃-H⁺: 185.12; found: 185.1.

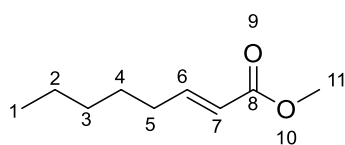
S-(2-Acetamidoethyl) 3-acetyloctanethioate **68**



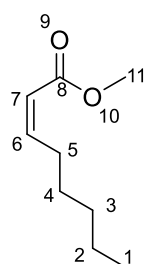
Carboxylic acid **69** (50 mg, 0.27 mmol, 1 eq.) were dissolved in DCM (0.5 ml) and cooled on ice. EDC (57 mg, 0.36 mmol, 1.3 eq.) and DMAP (6 mg, 50 nmol, 0.2 eq.) were added and the mixture stirred on ice for 15 min. N-Acetylcysteamine (36 mg, 0.3 mmol, 1.1 eq.) was added and the mixture was allowed to reach r.t. and was stirred overnight. The solvent was removed under reduced pressure and the residue dissolved in CHCl₃ (approx. 2 ml) and washed with hydrochloric acid (0.1 M) and brine. The aqueous layers were reextracted with CHCl₃. The organic layers were combined and dried (MgSO₄). The solvent was removed under reduced pressure. Purification by flash column chromatography (DCM/MeOH 9:1) gave **68** (13 mg, 16%). ¹H NMR (400 MHz, CDCl₃): δ 0.88 (3H, t, J 7.0 Hz, H₉), 1.27 (6H, m, H₆, H₇ and H₈), 1.43 (2H, m, H₅), 1.96 (3H, s, H₁₈), 2.21 (3H, s, H₁), 2.63 (1H, m, H_{10a}), 3.04 (4H, m, H₄, H_{10b} and H₁₄), 3.42 (2H, m, H₁₅); ¹³C NMR (100 MHz, CDCl₃, HMQC and HMBC used for assignments): δ 14.09 (C₉), 22.54 (C₈), 23.30 (C₁₈), 26.64 (C₆), 28.77 (C₁₄), 29.39 (C₁), 31.22 (C₅), 31.87 (C₇), 39.61 (C₁₅), 44.69 (C₁₀), 48.56 (C₄), 170.51 (C₁₇), 198.72 (C₁₁), 210.12 (C₂); IR (neat): ν_{\max} 2948m, 2932m, 2854m, 1709s (C=O ketone), 1687s and 1657s (C=O amide and thioester), 1541 M (NH bend); LC-MS m/z calcd for C₁₄H₂₅NO₃S+H⁺, 288.16; found: 288,16.

2.7. Synthesis of potential substrate of PigD

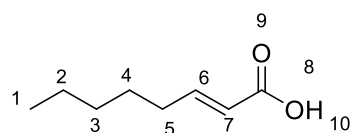


Methyl (E)-oct-2-enoate (E)-**90**

A RBF was charged with methyl (triphenylphosphoranylidene)acetate **91** (502 mg, 1.5 mmol, 1.5 eq.), hexanal (0.12 ml, 1 mmol, 1 eq.) and water. The mixture was stirred at r.t. for 1 hr. The mixture was then extracted with DCM and the organic layer was dried (MgSO_4) and concentrated under reduced pressure. Purification by flash column chromatography (hexane/ Et_2O) gave (E)-**90** as a colourless liquid (97 mg, 0.6 mmol, yield 60%). ^1H NMR (400 MHz, CDCl_3) δ : 0.86 (3H, t, J 7.0 Hz, H_1), 1.23-1.36 (4H, m, H_2 and H_3), 1.45 (2H, m, H_4), 2.19 (2H, m, H_5), 3.72 (3H, s, H_{11}), 5.81 (1H, d, J 16.0 Hz, H_7), 6.97 (dt, 1H, J 16.0 & 7.0 Hz, H_6); ^{13}C NMR (100 MHz, CDCl_3) δ 13.95 (C_1), 22.41, 27.70, 31.42, 32.20 (C_2 , C_3 , C_4 and C_5), 51.38 (C_{11}), 120.88 (C_6), 149.95 (C_7)

Methyl (Z)-oct-2-enoate (Z)-**90**

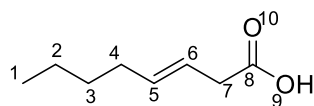
The conditions described for the formation of (E)-**90** were repeated with increased quantity of hexanal (10 mmol) and ylid (15 mmol). Proton NMR of the crude was consistent with the formation of (Z)-**90**. The product was not isolated, but the NMR spectra was consistent with a ratio 1:4 (Z)/(E). The quantity of (Z)-**90** could then be estimated (260 mg, 1.6 mmol, 16%) ^1H NMR (400 MHz, CDCl_3) 0.89 (3H, t, J 7.0 Hz, H_1), 1.3 (6H, m, H_2 , H_3 and H_4), 2.6 (2H, qd, J 7.0 & 2.0 Hz, H_5), 3.70 (3H, s, H_{11}), 5.76 (1H, dt, J 11.0 & 2.0 Hz, H_7), 6.24 (1H, dt, J 11.0 & 7.0 Hz, H_6)

2-Octenoic acid **89**

LiOH (81 mg, 3.5 mmol, 6 eq.) in H_2O (570 μl) was added slowly to methyl 2-octenoate E-**90** (100 mg, 0.6 mmol, 1 eq.) in solution in THF (1.14 ml) and $t\text{BuOH}$ (570 μl) at 0°C . The mixture was stirred overnight at r.t.. 5 ml of hydrochloric acid (1 M) were added to decrease the pH below 2. The mixture was extracted with 3x5ml DCM. The organic layer was dried with MgSO_4 and the solvent removed under reduced pressure. The crude mixture was redissolved in sat. NaHCO_3 , washed with DCM and the pH was decreased to 2 by adding hydrochloric acid (1 M) before extracting with DCM. After drying (MgSO_4) and concentrating under reduced pressure, carboxylic acid **89** was obtained (42 mg, 0.28 mmol, 47%) NMR ^1H (400 MHz, CDCl_3) δ 0.89 (3H, t, J 7.0 Hz, H_1), 1.25-1.39 (4H, m, H_2 and H_3), 1.47 (2H, m, H_4), 2.22 (2H, dt, J 7.0 & 7.0 Hz, H_5), 5.82 (d, 1H, J 16.0 Hz, H_7), 7.08 (dt, 1H, J 16.0 & 7.0 Hz, H_6); ^{13}C NMR (100 MHz, CDCl_3)

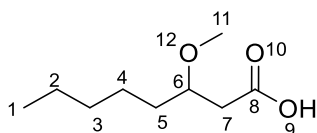
δ 13.94 (C₁), 22.41, 27.54, 31.29, 32.28 (C₂, C₃, C₄ and C₅), 120.42 (C₆), 152.52 (C₇); LC-MS: m/z calcd for C₈H₁₄O₂+H⁺ 143.21, found 143.2

3-Octenoic acid **89b**



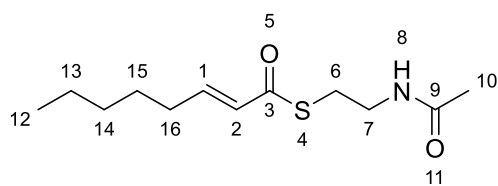
Demethylmalonate (502 mg, 5 mmol, 2.2 eq.) was added to a stirred solution of hexanal (270 μ l; 2.25 mmol, 1 eq.) in pyridine (13 ml) and piperidine (2 ml). the mixture was stirred at 110 °C for 1h. the mixture was cooled to 0 °C in an ice bath and hydrochloric acid (1 M) was added until pH = 2. After extraction with DCM, the organic layers were dried (MgSO₄) and concentrated under reduced pressure. Purification by flash column chromatography (hexane/EtOAc, 2:8) gave **89b** (55 mg, 17%). NMR ¹H (400 MHz, CDCl₃) δ 0.91 (3H, t, J 7.0 Hz, H₁), 1.24-1.45 (4H, m, H₇, H₃), 2.07 (2H, dt, J 7.0 & 7.0 Hz, H₄), 3.1 (2H, d, J 7.0 Hz, H₇), 5.49-5.67 (2H, m, H₅, H₆)

3-Methoxyoctanoic acid **89c**



LiOH (162 mg, 5.5 mmol, 3 eq.) in solution in H₂O (1.14 ml) was added slowly to a solution of ester (E)-**90** in THF (2.28 ml) and MeOH (1.14 ml) at 0 °C. The mixture was stirred overnight at r.t. After a wash with DCM, the pH was decreased to 2 with hydrochloric acid (1 M) and the product was extracted with DCM. The organic layer was dried (MgSO₄) and concentrated under reduced pressure. NMR was consistent with a mixture of **89** and by-product **89b** (ratio 4:1) but they could not be separated. NMR ¹H (400 MHz, CDCl₃) δ 2.56 (2H, m, H₇), 3.41 (3H, s, H₁₁), 3.66 (1H, m, H₆); The rest of the protons were hidden in the spectra of the main carboxylic acid.

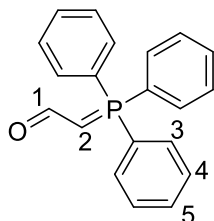
S-(2-Acetamidoethyl) (E)-oct-2-enethioate **70**



2-octenoic acid **89** (34 mg, 0.24 mmol, 1 eq.) in DCM was poured in a dry flask under N₂. At 0 °C N-(3-dimethylaminopropyl)-N'-ethylcarbodiimide hydrochloride (EDC HCl) (50 mg, 0.26 mmol, 1.1 eq.) and DMAP (0.05 eq.) were added. The mixture was stirred at 0 °C for 15 min. H-SNAC was added and the mixture was allowed to reach r.t. The mixture was stirred overnight. The solvent was removed under reduced pressure and the crude redissolved in chloroform. The solution was washed with hydrochloric acid (10 mM) and brine. The organic layer was dried (MgSO₄) and the solvent removed under reduced pressure. Purification by flash column chromatography gave **70** (19 mg, 0.08 mmol, 30%) NMR ¹H (400 MHz, CDCl₃) δ 0.88 (3H, t, J 7.0 Hz, H₁₂), 1.29 (4H, m, H₁₃ and H₁₄), 1.46 (2H, tt, J 7.0 & 7.0 Hz, H₁₅), 1.95 (3H, s, H₁₀), 2.19 (2H, dt, J 7.0 & 7.0 Hz, H₁₆),

3.08 (2H, t, J 6.0 Hz, H₆), 3.44 (2H, dt, J 6.0 & 6.0 Hz, H₇), 6.11 (1H, d, J 15.0 Hz, H₂), 6.92 (1H, dt, J 7.0 & 15.0 Hz, H₁); ¹³C NMR (100 MHz, CDCl₃) δ 13.91 (C₁₂), 22.39 (C₁₃), 23.20 (C₁₀), 27.58 (C₁₅), 28.23 (C₆), 31.31 (C₁₄), 32.20 (C₁₆), 39.82 (C₇), 128.27 (C₂), 146 (C₁), 170.26 (C₉), 190.41 (C₃); LC-MS: m/z calcd for C₁₂H₂₁NO₂S+H⁺: 244.14; found: 244.14

2-(Triphenyl-15-phosphanylidene)acetaldehyde **93**



A mixture of CHCl₃ (2 ml) and chloroethanal **92** (45% in H₂O, 160 mg, 0.92 mmol, 1 eq.) were distilled at 73 °C to remove the water. When approx. 1.6 ml of the azeotrope had been removed, triphenylphosphine (260 mg, 0.92 mmol, 1 eq.) was added to the yellow solution and the mixture was heated at reflux for 24 h. The solvent was removed under reduced pressure and the crude dissolved in water and washed with CHCl₃. Activated charcoal was added and the mixture stirred for 30 min before removing the charcoal by filtration. NaOH (1 M) was added dropwise under vigorous stirring until pH 12. The resulting precipitate was filtered and dried (86 mg). No further purification was performed. ¹H NMR (400 MHz, CDCl₃) δ 3.67 (1H, dd, J 25.0 & 4.0 Hz, H₂), 7.45-7.70 (15H, m, H₃, H₄ and H₅), 8.96 (1H, dd, J 38.0 & 4.0 Hz, H₁); ¹³C NMR (100 MHz, CDCl₃) δ 54.7 (d, J 98.0 Hz, C₂) 129.1, 132.3, 133.4 (C₃, C₄ and C₅), 181.8 (C₁); LC-MS: m/z calcd for C₂₀H₁₇NaOP+H⁺: 327.3, found 327.1

References

1. Splitstoser, J. C., Dillehay, T. D., Wouters, J. & Claro, A. Early pre-Hispanic use of indigo blue in Peru. *Sci. Adv.* **2**, 1501623 (2016).
2. Awtry, E. H. & Loscalzo, J. Aspirin. *Circulation* **101**, 1206–1218 (2000).
3. Newman, D. J. & Cragg, G. M. Natural Products as Sources of New Drugs from 1981 to 2014. *J. Nat. Prod.* **79**, 629–661 (2016).
4. Wohlleben, W., Mast, Y., Stegmann, E. & Ziemert, N. Antibiotic drug discovery. *Microb. Biotechnol.* **9**, 541–548 (2016).
5. UK, C. R. Cancer in the UK 2019. *Cancer Res. UK* (2019).
6. WHO. <https://www.who.int/news-room/fact-sheets/detail/antimicrobial-resistance>.
7. Hu, D. X., Withall, D. M., Challis, G. L. & Thomson, R. J. Structure, Chemical Synthesis, and Biosynthesis of Prodiginine Natural Products. *Chem. Rev.* **116**, 7818–7853 (2016).
8. Tsao, S. W., Rudd, B. A. M., He, X. G., Chang, C. J. & Floss, H. G. Identification of a red pigment from *Streptomyces coelicolor* A3(2) as a mixture of prodigiosin derivatives. *Journal of Antibiotics* **38**, 128–131 (1985).
9. Sydor, P. K., Barry, S. M., Odulate, O. M., Barona-Gomez, F., Haynes, S. W., Corre, C., Song, L. & Challis, G. L. Regio- and stereodivergent antibiotic oxidative carbocyclizations catalysed by Rieske oxygenase-like enzymes. *Nat. Chem.* **3**, 388–392 (2011).
10. Gerber, N. N. & Gauthier, M. J. New prodigiosin-like pigment from *Alteromonas rubra*. *Appl. Environ. Microbiol.* **37**, 1176–1179 (1979).
11. Gerber, N. N. Prodigiosin-like pigments from *Actinomadura (nocardia) pelletieri*. *J. Antibiot. (Tokyo)*. **24**, 636–640 (1971).
12. Fürstner, A. Chemistry and biology of roseophilin and the prodigiosin alkaloids: A survey of the last 2500 years. *Angew. Chemie - Int. Ed.* **42**, 3582–3603 (2003).
13. Wrede, F. & Hettche, O. Über das Prodigiosin, den roten Farbstoff des *Bacillus Prodigiosus*. *Berichte der Dtsch. Chem. Gesellschaft (A B Ser.)* **62**, 2678–2685 (1929).
14. Wrede, F. & Rothhaas, A. Über das Prodigiosin, den roten Farbstoff des *Bacillus*

References

- prodigiosus*, VI. *Hoppe-Seyler's Zeitschrift für Physiol. Chemie* **226**, 95–107 (1934).
15. Santer, U. V. & Vogel, H. J. Prodigiosin synthesis in *Serratia marcescens*: isolation of a pyrrole-containing precursor. *Biochim. Biophys. Acta* **19**, 578–579 (1956).
 16. Wasserman, H. H., McKeon, J. E., Smith, L. & Forgione, P. Prodigiosin. Structure and partial synthesis. *J. Am. Chem. Soc.* **82**, 506–507 (1960).
 17. Rapoport, H. & Willson, C. D. The Preparation and Properties of Some Methoxypyrroles. *J. Am. Chem. Soc.* **84**, 630–635 (1962).
 18. Rapoport, H. & Holden, K. G. The Synthesis of Prodigiosin. *J. Am. Chem. Soc.* **84**, 635–642 (1962).
 19. Rizzo, V., Morelli, A., Pinciroli, V., Sciangula, D. & D'Alessio, R. Equilibrium and Kinetics of Rotamer Interconversion in Immunosuppressant Prodigiosin Derivatives in Solution. *J. Pharm. Sci.* **88**, 73–78 (1999).
 20. Bhalara, H. D. Elucidation of the Biosynthetic Pathway of a Tripyrrole Secondary Metabolite, Prodigiosin. (Cambridge, 2011).
 21. Williams, R. P. Biosynthesis of Prodigiosin, a Secondary Metabolite of *Serratia marcescens*. *Appl. Environ. Microbiol.* **25**, (1973).
 22. Cerdeño, A. M., Bibb, M. J. & Challis, G. L. Analysis of the prodiginine biosynthesis gene cluster of *Streptomyces coelicolor* A3(2): new mechanisms for chain initiation and termination in modular multienzymes. *Chem. Biol.* **8**, 817–829 (2001).
 23. Thomson, N. R., Crow, M. A., McGowan, S. J., Cox, A. & Salmond, G. P. C. Biosynthesis of carbapenem antibiotic and prodigiosin pigment in *Serratia* is under quorum sensing control. *Mol. Microbiol.* **36**, 539–556 (2000).
 24. Harris, A. K. P., Williamson, N. R., Slater, H., Cox, A., Abbasi, S., Foulds, I., Simonsen, H. T., Leeper, F. J. & Salmond, G. P. C. The *Serratia* gene cluster encoding biosynthesis of the red antibiotic, prodigiosin, shows species- and strain-dependent genome context variation. *Microbiology* **150**, 3547–3560 (2004).
 25. Cox, A. R. J., Thomson, N. R., Bycroft, B., Stewart, G. S. A. B., Williams, P. & Salmond, G. P. C. A pheromone-independent CarR protein controls carbapenem antibiotic synthesis in the opportunistic human pathogen *Serratia marcescens*. *Microbiology* **144**, 201–209 (1998).

References

26. Williamson, N. R., Simonsen, H. T., Ahmed, R. A. A., Goldet, G., Slater, H., Woodley, L., Leeper, F. J. & Salmond, G. P. C. Biosynthesis of the red antibiotic, prodigiosin, in *Serratia*: identification of a novel 2-methyl-3-n-amylyl-pyrrole (MAP) assembly pathway, definition of the terminal condensing enzyme, and implications for undecylprodigiosin biosynthesis in *Streptomyces*. *Mol. Microbiol.* **56**, 971–989 (2005).
27. Gummadidala, P. M., Holder, M. E., O'Brien, J. L., Ajami, N. J., Petrosino, J. F., Mitra, C., Chen, Y. P., Decho, A. W. & Chanda, A. Complete Genome Sequence of *Vibrio gazogenes* ATCC 43942. *Genome Announc.* **5**, (2017).
28. Kim, D., Lee, J. S., Park, Y. K., Kim, J. F., Jeong, H., Oh, T. K., Kim, B. S. & Lee, C. H. Biosynthesis of antibiotic prodiginines in the marine bacterium *Hahella chejuensis* KCTC 2396. *J. Appl. Microbiol.* **102**, 937–944 (2007).
29. Schloss, P. D., Allen, H. K., Klimowicz, A. K., Mlot, C., Gross, J. A., Savengsuksa, S., McEllin, J., Clardy, J., Ruess, R. W. & Handelsman, J. Psychrotrophic strain of *Janthinobacterium lividum* from a cold Alaskan soil produces prodigiosin. *DNA Cell Biol.* **29**, 533–541 (2010).
30. Ravindran, A., Sunderrajan, S. & Pennathur, G. Phylogenetic Studies on the Prodigiosin Biosynthetic Operon. *Curr. Microbiol.* **76**, 597–606 (2019).
31. Stanley, A. E., Walton, L. J., Kourdi Zerikly, M., Corre, C. & Challis, G. L. Elucidation of the *Streptomyces coelicolor* pathway to 4-methoxy-2,2'-bipyrrole-5-carboxaldehyde, an intermediate in prodiginine biosynthesis. *Chem. Commun.* 3981–3983 (2006).
32. Williamson, N. R., Fineran, P. C., Leeper, F. J. & Salmond, G. P. C. The biosynthesis and regulation of bacterial prodiginines. *Nat. Rev. Microbiol.* **4**, 887–899 (2006).
33. Cho, H. J., Kim, K.-J., Kim, M. H. & Kang, B. S. Structural insight of the role of the *Hahella chejuensis* HapK protein in prodigiosin biosynthesis. *Proteins Struct. Funct. Bioinforma.* **70**, 257–262 (2007).
34. Sakai-Kawada, F. E., Ip, C. G., Hagiwara, K. A. & Awaya, J. D. Biosynthesis and Bioactivity of Prodiginine Analogs in Marine Bacteria, *Pseudoalteromonas*: A Mini Review. *Front. Microbiol.* **10**, 1715 (2019).
35. Lou, X., Ran, T., Han, N., Gao, Y., He, J., Tang, L., Xu, D. & Wang, W. Crystal structure of the catalytic domain of PigE: A transaminase involved in the biosynthesis of 2-methyl-3-n-amylyl-pyrrole (MAP) from *Serratia* sp. FS14. *Biochem. Biophys. Res. Commun.* **447**, 178–

References

- 183 (2014).
36. Dresen, C., Richter, M., Pohl, M., Lüdeke, S. & Müller, M. The Enzymatic Asymmetric Conjugate Umpolung Reaction. *Angew. Chem. Int. Ed.* **49**, 6600–6603 (2010).
 37. Couturier, M., Bhalara, H., Chawrai, S., Monson, R., Williamson, N., Salmond, G. & Leeper, F. J. Substrate flexibility of the flavin-dependent dihydropyrrole oxidases PigB and HapB involved in antibiotic prodigiosin biosynthesis. *ChemBioChem* cbic.201900424 (2019).
 38. Mo, S., Kim, B. S. & Reynolds, K. A. Production of Branched-Chain Alkylprodiginines in *S. coelicolor* by Replacement of the 3-Ketoacyl ACP Synthase III Initiation Enzyme, RedP. *Chem. Biol.* **12**, 191–200 (2005).
 39. Mo, S., Sydor, P. K., Corre, C., Alhamadsheh, M. M., Stanley, A. E., Haynes, S. W., Song, L., Reynolds, K. A. & Challis, G. L. Elucidation of the *Streptomyces coelicolor* Pathway to 2-Undecylpyrrole, a Key Intermediate in Undecylprodiginine and Streptorubin B Biosynthesis. *Chem. Biol.* **15**, 137–148 (2008).
 40. Whicher, J. R., Florova, G., Sydor, P. K., Singh, R., Alhamadsheh, M., Challis, G. L., Reynolds, K. A. & Smith, J. L. Structure and Function of the RedJ Protein, a Thioesterase from the Prodiginine Biosynthetic Pathway in *Streptomyces coelicolor*. *J. Biol. Chem.* **286**, 22558–22569 (2011).
 41. Wilks, J. C. & Slonczewski, J. L. pH of the cytoplasm and periplasm of *Escherichia coli*: rapid measurement by green fluorescent protein fluorimetry. *J. Bacteriol.* **189**, 5601–7 (2007).
 42. Haynes, S. W., Sydor, P. K., Stanley, A. E., Song, L. & Challis, G. L. Role and substrate specificity of the *Streptomyces coelicolor* RedH enzyme in undecylprodiginine biosynthesis. *Chem. Commun.* 1865 (2008).
 43. Chawrai, S. R., Williamson, N. R., Salmond, G. P. C. & Leeper, F. J. Chemoenzymatic synthesis of prodigiosin analogues--exploring the substrate specificity of PigC. *Chem. Commun. (Camb)*. **44**, 1862–1864 (2008).
 44. Barry, S. M. & Challis, G. L. Mechanism and catalytic diversity of rieske non-heme iron-dependent oxygenases. *ACS Catal.* **3**, 2362–2370 (2013).
 45. De Rond, T., Stow, P., Eigl, I., Johnson, R. E., Chan, L. J. G., Goyal, G., Baidoo, E. E. K., Hillson, N. J., Petzold, C. J., Sarpong, R. & Keasling, J. D. Oxidative cyclization of

References

- prodigiosin by an alkylglycerol monooxygenase-like enzyme. *Nat. Chem. Biol.* **13**, 1155–1157 (2017).
46. Boonlarpgradab, C., Kauffman, C. A., Jensen, P. R. & Fenical, W. Marineosins A and B, Cytotoxic Spiroaminals from a Marine-Derived *Actinomycete*. *Org. Lett.* **10**, 5505–5508 (2008).
 47. Salem, S. M., Kancharla, P., Florova, G., Gupta, S., Lu, W. & Reynolds, K. A. Elucidation of Final Steps of the Marineosins Biosynthetic Pathway through Identification and Characterization of the Corresponding Gene Cluster. *J. Am. Chem. Soc.* **136**, 4565–4574 (2014).
 48. Hayakawa, Y., Kawakami, K., Seto, H. & Furihata, K. Structure of a new antibiotic, roseophilin. *Tetrahedron Lett.* **33**, 2701–2704 (1992).
 49. Fürstner, A. & Weintritt, H. Total Synthesis of Roseophilin. *J. Am. Chem. Soc.* **120**, 2817–2825 (1998).
 50. Boger, D. L. & Hong, J. Asymmetric Total Synthesis of *ent* -(-)-Roseophilin: Assignment of Absolute Configuration. *J. Am. Chem. Soc.* **123**, 8515–8519 (2001).
 51. Harrington, P. E. & Tius, M. A. Synthesis and Absolute Stereochemistry of Roseophilin. *J. Am. Chem. Soc.* **123**, 8509–8514 (2001).
 52. Kawasaki, T., Sakurai, F. & Hayakawa, Y. A Prodigiosin from the Roseophilin Producer *Streptomyces griseoviridis*. *J. Nat. Prod.* **71**, 1265–1267 (2008).
 53. Hayakawa, Y., Nagatsuka, S. & Kawasaki, T. Dechlororoseophilin: a new cytotoxic metabolite from *Streptomyces griseoviridis*. *J. Antibiot. (Tokyo)*. **62**, 531–532 (2009).
 54. Withall, D. M., Haynes, S. W. & Challis, G. L. Stereochemistry and Mechanism of Undecylprodigiosin Oxidative Carbocyclization to Streptorubin B by the Rieske Oxygenase RedG. *J. Am. Chem. Soc.* **137**, 7889–7897 (2015).
 55. Burke, C., Thomas, T., Egan, S. & Kjelleberg, S. The use of functional genomics for the identification of a gene cluster encoding for the biosynthesis of an antifungal tambjamine in the marine bacterium *Pseudoalteromonas tunicata*. *Environ. Microbiol.* **9**, 814–818 (2007).
 56. Picott, K. J., Deichert, J. A., DeKemp, E. M., Schatte, G., Sauriol, F. & Ross, A. C. Isolation and characterization of tambjamine MYPI, a macrocyclic tambjamine analogue from

References

- marine bacterium *Pseudoalteromonas citrea*. *Medchemcomm* **10**, 478–483 (2019).
57. Papireddy, K., Smilkstein, M., Kelly, J. X., Shweta, Salem, S. M., Alhamadsheh, M., Haynes, S. W., Challis, G. L. & Reynolds, K. A. Antimalarial Activity of Natural and Synthetic Prodiginines. *J. Med. Chem.* **54**, 5296–5306 (2011).
 58. Isaka, M., Jaturapat, A., Kramyu, J., Tanticharoen, M. & Thebtaranonth, Y. Potent in vitro antimalarial activity of metacycloprodigiosin isolated from *Streptomyces spectabilis* BCC 4785. *Antimicrob. Agents Chemother.* **46**, 1112–3 (2002).
 59. Kim, H. S., Hayashi, M., Shibata, Y., Wataya, Y., Mitamura, T., Horii, T., Kawauchi, K., Hirata, H., Tsuboi, S. & Moriyama, Y. Cycloprodigiosin hydrochloride obtained from *Pseudoalteromonas denitrificans* is a potent antimalarial agent. *Biol. Pharm. Bull.* **22**, 532–4 (1999).
 60. Davidson, D. E., Tanticharoenyos, P., Johnsen, D. O., Kinnamon, K. E. & Hickman, R. L. Evaluating New Antimalarial Drugs against Trophozoite Induced *Plasmodium Cynomolgi* Malaria in Rhesus Monkeys. *Am. J. Trop. Med. Hyg.* **25**, 26–33 (1976).
 61. Castro, A. J. Antimalarial Activity of Prodigiosin. *Nature* **213**, 903–904 (1967).
 62. Kancharla, P., Kelly, J. X. & Reynolds, K. A. Synthesis and Structure–Activity Relationships of Tambjamines and B-Ring Functionalized Prodiginines as Potent Antimalarials. *J. Med. Chem.* **58**, 7286–7309 (2015).
 63. Herráez, R., Mur, A., Merlos, A., Viñas, M. & Vinuesa, T. Using prodigiosin against some gram-positive and gram-negative bacteria and *Trypanosoma cruzi*. *J. Venom. Anim. Toxins Incl. Trop. Dis.* **25**, (2019).
 64. *Cryptococcus*. (American Society of Microbiology, 2011).
 65. Kim, K., Alker, A., Shuster, K., Quirolo, C. & Harvell, C. Longitudinal study of aspergillosis in sea fan corals. *Dis. Aquat. Organ.* **69**, 95–99 (2006).
 66. Asano, S., Ogiwara, K., Nakagawa, Y., Suzuki, K., Hori, H. & Watanabe, T. Prodigiosin Produced by *Serratia marcescens* Enhances the Insecticidal Activity of *Bacillus thuringiensis* delta-Endotoxin (Cry1C) against Common Cutworm, *Spodoptera litura*. *J. Pestic. Sci.* **24**, 381–385 (1999).
 67. Moghaddam, E., Teoh, B.-T., Sam, S.-S., Lani, R., Hassandarvish, P., Chik, Z., Yueh, A., Abubakar, S., Zandi, K., Hidari, K. I., Talarico, L. B., Damonte, E. B., Zandi, K., Huh, S. U.,

References

- Paek, K. H., Kumar, S., Pandey, A. K., Lyu, S. Y. *et al.* Baicalin, a metabolite of baicalein with antiviral activity against dengue virus. *Sci. Rep.* **4**, 91–95 (2014).
68. Gutiérrez-Román, M. I., Holguín-Meléndez, F., Dunn, M. F., Guillén-Navarro, K. & Huerta-Palacios, G. Antifungal activity of *Serratia marcescens* CFFSUR-B2 purified chitinolytic enzymes and prodigiosin against *Mycosphaerella fijiensis*, causal agent of black Sigatoka in banana (*Musa spp.*). *BioControl* **60**, 565–572 (2015).
69. John Jimtha, C., Jishma, P., Sreelekha, S., Chithra, S. & Radhakrishnan, E. Antifungal properties of prodigiosin producing rhizospheric *Serratia sp.* *Rhizosphere* **3**, 105–108 (2017).
70. Danevčič, T., Borić Vezjak, M., Zorec, M. & Stopar, D. Prodigiosin - A Multifaceted *Escherichia coli* Antimicrobial Agent. *PLoS One* **11**, e0162412 (2016).
71. Lapenda, J. C., Silva, P. A., Vicalvi, M. C., Sena, K. X. F. R. & Nascimento, S. C. Antimicrobial activity of prodigiosin isolated from *Serratia marcescens* UFPEDA 398. *World J. Microbiol. Biotechnol.* **31**, 399–406 (2015).
72. Mimica, M. J., Carvalho, R. L., Berezin, E. N., Damaceno, N. & Caiaffa-Filho, H. H. Comparison of five methods for oxacillin susceptibility testing of *Staphylococcus aureus* isolates from cystic fibrosis patients. *Rev. Inst. Med. Trop. Sao Paulo* **54**, 305–306 (2012).
73. Lee, J. S., Kim, Y.-S., Park, S., Kim, J., Kang, S.-J., Lee, M.-H., Ryu, S., Choi, J. M., Oh, T.-K. & Yoon, J.-H. Exceptional production of both prodigiosin and cycloprodigiosin as major metabolic constituents by a novel marine bacterium, *Zooshikella rubidus* SI-1. *Appl. Environ. Microbiol.* **77**, 4967–73 (2011).
74. Feng, J., Shi, W., Zhang, S. & Zhang, Y. Identification of new compounds with high activity against stationary phase *Borrelia burgdorferi* from the NCI compound collection. *Emerg. Microbes Infect.* **4**, 1–15 (2015).
75. Darshan, N. & Manonmani, H. K. Prodigiosin inhibits motility and activates bacterial cell death revealing molecular biomarkers of programmed cell death. *AMB Express* **6**, 50 (2016).
76. Suryawanshi, R. K., Patil, C. D., Koli, S. H., Hallsworth, J. E. & Patil, S. V. Antimicrobial activity of prodigiosin is attributable to plasma-membrane damage. *Nat. Prod. Res.* **31**, 572–577 (2017).
77. Klein, A. S., Brass, H. U. C., Klebl, D. P., Classen, T., Loeschcke, A., Drepper, T., Sievers,

References

- S., Jaeger, K.-E. & Pietruszka, J. Preparation of Cyclic Prodiginines by Mutasyntesis in *Pseudomonas putida* KT2440. *ChemBioChem* **19**, 1545–1552 (2018).
78. Williamson, N. R., Fineran, P. C., Gristwood, T., Chawrai, S. R., Leeper, F. J. & Salmond, G. P. Anticancer and immunosuppressive properties of bacterial prodiginines. *Future Microbiol.* **2**, 605–618 (2007).
79. Songia, S., Mortellaro, A., Taverna, S., Fornasiero, C., Scheiber, E. A., Erba, E., Colotta, F., Mantovani, A., Isetta, A. M. & Golay, J. Characterization of the new immunosuppressive drug undecylprodigiosin in human lymphocytes: retinoblastoma protein, cyclin-dependent kinase-2, and cyclin-dependent kinase-4 as molecular targets. *J. Immunol.* **158**, 3987–95 (1997).
80. Nakamura, A., Magae, J., Tsuji, R. F., Yamasaki, M. & Nagai, K. Suppression of cytotoxic T cell induction in vivo by prodigiosin 25-C. *Transplantation* **47**, 1013–6 (1989).
81. Tsuji, R. F., Yamamoto, M., Nakamura, A., Kataoka, T., Yamasaki, M., Magae, J. & Nagai, K. Selective immunosuppression of prodigiosin 25-C and FK506 in the murine immune system. *J. Antibiot. (Tokyo)*. **43**, 1293–1301 (1990).
82. Tsuji, R. F., Magae, J., Yamashita, M., Nagai, K. & Yamasaki, M. Immunomodulating properties of prodigiosan 25-C, an antibiotic which preferentially suppresses induction of cytotoxic t cells. *J. Antibiot. (Tokyo)*. **45**, 1295–1302 (1992).
83. Azuma, T., Watanabe, N., Yagisawa, H., Hirata, H., Iwamura, M. & Kobayashi, Y. Induction of apoptosis of activated murine splenic T cells by cycloprodigiosin hydrochloride, a novel immunosuppressant. *Immunopharmacology* **46**, 29–37 (2000).
84. Nakai, K., Hamada, Y., Kato, Y., Yamamoto, D., Hirata, H. & Hioki, K. Cycloprodigiosin hydrochloride as an immunosuppressant in rat small bowel transplantation. *Transplant. Proc.* **32**, 1324–1325 (2000).
85. Magae, J., Miller, M. W., Nagai, K. & Shearer, G. M. Effect of metacycloprodigiosin, an inhibitor of killer T cells on murine skin and heart transplants. *J. Antibiot. (Tokyo)*. (1996).
86. Han, S.-B., Lee, C. W., Yoon, Y. D., Kang, J. S., Lee, K. H., Yoon, W. K., Kim, Y. K., Lee, K., Park, S.-K. & Kim, H. M. Effective prevention of lethal acute graft-versus-host disease by combined immunosuppressive therapy with prodigiosin and cyclosporine A. *Biochem. Pharmacol.* (2005).
87. Han, S. B., Kim, H. M., Kim, Y. H., Lee, C. W., Jang, E.-S., Son, K. H., Kim, S. U. & Kim, Y.

References

- K. T-cell specific immunosuppression by prodigiosin isolated from *Serratia marcescens*. *Int. J. Immunopharmacol.* **20**, 1-13 (1998).
88. Han, S. B., Park, S. H., Jeon, Y. J., Kim, Y. K., Kim, H. M. & Yang, K. H. Prodigiosin Blocks T Cell Activation by Inhibiting Interleukin-2R Expression and Delays Progression of Autoimmune Diabetes and Collagen-Induced Arthritis. *The Journal Of Pharmacology And Experimental Therapeutics* **299**, (2001).
89. D'Alessio, R., Bargiotti, A., Carlini, O., Colotta, F., Ferrari, M., Gnocchi, P., Isetta, A., Mongelli, N., Motta, P., Rossi, A., Rossi, M., Tibolla, M. & Vanotti, E. Synthesis and Immunosuppressive Activity of Novel Prodigiosin Derivatives. *J. Med. Chem.* **43**, 2557-2565 (2000).
90. Mortellaro, A., Songia, S., Gnocchi, P., Ferrari, M., Fornasiero, C., D'Alessio, R., Isetta, A., Colotta, F. & Golay, J. New immunosuppressive drug PNU156804 blocks IL-2-dependent proliferation and NF-kappa B and AP-1 activation. *J. Immunol.* **162**, 7102-9 (1999).
91. Stepkowski, S. M., Erwin-Cohen, R. A., Behbod, F., Wang, M.-E., Qu, X., Tejpal, N., Nagy, Z. S., Kahan, B. D. & Kirken, R. A. Selective inhibitor of Janus tyrosine kinase 3, PNU156804, prolongs allograft survival and acts synergistically with cyclosporine but additively with rapamycin. *Blood* **99**, 680-9 (2002).
92. Manderville, R. Synthesis, Proton-Affinity and Anti-Cancer Properties of the Prodigiosin-Group Natural Products. *Curr. Med. Chem. Agents* (2005).
93. Wang, Z., Li, B., Zhou, L., Yu, S., Su, Z., Song, J., Sun, Q., Sha, O., Wang, X., Jiang, W., Willert, K., Wei, L., Carson, D. A. & Lu, D. Prodigiosin inhibits Wnt/ β -catenin signaling and exerts anticancer activity in breast cancer cells. *Proc. Natl. Acad. Sci.* **113**, 13150-13155 (2016).
94. Francisco, R., Pérez-Tomás, R., Giménez-Bonafé, P., Soto-Cerrato, V., Giménez-Xavier, P. & Ambrosio, S. Mechanisms of prodigiosin cytotoxicity in human neuroblastoma cell lines. *Eur. J. Pharmacol.* (2007).
95. Ho, T.-F. F., Ma, C.-J. J., Lu, C.-H. H., Tsai, Y.-T. T., Wei, Y.-H. H., Chang, J.-S. S., Lai, J.-K. K., Cheuh, P.-J. J., Yeh, C.-T. T., Tang, P.-C. C., Tsai Chang, J., Ko, J.-L. L., Liu, F.-S. S., Yen, H. E. & Chang, C.-C. C. Undecylprodigiosin selectively induces apoptosis in human breast carcinoma cells independent of p53. *Toxicol. Appl. Pharmacol.* **225**, 318-328 (2007).

References

96. Yamamoto, C., Takemoto, H., Kuno, K., Yamamoto, D., Tsubura, A., Kamata, K., Hirata, H., Yamamoto, A., Kano, H., Seki, T. & Inoue, K. Cycloprodigiosin hydrochloride, a new H⁺/Cl⁻ symporter, induces apoptosis in human and rat hepatocellular cancer cell lines in vitro and inhibits the growth of hepatocellular carcinoma xenografts in nude mice. *Hepatology* **30**, 894–902 (1999).
97. Schimmer, A. D., O'Brien, S., Kantarjian, H., Brandwein, J., Cheson, B. D., Minden, M. D., Yee, K., Ravandi, F., Giles, F., Schuh, A., Gupta, V., Andreeff, M., Koller, C., Chang, H., Kamel-Reid, S., Berger, M., Viallet, J. & Borthakur, G. A phase I study of the pan bcl-2FamilyInhibitor obatoclax mesylate in patients with advanced hematologic malignancies. *Clin. Cancer Res.* (2008).
98. Zhang, J., Shen, Y., Liu, J. & Wei, D. Antimetastatic effect of prodigiosin through inhibition of tumor invasion. *Biochem. Pharmacol.* **69**, 407–414 (2005).
99. Schimmer, A. D., Raza, A., Carter, T. H., Claxton, D., Erba, H., DeAngelo, D. J., Tallman, M. S., Goard, C. & Borthakur, G. A Multicenter Phase I/II Study of Obatoclax Mesylate Administered as a 3- or 24-Hour Infusion in Older Patients with Previously Untreated Acute Myeloid Leukemia. *PLoS One* **9**, e108694 (2014).
100. Oki, Y., Copeland, A., Hagemester, F., Fayad, L. E., Fanale, M., Romaguera, J. & Younes, A. Experience with obatoclax mesylate (GX15-070), a small molecule pan-Bcl-2 family antagonist in patients with relapsed or refractory classical Hodgkin lymphoma. *Blood* **119**, 2171–2 (2012).
101. Paik, P. K., Rudin, C. M., Pietanza, M. C., Brown, A., Rizvi, N. A., Takebe, N., Travis, W., James, L., Ginsberg, M. S., Juergens, R., Markus, S., Tyson, L., Subzwari, S., Kris, M. G. & Krug, L. M. A phase II study of obatoclax mesylate, a Bcl-2 antagonist, plus topotecan in relapsed small cell lung cancer. *Lung Cancer* **74**, 481–485 (2011).
102. Langer, C. J., Albert, I., Ross, H. J., Kovacs, P., Blakely, L. J., Pajkos, G., Somfay, A., Zatloukal, P., Kazarnowicz, A., Moezi, M. M., Schreeder, M. T., Schnyder, J., Ao-Baslock, A., Pathak, A. K. & Berger, M. S. Randomized phase II study of carboplatin and etoposide with or without obatoclax mesylate in extensive-stage small cell lung cancer. *Lung Cancer* **85**, 420–428 (2014).
103. Li, D., Liu, J., Wang, X., Kong, D., Du, W., Li, H., Hse, C.-Y., Shupe, T., Zhou, D. & Zhao, K. Biological Potential and Mechanism of Prodigiosin from *Serratia marcescens* Subsp. lawsoniana in Human Choriocarcinoma and Prostate Cancer Cell Lines. *Int. J. Mol. Sci.*

References

- 19, 3465 (2018).
104. Soto-Cerrato, V., Llagostera, E., Montaner, B., Scheffer, G. L. & Perez-Tomas, R. Mitochondria-mediated apoptosis operating irrespective of multidrug resistance in breast cancer cells by the anticancer agent prodigiosin. *Biochem. Pharmacol.* **68**, 1345–1352 (2004).
105. Nakashima, T., Tamura, T., Kurachi, M., Yamaguchi, K. & Oda, T. Apoptosis-Mediated Cytotoxicity of Prodigiosin-Like Red Pigment Produced by γ -Proteobacterium and Its Multiple Bioactivities. *Biol. Pharm. Bull.* **28**, 2289–2295 (2005).
106. Montaner, B. & Pérez-Tomás, R. The cytotoxic prodigiosin induces phosphorylation of p38-MAPK but not of SAPK/JNK. *Toxicol. Lett.* **129**, 93–8 (2002).
107. Ramoneda, B. M. & Pérez-Tomás, R. Activation of protein kinase C for protection of cells against apoptosis induced by the immunosuppressor prodigiosin. *Biochem. Pharmacol.* (2002).
108. Hong, B., Prabhu, V. V., Zhang, S., Van Den Heuvel, A. P. J., Dicker, D. T., Kopelovich, L. & El-Deiry, W. S. Prodigiosin rescues deficient p53 signaling and antitumor effects via upregulating p73 and disrupting its interaction with mutant p53. *Cancer Res.* (2014).
109. Fürstner, A., Reinecke, K., Prinz, H. & Waldmann, H. The core structures of roseophilin and the prodigiosin alkaloids define a new class of protein tyrosine phosphatase inhibitors. *ChemBioChem* (2004).
110. Pérez-Tomás, R., Montaner, B., Llagostera, E. & Soto-Cerrato, V. The prodigiosins, proapoptotic drugs with anticancer properties. *Biochem. Pharmacol.* **66**, 1447–1452 (2003).
111. Konno, H., Matsuya, H., Okamoto, M., Sato, T., Tanaka, Y., Yokoyama, K., Kataoka, T., Nagai, K., Wasserman, H. H. & Ohkuma, S. Prodigiosins uncouple mitochondrial and bacterial F-ATPases: Evidence for their H⁺/Cl⁻ symport activity. *J. Biochem.* (1998).
112. Sato, T., Konno, H., Tanaka, Y., Kataoka, T., Nagai, K., Wasserman, H. H. & Ohkuma, S. Prodigiosins as a new group of H⁺/Cl⁻ symporters that uncouple proton translocators. *J. Biol. Chem.* (1998).
113. Nakayasu, T., Kawauchi, K., Hirata, H. & Shimmen, T. Demonstration of Cl⁻ Requirement for Inhibition of Vacuolar Acidification by Cycloprodigiosin in Situ. *Plant Cell Physiol.* **41**, 857–863 (2000).

References

114. Togashi, K., Kataoka, T. & Nagai, K. Characterization of a series of vacuolar type H(+)-ATPase inhibitors on CTL-mediated cytotoxicity. *Immunol. Lett.* **55**, 139–44 (1997).
115. Ohkuma, S., Sato, T., Okamoto, M., Matsuya, H., Arai, K., Kataoka, T., Nagai, K. & Wasserman, H. H. Prodigiosins uncouple lysosomal vacuolar-type ATPase through promotion of H⁺/Cl⁻ symport. *Biochem. J.* **334** (Pt 3, 731–41 (1998).
116. Kawauchi, K., Shibutani, K., Yagisawa, H., Kamata, H., Nakatsuji, S., Anzai, H., Yokoyama, Y., Ikegami, Y., Moriyama, Y. & Hirata, H. A Possible Immunosuppressant, Cycloprodigiosin Hydrochloride, Obtained from *Pseudoalteromonas denitrificans*. *Biochem. Biophys. Res. Commun.* **237**, 543–547 (1997).
117. Matsuya, H., Okamoto, M., Ochi, T., Nishikawa, A., Shimizu, S., Kataoka, T., Nagai, K., Wasserman, H. H. & Ohkuma, S. Reversible and potent uncoupling of hog gastric (H⁺+K⁺)-ATPase by prodigiosins. *Biochem. Pharmacol.* **60**, 1855–63 (2000).
118. Gale, P. A., Light, M. E., McNally, B., Navakhun, K., Sliwinski, K. E. & Smith, B. D. Co-transport of H⁺/Cl⁻ by a synthetic prodigiosin mimic. *Chem. Commun.* (2005).
119. Fürstner, A., Grabowski, J., Lehmann, C. W., Kataoka, T. & Nagai, K. Synthesis and Biological Evaluation of Nonylprodigiosin and Macrocyclic Prodigiosin Analogues. *ChemBioChem* **2**, 60–68 (2001).
120. Diaz, R. I. S., Regourd, J., Santacroce, P. V., Davis, J. T., Jakeman, D. L. & Thompson, A. Chloride anion transport and copper-mediated DNA cleavage by C-ring functionalized prodigiosenes. *Chem. Commun.* 2701–2703 (2007).
121. Melvin, M. S., Wooton, K. E., Rich, C. C., Saluta, G. R., Kucera, G. L., Lindquist, N. & Manderville, R. A. Copper-nuclease efficiency correlates with cytotoxicity for the 4-methoxypyrrrolic natural products. *J. Inorg. Biochem.* **87**, 129–135 (2001).
122. Melvin, M. S., Tomlinson, J. T., Saluta, G. R., Kucera, G. L., Lindquist, N. & Manderville, R. A. Double-strand DNA cleavage by copper-prodigiosin. *J. Am. Chem. Soc.* **122**, 6333–6334 (2000)
123. Melvin, M. S., Calcutt, M. W., Nofle, R. E. & Manderville, R. A. Influence of the A-ring on the redox and nuclease properties of the prodigiosins: Importance of the bipyrrrole moiety in oxidative DNA cleavage. *Chem. Res. Toxicol.* (2002).
124. Park, G., Tomlinson, J. T., Melvin, M. S., Wright, M. W., Day, C. S. & Manderville, R. A. Zinc and copper complexes of prodigiosin: Implications for copper-mediated double-

References

- strand DNA cleavage. *Org. Lett.* (2003).
125. Regourd, J., Ali, A. A. S. & Thompson, A. Synthesis and anti-cancer activity of C-ring-functionalized prodigiosin analogues. *J. Med. Chem.* **50**, 1528–1536 (2007).
126. Rastogi, S., Zhang, D. & Davis, J. T. The natural product prodigiosin binds G-quadruplex DNA. *Supramol. Chem.* **28**, 18–28 (2016).
127. Rastogi, S., Marchal, E., Uddin, I., Groves, B., Colpitts, J., McFarland, S. A., Davis, J. T. & Thompson, A. Synthetic prodigiosenes and the influence of C-ring substitution on DNA cleavage, transmembrane chloride transport and basicity. *Org. Biomol. Chem.* **11**, 3834 (2013).
128. Dejean, L. M., Martinez-Caballero, S., Guo, L., Hughes, C., Teijido, O., Ducret, T., Ichas, F., Korsmeyer, S. J., Antonsson, B., Jonas, E. A. & Kinnally, K. W. Oligomeric Bax Is a Component of the Putative Cytochrome c Release Channel MAC, Mitochondrial Apoptosis-induced Channel. *Mol. Biol. Cell* **16**, 2424–2432 (2005).
129. Pérez-Galán, P., Roué, G., Villamor, N., Campo, E. & Colomer, D. The BH3-mimetic GX15-070 synergizes with bortezomib in mantle cell lymphoma by enhancing Noxa-mediated activation of Bak. *Blood* (2007).
130. Trudel, S., Zhi, H. L., Rauw, J., Tiedemann, R. E., Xiao, Y. W. & Stewart, A. K. Preclinical studies of the pan-Bcl inhibitor obatoclax (GX015-070) in multiple myeloma. *Blood* (2007).
131. Nguyen, M., Marcellus, R. C., Roulston, A., Watson, M., Serfass, L., Murthy Madiraju, S. R., Goulet, D., Viallet, J., Belec, L., Billot, X., Acoca, S., Purisima, E., Wiegmanns, A., Cluse, L., Johnstone, R. W., Beauparlant, P., Shore, G. C., Bélec, L. *et al.* Small molecule obatoclax (GX15-070) antagonizes MCL-1 and overcomes MCL-1-mediated resistance to apoptosis. *Proc. Natl. Acad. Sci. U. S. A.* (2007).
132. Fulda, S., Galluzzi, L. & Kroemer, G. Targeting mitochondria for cancer therapy. *Nat. Rev. Drug Discov.* **9**, 447–464 (2010).
133. Mann, J. *Chemical aspects of biosynthesis.* (Oxford University Press, 1994).
134. Weissman, K. J. Mutasynthesis – uniting chemistry and genetics for drug discovery. *Trends Biotechnol.* **25**, 139–142 (2007).
135. Chawrai, S. R., Williamson, N. R., Mahendiran, T., Salmond, G. P. C. & Leeper, F. J.

References

- Characterisation of PigC and HapC, the prodigiosin synthetases from *Serratia sp.* and *Hahella chejuensis* with potential for biocatalytic production of anticancer agents. *Chem. Sci.* **3**, 447–454 (2012).
136. Domröse, A., Klein, A. S., Hage-Hülsmann, J., Thies, S., Svensson, V., Classen, T., Pietruszka, J., Jaeger, K.-E. E., Drepper, T. & Loeschcke, A. Efficient recombinant production of prodigiosin in *Pseudomonas putida*. *Front. Microbiol.* **6**, 972 (2015).
137. Klein, A. S., Domröse, A., Bongen, P., Brass, H. U. C., Classen, T., Loeschcke, A., Drepper, T., Laraia, L., Sievers, S., Jaeger, K.-E. & Pietruszka, J. New Prodigiosin Derivatives Obtained by Mutasynthesis in *Pseudomonas putida*. *ACS Synth. Biol.* **6**, 1757–1765 (2017).
138. Trofimov, B. A., Mikhaleva, A. I., Ivanov, A. V., Shcherbakova, V. S. & Ushakov, I. A. Expedient one-pot synthesis of pyrroles from ketones, hydroxylamine, and 1,2-dichloroethane. *Tetrahedron* **71**, 124–128 (2015).
139. Chawrai, S. R. Studies on Biosynthetic Pathway of a Tripyrrole secondary Metabolite, Prodigiosin. (Cambridge, 2009).
140. Bates, T. F., Clarke, M. T. & Thomas, R. D. Unusual stability of an alkyllithium dimer. Preparation, properties, and decomposition mechanism of tert-butyllithium dietherate dimer. *J. Am. Chem. Soc.* **110**, 5109–5112 (1988).
141. Seo, Y. H., Kim, J.-K. & Jun, J.-G. Synthesis and biological evaluation of piperlongumine derivatives as potent anti-inflammatory agents. *Bioorg. Med. Chem. Lett.* **24**, 5727–5730 (2014).
142. Alves, J. C. F. 2-Pyrrolidinones and 3-Pyrrolin-2-ones: A Study on the Chemical Reactivity of These Structural Moieties. *Org. Chem. Int.* **2011**, 1–10 (2011).
143. Piel, I., Pawelczyk, M. D., Hirano, K., Fröhlich, R. & Glorius, F. A Family of Thiazolium Salt Derived N-Heterocyclic Carbenes (NHCs) for Organocatalysis: Synthesis, Investigation and Application in Cross-Benzoin Condensation. *European J. Org. Chem.* **2011**, 5475–5484 (2011).
144. Tanemura, K., Suzuki, T., Nishida, Y., Satsumabayashi, K. & Horaguchi, T. A mild and efficient procedure for alpha-bromination of ketones using N-bromosuccinimide catalysed by ammonium acetate. *Chem. Commun.* 470–471 (2004).
145. Carver, T. J., Rutherford, K. M., Berriman, M., Rajandream, M.-A., Barrell, B. G. & Parkhill, J. ACT: the Artemis comparison tool. *Bioinformatics* **21**, 3422–3423 (2005).

References

146. McWilliam, H., Li, W., Uludag, M., Squizzato, S., Park, Y. M., Buso, N., Cowley, A. P. & Lopez, R. Analysis Tool Web Services from the EMBL-EBI. *Nucleic Acids Res.* **41**, W597-600 (2013).
147. Kelley, L. A. & Sternberg, M. J. E. Protein structure prediction on the Web: a case study using the Phyre server. *Nat. Protoc.* **4**, 363–371 (2009).
148. Niwa, H. & Umehara, T. Structural insight into inhibitors of flavin adenine dinucleotide-dependent lysine demethylases. *Epigenetics* **12**, 340–352 (2017).
149. Couturier, M., Bhalara, H., Salmond, G. P. C. & Leeper, F. J. Mutasythesis of novel prodiginines derived from the antibiotic prodigiosin by exploiting substrate specificity of H₂MAP oxidases PigB and HapB. *Access Microbiol.* **1**, 318 (2019).
150. Slater, H., Crow, M., Everson, L. & Salmond, G. P. C. Phosphate availability regulates biosynthesis of two antibiotics, prodigiosin and carbapenem, in *Serratia* via both quorum-sensing-dependent and -independent pathways. *Mol. Microbiol.* **47**, 303–320 (2008).
151. DeBerardinis, A. M., Turlington, M., Ko, J., Sole, L. & Pu, L. Facile Synthesis of a Family of H8 BINOL-Amine Compounds and Catalytic Asymmetric Arylzinc Addition to Aldehydes. *J. Org. Chem.* **75**, 2836–2850 (2010).
152. Cossy, J. & Pale-Grosdemange, C. A convenient synthesis of amides from carboxylic acids and primary amines. *Tetrahedron Lett.* **30**, 2771–2774 (1989).
153. Bolotin, A., Quinquis, B., Sorokin, A. & Ehrlich, S. D. Clustered regularly interspaced short palindrome repeats (CRISPRs) have spacers of extrachromosomal origin. *Microbiology* **151**, 2551–2561 (2005).
154. Evans, T. J., Crow, M. A., Williamson, N. R., Orme, W., Thomson, N. R., Komitopoulou, E. & Salmond, G. P. C. Characterization of a broad-host-range flagellum-dependent phage that mediates high-efficiency generalized transduction in, and between, *Serratia* and *Pantoea*. *Microbiology* **156**, 240–247 (2010).
155. Bainton, N. J., Stead, P., Chhabra, S. R., Bycroft, B. W., Salmond, G. P. C., Stewart, G. S. A. B. & Williams, P. N-(3-oxohexanoyl)-l-homoserine lactone regulates carbapenem antibiotic production in *Erwinia carotovora*. *Biochem. J.* **288**, 997–1004 (1992).
156. Sumathi, C., MohanaPriya, D., Swarnalatha, S., Dinesh, M. G. & Sekaran, G. Production of prodigiosin using tannery fleshing and evaluating its pharmacological effects. *ScientificWorld Journal.* **2014**, 290327 (2014).

References

157. Lin, P. Bin, Shen, J., Ou, P. Y., Liu, L. Y., Chen, Z. Y., Chu, F. J., Wang, J. & Jin, X. B. Prodigiosin isolated from *Serratia marcescens* in the *Periplaneta americana* gut and its apoptosis-inducing activity in HeLa cells. *Oncol. Rep.* **41**, 3377–3385 (2019).
158. Herrero, M., de Lorenzo, V. & Timmis, K. N. Transposon vectors containing non-antibiotic resistance selection markers for cloning and stable chromosomal insertion of foreign genes in gram-negative bacteria. *J. Bacteriol.* **172**, 6557–67 (1990).
159. de Lorenzo, V., Herrero, M., Jakubzik, U. & Timmis, K. N. Mini-Tn5 transposon derivatives for insertion mutagenesis, promoter probing, and chromosomal insertion of cloned DNA in gram-negative eubacteria. *J. Bacteriol.* **172**, 6568–72 (1990).
160. Oliveira, B. L., Guo, Z., Boutureira, O., Guerreiro, A., Jiménez-Osés, G. & Bernardes, G. J. L. A Minimal, Unstrained S-Allyl Handle for Pre-Targeting Diels–Alder Bioorthogonal Labeling in Live Cells. *Angew. Chemie - Int. Ed.* (2016).
161. Wheeldon, I., Minter, S. D., Banta, S., Barton, S. C., Atanassov, P. Sigman, M. Substrate channelling as an approach to cascade reactions. *Nat. Chem.* **8**, 299–309 (2016).
162. Manjasetty, B. A., Powlowski, J. & Vrielink, A. Crystal structure of a bifunctional aldolase-dehydrogenase: sequestering a reactive and volatile intermediate. *Proc. Natl. Acad. Sci. U. S. A.* **100**, 6992–7 (2003).
163. Wu, F. & Minter, S. Krebs Cycle Metabolon: Structural Evidence of Substrate Channeling Revealed by Cross-Linking and Mass Spectrometry. *Angew. Chem. Int. Ed.* **54**, 1851–1854 (2015).
164. Smith, S. & Tsai, S.-C. The type I fatty acid and polyketide synthases: a tale of two megasynthases. *Nat. Prod. Rep.* **24**, 1041–72 (2007).
165. Mullaney, M. W., McClure, R. A., Robey, M. T., Kelleher, N. L. & Thomson, R. J. Natural products from thioester reductase containing biosynthetic pathways. *Nat. Prod. Rep.* **35**, 847–878 (2018).
166. Awodi, U. R., Ronan, J. L., Masschelein, J., de los Santos, E. L. C. & Challis, G. L. Thioester reduction and aldehyde transamination are universal steps in actinobacterial polyketide alkaloid biosynthesis. *Chem. Sci.* **8**, 411–415 (2017).
167. Chhabra, A., Haque, A. S., Pal, R. K., Goyal, A., Rai, R., Joshi, S., Panjikar, S., Pasha, S., Sankaranarayanan, R. & Gokhale, R. S. Nonprocessive [2 + 2]e⁻ off-loading reductase domains from mycobacterial nonribosomal peptide synthetases. *Proc. Natl. Acad. Sci. U.*

References

- S. A. **109**, 5681–6 (2012).
168. Gahlloth, D., Dunstan, M. S., Quaglia, D., Klumbys, E., Lockhart-Cairns, M. P., Hill, A. M., Derrington, S. R., Scrutton, N. S., Turner, N. J. & Leys, D. Structures of carboxylic acid reductase reveal domain dynamics underlying catalysis. *Nat. Chem. Biol.* **13**, 975–981 (2017).
169. LoPachin, R. M. & Gavin, T. Molecular Mechanisms of Aldehyde Toxicity: A Chemical Perspective. *Chem. Res. Toxicol.* **27**, 1081–1091 (2014).
170. Lopachin, R. M., Geohagen, B. C. & Gavin, T. Synaptosomal toxicity and nucleophilic targets of 4-hydroxy-2-nonenal. *Toxicol. Sci.* (2009).
171. Zhang, L., Gavin, T., DeCaprio, A. P. & LoPachin, R. M. γ -Diketone Axonopathy: Analyses of Cytoskeletal Motors and Highways in CNS Myelinated Axons. *Toxicol. Sci.* **117**, 180–189 (2010).
172. Lu, K., Collins, L. B., Ru, H., Bermudez, E. & Swenberg, J. A. Distribution of DNA adducts caused by inhaled formaldehyde is consistent with induction of nasal carcinoma but not leukemia. *Toxicol. Sci.* (2010).
173. Kehrer, J. P. The Molecular Effects of Acrolein. *Toxicol. Sci.* **57**, 6–15 (2000).
174. Esterbauer, H., Schaur, R. J. & Zollner, H. Chemistry and biochemistry of 4-hydroxynonenal, malonaldehyde and related aldehydes. *Free Radic. Biol. Med.* **11**, 81–128 (1991).
175. Ahmed Laskar, A. & Younus, H. Aldehyde toxicity and metabolism: the role of aldehyde dehydrogenases in detoxification, drug resistance and carcinogenesis. *Drug Metab. Rev.* **51**, 42–64 (2019).
176. Altschul, S. F., Gish, W., Miller, W., Myers, E. W. & Lipman, D. J. Basic local alignment search tool. *J. Mol. Biol.* **215**, 403–410 (1990).
177. Schirmer, A., Rude, M. A., Li, X., Popova, E. & del Cardayre, S. B. Microbial Biosynthesis of Alkanes. *Science (80)*. **329**, 559–562 (2010).
178. Cha, H. J., Jeong, J.-H., Rojviriyaya, C. & Kim, Y.-G. Structure of Putrescine Aminotransferase from *Escherichia coli* Provides Insights into the Substrate Specificity among Class III Aminotransferases. *PLoS One* **9**, e113212 (2014).
179. Moser, J., Schubert, W. D., Beier, V., Bringemeier, I., Jahn, D. & Heinz, D. W. V-shaped

References

- structure of glutamyl-tRNA reductase, the first enzyme of tRNA-dependent tetrapyrrole biosynthesis. *EMBO J.* **20**, 6583–6590 (2001).
180. Wass, M. N., Kelley, L. A. & Sternberg, M. J. E. 3DLigandSite: Predicting ligand-binding sites using similar structures. *Nucleic Acids Res.* (2010).
181. Raach, A. & Reiser, O. Sodium Chlorite-Hydrogen Peroxide — A Mild and Selective Reagent for the Oxidation of Aldehydes to Carboxylic Acids. *J. für Prakt. Chemie* **342**, 605–608 (2000).
182. Huang, Y.-T., Lu, S.-Y., Yi, C.-L. & Lee, C.-F. Iron-catalyzed synthesis of thioesters from thiols and aldehydes in water. *J. Org. Chem.* **79**, 4561–8 (2014).
183. Poon, P. S., Banerjee, A. K. & Laya, M. S. Advances in the Krapcho decarboxylation. *J. Chem. Res.* **35**, 67–73 (2011).
184. Chandrasekhar, S., Kumar, M. S. & Muralidhar, B. One pot conversion of carboxylic acids to aldehydes with DIBAL-H. *Tetrahedron Lett.* **39**, 909–910 (1998).
185. Vogel, A. I., Furniss, B. S. & Vogel, A. I. *Vogel's Textbook of practical organic chemistry.* (Longman Scientific & Technical, 1989).
186. Uyeda, C. & Jacobsen, E. N. Enantioselective Claisen rearrangements with a hydrogen-bond donor catalyst. *J. Am. Chem. Soc.* **130**, 9228–9229 (2008).
187. Eckelmann, D., Spitteller, M. & Kusari, S. Spatial-temporal profiling of prodiginines and serratamolides produced by endophytic *Serratia marcescens* harbored in *Maytenus serrata*. *Sci. Rep.* **8**, 5283 (2018).
188. Monson, R., Smith, D. S., Matilla, M. A., Roberts, K., Richardson, E., Drew, A., Williamson, N., Ramsay, J., Welch, M. & Salmond, G. P. C. A Plasmid-Transposon Hybrid Mutagenesis System Effective in a Broad Range of *Enterobacteria*. *Front. Microbiol.* **6**, 1442 (2015).
189. Henrici, R. C., Pecen, T. J., Johnston, J. L. & Tan, S. The pPSU Plasmids for Generating DNA Molecular Weight Markers. *Sci. Rep.* **7**, 2438 (2017).
190. Vince, A., Dawson, A. M., Park, N. & O'Grady, F. Ammonia production by intestinal bacteria. *Gut* **14**, 171–7 (1973).
191. Kelly, S. M., Jess, T. J. & Price, N. C. How to study proteins by circular dichroism. *Biochim. Biophys. Acta - Proteins Proteomics* **1751**, 119–139 (2005).

References

192. Sreerama, N., Venyaminov, S. Y. U. & Woody, R. W. Estimation of the number of α -helical and β -strand segments in proteins using circular dichroism spectroscopy. *Protein Sci.* **8**, 370–380 (2008).
193. Andrade, M. A., Chacón, P., Merelo, J. J. & Morán, F. Evaluation of secondary structure of proteins from UV circular dichroism spectra using an unsupervised learning neural network. *Protein Eng. Des. Sel.* **6**, 383–390 (1993).
194. van Stokkum, I. H. M., Spoelder, H. J. W., Bloemendal, M., van Grondelle, R. & Groen, F. C. A. Estimation of protein secondary structure and error analysis from circular dichroism spectra. *Anal. Biochem.* **191**, 110–118 (1990).
195. Sreerama, N. & Woody, R. W. A Self-Consistent Method for the Analysis of Protein Secondary Structure from Circular Dichroism. *Anal. Biochem.* **209**, 32–44 (1993).
196. Nicotinamide adenine dinucleotide - Wikipedia.
197. Kim, H. R. H. R., Rho, H. W. H. W., Park, J. W. J. W., Park, B. H. B. H., Kim, J. S. J. S. & Lee, M. W. M. W. Assay of Ornithine Aminotransferase with Ninhydrin. *Anal. Biochem.* **223**, 205–207 (1994).
198. Bycroft, B. W., Maslen, C., Box, S. J., Brown, A. G. & Tyler, J. W. The isolation and characterisation of (3R,5R)- and (3S,5R)-carbapenam-3- carboxylic acid from *Serratia* and *Erwinia* species and their putative biosynthetic role. *J. Chem. Soc. Chem. Commun.* **0**, 1623–1625 (1987).
199. Grant, S. G., Jessee, J., Bloom, F. R. & Hanahan, D. Differential plasmid rescue from transgenic mouse DNAs into *Escherichia coli* methylation-restriction mutants. *Proc. Natl. Acad. Sci.* **87**, 4645–4649 (1990).
200. Studier, F. W. & Moffatt, B. A. Use of bacteriophage T7 RNA polymerase to direct selective high-level expression of cloned genes. *J. Mol. Biol.* **189**, 113–30 (1986).
201. Ramsay, J. P., Williamson, N. R., Spring, D. R. & Salmond, G. P. C. A quorum-sensing molecule acts as a morphogen controlling gas vesicle organelle biogenesis and adaptive flotation in an enterobacterium. *Proc. Natl. Acad. Sci. U. S. A.* **108**, 14932–7 (2011).
202. Takebe, I., Singer, H. J., Wise, E. M. & Park, J. T. *Staphylococcus aureus* H autolytic activity: general properties. *J. Bacteriol.* **102**, 14–9 (1970).

Appendix

1. Bioinformatic of PigE

1.1 Phyre alignment

```

>PigE          1      MKFGFIAHPTSVGLKRYVKMIDLLQRNSTELHSGYKRDLRRENLVPFMNFAKITSATGA
>UniRef50_Q2S9J6 1      MKFGFIGHPTSIGLKRYVKMLDLLDRSSRDQVGYQRDIWHRNLVFFVDFGRIQSPAGV
>UniRef50_A4FH75 1      MKFGFLAHPVNTGQRNYVRAAALLSSMADERTGRAPSGAARHT--VPMPMFGTVVVSATGH
>UniRef50_Q2LW66 1      -----

>PigE          61     TCEGVIKYMPLVADEMLADARGIANRVVSGIEELVEDGAELVGLGGFTSIVGRRGEATAE
>UniRef50_Q2S9J6 61     SCEGIVHYLPLTAEEMLSTPRAVQQRIFEGIESLQAQGAQLVGLGGFTS IIGKRGLVTAE
>UniRef50_A4FH75 61     RCEGDLRYPHTAEDLLRRATDAVDHVVAQVEDLRRAGAQLVGLGGATSIVGNRGLTTQR
>UniRef50_Q2LW66 61     -----

>PigE          121    KSPVPVTSGNSLTTYAGYKALMQIQSWLDIQPEQEPVAIVGYPGSICLALSRLLLAQGFS
>UniRef50_Q2S9J6 121    RAGIPVTSGNSLTTYAGYTVLLQTLERLQLDPADAQVAIVGYPGSICLALAKLLLQLGCR
>UniRef50_A4FH75 121    RVDVPLTSGNSLTTYSAHELLRVTIARLGRRPSDVEVGIVGFPGAIGLAMARLLDDGCR
>UniRef50_Q2LW66 121    -----

>PigE          181    LHLHRAGHKDEDELLSHLPEQYRSRVTLTSDPEDLYPRCKLFVAATSAGGVIDPYKLQP
>UniRef50_Q2S9J6 181    LDLVHRGTADDAQLL-EHLPEHWRSRVTLNLSMDAAYERNRFAAATSSGGVIDVSR LAP
>UniRef50_A4FH75 181    LHLVHRKGRMRPEQLLDELPAAAHDRVTIGDDVAECLRRLRIVAASSAGGLIDCDDL RP
>UniRef50_Q2LW66 181    -----

>PigE          241    GSVFIDVALPRDINS DTRPDRDILIIDGGCVTATDAVKLGGESLNVTIKQQ LNGCMAET
>UniRef50_Q2S9J6 241    GSIVVDIALPRDAERPPTP-RTDVLVLDGGCVTAS PATKLGGESMMSIKQQINGCLAET
>UniRef50_A4FH75 241    GSVVVDVALPRDVRPRRERR-DVLVLDGGLVSASDAVVLDGM--ELATSEQINGCLAET
>UniRef50_Q2LW66 241    -----

>PigE          301    IVLALENRRENFSLGRYLALDNVLEIGELAEKHGFLVYPLASYGERIDRQRVINLKRYHY
>UniRef50_Q2S9J6 301    MVLALEGRAECFSIGRDL PPEKVLEIGEIAERHGFRAFPLASYGERINIELINGLRRFHH
>UniRef50_A4FH75 301    VVLALEERAESFSLGRELD PGRVREIGELARRHGFLPSAPSSWGRLVRLDRIDELPGWSA
>UniRef50_Q2LW66 301    -----

>PigE          361    HDIYSDEPDTEQPPASQLAFIDAI IAQDPAREDTLDRYHQFINPMMVEFLKLQHC DNVFR
>UniRef50_Q2S9J6 361    RGNAQAPGYT-----PSDLAATEPDSGEARRSQT VQRYRSYINPMLADFLQMQRCDK VFE
>UniRef50_A4FH75 361    -----ERPDPAESTRRRFRDNVNPPLAGFYAVHGM DRVFT
>UniRef50_Q2LW66 361    -----NSCSGTRMSKEGETMREDLVTRTQRLLAPSLVIHS-----DIVVK

>PigE          421    RASGTQLFTADGEAFLDMVAGYGCINLGHNPQPIIDALKAYLDAQGNFIQYIS IPEQAA
>UniRef50_Q2S9J6 421    RAEGCTLTDTDGERFLDMVSGYGCLNLGHNPQVVTEAIQKYVANMGPNFVQYVSL PEETS
>UniRef50_A4FH75 421    RSGSTLTADGVEYLDFIGGYGSLNVGHNHPAVTAAVQFLTAGEPTFVQYASIPHR TA
>UniRef50_Q2LW66 421    RGHGVYLESDVGKRYLDFTSGLAVANVGHSHPKIVEAIKKQAEELVHAGCMFY Y--EPLA

>PigE          481    KLAEVLCHFAPGNMGRVFFS NSGTEAVEAAMKLAKASTGKAGIAYLKNSYHGKTLGALS I
>UniRef50_Q2S9J6 481    KLAERLCVAPGRFERVFFS NSGTEAVEAALKLAKAASRRSRFVFANNSYHGKTLGALS V
>UniRef50_A4FH75 481    ELAERLCEIAPGMRRAFFG NSGAEAVEAALKLARAATGRTRFVHAENSYHGKTFGALS V
>UniRef50_Q2LW66 481    EYPERLKEVTPPGLDRFFF SNGAEAEIEGALKLARYFTGRQGILAFSGAFHGRTYGALS L

>PigE          541    TGREKHRRHFKPLLASMIEVPFADIEALRQTL SRDDIGALMIEPIQEGGVHVPPPGYL R
>UniRef50_Q2S9J6 541    TGREKHQKHFRPLLPGCTGVPFGDLEALRVELEQGDVCAFIIEPIQEGGVYLPDPGYL K

```

Appendix

```

>UniRef50_A4FH75      541  TGRDHYRDPFRMPVDCVGVFPGDENALREAIAG--AAAFIVEPVQEGGVVLPVPPGYLT
>UniRef50_Q2LW66     541  TSNAKYRNRYAPLLPSVYHAPYPYCYRLNRLIAPEE IACAVIEPMLGEGGYVVPARYLK

>PigE                 601  TVQEICRQTD TLLMVDEVQTGLGRTGKLFACEWEGIEPDVLMLSKSLSGGVMPIGATLCR
>UniRef50_Q2S9J6     601  AAQELCRRTG TLLIVDEIQ TGLGRTGRLFACEWEGVEPDIMVLSKSLSGGLIPIGATLSS
>UniRef50_A4FH75     601  AAQRICREAG AVFIVDEIQ TGLGRTGAMFACEHEGVEPDVLC LAKSLSGGLVPIAATLST
>UniRef50_Q2LW66     601  KLRKLCDREG ILLIFDEVQ SGMGRGTGRWFASEHFGIVPDI MTLAKGIANG-MPLSAVVSS

>PigE                 661  AIFGNGPYGT ADRFLMHSST FGGGNIAAVVALSALREILAQDLV GNAERLGT YFKQALTD
>UniRef50_Q2S9J6     661  AQIWDAAAY A TGRFLLHTS TFGGCNLAGVAGLAALEGVIEQDLPRRAQ EMDGYFKAE LQQ
>UniRef50_A4FH75     661  AEVWDAAYG SSSGSLHTS TFGGCNLSVAALATLDLIESEKLAARAEVM GRRLRDALTE
>UniRef50_Q2LW66     661  GRIMD-----GWAPGTHGTTFGGNPVSLCAA AATLRVIEEERLLENAAVVGSKALERLES

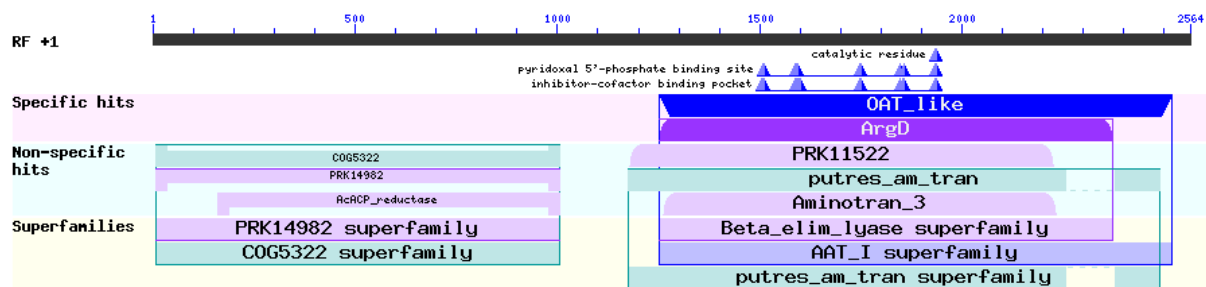
>PigE                 721  VAARYPFVAE IAGRGLMLGIQFDQTFAGAVGASAREFAT RLPGDWHTTWKFLPDPVQAHL
>UniRef50_Q2S9J6     721  AVQAYPFIK EVRGRGLMLGIQFNND FSGAVEACAREFGTRLPGDWHLAYRFFPDEVREHL
>UniRef50_A4FH75     721  ACAPFEFVGE VRGIGLMAIAFDARYD GAVRTAVEDMASRLPGDFRAIAE LLPDPVREVL
>UniRef50_Q2LW66     721  MKDRHPVIGD VRGRGLMIGVEFVREGK-----

>PigE                 781  KAAMERMEQS LGEMFCMKFVTKLCQDHNILTFITANSSTVIRIQPPLTISKAEIDRFVSA
>UniRef50_Q2S9J6     781  AAAVGKMEES LAEMFCMRFVTKLSNDHRILTFVTANSSTVIRIQPPLIISKEEVDHFVKS
>UniRef50_A4FH75     781  RQAGSSVETA LGDLLCLRFVAAAMGRDHRILTFVTANRNQVVR LQPPLVVTEAEIDRFAES
>UniRef50_Q2LW66     781  -----EPDRATVEKIMKTCLDRGLLLVECGGDKN IRLR LIPPLVITREEMDHGLDI

>PigE                 841  FATVCDDELST FLE
>UniRef50_Q2S9J6     841  FATVCEEMS----
>UniRef50_A4FH75     841  ARAVCETAT----
>UniRef50_Q2LW66     841  LEEAI-----

```

1.2 BLAST



2. Bioinformatic of PigD

```

>PigD      1      MTTMIGQTRQAGSSSYEQAWQAEQAPCPGMEPDTLTVGVVVVTRNPTFFQTGLSVLNDIR
>UniRef50_Q2S9J7  1      -----EITIGVIVVTRSRGFFETGLSVLSDIR
>UniRef50_B9KBA0  1      -----
>UniRef50_C6VV63  1      -----

>PigD      61      DYVFNRVHIQSELPLKLELASDPLYSEAREKAIHFLKNQSKALNIQVIQCASLAEATGK
>UniRef50_Q2S9J7  61      GEVFQQVSLDADIEFEEKLPSTHPVYEEARDKAVRFLGKRKERISMRVIQADSLARAQDK
>UniRef50_B9KBA0  61      -----
>UniRef50_C6VV63  61      -----

>PigD      121     I IYTHALEQQPEFQMGMLFYDQTSLGNVDDSEIKIDRDLDAFYSAMQRGGIPAFYTTTFST
>UniRef50_Q2S9J7  121     ILQAPLLGTN--FQVGMVYVDYADPQFEDLAPQQIDAQLRDFYAVLRQADIPVFQSSFST
>UniRef50_B9KBA0  121     -----
>UniRef50_C6VV63  121     -----

>PigD      181     VTFIRDVRSSFRYLPQQYREIVRSEDPAIFQTELLCLWMDFFEMNYTNRRVKPIGALALH
>UniRef50_Q2S9J7  181     VVYTLQPQRPRIRHQPMYIERQLPDDRSLLQADLLCLWMDFFEMSYANRRVKPAARVLPH
>UniRef50_B9KBA0  181     -----K
>UniRef50_C6VV63  181     -----PVVSVAKPEL

>PigD      241     NTLAEQLIQFFERTAASRWLVSYTGSIIISNLIGYLDRHAEAHGALVLRGPNEHAIACGA
>UniRef50_Q2S9J7  241     NTLGEHLINFLSARAGSEWLGIFYFTGSLVSNMINYLEQEAHRDVLVLRGPSEHSLACGA
>UniRef50_B9KBA0  241     MKGSKMLFEAFLRREGVDT--IFGIPGGAIINVYDELCNYED--KINFYLFREHQGATHAA
>UniRef50_C6VV63  241     INGSHAVIQSLIAEGVKT--IFGYPGGAIMPVYDAIYDYQDQ--IDHILVRHEQGAAHAA

>PigD      301     MANWQLYRMPFLGVVTSGMMDEFKGTLINLKETAAQGIIVAAENRNNQWYSFQGTQTPTE
>UniRef50_Q2S9J7  301     MANWQLYRRPFLIVVTSGMIDEFKGTIANLREARAQGFIVCAENRHDQWFAFQGTVSAEE
>UniRef50_B9KBA0  301     DGYARVTGKPGVVIVTSGPgtNTVTGIATAYMDSIPLVVITGQVPTSFIG---TDAFQEV
>UniRef50_C6VV63  301     EGFARISGEVGVCLVTSGPgtNLVTGIADAIIDSTPMVCIIGQVASHLLG---TDAFQET

>PigD      361     DMRDVLAAKRIPYVYIDDVDGIADGLAEVFRLYHQAGQGPVVILATQNVLESTLSLEPVPG
>UniRef50_Q2S9J7  361     DSREVIKARGLPCLYLNDVDRLQEDLQKAMELYDAKRGFPVLLATQAVLEACSRFDIAYP
>UniRef50_B9KBA0  361     DVTGITMPITKHNHLVTSIEELPYAIKEAFYVatGRPGPVVLDLDFPKDIQTAEGEFNYPDE
>UniRef50_C6VV63  361     DVMGITIPITKWNQITNADEIPEIIAKAFYIasGRPGPVLIDITKDAQ-QKLMTKPFVH

>PigD      421     DLPPVSGLPAYDCPPISDSFEQAMALINEGPEKLVWQLGPPVSDDEYALVHEIADAAGLAL
>UniRef50_Q2S9J7  421     PAPEAPSDTI--PESVQVLDQVMSLLNDGPKLVWQC GAMDEEELELTLIAERAGVAL
>UniRef50_B9KBA0  421     IEILGYKPTVKGHP---KQIKKAMELLKESKRpvIVGGGANLSGAMDLVNRFIDKFGVPA
>UniRef50_C6VV63  421     KKTETLLSYHPRVAPKEEQAAAAKLINQAKRp1FVGHGVQISGAEQELIQFIEKTDIPA

>PigD      481     VDSLAPHGSAPKYYQGKRNPYHLGTLAIYGYSPRVYNFLHTNDKLNPMSDQSVFMIKSRV
>UniRef50_Q2S9J7  481     VDSLTYPGSVPKFRHCQRNRNYLGALAVYGYSPRVYNFLHTNDKMNPPQSEQCLFFIKSKL
>UniRef50_B9KBA0  481     VSTLMGRGVNPSDER-----LYYDGI GMHGAYYGN YAV-----ANADLI IALGVRF
>UniRef50_C6VV63  481     ASTLLGLSSVSDH-----PNYVGWLG MHGNYGT-----NVL TNQCDLI IAVGMRF

>PigD      541     AQITTPFSDGRLERKVHLVQLTHDERHLSPYADLKLHMDCLTFLRAVKANLHVDAALREK
>UniRef50_Q2S9J7  541     HQVCTPFSDGRLQRKLQIVQLTDNPEHISPYTDFPLVLEHKQFLRYVDKHLAPSPELVAR
>UniRef50_B9KBA0  541     SDRILG-NPRTFTRNARIHVHDIDPAEIGKnVDVPIVGDLRNVLEEFKY--DLDTDFSE
>UniRef50_C6VV63  541     DDRVTGDLS-RYAKQAKVVHIEIDPAEIDKIvdAPVVGDAKKALELLLPLVNENNH----

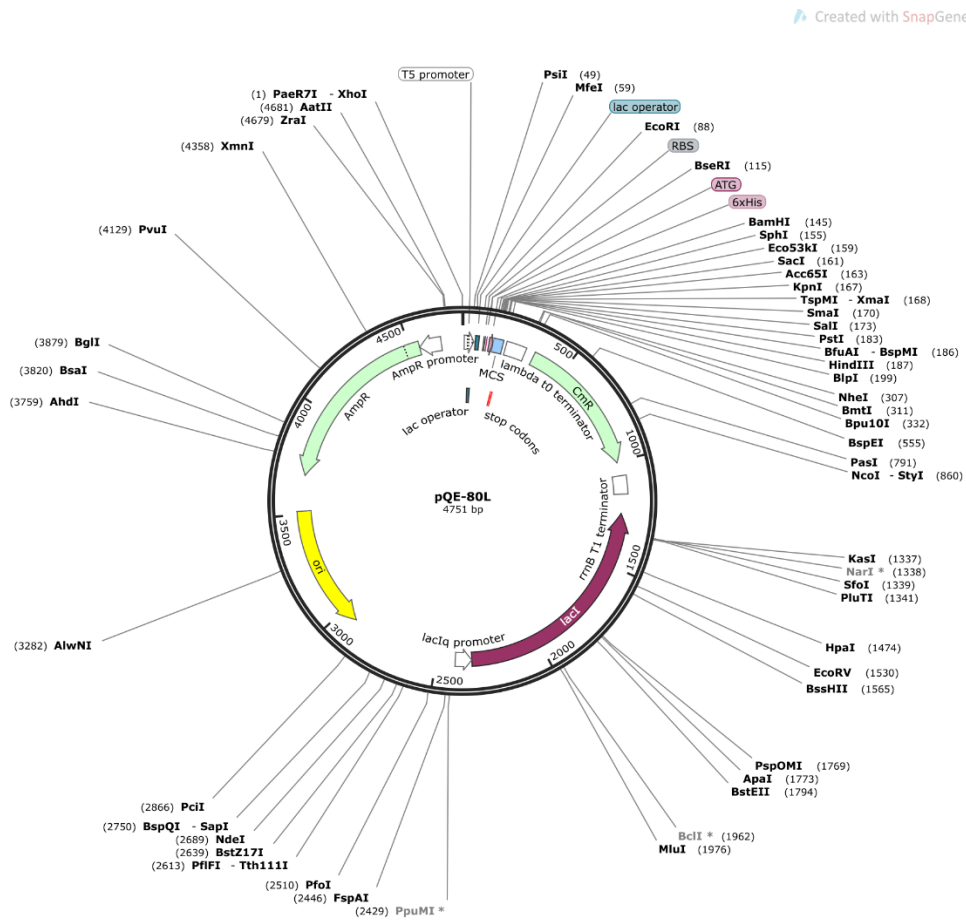
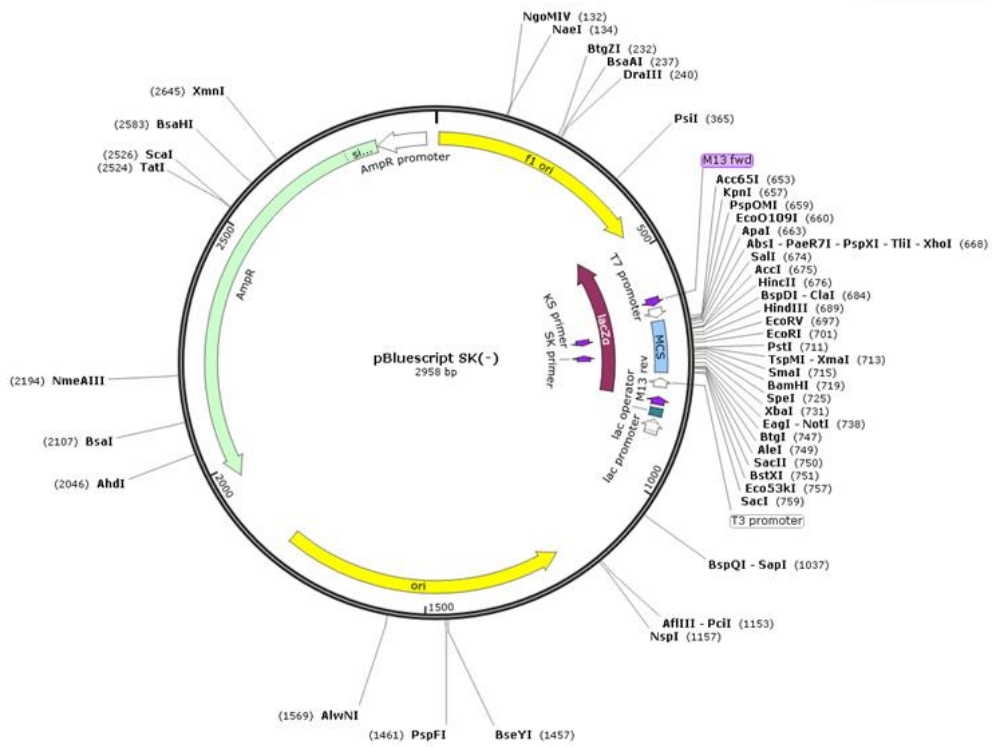
>PigD      601     RKALIAAYLDSPSDVVSQPLSPLMSANYFFCQLNRVIENLIKTFNFDFTGVYDVGRCGIS
>UniRef50_Q2S9J7  601     RYQAIASVPDPSDPMASRLPTTPMTPNYFFARLNKLMEKLIVEHGYDYTGLYDVGRCGIS
    
```

Appendix

```
>UniRef50_B9KBA0 601 WIEELQEVKKKYPLTYK-RDGKLIKPOY-----IVEKVNVEVFPDDTIIVVADVGNQMW
>UniRef50_C6VV63 601 -EAWKAEFKKYDAIEDEKITQPELAPTTEKIKMAEVIRTLSDKTKGEAVIVADVGNQMM
>PigD 661 AVRNVAKTRRGFSGWYGRALMGDALLATSylahtSPthVvAFIGDgAKGIVPDILPAFID
>UniRef50_Q2S9J7 661 AVRNLAtrRGFSGWYGRALMGDALMASISLAFTSPSNVvAFIGDgAKGLTPDVLPSLLE
>UniRef50_B9KBA0 661 VAQYYRFKHQrfLCSGGLGTMGYALPAGIGAKiaPDREVVIFAGDGGFQMNIQELMTV--
>UniRef50_C6VV63 661 TARYYQFKKpsFITSGGLGTMGYALPASFGAKvaPDREVVAMIGDGCfQMTIQELGTIAQ
>PigD 721 NILTHPQLLNKSITIFyFCNGGLSVINTYqERILFNrTSRQmRLVNVdQPafEQTVDDFH
>UniRef50_Q2S9J7 721 NALSYpGRMNRNLTIfyFCNGGHsvINTYqERILFNyTSRQmRLVNVtdQdweDELGGLR
>UniRef50_B9KBA0 721 -----KRYNLPVKIIVMDNKALGMVRQWQQLFFNCRYSATILA---DNPdFAKIAEAVG
>UniRef50_C6VV63 721 S-----GLPVKIIILNNNfLGMVRQWQQLFHqKRYs----FVELQNPdFITIAKGFg
>PigD 781 IQGKTLTHfDEdTIRHALMTPKRLNLFsvVLGHnNEGDGIsLATAKwQRDPsDREALQE
>UniRef50_Q2S9J7 781 FTsRtLTtFDpAALtsALLrPGcVnLFSvmVshNNEGDGIsLATATgWRDP----ATQP
>UniRef50_B9KBA0 781 IKAMRIEKpDerAVEE-LARSKEPMLIHAVVDPAENVLPMVPPGG-----
>UniRef50_C6VV63 781 INGHTCSKRedaSLDTMLA-SDKPYLLEVIVEKEENVfPMVPTGA-----
>PigD 841 RKDWAARQPESTSTSFdQGQnKEAIS
>UniRef50_Q2S9J7 841 QAEAKAQATATGTDtETDK-----
>UniRef50_B9KBA0 841 -----
>UniRef50_C6VV63 841 -----
```

Appendix

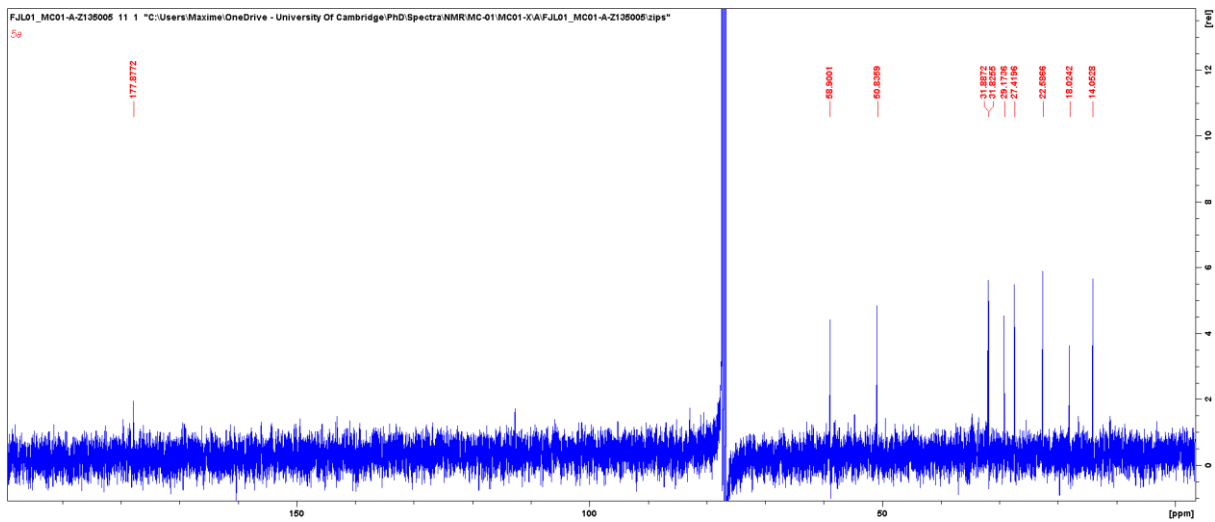
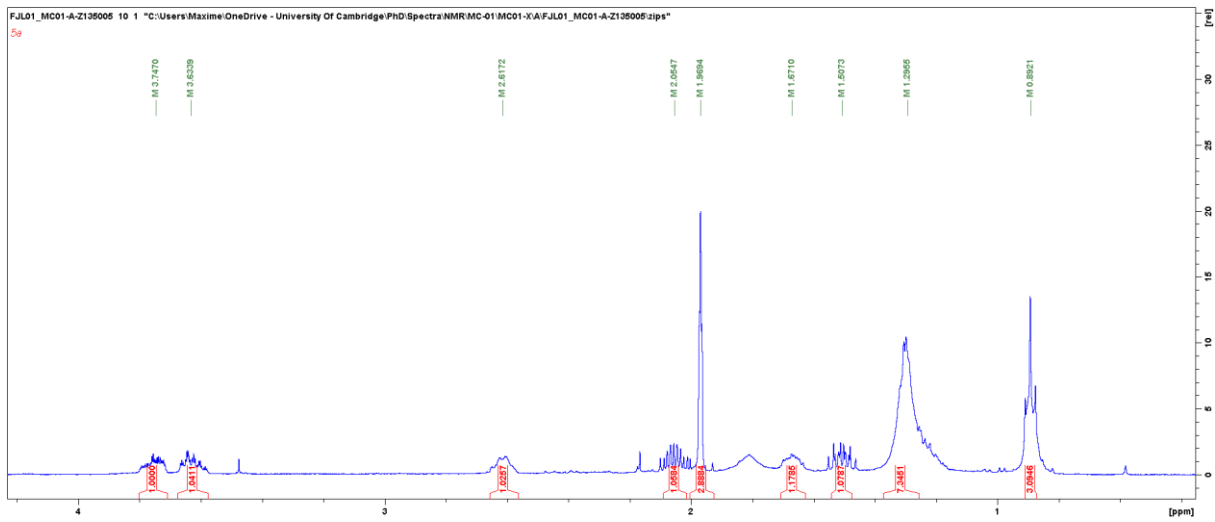
3. Vector sequences



Appendix

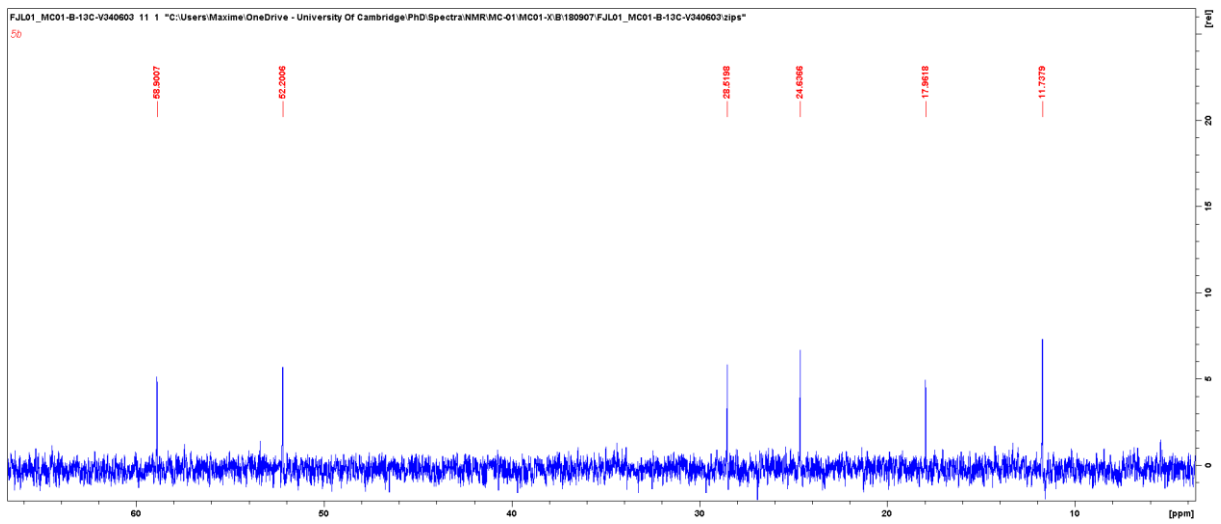
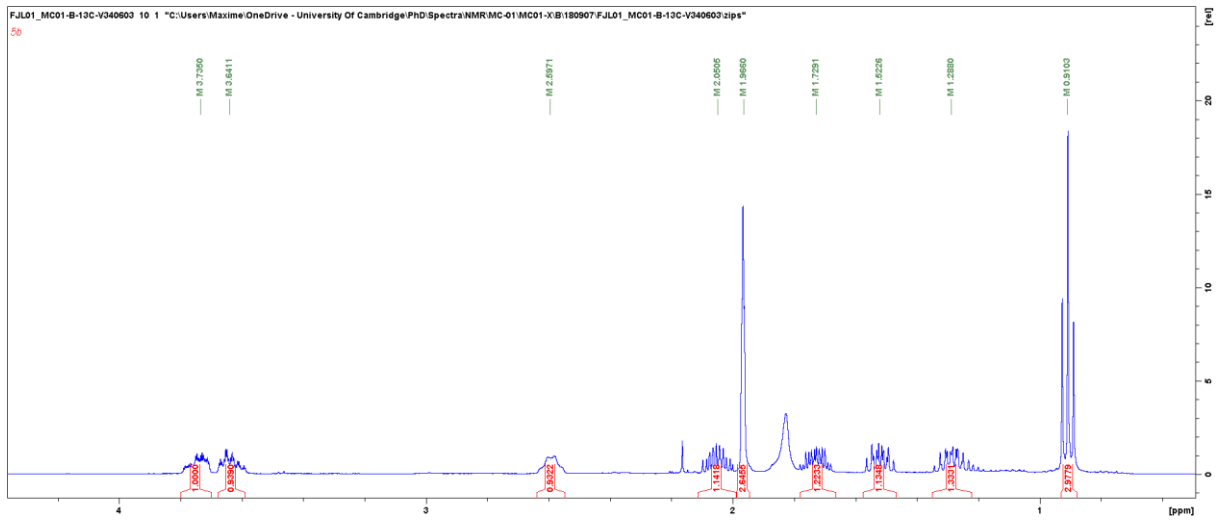
4. NMR Spectras

19a



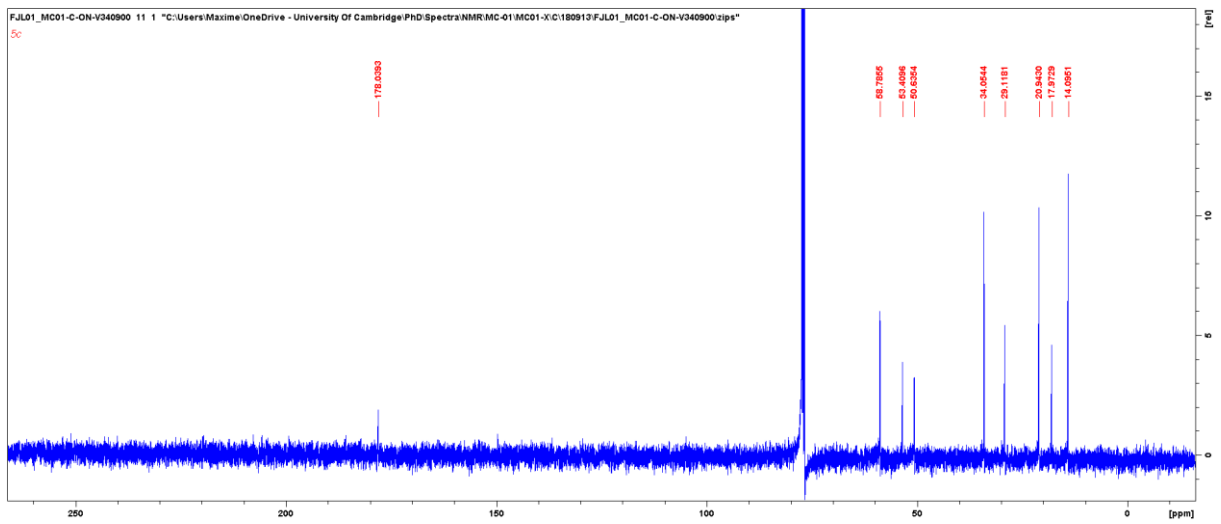
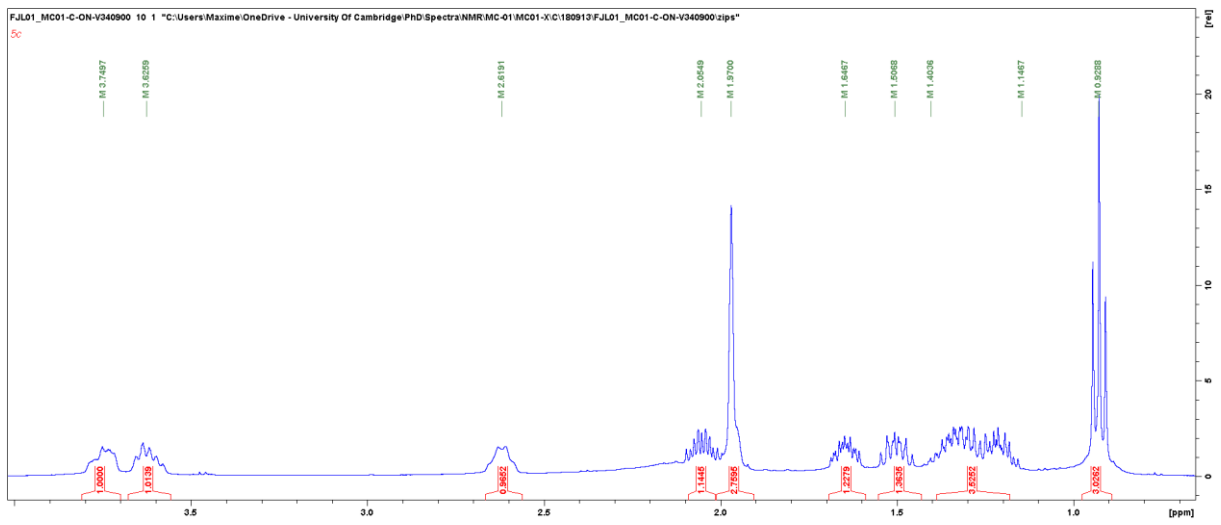
Appendix

19b



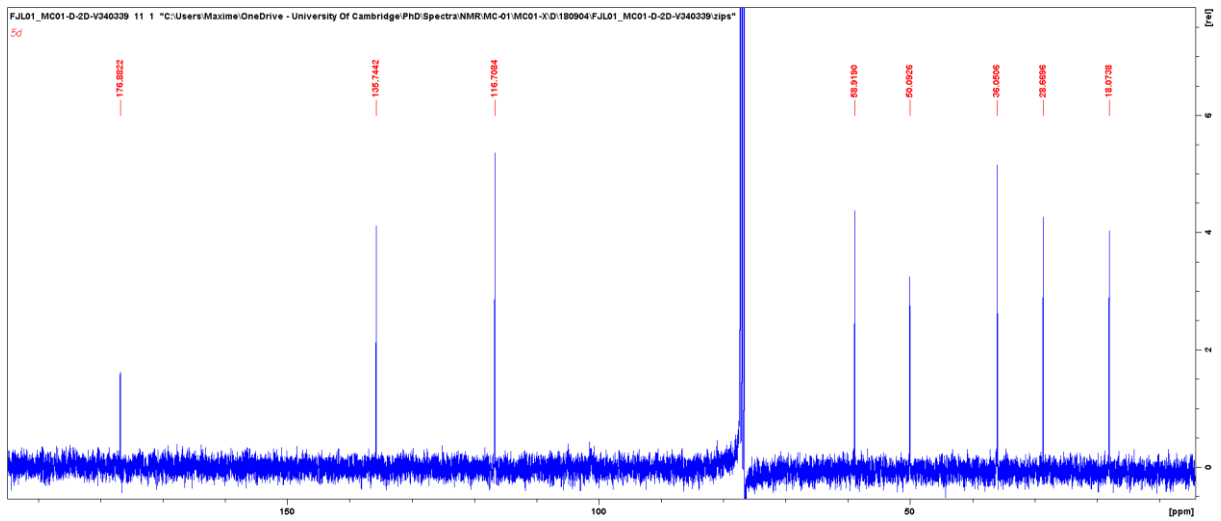
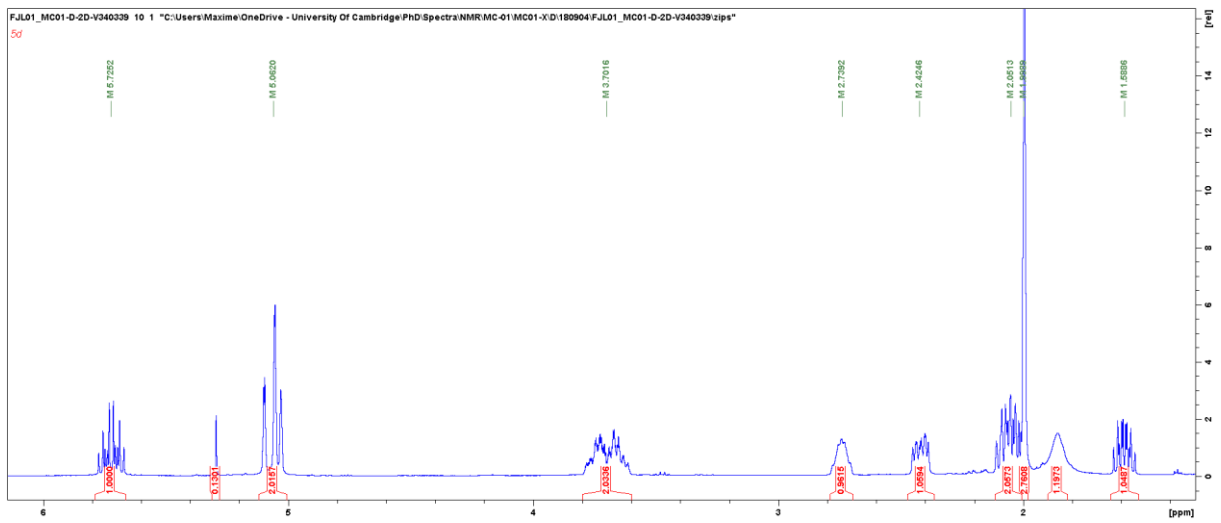
Appendix

19c



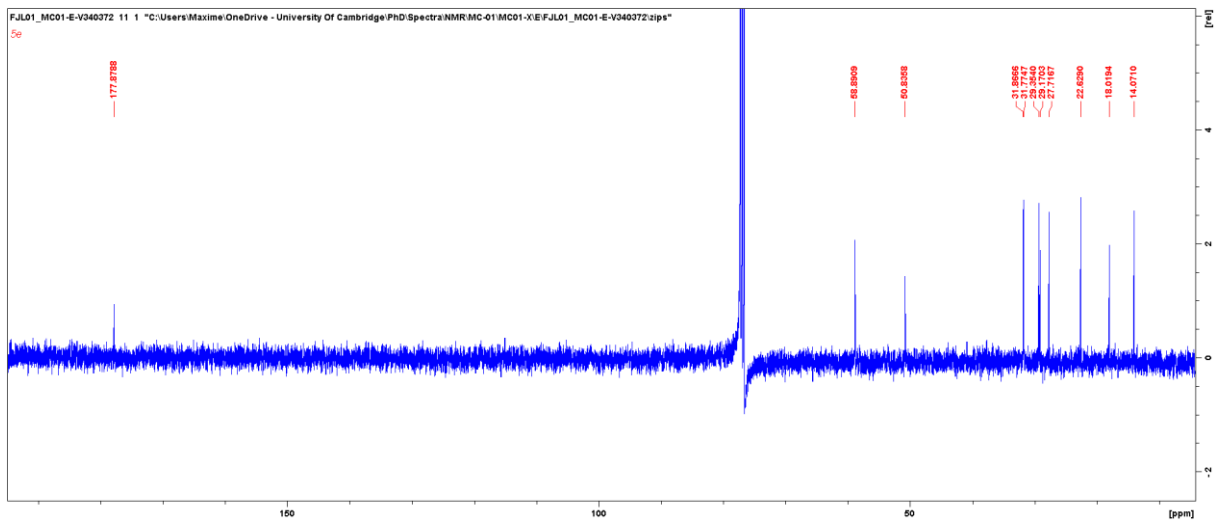
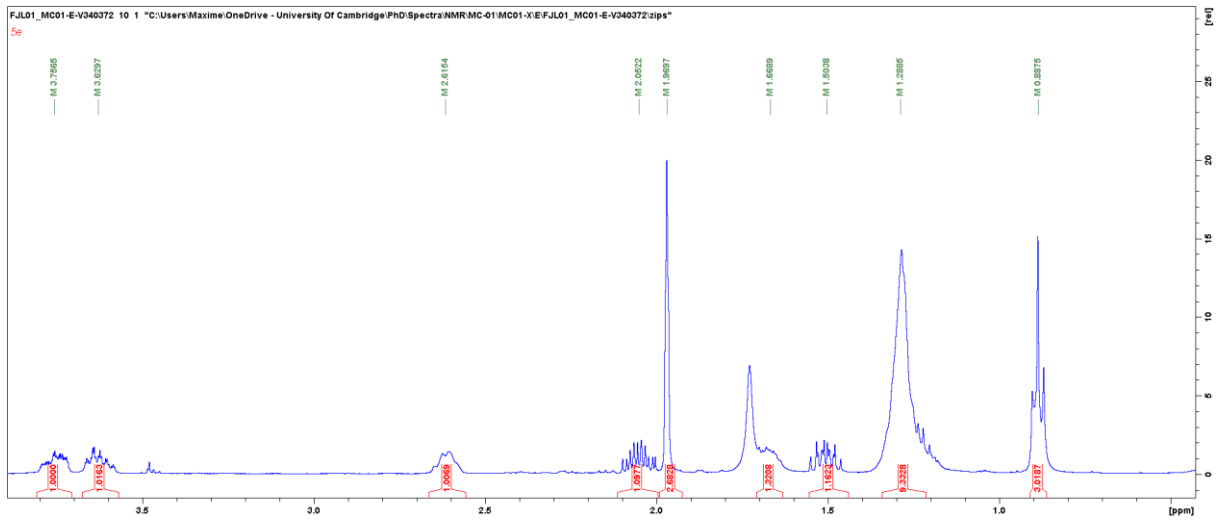
Appendix

19d

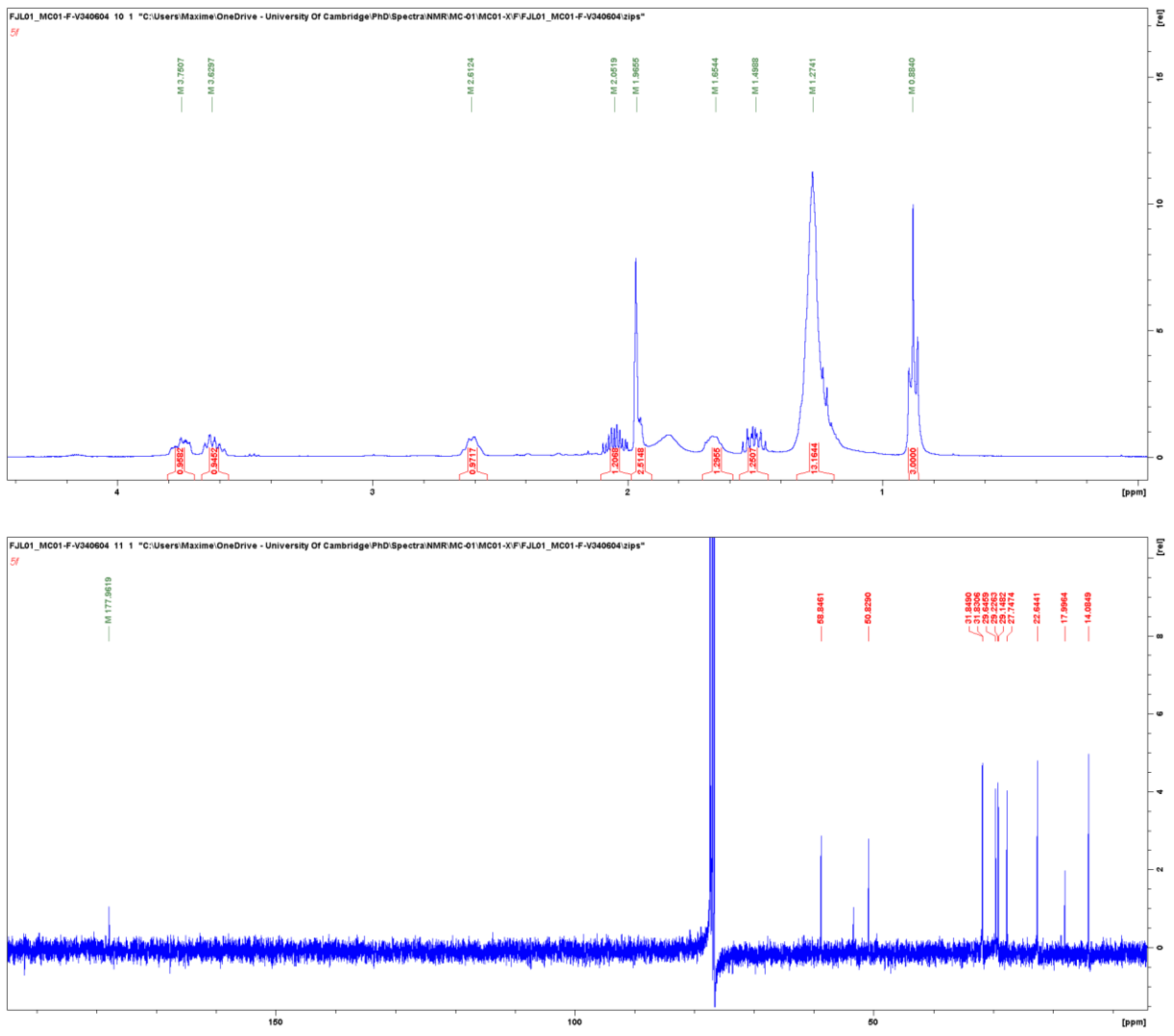


Appendix

19e

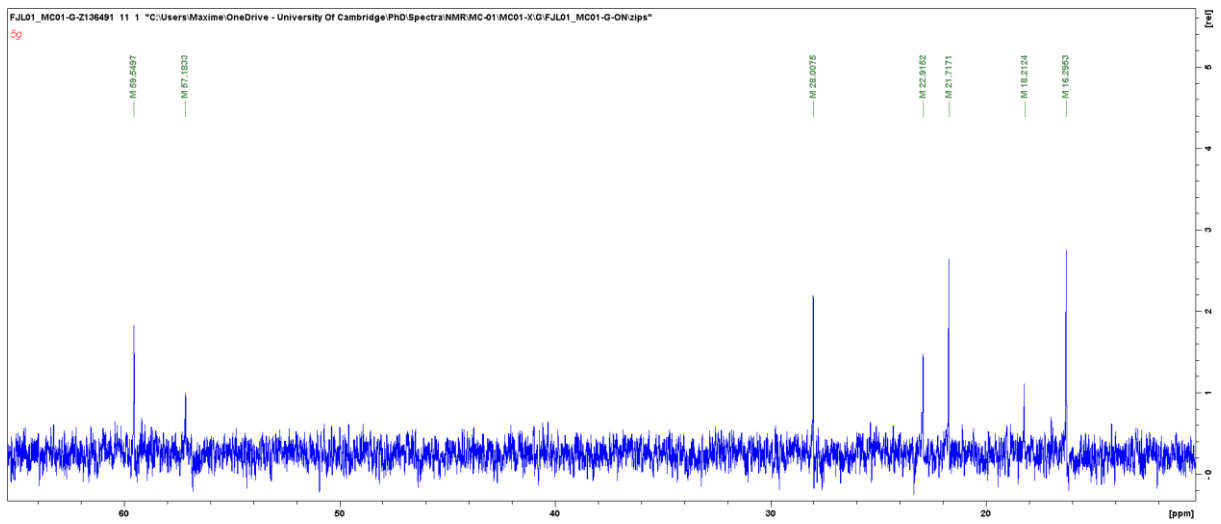
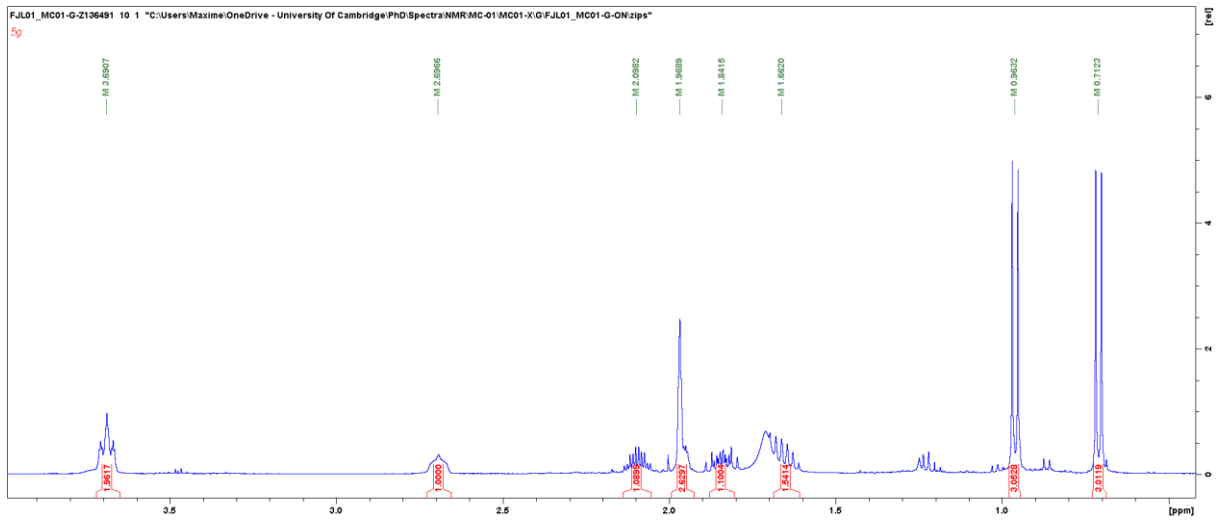


19f



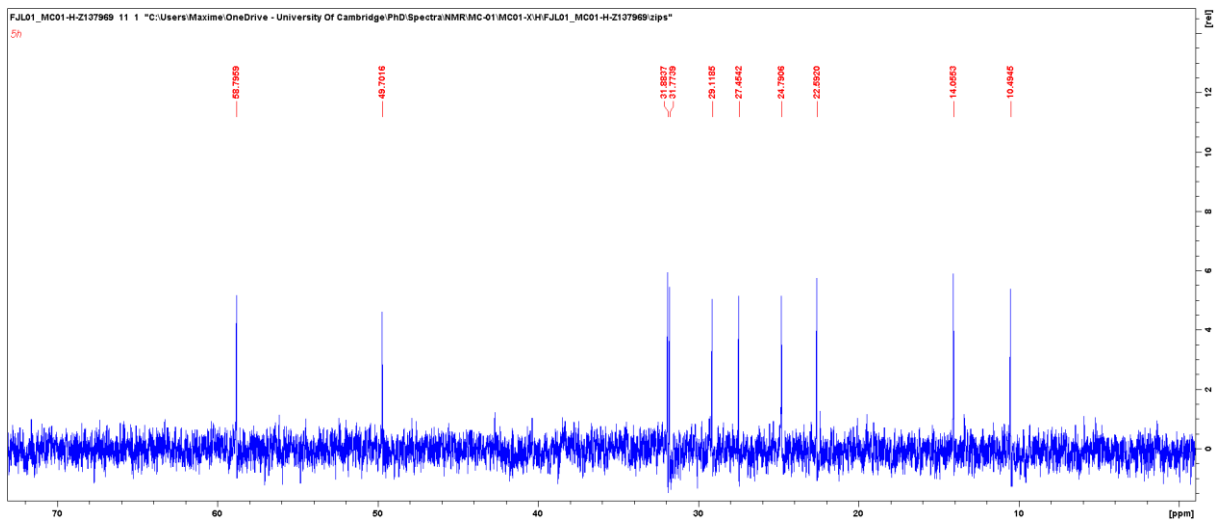
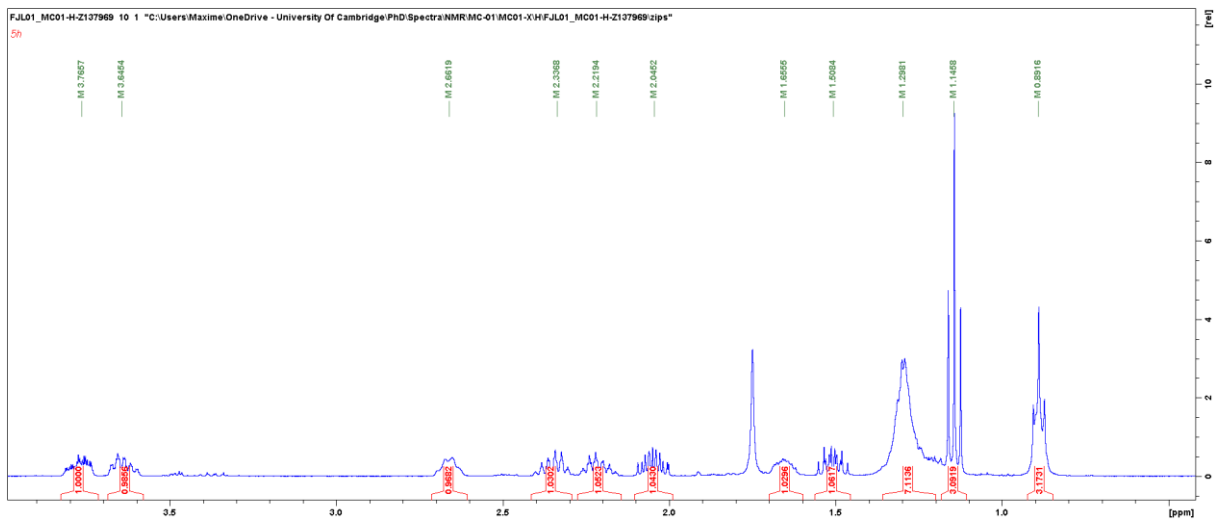
Appendix

19g



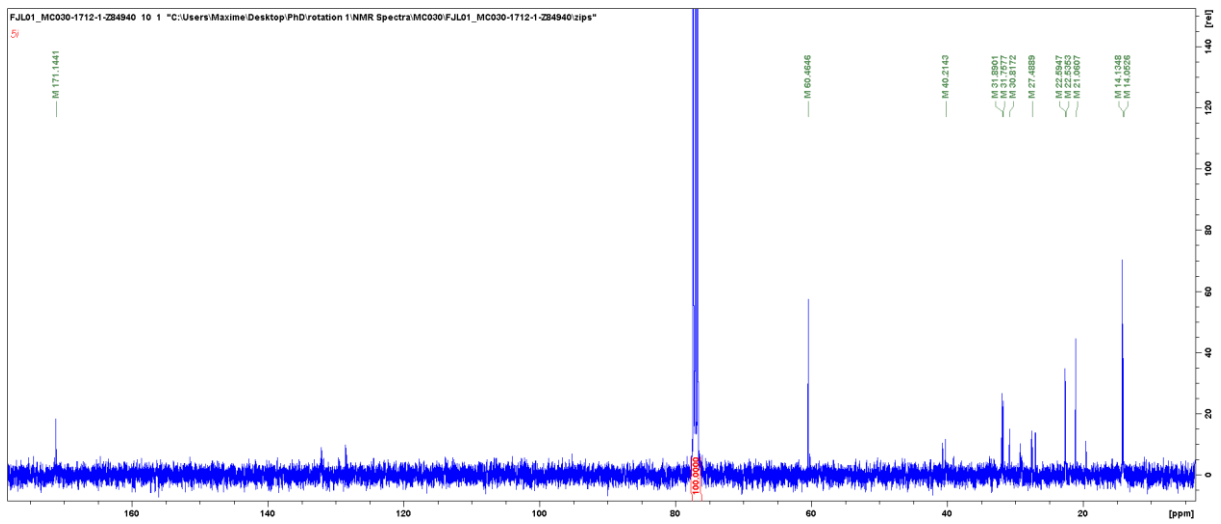
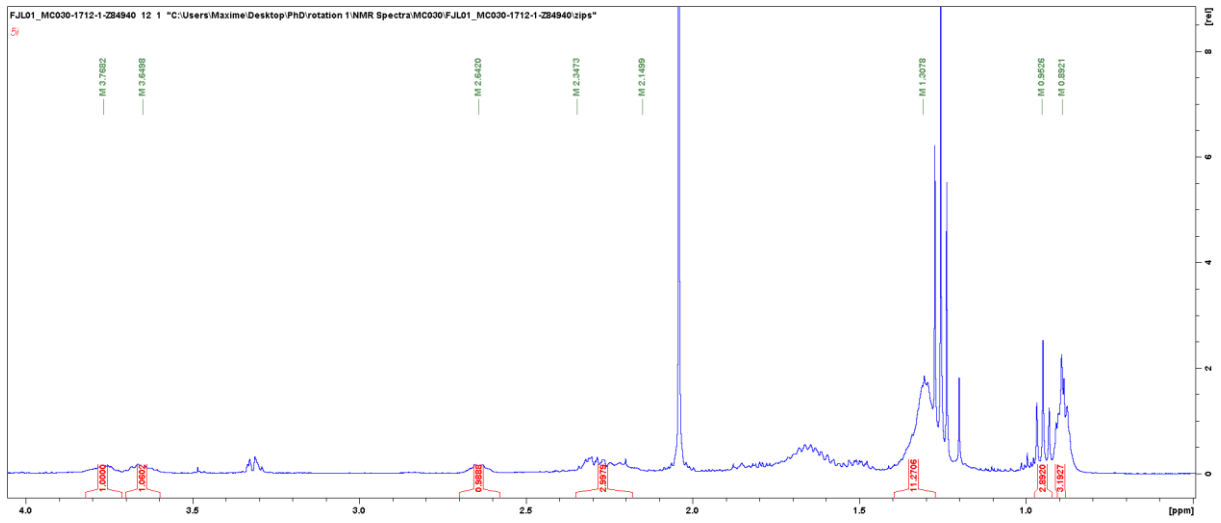
Appendix

19h



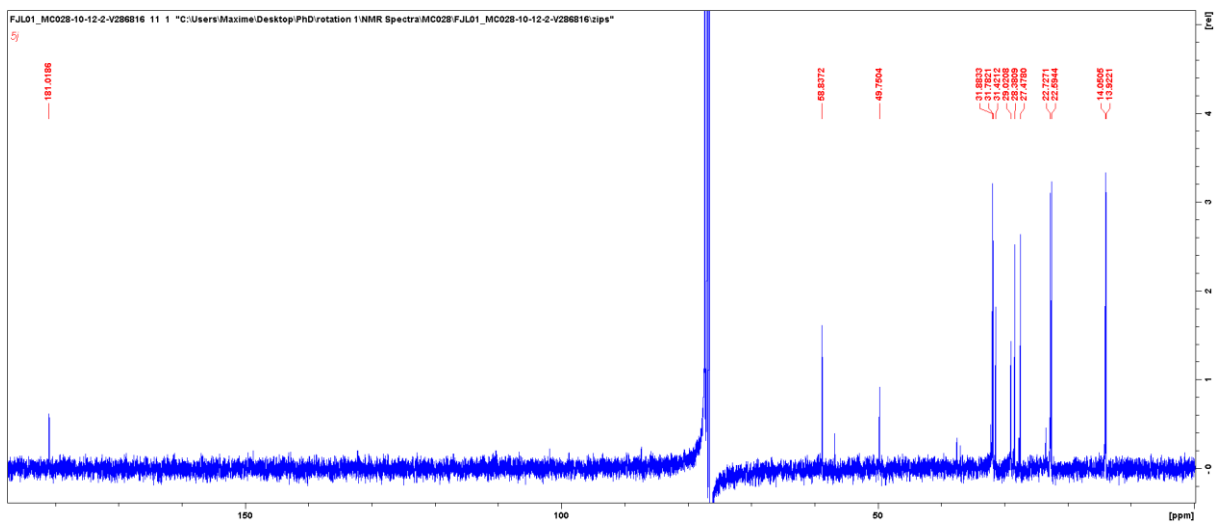
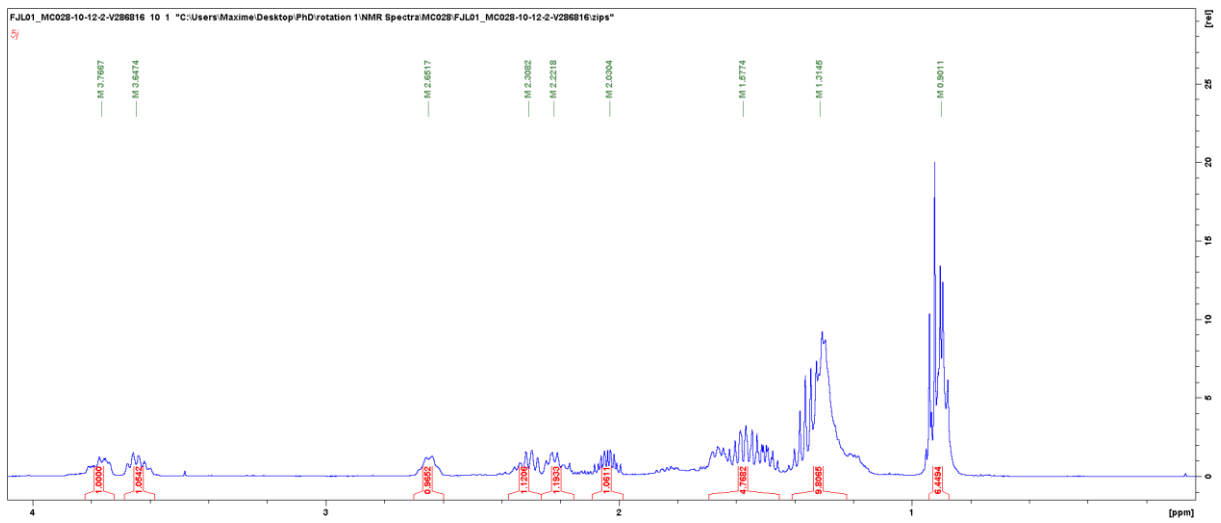
Appendix

19i



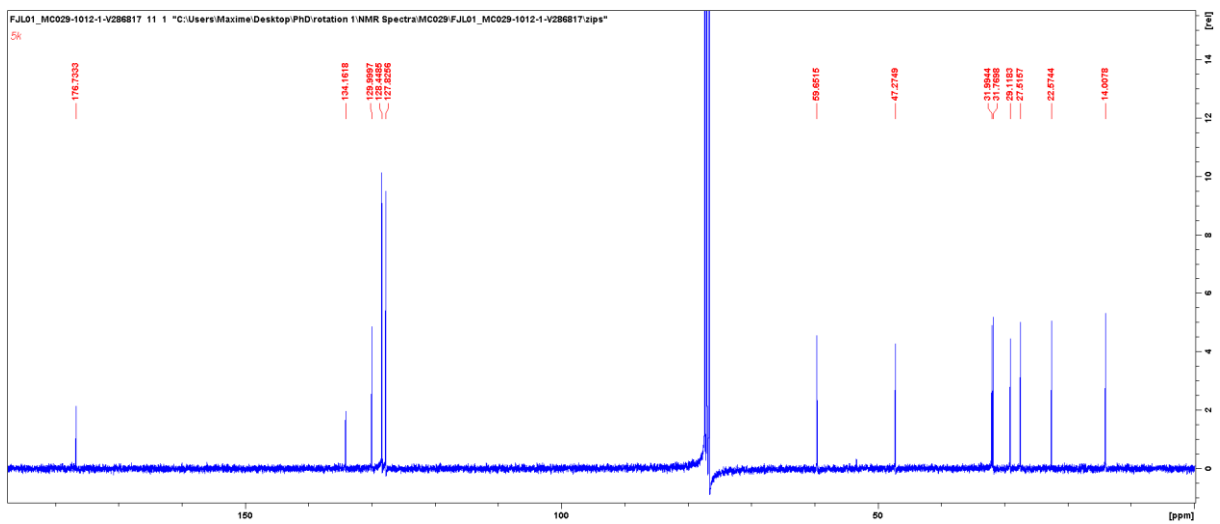
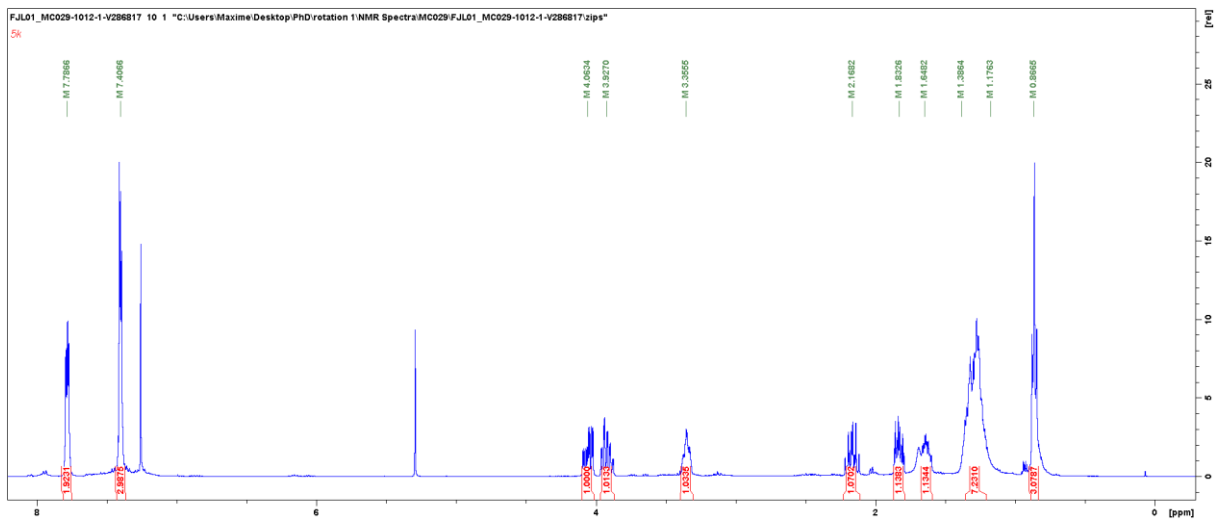
Appendix

19j



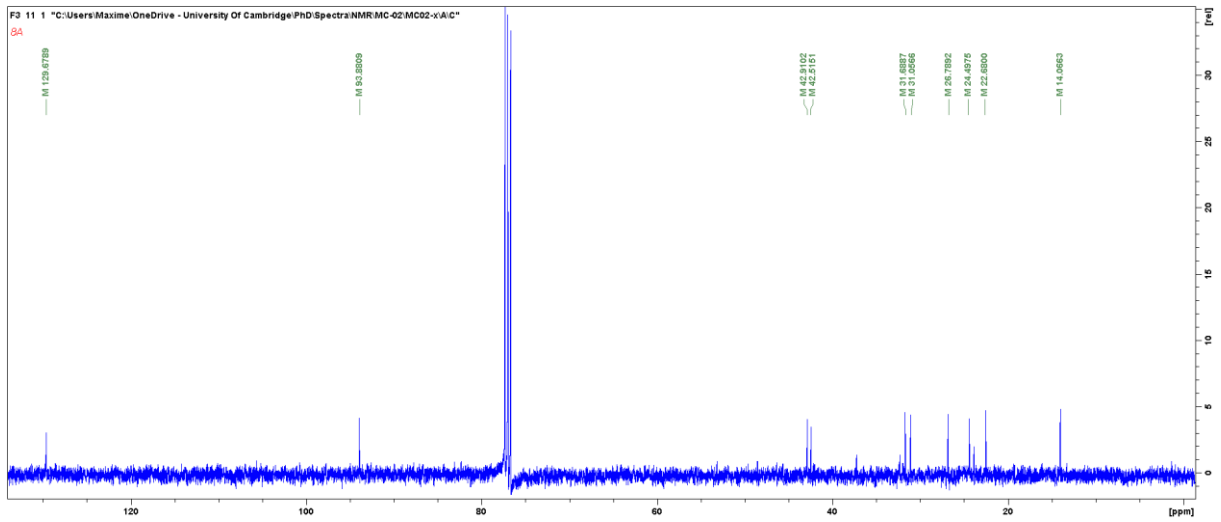
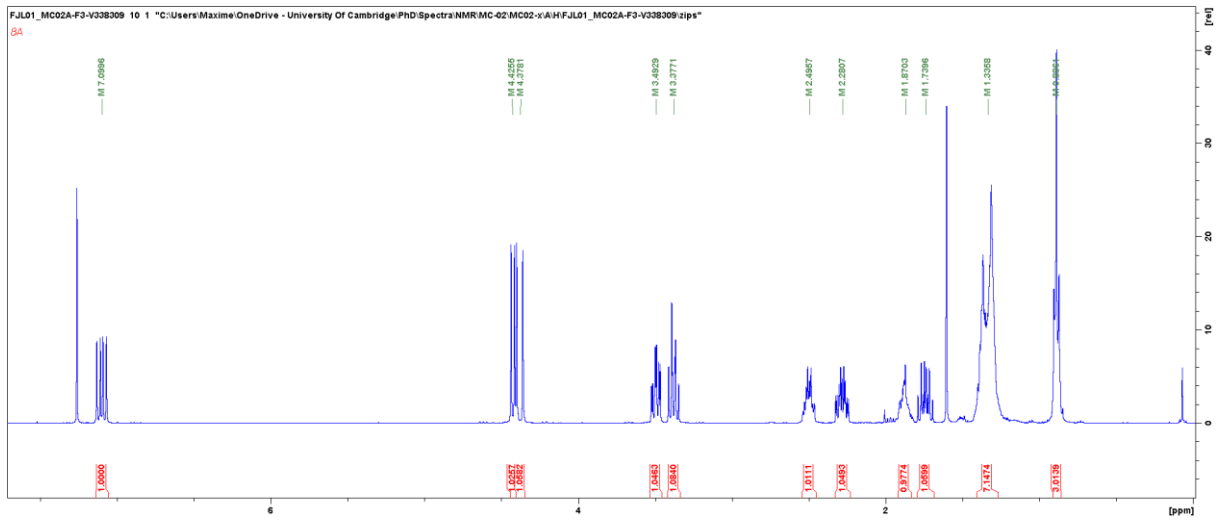
Appendix

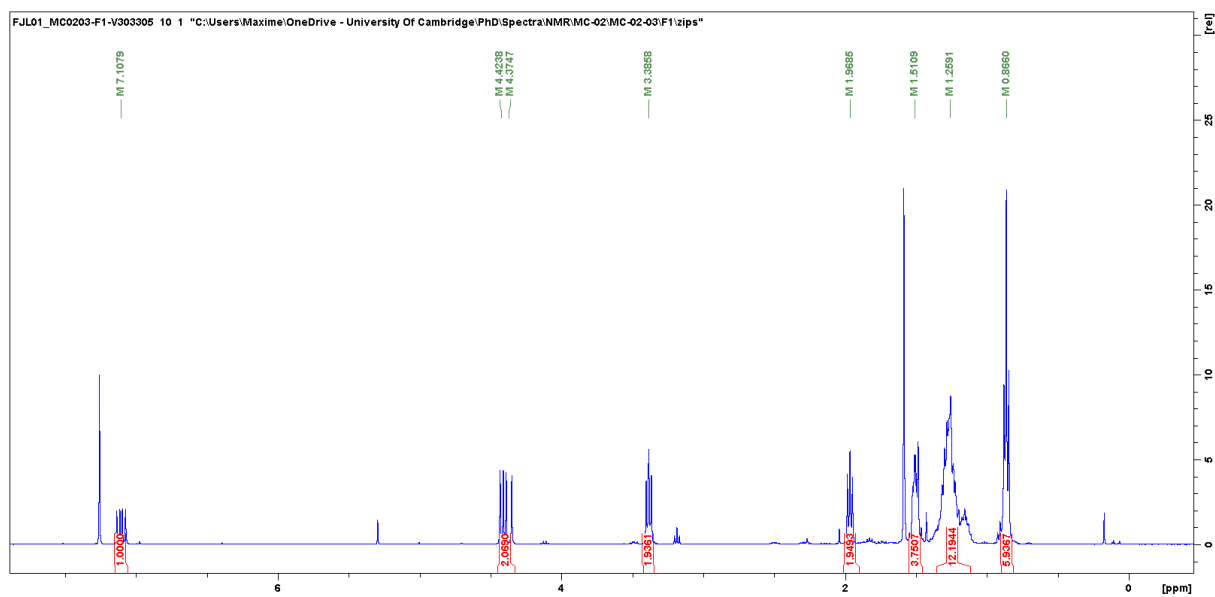
19k



Appendix

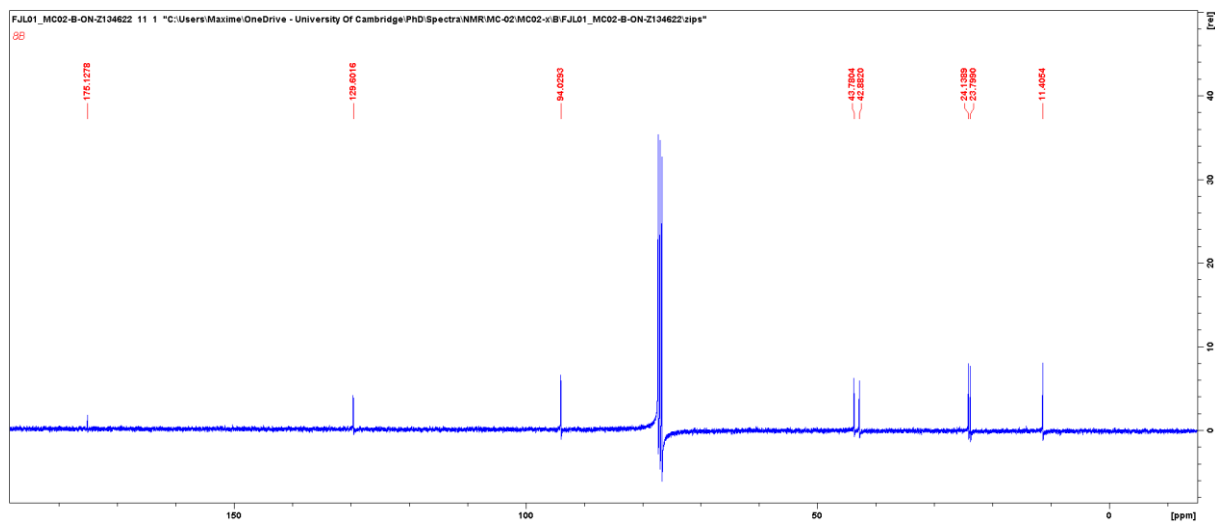
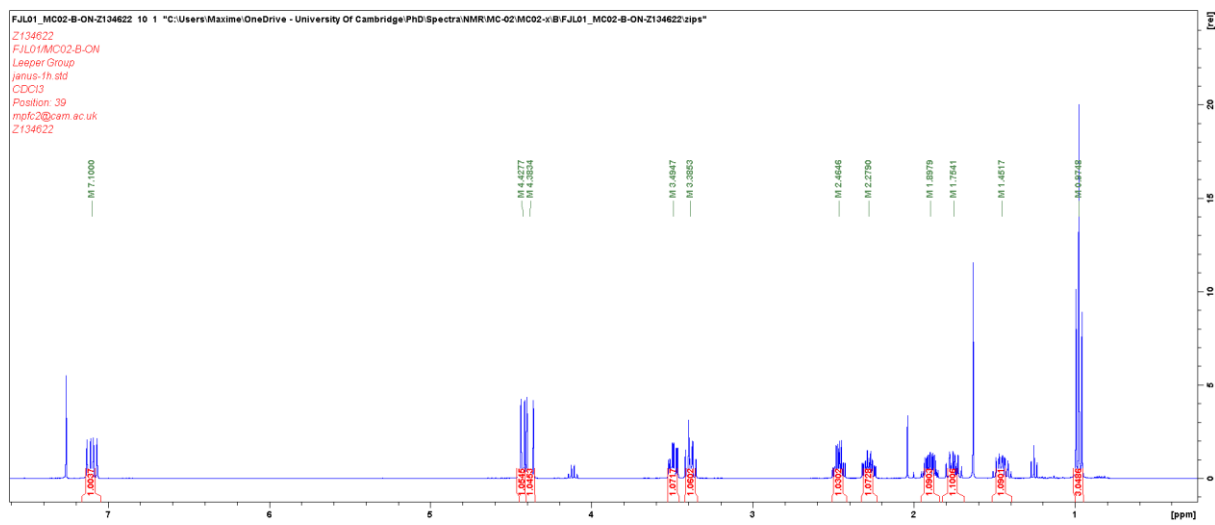
40a





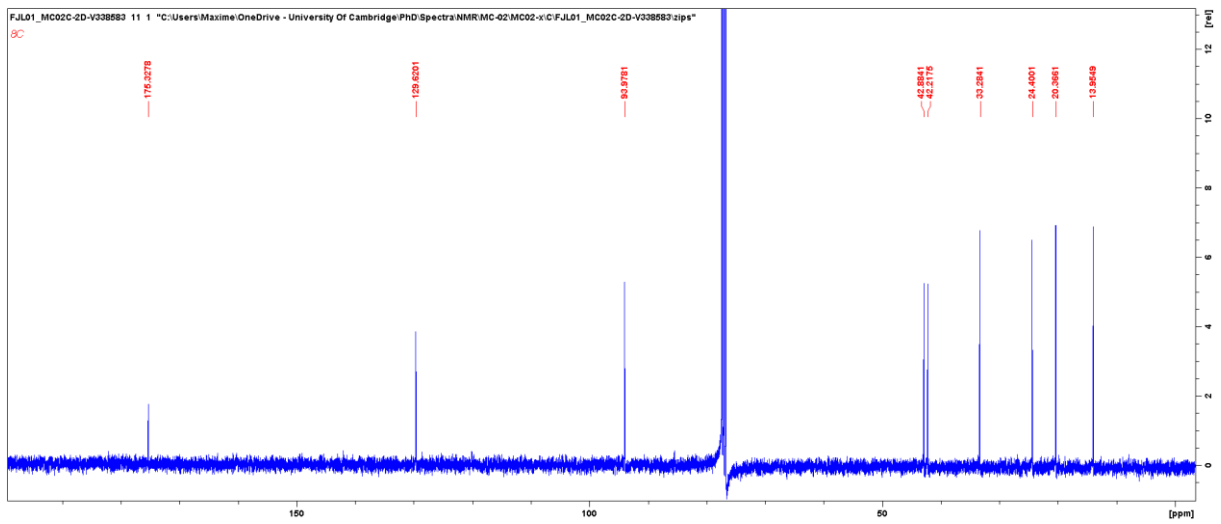
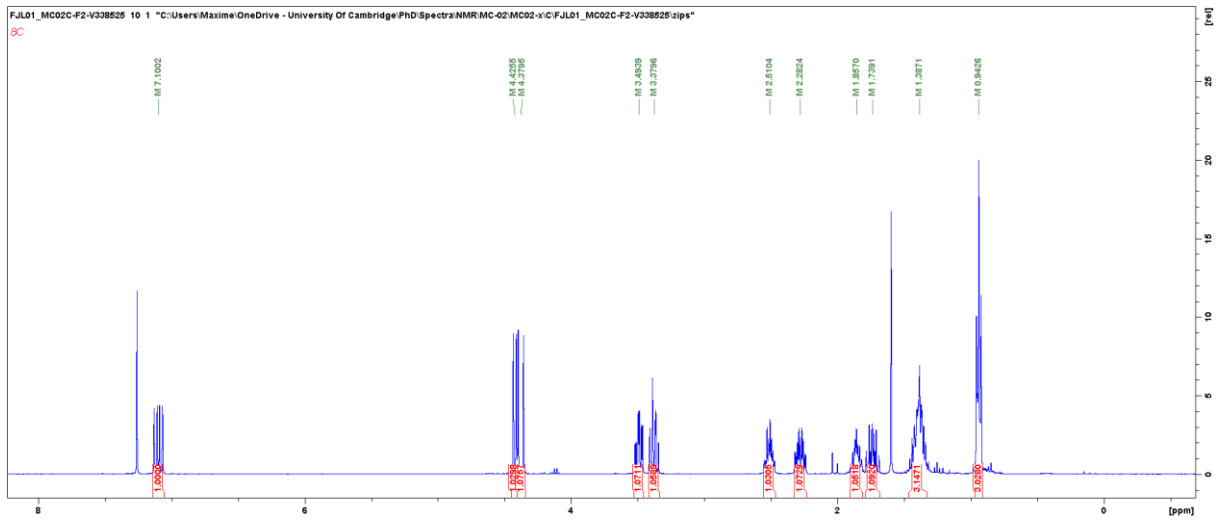
Appendix

40b



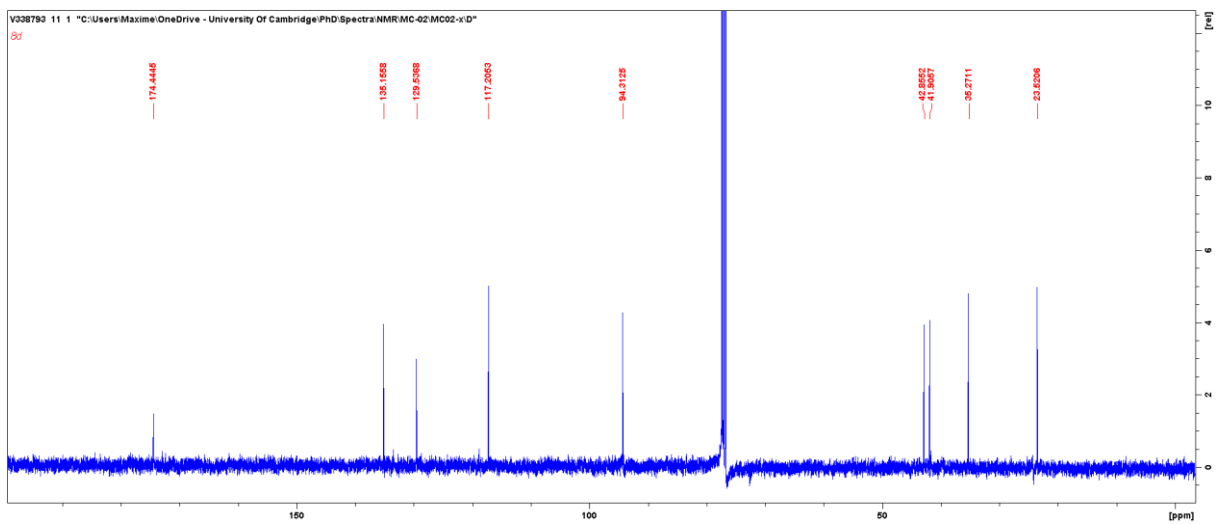
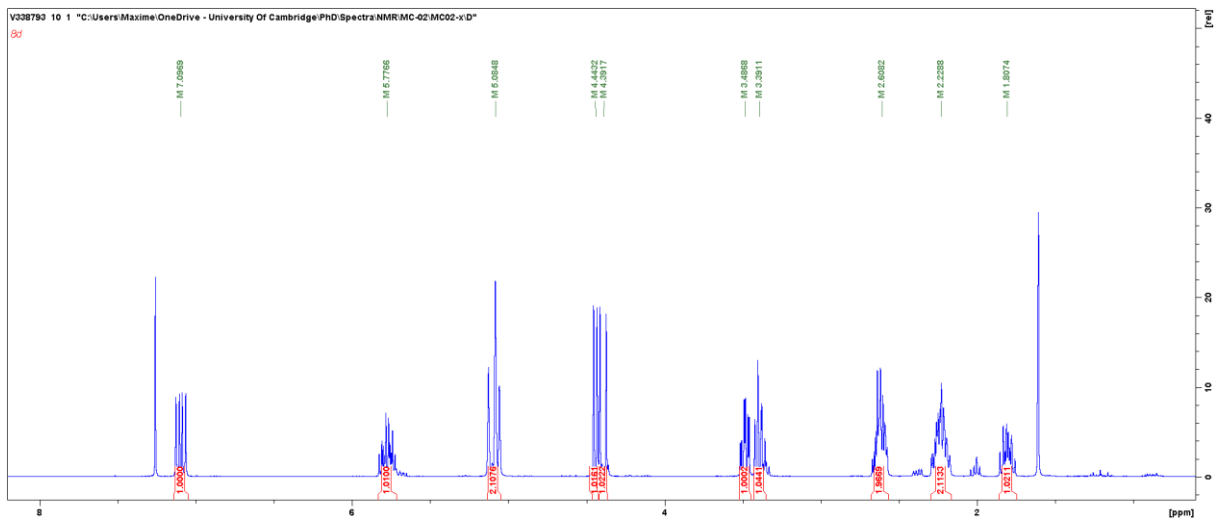
Appendix

40c



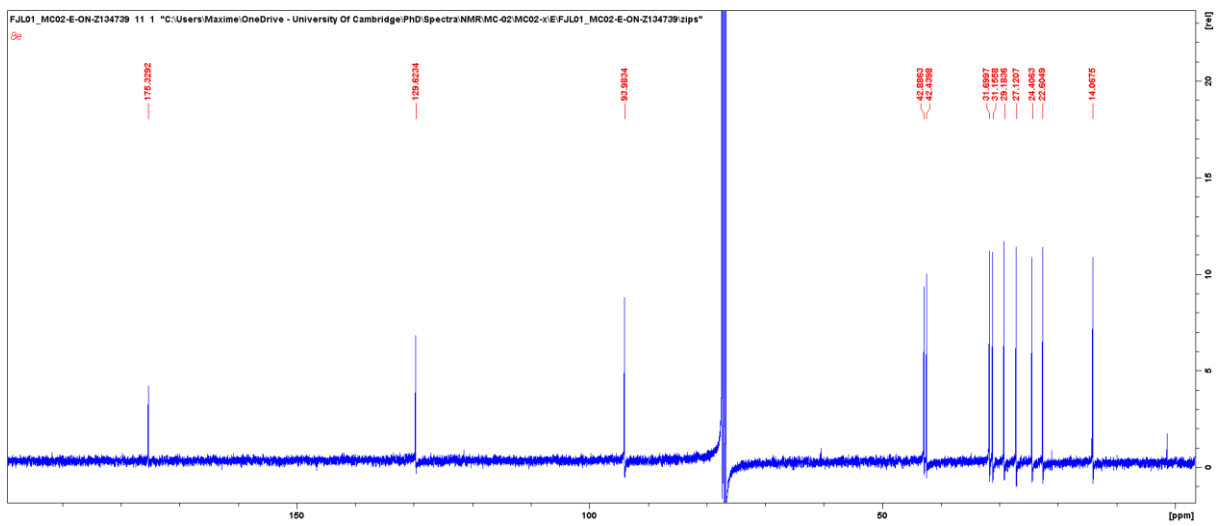
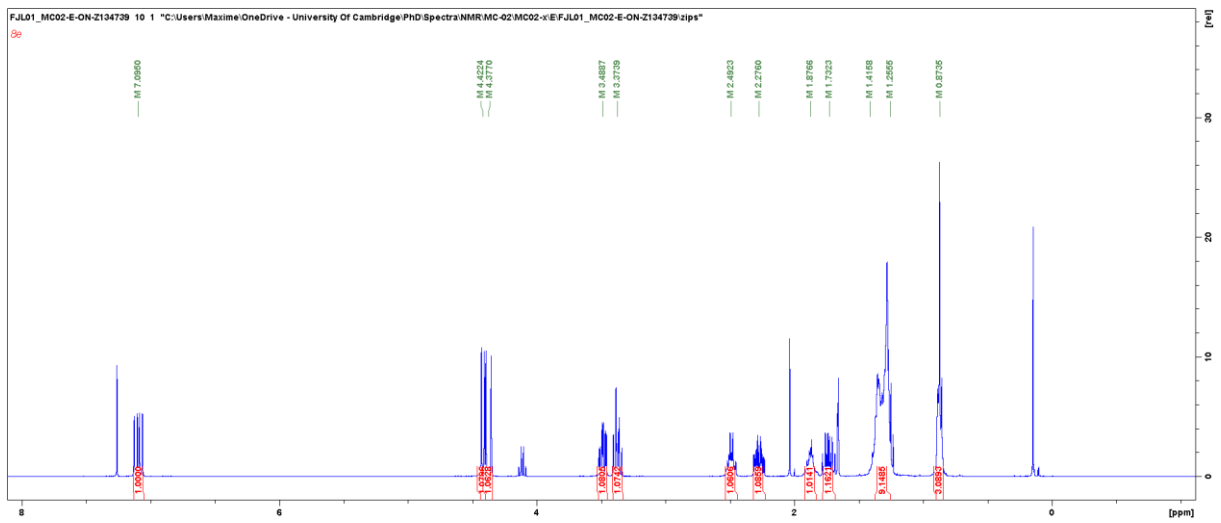
Appendix

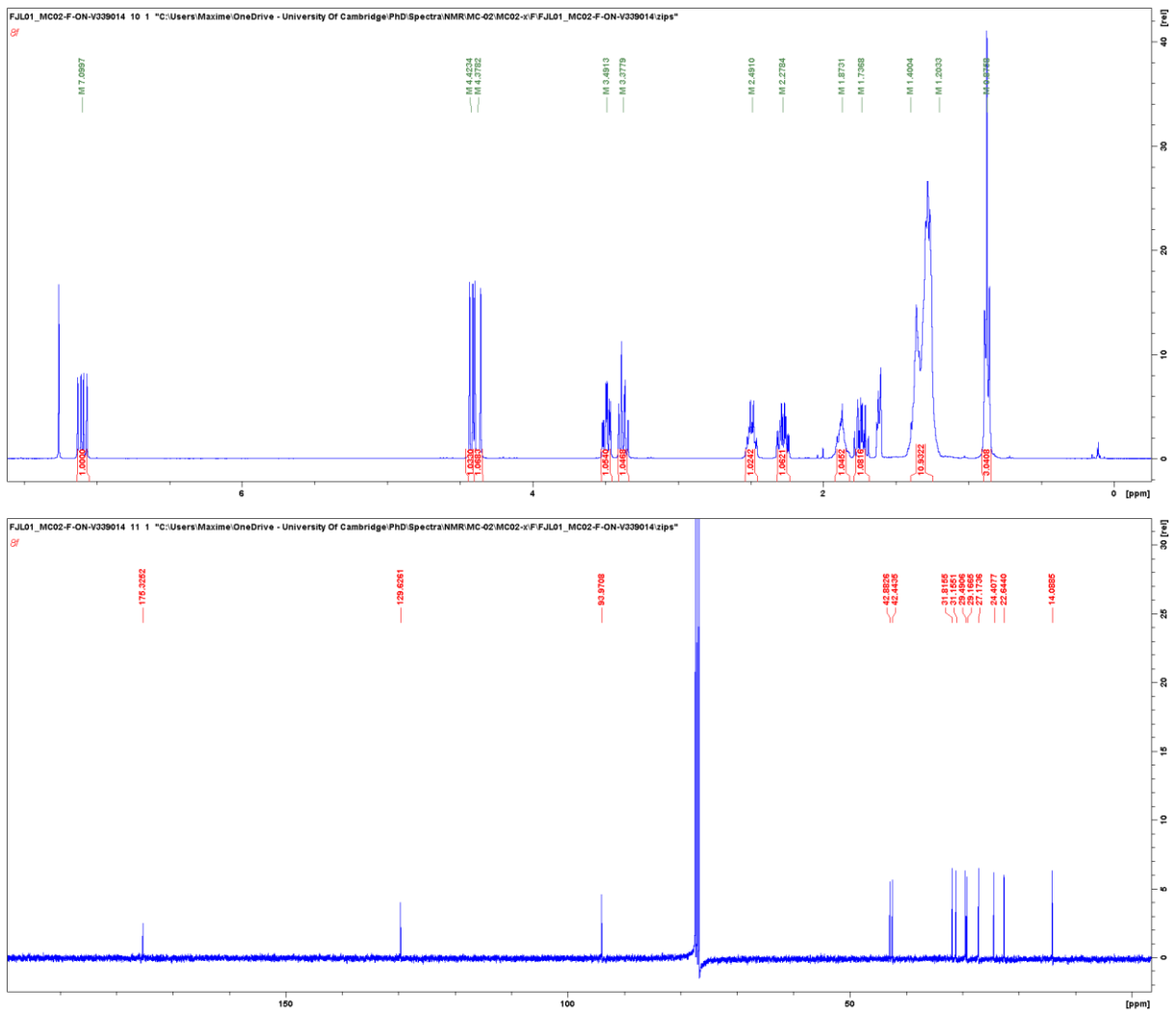
40d



Appendix

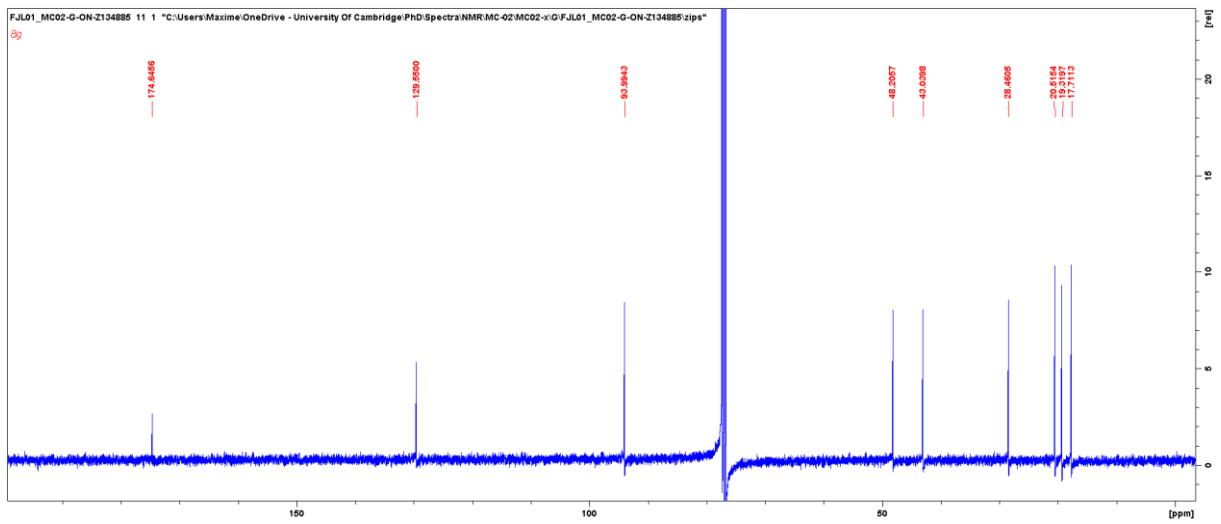
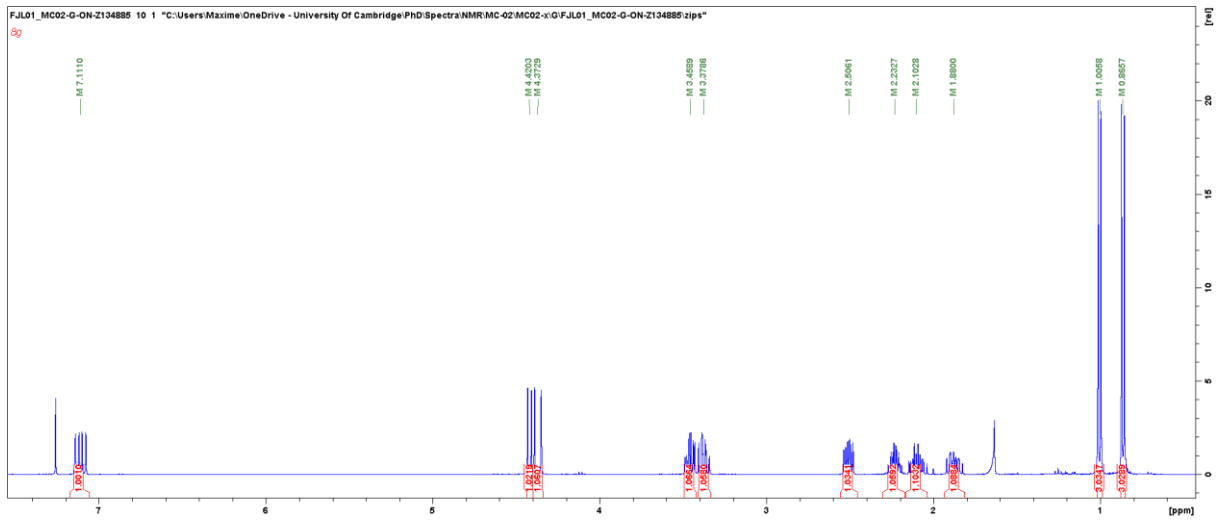
40e





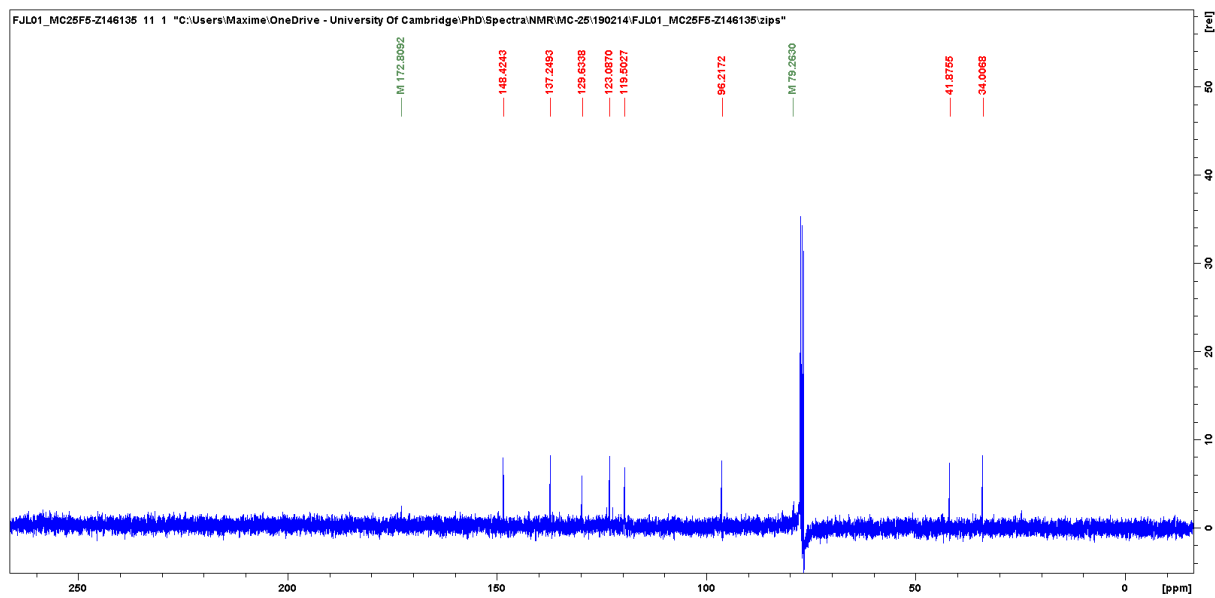
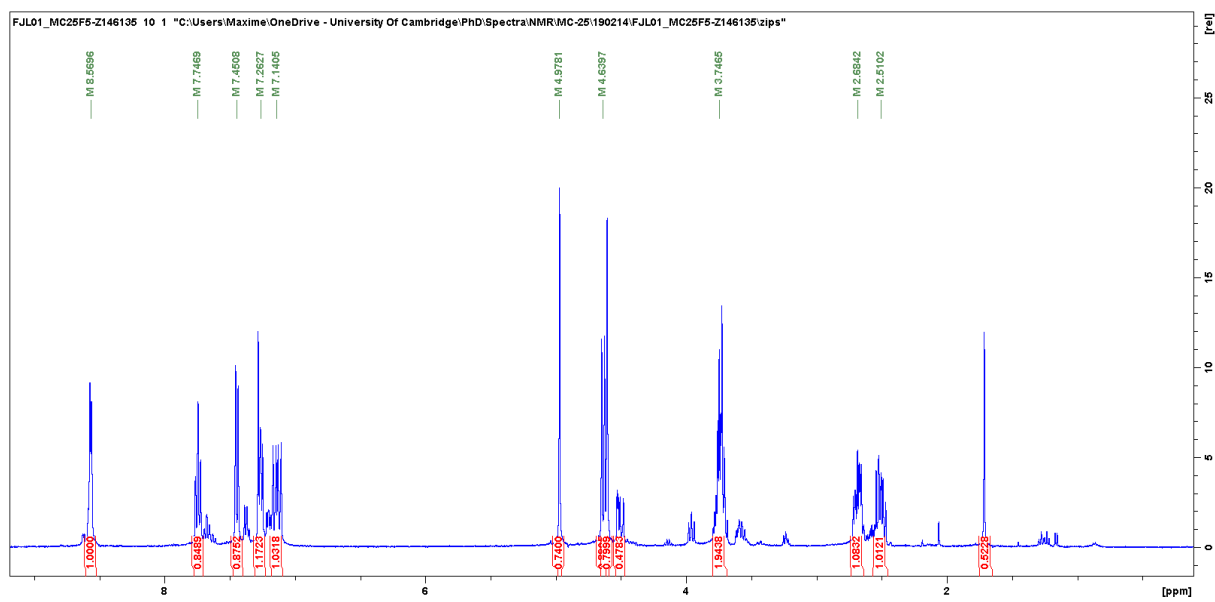
Appendix

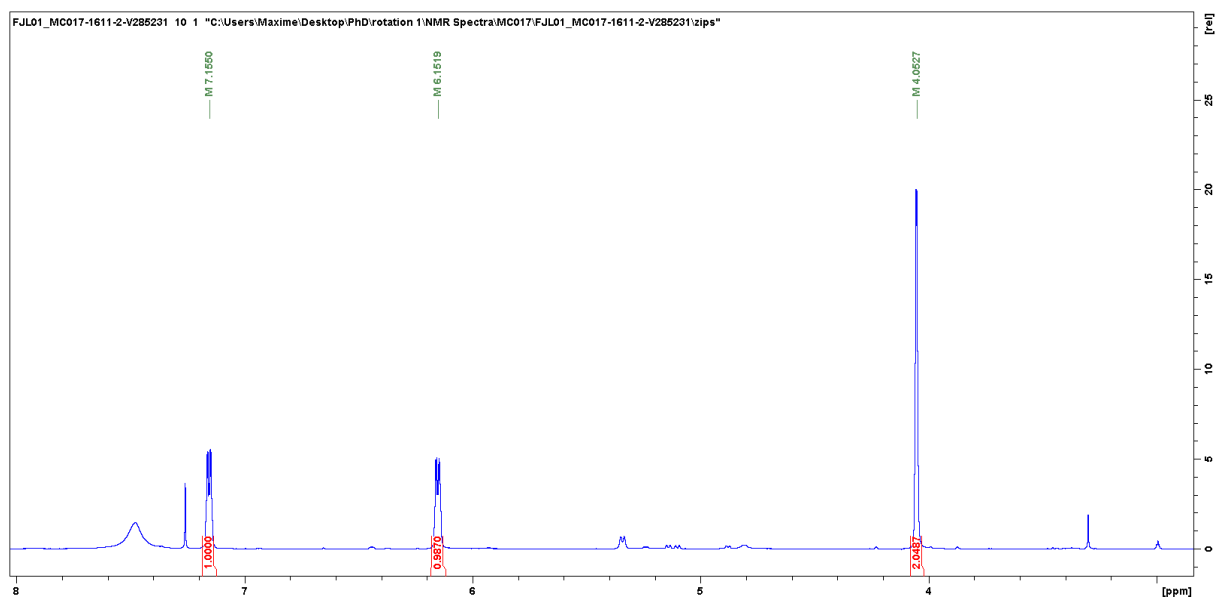
40g

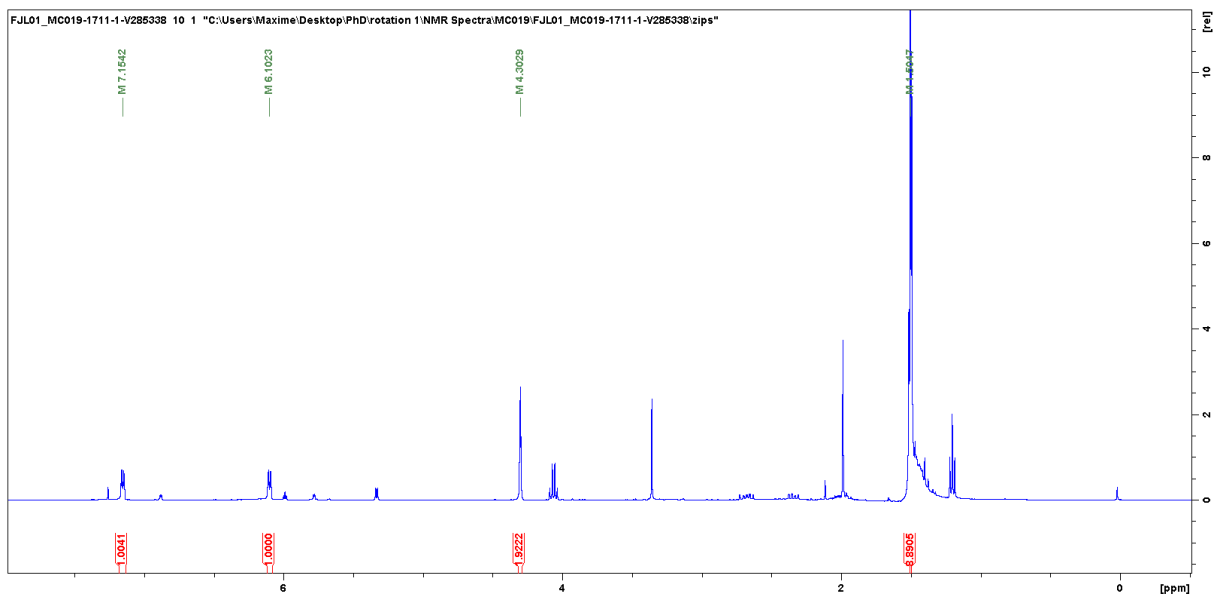
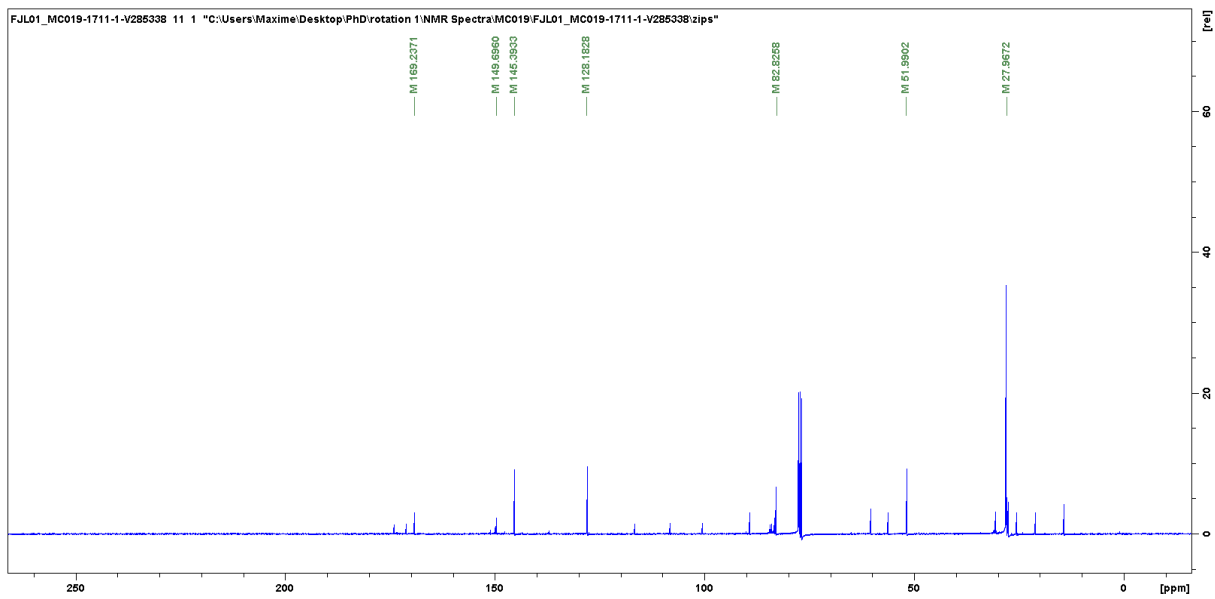


Appendix

41

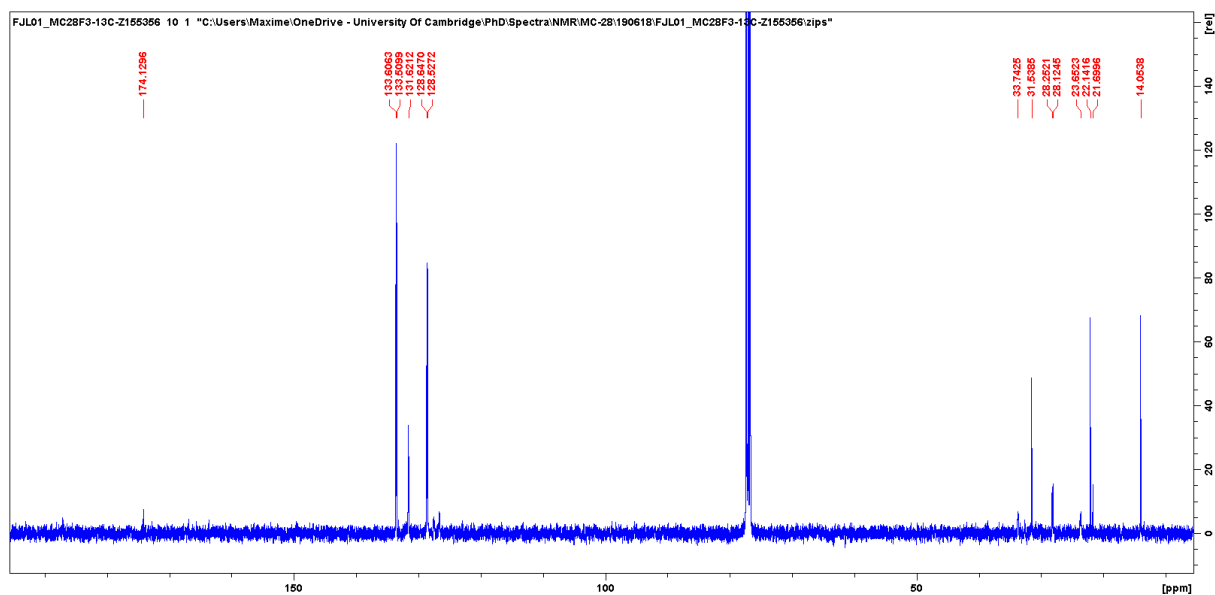
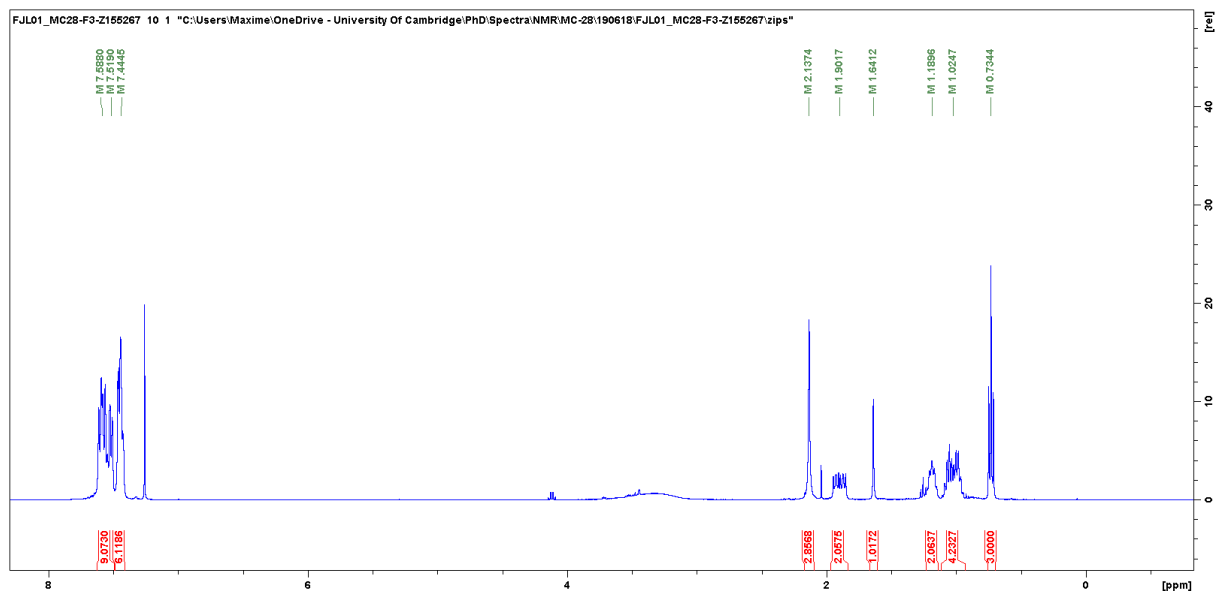






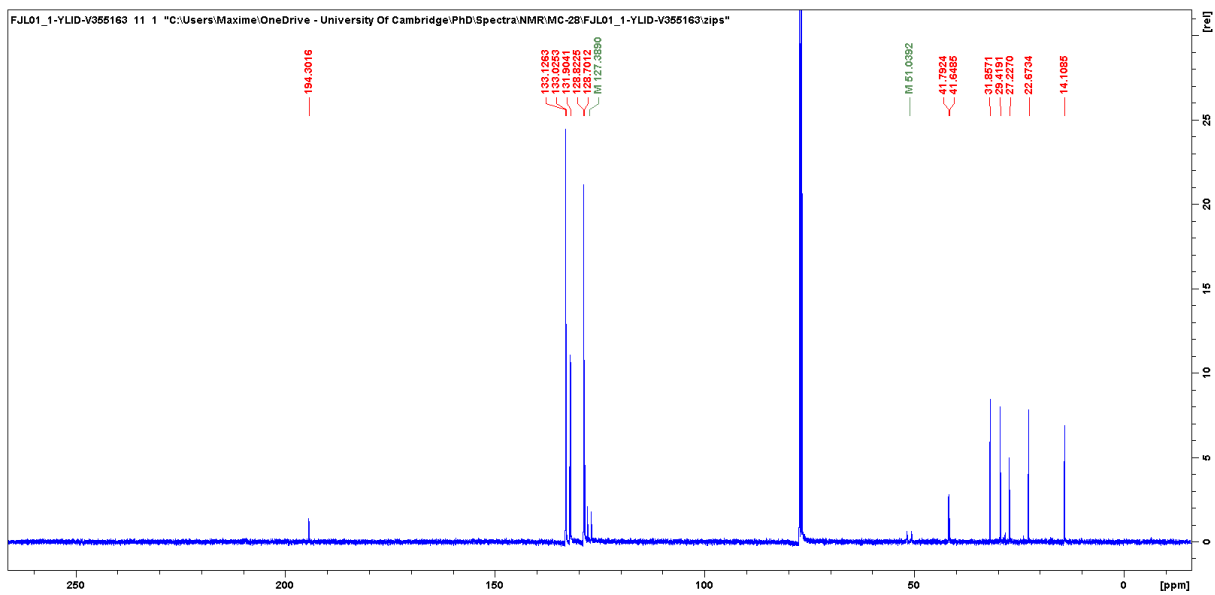
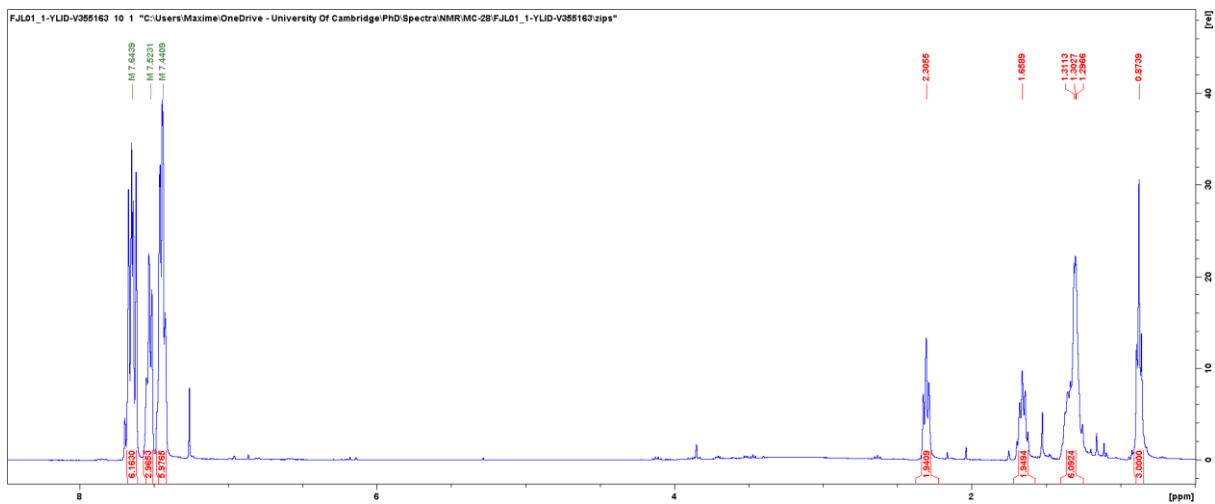
Appendix

49a



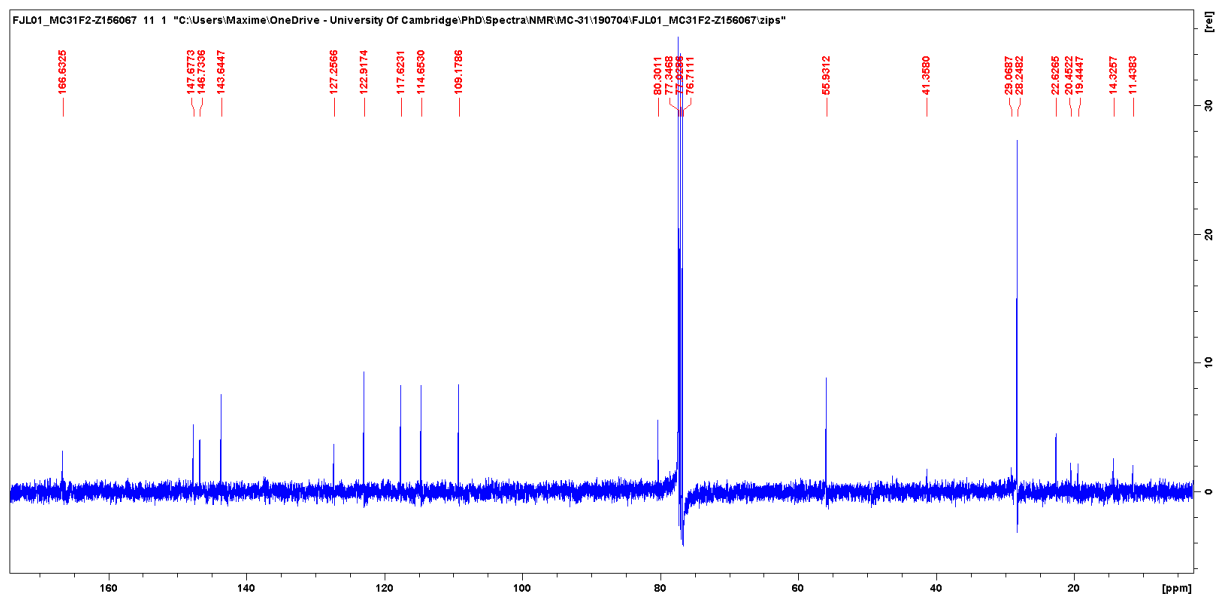
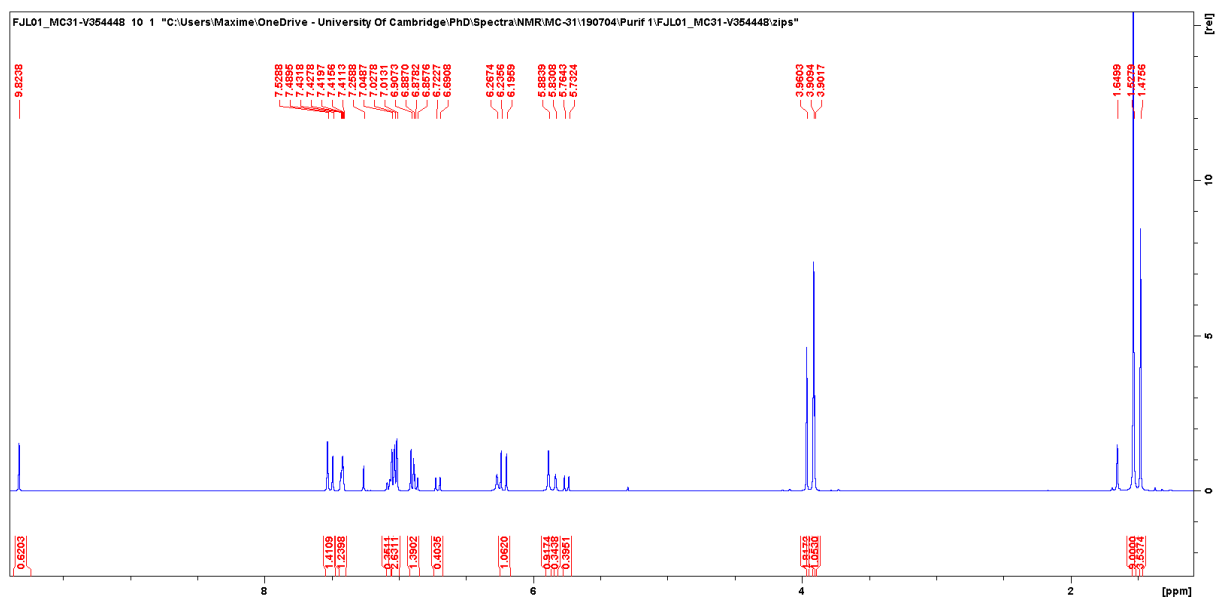
Appendix

49b



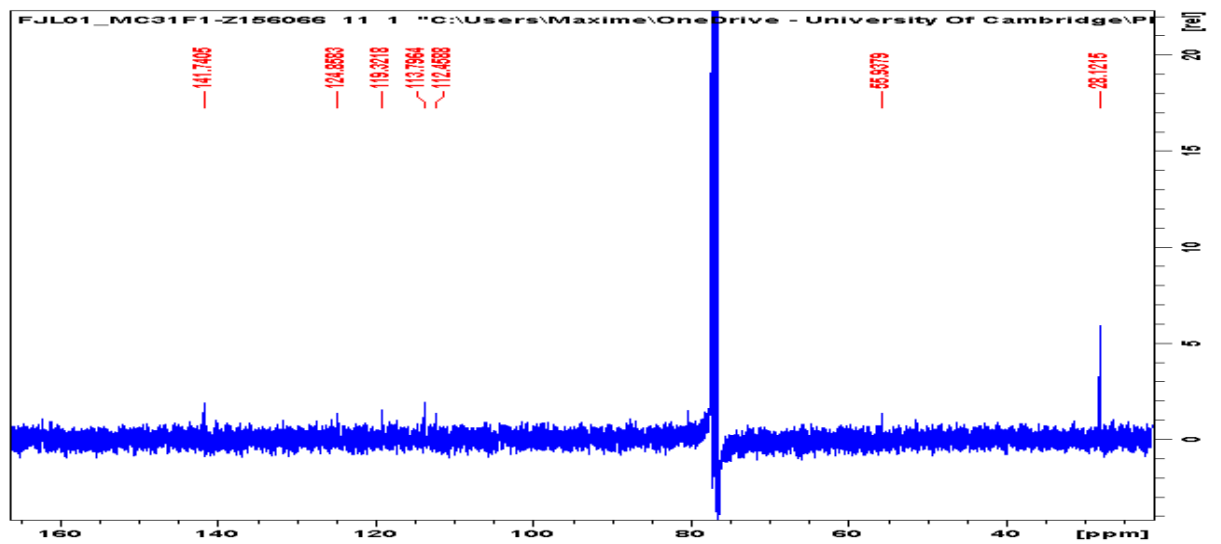
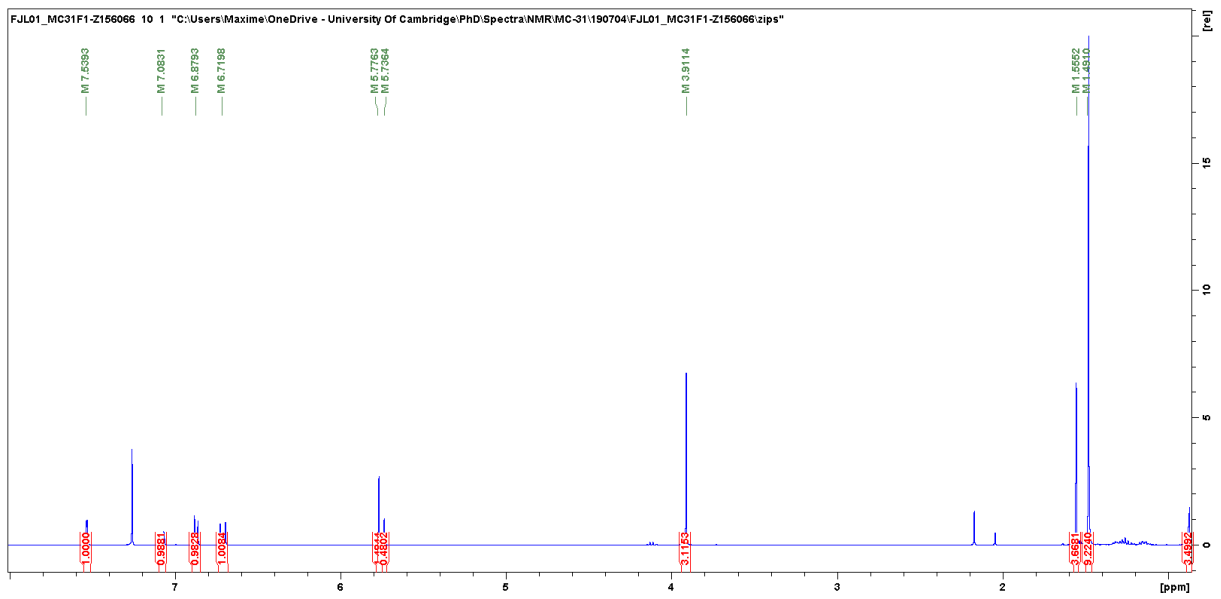
Appendix

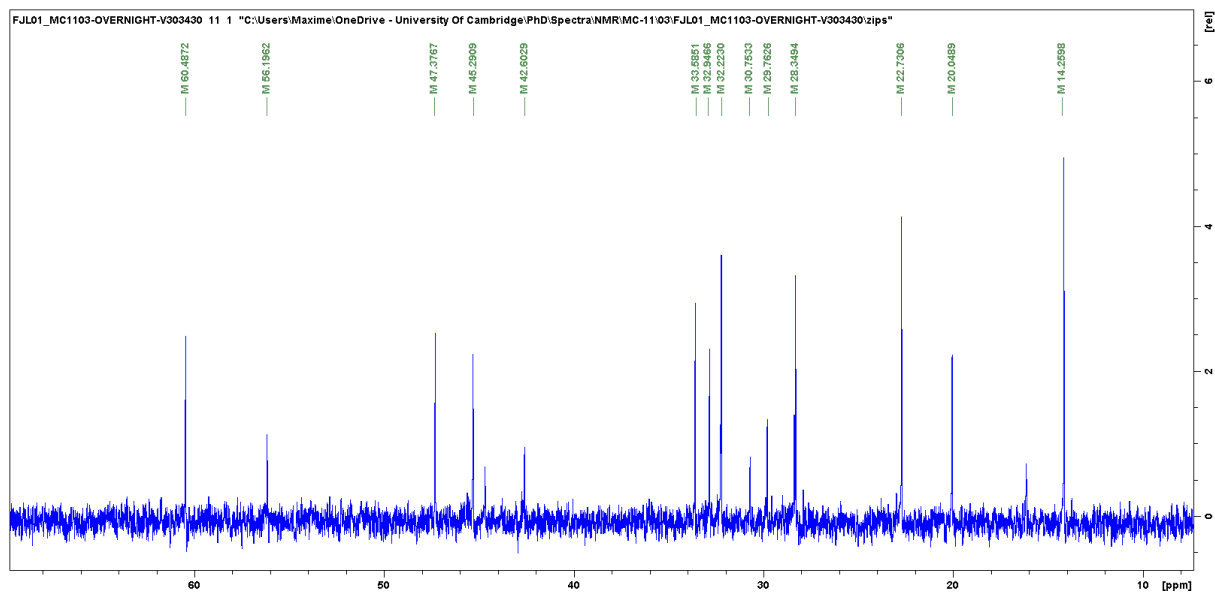
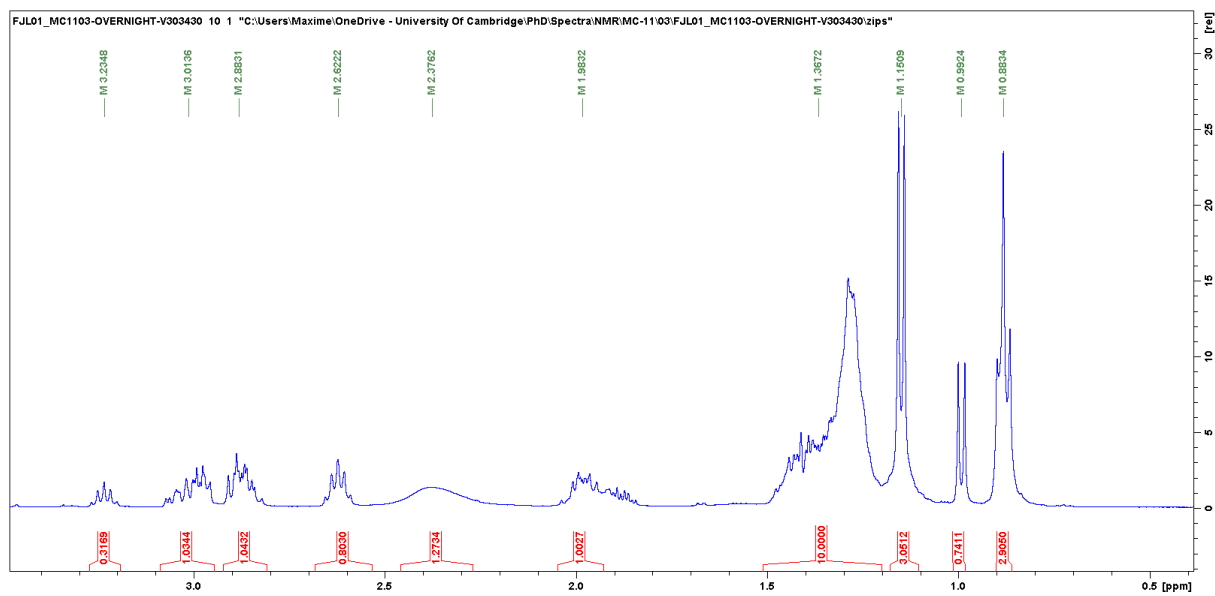
(E)-55

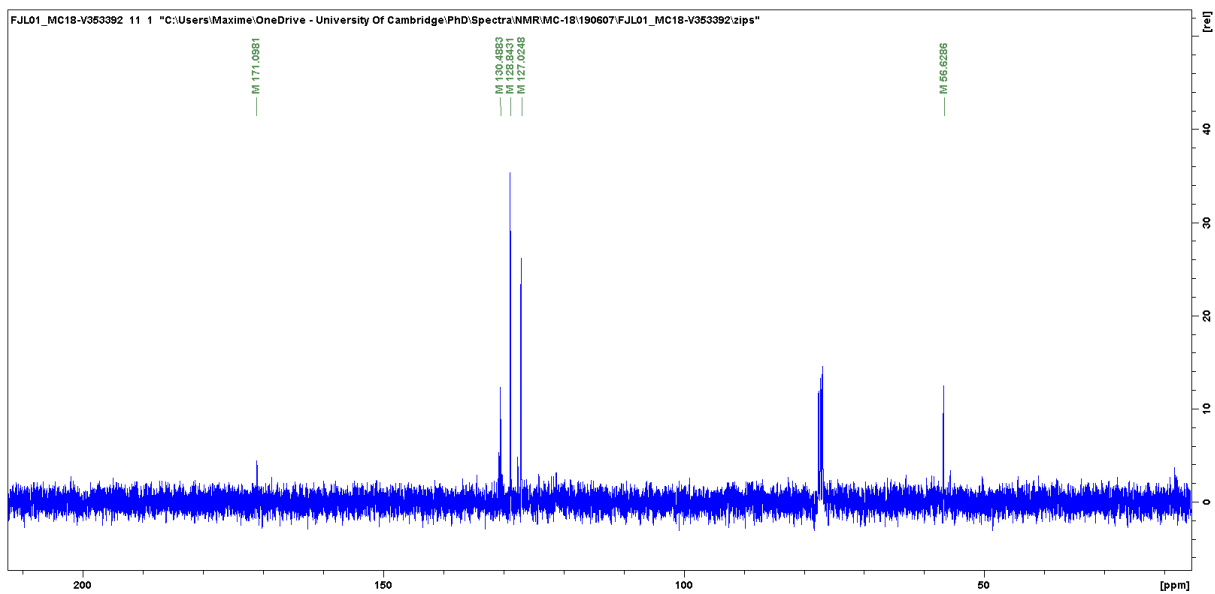
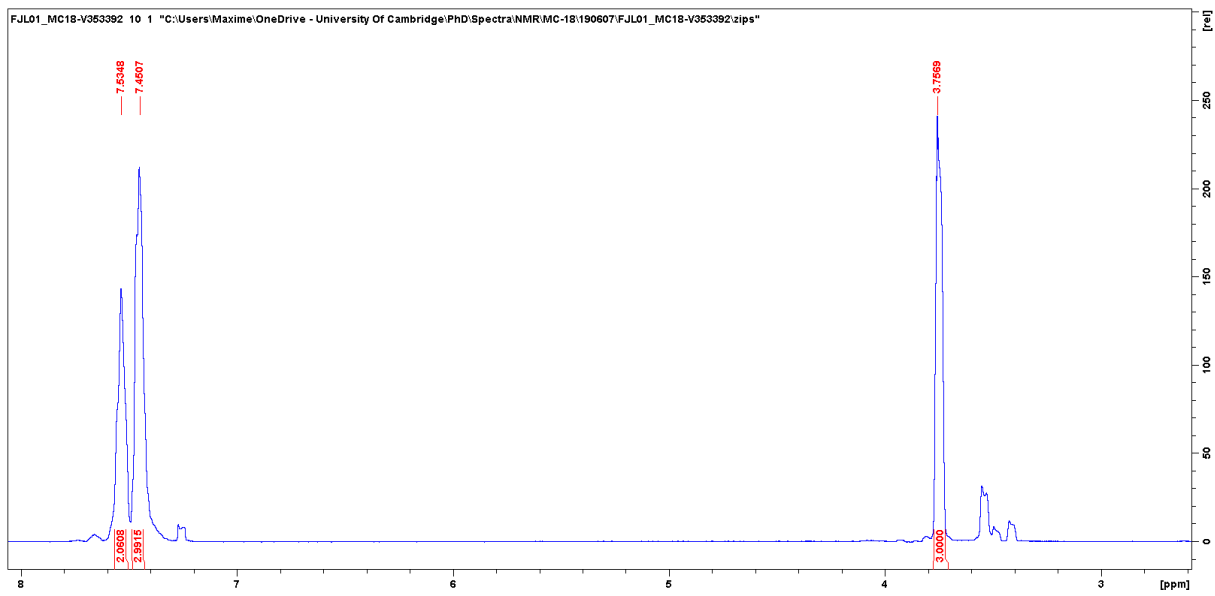


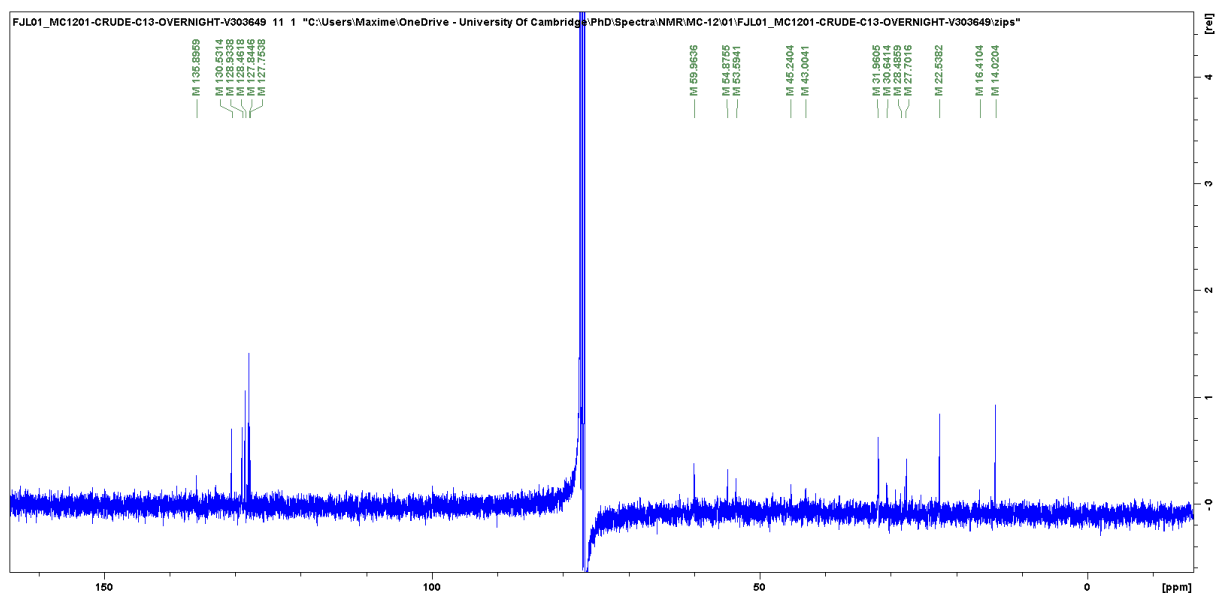
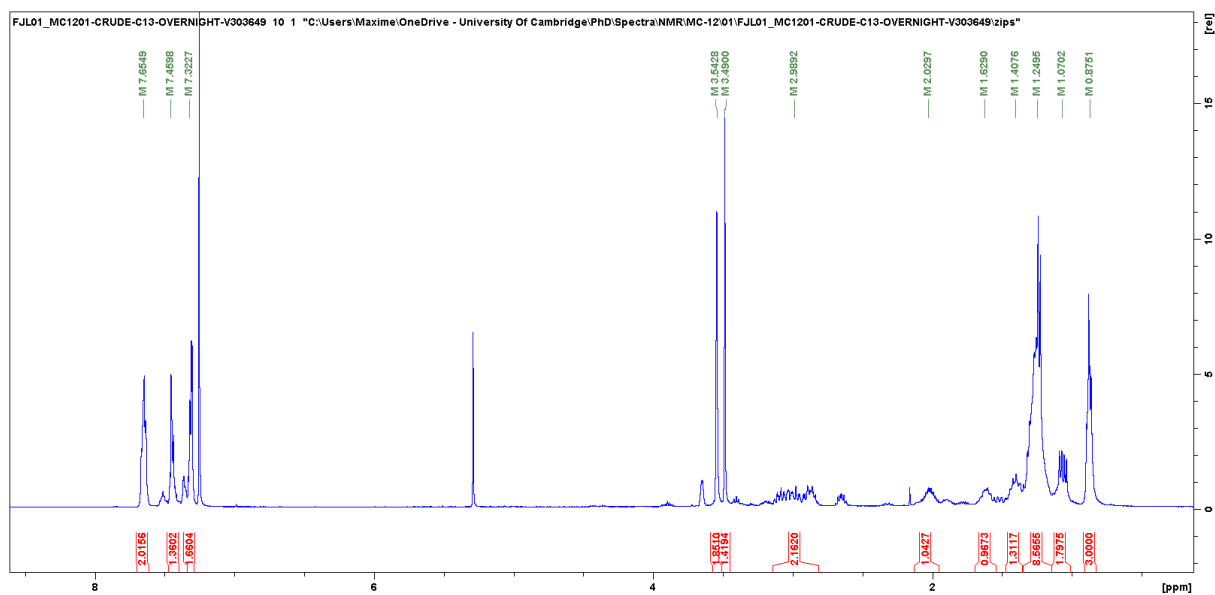
Appendix

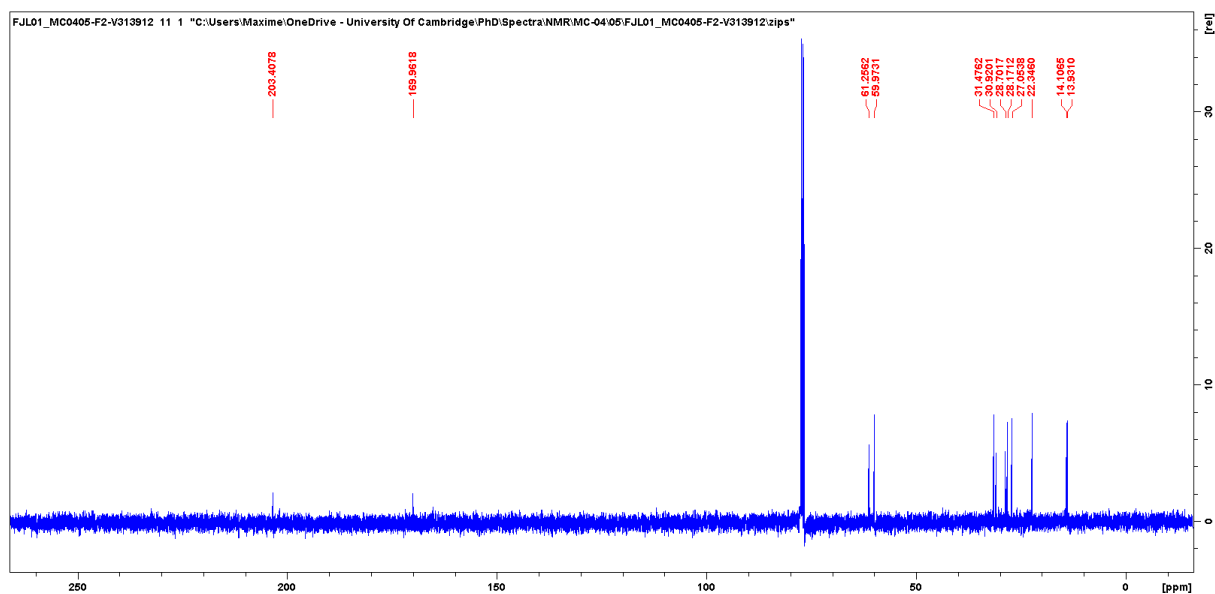
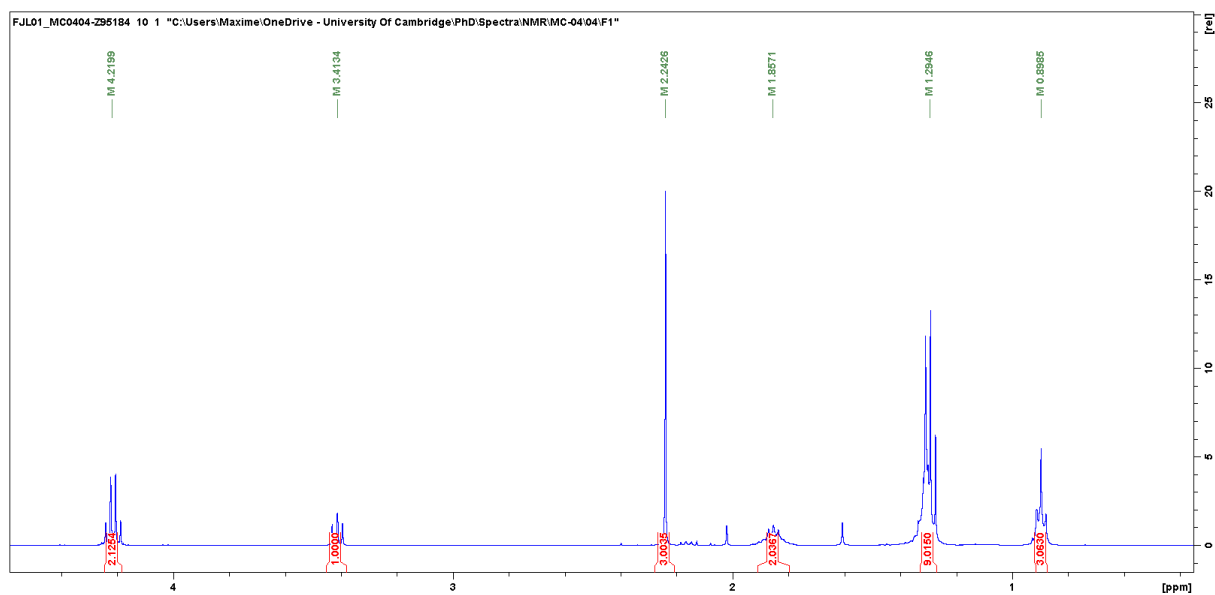
(Z)-55

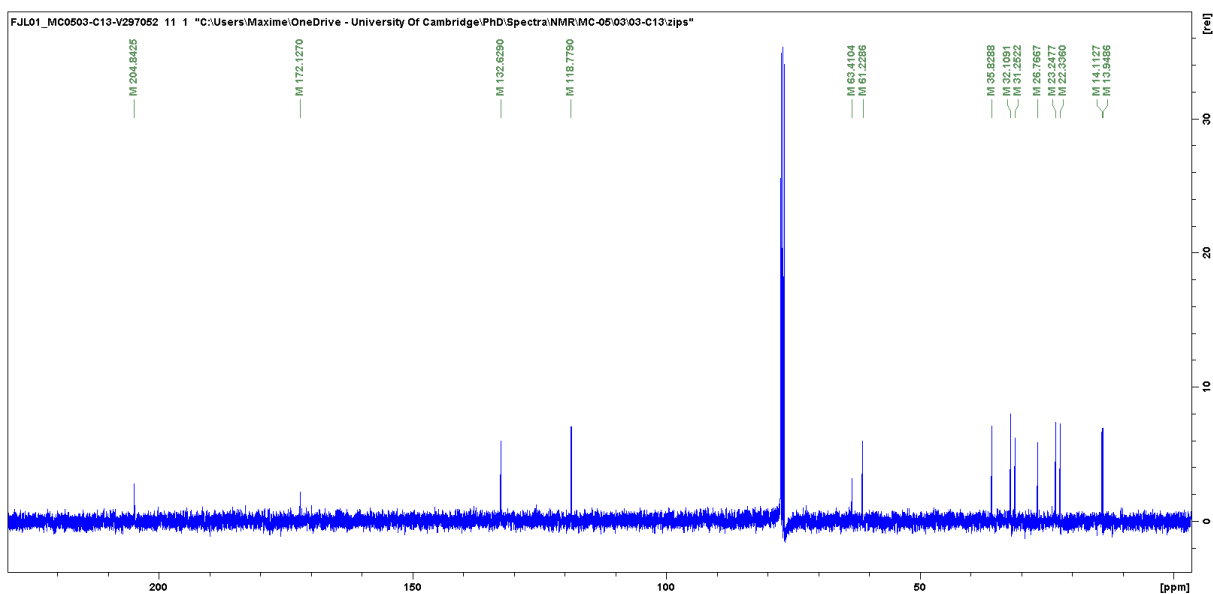
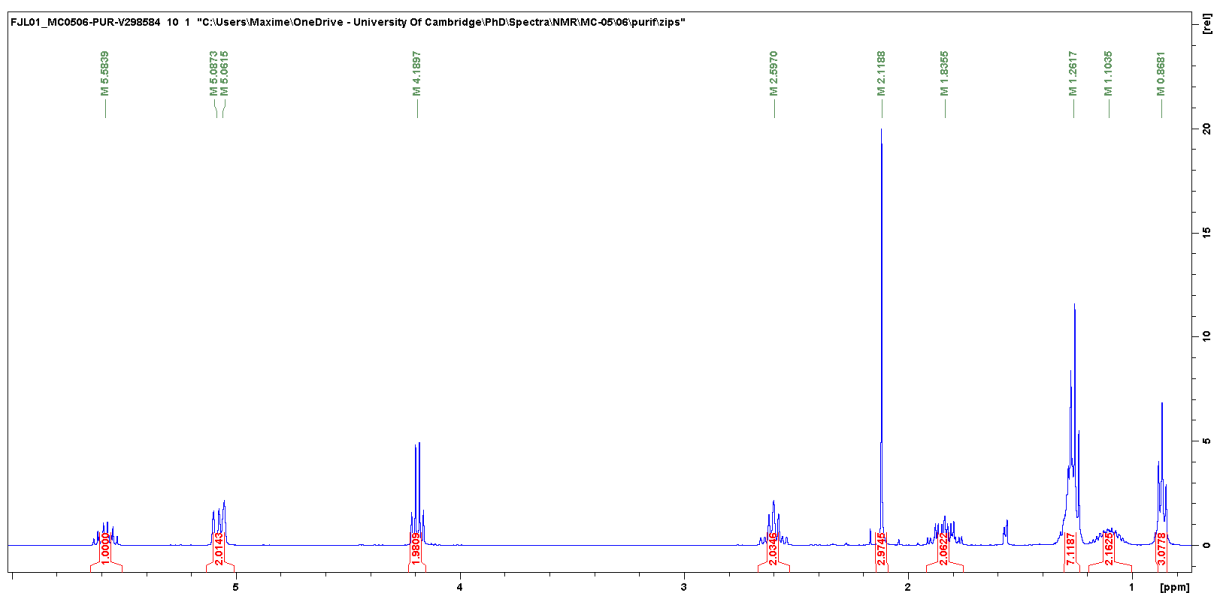


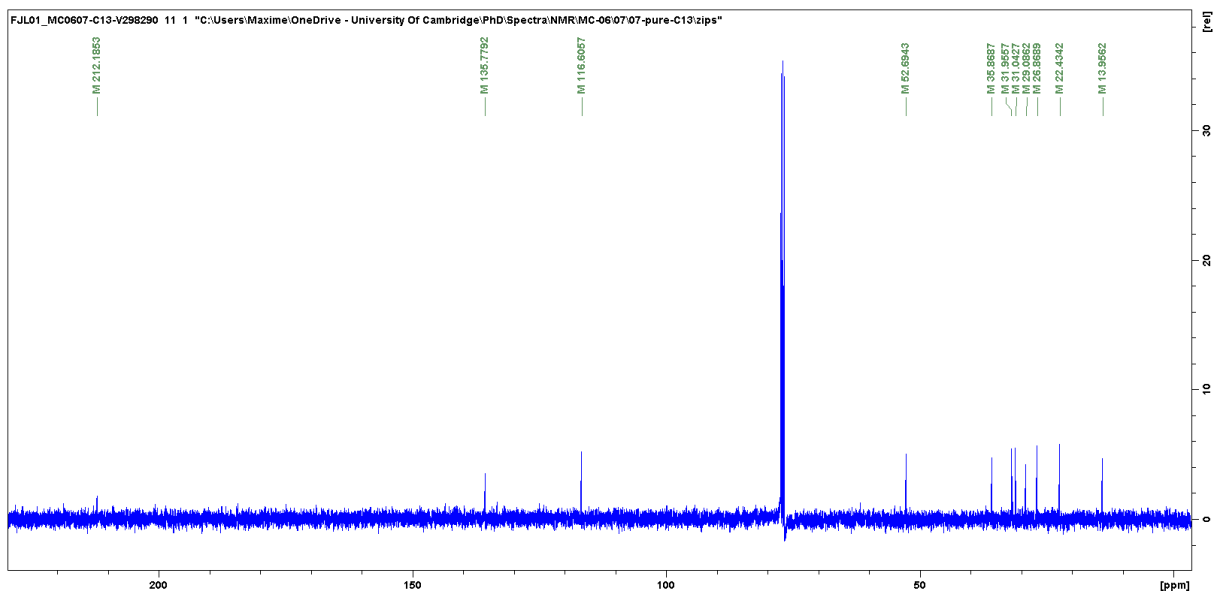
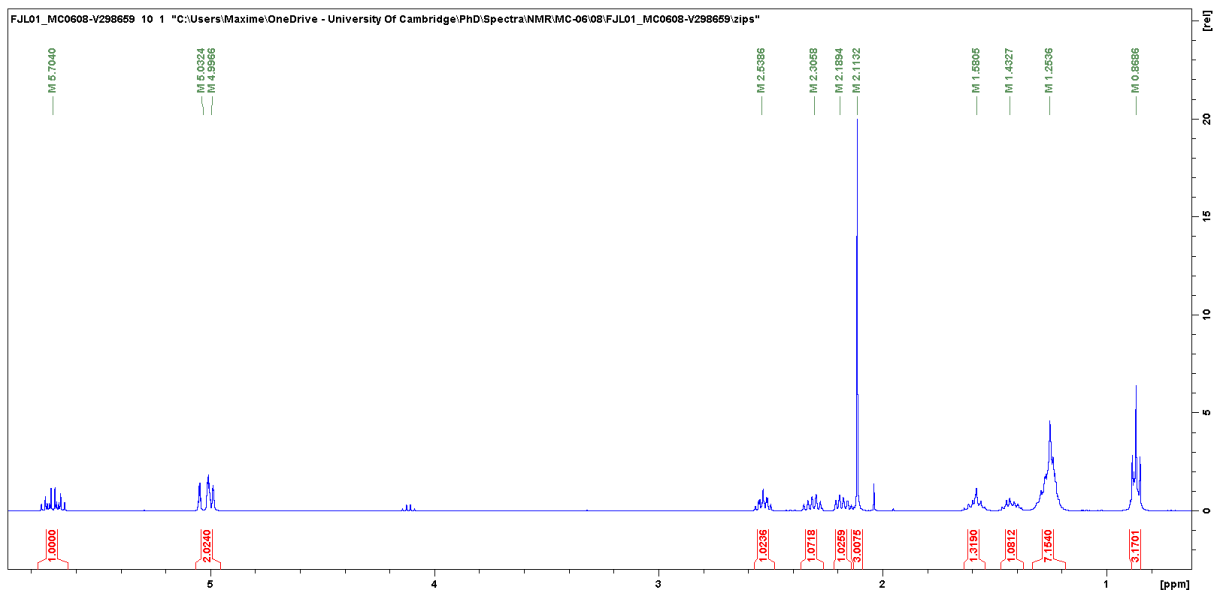






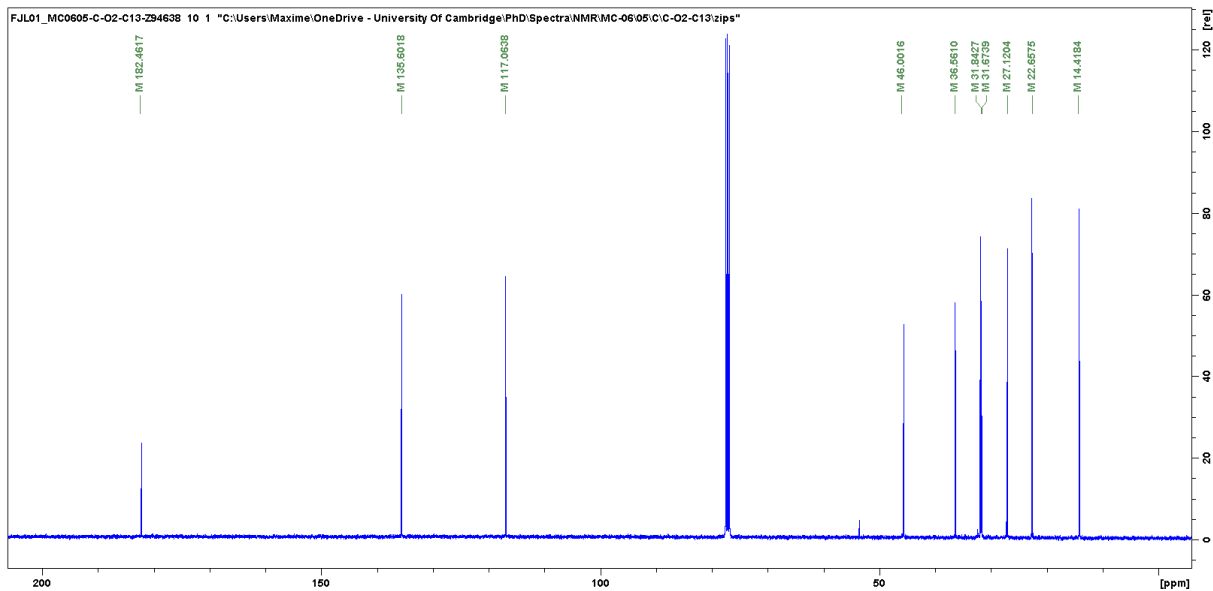
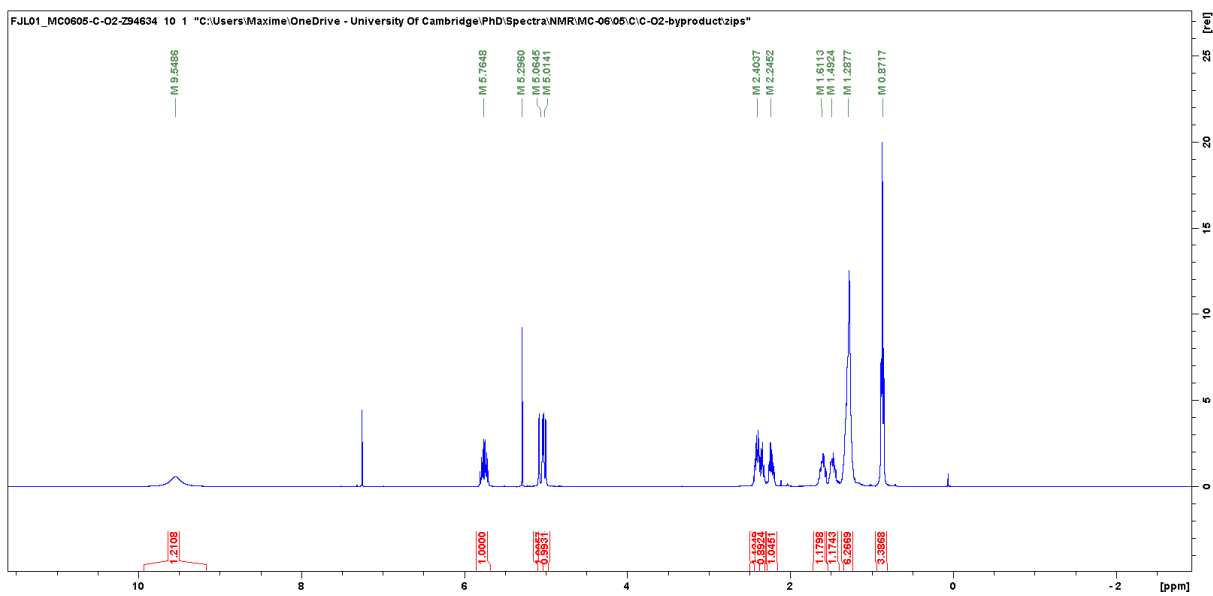






Appendix

74b



Appendix

20

